Synthesis of tailored ligands for radiopharmaceutical applications

Morag Ann Maccall Easson

Synthesis of Tailored Ligands for Radiopharmaceutical Applications

by

Morag Ann Maccall Easson

Department of Chemistry
University of Durham

A thesis submitted for the degree of Doctor of Philosophy

September 1997

Abstract

Synthesis of Tailored Ligands for Radiopharmaceutical Applications

An important aspect of clinical imaging techniques involves the use of complexed gamma or positron-emitting radionuclides. e.g. ^{99m}Tc (γ, $t_{1/2}$ = 6.02 h, 141 keV) for Single Photon Emission Tomography (SPET), ^{62}Cu (β^+,$t_{1/2}$ = 9.74 min, 1.315 MeV) for Positron Emission Tomography (PET). With such radiopharmaceuticals in mind, two new classes of acyclic tetradentate ligands have been synthesised, featuring an N_2S_2 donor system. This array of donor atoms is particularly attractive for its 'soft' metal preference, favouring the complexation of radionuclides such as ^{64}Cu and ^{99m}Tc in diagnostic imaging of disease states, and $^{186/188}Re$ (β^-, $t_{1/2}$ = 90h) in targeted radiotherapy. In both ligand systems the sulfur donor is adjacent to pentavalent phosphorus. Substitution at phosphorus allows easy modification of aryl or alkyl groups to vary the lipophilicity of the complex without affecting the binding properties.

The first class of new ligands presented incorporate thiophosphinic acid groups which are more acidic than their corresponding phosphinates and carboxylates, increasing the stability of the complexes in acidic media. The synthetic routes to series of such ligands have been investigated and optimised. Initial attempts to access the aza-thiophosphinates via treatment of the sulfur-containing P(III) species with the diamine and paraformaldehyde failed to show any significant reaction. The best method of P=S bond formation was found to be via sulfur transfer to the corresponding P(V) phosphinate. The other class of ligands synthesised incorporate the dialkylthiophosphoryl group in conjunction with hydrazide or aminopyridyl moieties. The solid state structures of the ligands were determined by X-ray crystallography.

The solution complexation behaviour of the ligands with a variety of metals, particularly copper and rhenium was studied. The thiophosphinic acid ligands form 1:1 complexes with copper(II) under dilute conditions and oligomeric complexes at high solution concentrations. The complexes formed with copper(II) and oxorhenium(V) appear to be charge neutral. Several of the dialkylthiophosphoryl ligands formed copper(I) complexes by spontaneous reduction of a copper(II) source, and redox behaviour was also shown towards oxorhenium(V).

Some of the ligands radiolabel efficiently with technetium-99m and copper-64 and their preliminary evaluation shows promise for further development.

Morag Ann M. Easson, 1997

Declaration

The content of this thesis represents the work of the author unless indicated to the contrary or acknowledged by reference. The thesis describes the results of research carried out in the Department of Chemistry at the University of Durham, and also at the MRC Cyclotron Unit at Hammersmith Hospital and Amersham International between October 1994 and September 1997. This work has not been submitted for a higher degree in any other academic institution.

Statement of Copyright

Acknowledgements

I would like to thank my supervisor, Professor David Parker, for his enthusiasm, help and encouragement during the course of this project. Many thanks are also due to Dr Jamal Zweit at Hammersmith and Dr Alex Gibson at Amersham for short, but hectic, times radiolabelling. It was terrific experience.

I am also very grateful to Andrei Batsanov, Janet Moloney and Christian Lehman for X-ray crystallography; Alan Kenwright, Julia Say and Ray Matthews for NMR; Lenny Laughlin for help with HPLC; Mike Jones and Lara Turner for Mass Spectrometry; Ritu Kataky for electrochemistry; and all the technical staff of the department for their fantastic support.

Special thanks are due to all the boys and girls of lab 27, both past and present, for their support, friendship and laughs.

Financial support from EPSRC is gratefully acknowledged

Most of all, thanks to the 'support services' (my parents).

To Mum and Dad

This world, where much is to be done,
and little is known....

Dr. Samuel Johnson

CONTENTS

Chapter One

Chapter Two

Chapter Three

Chapter Four

Chapter Five

Chapter Six

Abbreviations

Ac	Acetyl
Ar	Aromatic
aq	Aqueous
BBB	Blood Brain Barrier
bn	Benzyl
BGO	Bismuth Germanate
β^-	Beta Particle
β^+	Positron
Bu	Butyl
Bq	Becquerel
°C	Degrees Celsius
CAD	Coronary Artery Disease
Ch.	Chapter
cy	Cyclohexyl
Cyclam	1, 4, 8, 11 Tetraaza cyclotetradecane
Cyclen	1, 4, 7, 10 Tetraaza cyclododecane
d	Doublet
δ	Chemical Shift
2D	Two Dimensional
3D	Three Dimensional
DADS	Diamide Dithiol
DADT	Diamino Dithiol
DCI	Desorption Chemical Ionisation
DCM	Dichloromethane
dd	Doublet of Doublets
DIBAL	Di-*iso*-Butyl Aluminium Hydride
DMF	N, N-Dimethylformamide
DMPE	bis(Dimethyl Phosphine) Ethane
DMPU	N, N' Dimethylpropyleneurea
DMSO	Dimethylsulfoxide
DOTA	1, 4, 7, 10 Tetraaza Cyclododecane N, N', N'', N''' Tetraacetic acid
DTPA	Diethylenetriamine N,N,N'N",N" Pentaacetic Acid
e^-	Electron
EDDA	Ethylene Diamine Diacetic Acid
EDTA	Ethylene Diamine Tetraacetic Acid
EDDPi	Ethylene Diamine N, N' Di-phosphinic acid
EDTPi	Ethylene Diamine N, N, N', N' tetra phosphinic acid

EI	Electron Impact Ionisation
en	Ethylenediamine
ESMS	ElectroSpray Mass Spectrometry
Et	Ethyl
eV	Electron Volt
FDA	Food and Drug Administration
FTIR	Fourier Transform Infra Red
h	Hours
HPLC	High Performance Liquid Chromatography
Hz	Hertz
I	Ionic Strength
IR	Infra Red
J	Coupling constant
K	Kelvin
L	Ligand
LDA	Lithium Diisopropylamine
lit.	Literature
LR	Lawesson's Reagent
M	Metal
MAb	Monoclonal Antibody
Me	Methyl
MeOH	Methanol
m	Multiplet
min	Minute
m. p.	Melting Point
MRI	Magnetic Resonance Imaging
Ms	Methane Sulfonyl
MS	Mass Spectrometry
n	Neutron
ν	Neutrino
$12N_4$	1, 4, 7, 10 tetra-aza cyclododecane
NMR	Nuclear Magnetic Resonance
NOTA	1, 4, 7-Triazacyclononane N, N', N'' triacetic acid
p^+	Proton
pda	Phenylene Diamine
PET	Positron Emission Tomography
Ph	Phenyl
py	Pyridyl
q	Quartet
RBC	Red Blood Cells

R_t	Retention Time
s	Singlet
SPET	Single Photon Emission Tomography
TBDMS	*tert*-Butyl DiMethyl Silyl
$t_{1/2}$	Half Life
t	Triplet
td	Triplet of Doublets
tt	Triplet of Triplets
Tf	Trifluoromethane sulfonyl
TFA	Trifluoroacetic acid
THF	Tetrahydrofuran
TLC	Thin Layer Chromatography
Ts	Toluene Sulfonyl
UV	Ultra Violet

Chapter One

Introduction

1. Introduction

A brief outline of the applications of radiopharmaceuticals is given (1.1) along with their importance within the range of imaging techniques available in diagnostic medicine (1.2). The processes involved for imaging with gamma-emitters and positron-emitters are discusssed (1.3) with relevance to suitable radionuclides (1.4) and their potential extension to therapeutic applications (1.5). The administration of metal radionuclides as coordination complexes is assessed (1.6) with particular attention to technetium, rhenium and copper prior to illustration of their corresponding radionuclides in nuclear medicine (1.7). Finally, the subject matter presented in subsequent chapters is outlined (1.8).

1.1 Radiopharmaceuticals

Radiopharmaceuticals are drugs which contain a radioactive component for the diagnosis or therapy of disease. Quite simply, the radioactivity can act as a signal or tracking device in the former case, or it can be used to destroy diseased cells in the latter. They exploit both the nuclear properties of the radionuclide and the pharmacological properties of the radiopharmaceutical. Now in routine use in clinical nuclear medicine for disease diagnosis in a variety of imaging protocols, they are also under investigation for their use in treatment.

1.2 Diagnostic Imaging in Medicine

Imaging techniques are important for medical diagnosis: diagnosis can be crucial for health and life itself. Diagnostic techniques are essential in medicine for a range of investigations from the detection of cancer - where early diagnosis is vital - to the study of neurological diseases and cardiology. Metabolic pathways and drug metabolism can be studied to give a greater understanding of a variety of disorders and perhaps progress towards an effective treatment of these diseased states. A whole range of techniques are available - each with different advantages and abilities to gain different levels of information. All are complementary as they range from providing structural information to molecular detail. A particular technique is chosen according to the level of information required. For example, a ruler is a useful tool for measuring the breadth of this page but quite inadequate for measuring the length of a football pitch. Different techniques and instrumentation are required to answer different medical questions. Current imaging techniques available include *X-ray computed tomography* (X-ray CT), *magnetic resonance imaging* (MRI), *ultrasound* and the radiopharmaceutical modalities - *single photon emission tomography* (SPET) and *positron emission tomography* (PET). The level of information which can be gained by each of these techniques is illustrated

schematically (Figure 1.1). The range in sensitivity is from the detection of millimolar concentrations by MRI to picomolar concentrations in PET - a billion-fold (10^9) difference.[1] With respect to specificity, the range is from tissue density/water content by MRI to a clearly identifiable molecule (radiolabelled) by PET. The real advantage of radionuclide imaging is the ability to monitor biochemical and physiological processes as they occur in living systems.

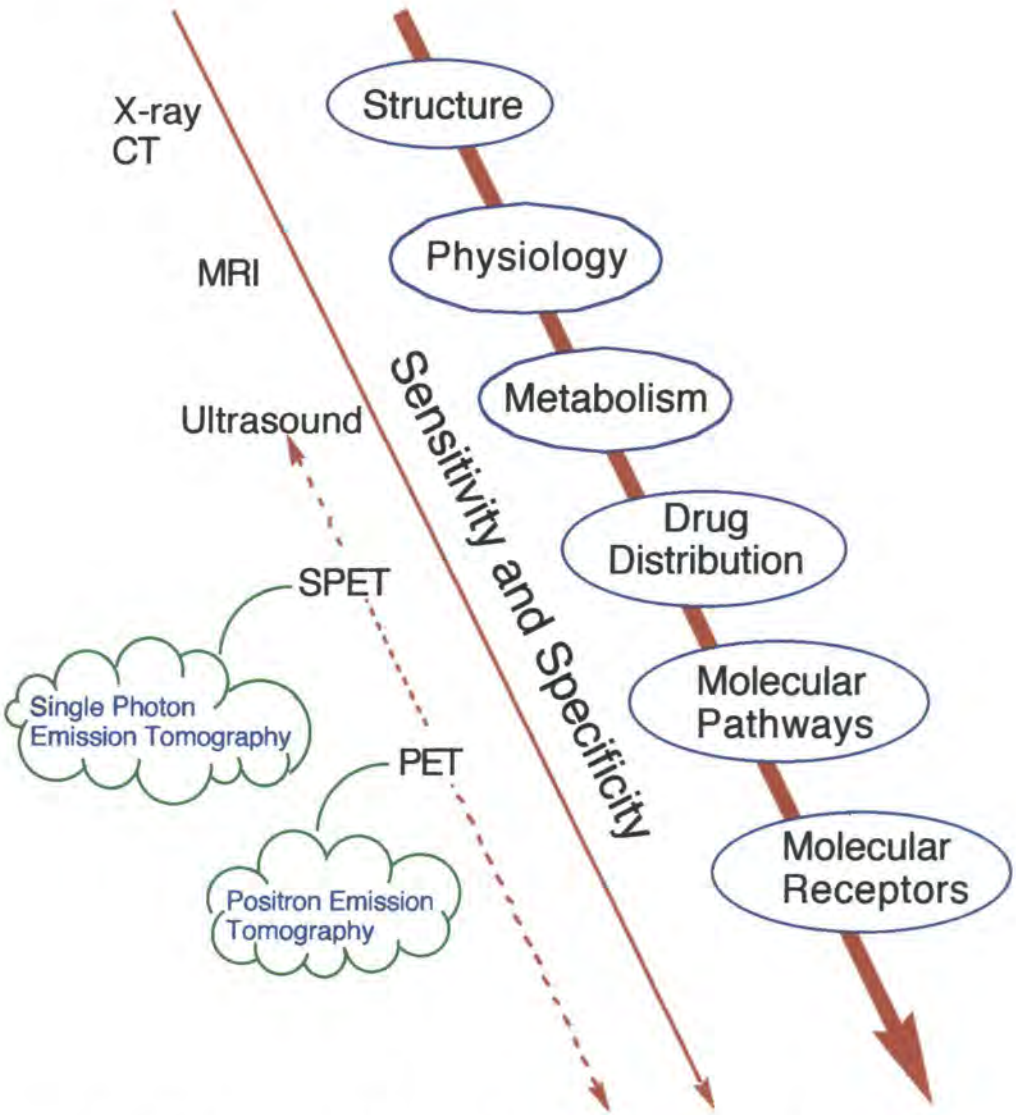

Figure 1.1 The spectrum of diagnostic imaging in medicine (level of information from various imaging modalities) reproduced from reference[1]

1.3 Radionuclide Imaging

The requirements of any imaging technique are: an energy source; the interaction of this energy with the studied matter in a useful and non-uniform manner; a means of detecting the contrast attained; and a method of displaying this information. This can be easily envisaged by considering a routine X-ray that most of the population will have experienced at some point. In this case, the X-rays from an external source pass through

the subject under investigation and are attenuated more or less strongly by different tissues. It is this contrast which produces a picture of the subject. The important difference in radionuclide imaging is that the energy source is internal, arising from radioactivity emitted by the radiopharmaceutical (Figure 1.2). Several imaging techniques utilise the characteristic emissions produced by unstable nuclei. A choice of emission pathways provide scope for highly sensitive imaging protocols as well as therapy. It is therefore appropriate to consider the processes involved for radiation to occur.

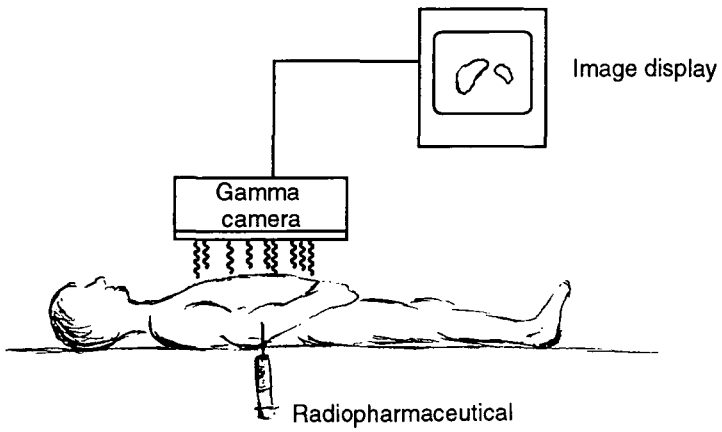

Figure 1.2 Schematic representation of radionuclide imaging reproduced from reference[2]

The Rutherford-Bohr model provides the basic picture of a neutral atom with its nucleus consisting of protons and neutrons (providing the mass number, A) and electrons remaining in their discrete orbits. Nuclei are stable in their ground state but unstable if they possess too much energy in an excited state. Unstable nuclei lose energy in the form of electromagnetic radiation or particle emissions to decay to their stable ground state. The ratio of protons to neutrons determines the stability of the nuclei and the particular deficiency (proton or neutron) determines the mode of decay. Alpha, beta, positron and gamma-ray emissions are common, but only electromagnetic radiation, such as gamma-rays, has sufficient energy to allow external detection as required for imaging. Detection of this radiation as a function of time forms the fundamental basis of SPET and PET, providing data which allows extrapolation of the spatial and temporal distribution of the radionuclide. Construction of a 3D distribution of radiopharmaceuticals *in vivo* is effected from a set of two dimensional projectional images. The planar mode of SPET, widely available in clinical practice, provides only a 2D projection of a 3D source of activity.

SPET (Single Photon Emission Tomography)

The basis of SPET is the detection of γ-rays emitted (often mono-energetically) from radionuclides. If a nucleus remains in the excited state for a measurable time then it is *metastable* (denoted by 'm' after the mass number). Isomers are therefore possible due to two nuclides having the same number of protons and neutrons but different energies. The metastable nuclide decays by isomeric transition by emission of a gamma-ray or a 'conversion electron'. Metastable nuclides are particularly favourable as they often have a single gamma emission and may not be complicated by other accompanying emissions, for example, alpha or beta particles (see 1.5). These particles have a short range and deposit most of their radiation close to the source, which would increase the dose of radiation to the patient unnecessarily. Other decay processes affecting SPET radionuclides are *electron capture* and *internal conversion*. 'Capture' of an orbital electron by a proton of a neutron deficient nucleus results in the formation of a new neutron (and a neutrino), followed by the emission of an X-ray (equation 1.1). The neutrino does not affect the imaging process and will not be considered here.

$$p^+ + e^- \longrightarrow n + \nu \qquad \text{equation 1.1}$$

The atomic number therefore decreases by one unit:

$$^{A}_{Z}X + ^{0}_{-1}e \longrightarrow ^{A}_{Z-1}Y \qquad \text{equation 1.2}$$

The X-ray emitted is characteristic of the daughter radionuclide (Y, equation 1.2) as it is produced when the vacancy left in the particular electron shell is filled by another electron from a higher energy level (Figure 1.3). The radionuclide, thallium-201, for example, decays by electron capture and is used in diagnostic nuclear medicine.

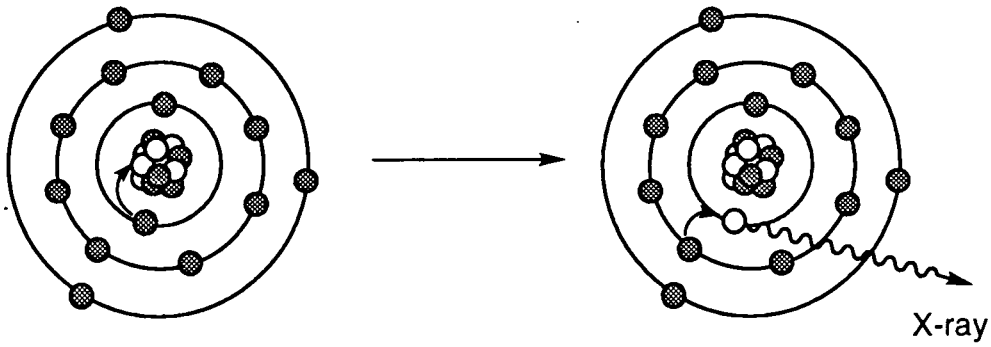

Figure 1.3 Electron capture followed by X-ray emission

Internal conversion is the result of excess energy from the nucleus being transferred to an orbital electron rather than emission of this energy as a gamma-ray. The orbital electron is then ejected, followed by the emission of characteristic X-rays or a second (Auger) electron (Figure 1.4). As short range ionising radiation, Auger emission is potentially useful for therapeutic applications.

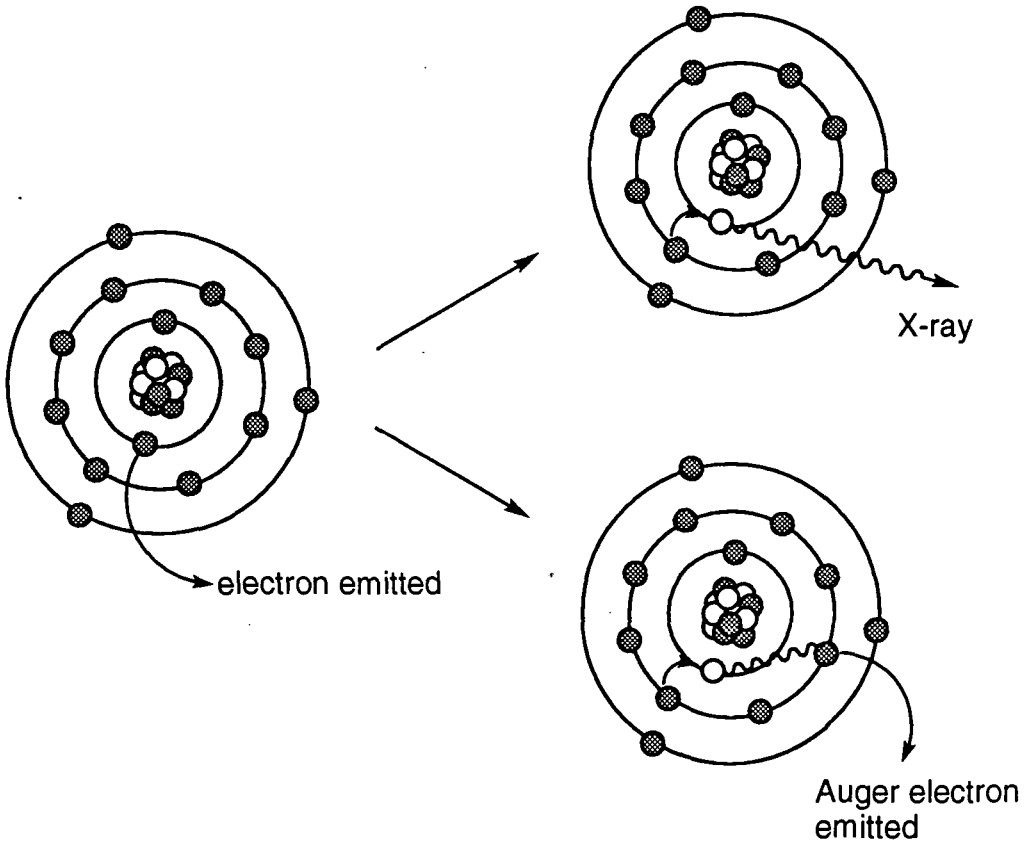

Figure 1.4 Internal conversion is followed by X-ray emission or Auger emission

Gamma-rays and X-rays are both forms of electromagnetic radiation, differing only in their origin. Gamma-rays are emitted from the nucleus: X-rays are emitted from electron orbitals.

Efficient detection of this radiation is then required for imaging the position of their source. The most important interactions of photons with matter (within the energy range applicable to nuclear medicine) are the photoelectric effect and Compton scattering. In a photoelectric interaction, the atom absorbs all of the energy of the gamma-ray and uses it to eject an inner-shell electron called a photoelectron (Figure 1.5a). This photoelectron has an energy equal to the γ-ray energy minus the binding energy of the electron shell. Since the detection of radiation is dependent on its interaction with matter, the absorbing material must possess a suitable atomic number (Z) since the number of photoelectrons produced is related to Z and the energy (E) of the incident γ-ray. Sodium iodide (Z=53) is commonly used in nuclear medicine as the

detector scintillate material for this reason and doping with thallium (Tl) improves the scintillation quality of the crystal. Another consequence of the photoelectric effect is that radionuclides emitting low energy γ-rays are unsuitable for imaging protocols, since the emitted γ-rays are absorbed by tissue and never reach an external detector - merely giving the radiation dose to the patient. Medium energy rather than high energy γ-rays are required as the photoelectric effect drops off with increased energy. Compton scattering dominates for high energies and is caused by the interaction of a photon with an outer-shell electron. The photon loses some of its energy which is transfered to the electron, resulting in the photon being scattered in a new direction (Figure 1.5b).

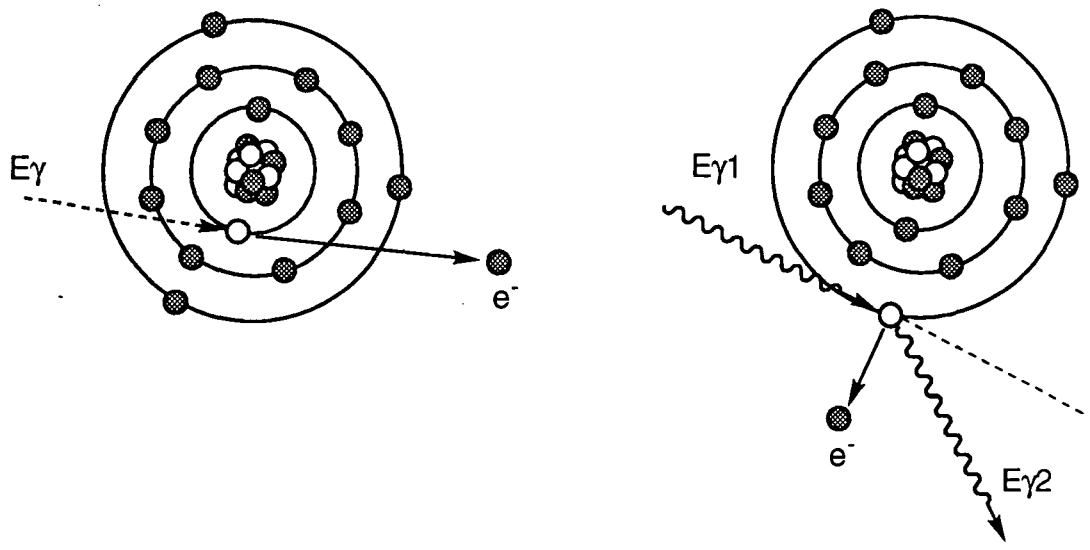

Figure 1.5 (a) Photoelectric effect (b) Compton scattering

A balance in the energy of the radionuclide is required as it has to be high enough to penetrate the tissue and be detected externally, but low enough to avoid Compton scattering becoming the predominant interaction. Radionuclides with energies in the range 100-200 keV are suitable for imaging protocols as this energy window provides the highest detection efficiency for NaI detectors. Therefore, the photoelectric effect governs the design of instrumentation for SPET and the choice of radionuclide emitting radiation in the correct energy range. A source of error in the absolute quantification of the technique can arise from Compton Scattering by causing loss of intensity or degrading the image if a detected photon has been scattered in tissue and its path altered prior to external detection.

Conventional SPET systems using gamma cameras can be used for both the planar and tomographic modes of imaging. Either the camera system rotates 360° around the patient or a 'dedicated' system (Figure 1.6) encompasses the patient completely with a ring of sodium iodide crystals. The latter system is more effective as information can be acquired more efficiently and cross-sectional pictures of the distribution of the radiation source within the body can be produced. The spatial resolution, field-of-view size and

and detection efficiency can be optimised by the use of collimators which act in a similar manner to optical lenses focusing light rays. Improvement of these characteristics leads to an improvement in the sensitivity and specificity of SPET imaging of radiopharmaceutical localisation and disease detection.

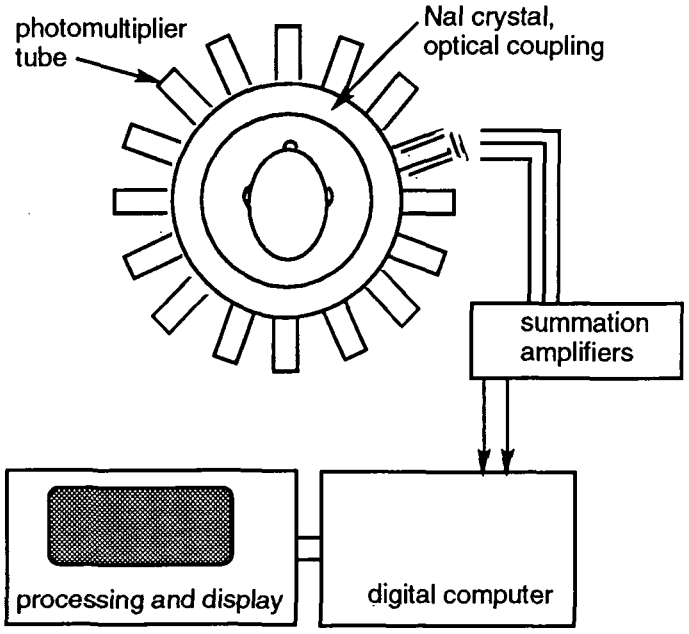

Figure 1.6 Representation of a dedicated SPET system reproduced from reference[3]

PET (Positron Emission Tomography)

A positron can be considered as an anti-electron, having the same mass as an electron but the opposite charge. Positron-emitting nuclides are unstable due to their excess of protons and neutron deficiency. Thus, a proton in the nucleus is transformed into a neutron, a positron and a neutrino (equation 1.3).

$$p \longrightarrow n + \beta^{+} + \nu \qquad \text{equation 1.3}$$

Thus, the nuclide, X, is transformed to its daughter nucleus, Y, with a decrease in the atomic number of one (equation 1.4).

$$^{A}_{Z}X \longrightarrow {}^{A}_{Z-1}Y + {}^{0}_{+1}e + n \qquad \text{equation 1.4}$$

The initial kinetic energy possessed by the positron is lost by collision deactivation after it has travelled a short distance (1-4 mm). The positron then combines with an electron to form the short-lived positronium species which annihilates to emit two γ-rays of 511 keV at 180° to each other (Figure 1.7). This self-destruction emitting

collinear photons is fundamental to the high spatial resolution in PET. Simultaneous detection of these two γ-rays by the use of coincidence circuitry allows a line to be constructed upon which the annihilation event took place.

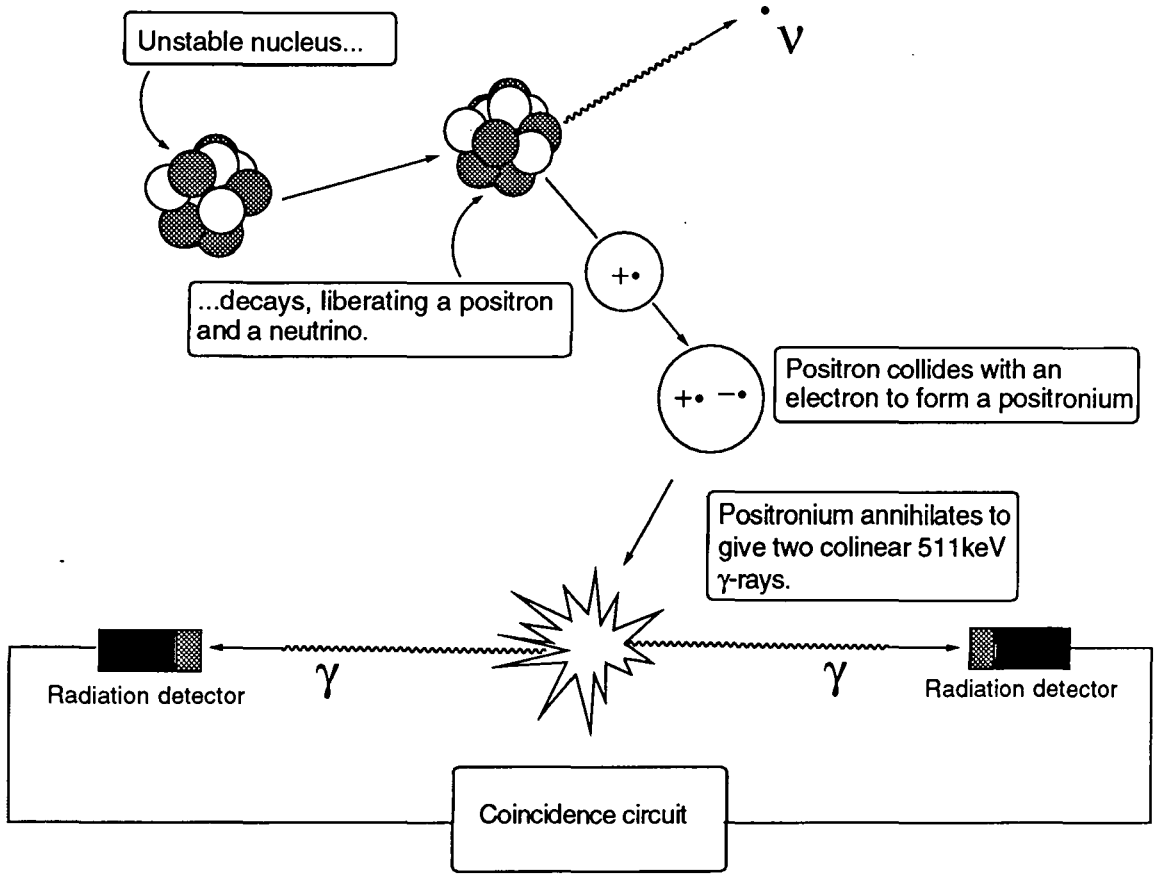

Figure 1.7 Positron annihilation and coincidence detection

The electronic circuit only registers the event if both the opposing detectors register radiation at the same time. Several million coincidences are recorded in a PET scan, forming a large number of intersecting coincidence lines. A circumferential array of opposing crystal detectors linked in pairs and complex circuitry make up a PET camera (Figure 1.8) and allow the determination of the intersection of many lines of annihilation which define the spatial location and quantity of positron emitters within the subject scanned. The spatial resolution of PET is limited by the size of each individual detector, non-collinearity of the two photons (arising from some net directional component, <0.5°) and the range of the positron as it travels between 1-4 mm before undergoing the annihilation event that is recorded.

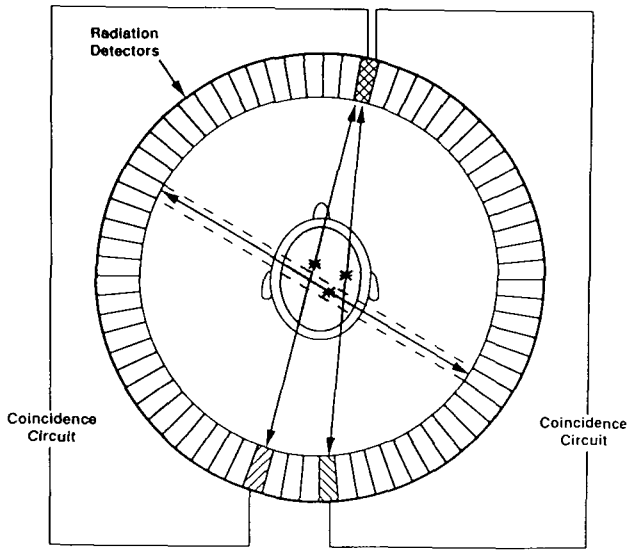

Figure 1.8 Schematic illustration of a PET camera
reproduced from reference[4]

Detection of different positron-emitting radionuclides does not require adaption of the equipment as annihilation of the particles always gives rise to photons of the same energy (511 keV). However, this energy is significantly higher than the energies of commonly detected photons in SPET imaging and therefore, requires a different scintillation material.[5,6] Bismuth germanate (BGO) is a suitable material exhibiting high absorbing power (high stopping power) for 511 keV radiation. The advent of new gamma-cameras for PET with 1000 times greater sensitivity than systems previously employed, has resulted from improvements in scintillation materials. Research is continuing to find materials which have the same high absorbing power as BGO currently employed, but emit more light per event and with faster rise and decay times. Bismuth germanate remains the chosen material for the scintillation detection of 511 keV photons although its light output and therefore energy resolution is lower than its NaI(Tl) counterpart.

In clinical practice

SPET is currently in widespread use for investigating regional cerebral blood flow and for bone and myocardial perfusion imaging. Although SPET does not offer as high resolution and sensitivity as PET, it is more widely available due to the supply and far lower cost of the appropriate radionuclides. ^{123}I, ^{201}Tl, ^{111}In and particularly ^{99m}Tc are extensively used in SPET scans. The preeminence of ^{99m}Tc in nuclear medicine is due to its favourable properties (see below), low cost and availability. PET facilities continue to expand despite the huge expense encountered. The cost-effectiveness of the

technique in terms of radiation dose versus information gained has been questioned. However, it remains the most specific and sensitive means for quantitative imaging of molecular interactions and pathways in human tissue and is consequently a valuable tool for the clinician. Quantitative changes can be assessed by the magnitude of the change in blood flow measured in ml min^{-1}. It has enormous potential considering its ability to study neurotransmitters, receptors and drug binding and gain vital information for neurology, cardiology and oncology in assessing disease staging. Psychiatric studies are also receiving increased interest and investigation.

Research in many disciplines associated with radionuclide imaging and equipment is continuing. These include the design of cameras, new scintillation materials, collimators and improvements in radionuclide availability and production to reduce the tiny amount of carrier molecules (stable isotopes) present. Indeed, the approach appears to be multidisciplinary.[7] A further area for continuing innovation and improvement is in the design and development of new radiopharmaceuticals, which provides, in part, the motivation for the following chapters of this work.

1.4 Choice of Radionuclide

There is an abundance of radionuclides suitable for imaging applications with a variety of physical and chemical properties. The mode of radioactive decay determines the radiation dose to the patient as well as the imaging properties required by the detection system. Production of the chosen radionuclide dominates the feasibility of the logistics of the study.

Availability

Many short-lived radionuclides are only available from very expensive cyclotrons, limiting their availability, although some cyclotron-produced nuclides with slightly longer half-lives are accessible by regional distribution. Half-lives of the order of minutes can only be considered if a cyclotron is available at the hospital where the study is to take place. By far the most convenient method for the production of radionuclides is the generator system which allows SPET and PET studies to be carried out at centres remote from a cyclotron. Generators rely upon a longer-lived nucleus - the parent nucleus - decaying to the more stable yet radioactive 'daughter' nucleus which can be eluted from the generator as it is required in the hospital. The parent isotope can be produced at a remote site and transported to the required site for its use in a generator. The half-life of the parent isotope is important as it dictates the 'shelf-life' of the generator between replenishments. More radionuclides are becoming accessible from generator systems: the most common example in clinical use is the $^{99}Mo/^{99m}Tc$ generator for the convienient production of ^{99m}Tc.[8] Molybdenum-99 is

bound to an alumina column and a supply of ^{99m}Tc daughter product is continually produced by decay of the parent.[9] The metastable product is extracted from the generator by repeated elution so that a fresh supply is available for numerous radiopharmaceutical applications.

$$^{99}MoO_4^{2-} \xrightarrow[66\ h]{\beta^-} {}^{99m}TcO_4^- \xrightarrow[6\ h]{\gamma} {}^{99}TcO_4^-$$

The increasing accessibility of many β^+-emitters from generators (Table 1.1) provides another driving force for further increase in the amount of PET radiotracers and facilities. Nuclear medicine requires radionuclides to be produced in high chemical and radiochemical purity in a no-carrier added form, that is, free from contamination by any stable isotopes.

Table 1.1 Generator produced β^+- emitting radionuclides

Parent	$t_{1/2}$ (d)	Daughter	$t_{1/2}$ (min)	Positron yield (%)
^{52}Fe	0.34	^{52m}Mn	21.1	97
^{62}Zn	0.39	^{62}Cu	9.74	97
^{68}Ge	288	^{68}Ga	68.1	89
^{72}Se	8.40	^{72}As	1560	88
^{82}Sr	25.6	^{82}Rb	1.27	95
^{110}Sn	4.11	^{110}In	69.0	62
^{118}Te	6.0	^{118}Sb	3.60	74
^{122}Xe	0.83	^{122}I	3.62	77
^{128}Ba	2.43	^{128}Cs	3.80	69
^{134}Ce	3.0	^{134}La	6.70	61
^{140}Nd	3.3	^{140}Pr	3.39	54

Radionuclear Properties

Accurate spatial and temporal detection of a radiopharmaceutical requires large numbers of emitted photons. Diagnostic imaging procedures require a radionuclide possessing a suitable emission (or a range of emissions) which penetrate the body to give a detectable signal externally. The energy of emitted photons should be greater than about 80 keV for practical use in obtaining high detection efficiency,[10] but not so great that the patient is exposed to unnecessary radiation. Current instrumentation in nuclear medicine requires the energy of γ-emitters to be in the range of 80-300 keV, while PET requires special instrumentation for the uniform 511 keV resulting from positron annihilation. The half-life of a suitable candidate nuclide is probably the most obvious criterion for its selection as it must possess a half-life appropriate to the time

frame of study. Sufficient time is required to synthesise and purify the radiotracer, inject the compound into the patient and image its distribution. The time required varies according to the nature of the study: a short time is required for perfusion (blood-flow) studies while a longer time is required for more prolonged studies such as the localisation of a radiopharmaceutical incorporating a targeting vehicle like a monoclonal antibody (MAb). The nuclide should possess the shortest practical half-life compatible with the particular physiological investigation.

γ-Emitters for SPET

The gamma-emitter ^{99m}Tc is the mainstay of nuclear medicine,[11] occuring in > 90% of all scans, for several reasons. It is readily available from a generator system at low cost and its 6 hour half-life and single gamma ray emission (accompanied only by low energy Auger electrons) offer ample time for imaging and deny any harmful effects of accompanying emissions. Radiopharmaceuticals containing ^{99m}Tc have been developed into 'cold' kit packages for convenience. Only rejuvenation of a single vial containing the other essential components with radiotechnetium eluant is required to form the radiopharmaceutical (see below). Formation of such tracers is rapid at room temperature and occurs in high yields (> 90%) of radiochemical purity. The challenge of technetium radiopharmaceuticals is in the development of complexes suitable for *in vivo* use as technetium, unlike copper, is not a natural physiological metal.

Table 1.2 γ-Emitting radionuclides for SPET

Radionuclide	$t_{1/2}$ (h)	Principle E_γ (keV)	Source
^{99m}Tc	6.02	141	Generator
^{111}In	68	171, 247	Cyclotron
^{67}Ga	78	93, 184	Cyclotron
^{131}I	193	364, 367	Reactor
^{123}I	13.2	159	cyclotron

Other useful nuclides for SPET are gallium-67 and indium-111. Their half-lives are somewhat longer than required, leading to excessive exposure of the patient to radiation. However, nuclides with longer half-lives are suitable for targeted applications (radioimmunoscintigraphy) where time for the localisation of the conjugate is required. Iodine-123 has a suitable half-life and energy (159 keV) for imaging, and indeed one of the common radiopharmaceuticals commmercially available as a blood-flow agent is [^{123}I]-iodoamphetamine (IMP). Although it is commonly and efficiently used in many applications, it may suffer from problems of deiodination and subsequent localisation of the iodine-123 in the thyroid.

β^+-emitters for PET

Much of the driving force for the evolution of PET was provided by the short-lived 'organic' nuclides, ^{11}C, ^{13}N, ^{15}O and ^{18}F (Table 1.3). These nuclides can be incorporated into natural metabolites such as amino-acids, sugars and steroids by replacement of their analogous stable atom without affecting the *in vivo* metabolism of the molecules. This provides a useful method of gaining information about the physiological fate of such naturally occuring compounds and can be similarly applied to therapeutic drugs to find out more about their modes of action. Studies with ^{11}C and ^{18}F are the most common although relatively simple molecules such as ammonia labelled with ^{13}N and water labelled with ^{15}O have found application in perfusion studies.[12] Myocardial uptake proportional to blood flow is exhibited by $^{13}NH_3$ and a high sensitivity and accuracy has been obtained in detecting coronary artery diseases (CADs). Radiolabelled water, $H_2{}^{15}O$, has been used to assess both cerebral and myocardial perfusion.

Table 1.3 Non-metallic positron-emitting radionuclides

Radionuclide	$t_{1/2}$ (min)	Positron yield (%)
^{11}C	20.4	> 99
^{13}N	9.96	> 99
^{15}O	2.04	> 99
^{18}F	110.0	96.9

Fluorine is useful for the radiolabelling of such molecules despite not being a natural constituent of bio-organic molecules. It is a good isostere for hydrogen and its inclusion offers a slightly longer time-frame (110 mins) than the other non-metallic nuclides for studies to take place. ^{18}F-Fluorodeoxyglucose (FDG) ((**1**), Figure 1.9) has been extensively used in metabolic studies of the heart and brain.[13] It is enzymatically phosphorylated after injection to FDG-6-phosphate which is not a substrate for the normal glycolysis pathway of glucose metabolism. As a result, it is trapped in the cell. Despite the usefulness of these radionuclides they are, however, limited to research applications as their production is too expensive and their distribution is unfeasible for routine use.

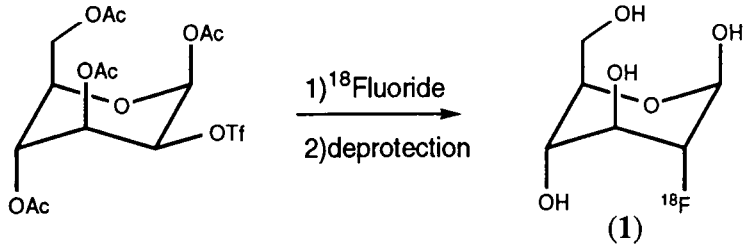

(1)

Figure 1.9

The exploitation of metallic positron-emitting radionuclides is becoming more widespread for PET studies. In particular, the use of medium half-life nuclides is receiving more attention as the sensitivity and quantitative accuracy of PET can potentially be combined with a large number of specific tracers such as those developed for SPET imaging.[14] An abundance of metallic β-emitting nuclides offer huge scope for the development of PET due to their vast range of half-lives (Table 1.4) and a variety of chemical properties. Ranging from transition metals to alkali metals and lanthanides, there is a diversity of chemistry available to be explored and developed. Bromine and iodine, although non-metallic, are recognised for their suitable nuclear and chemical properties for imaging applications.

Table 1.4 Examples of positron-emitting radionuclides

Radionuclide	$t_{1/2}$ (h or stated)	β^+ Yield (%)	Radionuclide	$t_{1/2}$ (h or stated)	β^+ Yield (%)
^{52}Fe	8.2	57	^{75}Br	1.6	76
^{55}Co	18	77	^{76}Br	16	57
^{57}Ni	36	40	^{83}Sr	33	24
^{61}Cu	3.4	62	^{89}Zr	78	22
^{62}Cu	9.8 mins	98	^{94g}Tc	4.9	11
^{64}Cu	12.7	19	^{94m}Tc	0.9	72
^{66}Ga	9.5	57	^{134}La	6.7	62
^{68}Ga	68 mins	89	^{124}I	100	22

$^{82}Rb^+$ was the first FDA (Food and Drug Administration)-approved radiopharmaceutical for PET imaging and is widely used in clinical practice for the imaging of myocardial blood flow in the detection of CADs, by administration simply as a chloride salt ($^{82}RbCl$). It can be considered as an analogue of K^+ and is taken up by mycocytes using the Na^+-K^+ ATP pump mechanism.[15] Although it is conveniently available from the $^{82}Sr/^{82}Rb$ generator, the scope of Rb^+ for PET imaging is somewhat restricted by its short half-life (1.27 min) and limited coordination chemistry. ^{68}Ga, produced by the $^{68}Ge/^{68}Ga$ generator has a more suitable half-life (68 mins) and useful coordination chemistry for complexation with some multidentate ligands. Another generator produced positron-emiiter is ^{110}In from the $^{110}Sn/^{110}In$ system. Despite the half-life of the parent isotope being a mere 4.15 h, the use of ^{110}In has been suggested for the labelling of white blood cells with regard to organ transplant rejection.[16]

Copper-62 has received more attention than most generator-produced positron emitters, due to its favourable chemistry, potential applications and the existence of several other useful copper radioncuclides of different emissions and half-lives. Whilst there are only two stable isotopes of copper (with slight variation of abundances), there are a range of

copper radioisotopes possessing various emissions and various half-lives (Table 1.5).[17] This itself is advantageous, as a new copper radiotracer in the early stages of development can be studied using a longer-lived copper radioisotope before employment of the relatively short-lived ^{62}Cu species which allows less handling time. However, practical application of the generator system may be limited due to short half-life of the parent isotope ^{62}Zn ($t_{1/2}$ 9.36 h). Replenishment is often required and this particular isotope can be available from many medium-energy cyclotrons.[18] Copper-64 and copper-67 also offer scope for therapy because of their beta-emission and suitable half-lives (see section **1.5**).

Another opportunity which may soon be exploited is ^{94m}Tc. As a positron-emitter with a suitable half-life for imaging, ^{94m}Tc could access all the radiopharmaceuticals used in the clinic for SPET by swapping technetium nuclides.

Table 1.5 Physical properties of Cu radionuclides for imaging and therapy

Radionuclide	t1/2 (h)	Emission (%)	E_p (keV)	E_{np} (keV)	R_{np} (mm)	Source
^{60}Cu	0.38	β^+ (93)	511	873	4.4	cyclotron
		EC (7)	1332			
^{61}Cu	3.3	β^+ (62)	511	527	2.6	cyclotron
		EC (38)	283			
^{62}Cu	0.16	β^+(98)	511	1315	6.6	generator/
		EC (2)				cyclotron
^{64}Cu	13	β^+ (19)	511	278	1.4	reactor/
		EC (41)	1346			cyclotron
		β^- (40)		190	0.95	
^{66}Cu	0.09	β^- (100)		1109	5.6	reactor/
						cyclotron
^{67}Cu	62	β^- (100)	93	121	0.61	reactor/
						cyclotron

E_p=energy of the most abundant penetrating (γ) radiation following the coresponding decay

E_{np}=average energy of the most abundant nonpenetrating (β^-/(β^+) radiation

R_{np}=average range of nonpenetrating radiation in tissue

1.5 Complementary radiopharmaceuticals for therapy

As radiopharmaceuticals depend upon both their biological behaviour and physical decay, maintaining effectively the same chemical properties but altering the mode of decay (by substitution of a different isotope) allows potential for therapy. The replacement of different metal nuclides in the same radiopharmaceutical is not limited

to isotopes of the same element (e.g. technetium-99m or 94m) nor to imaging applications. Some radionuclides, such as ^{188}Re and ^{186}Re, have suitable emissions for therapeutic and simultaneous imaging applications. There is interest in developing radiopharmaceuticals for therapy based on rhenium for two main reasons: rhenium complexes are very closely related structurally to their analogous technetium-containing compounds and ^{188}Re is available from the $^{188}W/^{188}Re$ generator. It is their analagous chemical behaviour and potential for complementary imaging and therapy which merits the discussion of rhenium radionuclides here as there are many other nuclides with suitable properties for therapeutic applications.[19] Sufficient radioactivity must be transported to the tissue being targeted to kill the diseased cells whilst keeping the uptake in non-target tissue to a minimum. The ionising emission processes with potential suitability for therapeutic use decay by alpha, beta and Auger emission.

Very heavy elements (Z>83) emit alpha particles which consist of two protons and two neutrons (helium nuclei) (equation 1.5). Despite their relatively large size and consequently short range (40-90 μm or several cell diameters), alpha particles are suitable for therapy due to their strong ionising ability.

$$^{A}_{Z}X \longrightarrow {}^{A-4}_{Z-2}Y + {}^{4}_{2}\alpha \qquad \text{equation 1.5}$$

Beta emission results from an excess of neutrons (and proton deficiency) and is the transformation of a neutron to a proton, an electron (β^-) and a neutrino (equation 1.6).

$$n \longrightarrow p + \beta^- + \nu \qquad \text{equation 1.6}$$

Therefore, the daughter nuclide is a different element, with an atomic number increased by one (equation 1.7).

$$^{A}_{Z}X \longrightarrow {}^{A}_{Z+1}Y + {}^{0}_{-1}e + \nu \qquad \text{equation 1.7}$$

Although beta particles are lighter than alpha particles with a single charge enabling them to penetrate further, they still have a short range in tissue (in the order of several mm), giving most of their energy to matter close to the parent atom.

Auger electrons (see section **1.3**) may also prove useful in this context, although their range is extremely short - about one cell nucleus in diameter.

Copper-64 uniquely combines positron, beta, and Auger emission, giving it the ability to be used in therapy and imaging simultaneously (Table 1.5, section **1.4**). Both

radioisotopes of rhenium emit energetic beta particles possessing a strong ability to penetrate tissue (90% of the radiation is deposited within 5.5 mm). ^{188}Re emits a high energy beta-particle (E_{max}=2.1 MeV) suitable for the treatment of diseases requiring longer ranges. ^{186}Re has a longer half-life (3.78 days) but less energetic emission (E_{max}=1.08 MeV) which gives it a slightly shorter range (around 2 mm) compared with the range of ^{188}Re (around 5.5 mm). Both rhenium radionuclides are suitable for therapy, providing variability in the half-life and positron energy, depending upon the target size and volume.

These particle emissions are sometimes accompanied by emission of gamma rays. If these photons are of a suitable energy then they can be used for simultaneous imaging to monitor the localisation properties, pharmacokinetics and dosimentry in patients. The gamma-ray abundance should be low to minimise the adverse radiation dose, yet produce enough photons for imaging. Pure gamma-emitters like ^{99m}Tc can be used for imaging to establish the targeting suitability and a therapeutic analogue then prepared. For example, ^{99m}Tc diphosphonates are used for skeletal-metastases imaging. The therapeutic congener of technetium, ^{186}Re, was subsequently prepared in the form of a diphosphonate - ^{186}Re-HEDP (hydroxyethyldiaminetetramethylene-phosphonate) (**2**) - to act as an agent for the pain relief of patients suffering from bone-cancer.

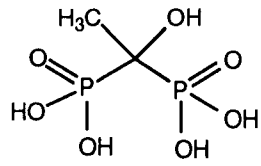

(2) HEDP

1.6 Administration of Metal Radionuclides

The term 'pharmaceutical' may evoke images of natural products and organic molecules as therapeutic drugs. This is quite natural, considering the composition of biological matter. But metals have been used in medicine since antiquity and examples of these range from bismuth anti-ulcer treatments to platinum anti-cancer compounds.[20] Metal radionuclides offer significantly more appropriate nuclear properties for imaging and therapy in many cases. They may appear more challenging to administer than their 'organic' counterparts but this challenge highlights the value of coordination chemistry in medicine and offers scope to exploit the properties of the complexes and use them to best advantage. Increasing numbers of radiopharmaceuticals are based on well-defined coordination complexes.

Metals must be administered to the patient in the form of coordination complexes and desirable metals must form stable complexes with good kinetics of complexation.

Thermodynamic stability is not the real issue: *in vivo* stability is important in this biological context. Although physiological conditions are pH7.4 and 37°C, there are various enzymes, proteins and cells as well as local variations in pH which may challenge the integrity of the coordination complex. Thus, it is the kinetic stability which determines the fate of the complex. Kinetic stability is favoured when the coordination sphere of the metal is saturated and the metal is in an oxidation state which is stable *in vivo*. The complex should be charge neutral or cationic to disfavour protonation and acid-catalysed dissociation pathways on electrostatic grounds. Charge neutrality is also necessary for passive diffusion through cell membranes and penetration of the blood-brain barrier (BBB) in humans. The BBB is a special membrane which protects the brain from fluctuations in the composition of the blood and from circulatory neurotransmitters and neuroactive agents.[21] It is selective in the choice of molecules allowed through and acts to restrain ions and peptides. Crossing the BBB also requires complexes to be lipophilic and of relatively low molecular weight[22] in order to become useful agents for imaging brain and heart. Additional functionalities present as part of a neutral complex - such as amide, alcohol or carbonyl groups - may exhibit some hydrogen-bonding and thus lower the overall lipophilicity of the complex. This would reduce the ability of the complex to cross the blood-brain barrier. Many radiopharmaceuticals are excluded from the BBB in a normal brain and can consequently diagnose brain abnormalities. For example, in brain tumours, the BBB breaks down (post radiotherapy or chemotherapy) and many non-diffusable compounds enter. A positive scan provides information about these abnormalities.[23]

Another practical consideration is that the radionuclide must be added in a synthetically easy step which occurs rapidly in order that the time available from the decay is usefully employed for imaging.

Design of Radiopharmaceuticals

Radiopharmaceuticals can be classed as 'metal-esssential' and 'metal tagged'. Metal-essential radiotracers rely on their own intrinsic properties such as charge, shape, lipophilicity and redox properties to determine their biological distribution. Metal-tagged radiopharmaceuticals are regarded as bifunctional chelators where the ligand that binds the radionuclide is attached to a targeting vector or carrier molecule such as a monoclonal antibody or small peptide which determines its biodistribution. The metal is simply transported by this vehicle to act as a marker. In both cases, the metal coordination chemistry determines the ultimate geometry and stability of the radiopharmaceutical. A high kinetic stability is sought in order that the radiopharmaceutical localises in the target organ, or is excreted intact.

Features of Ligand Design

Observations of a great many coordination compounds have led to the definition of certain general trends which can form the foundations for the design of new ligand architecture. Selection of donor atoms within a ligand can provide a means of increasing or decreasing the binding interactions with certain cations and affects the rate of formation of the complex. Pearson's classification of hard/soft acids and bases[24] provides a useful preliminary guide for the selection of a particular donor atom to favour binding for a specific metal cation. Metals are classified as 'hard' (class a), 'soft' (class b) or 'borderline' (Figure 1.10).

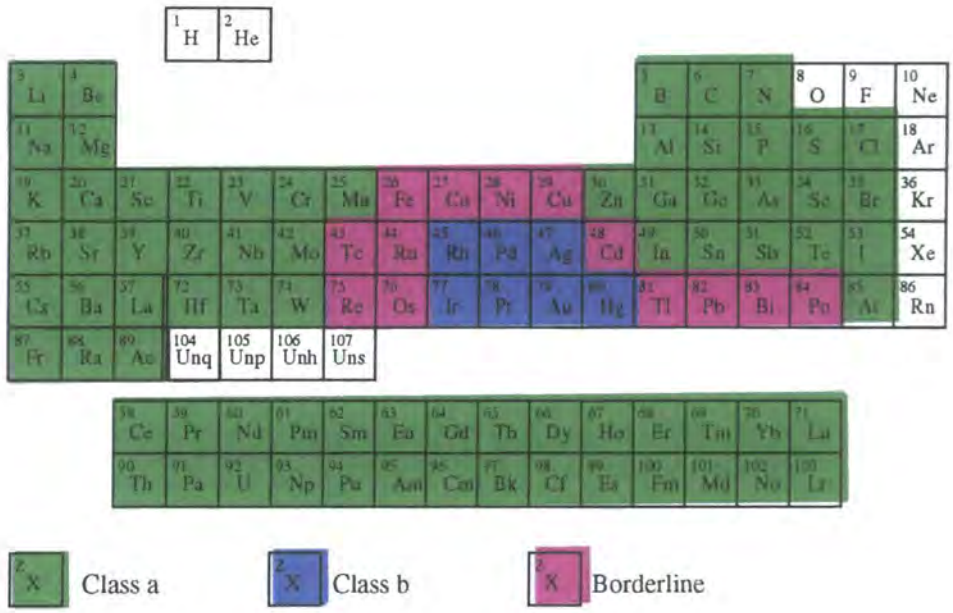

Figure 1.10 Classification of acceptor atoms in their common oxidation states[25]

By selecting suitable complementary donors (Lewis bases) for a particular metal, the complex stability and ligand selectivity can be maximised. For example, a hard cation like Li^+ could be matched with oxygen donors but a soft more polarisable cation like Au^+ would be better matched with sulfur, while borderline cations may tolerate both.

The common donors are:

hard	nitrogen	as amines, imines, amides
	oxygen	as ethers, carbonyls, carboxylates, alcohols
soft	phosphorus	as phosphines
	sulfur	as thiols, thiolates, thioethers

The influence of donor atoms is manifest in the coordination number as their charge can satisfy the charge demands of the metal and consequently affects the number of them which can be present. Metal-ligand attractions must exceed destabilising repulsions. Coordination number generally increases with the size of the metal ion to increase the complex stability; for example, first transition row elements favour 4, 5, or 6-coordinate complexes while larger cations such as lanthanides prefer an 8 or higher coordinate environment. The complex geometry is associated with the coordination number as 4-coordinate complexes tend to adopt tetrahedral or square planar geometry while 6-coordinate complexes of the same metal are octahedral in order to minimise charge and steric repulsions.

The chelate effect is another important consideration. Generally, a complex containing one or more 5- or 6-membered chelate rings is thermodynamically more stable than a complex with the same donors as monodentate ligands. The chelate ring size favoured for controlling metal ion selectivity and complex stability is dependent on the size of the metal cation. 5-Membered chelate rings are favoured by larger metal ions while 6-membered chelate rings are favoured by smaller ions by virtue of the relative bite angles, metal-ligand bond length and the ring-strain which results (Figure 1.11).[26]

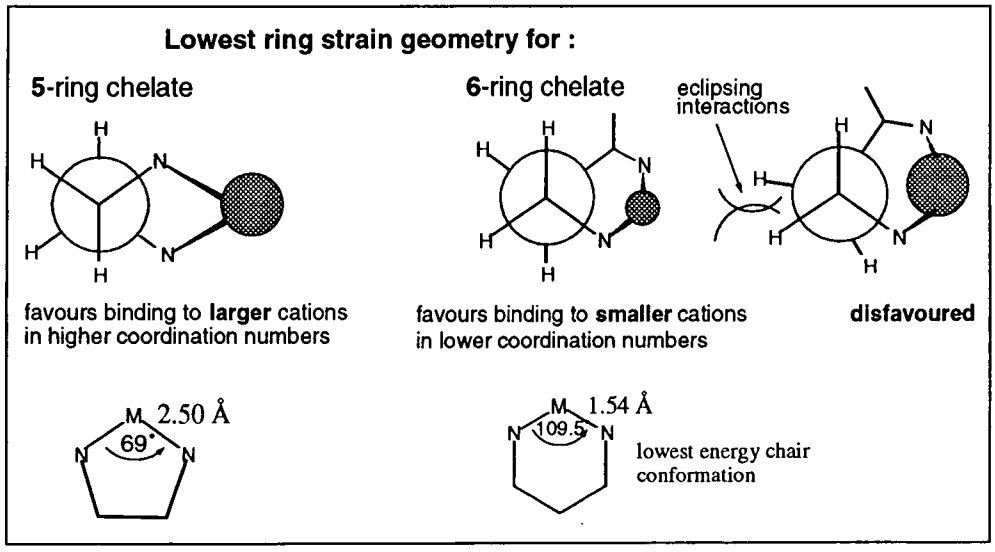

Figure 1.11 Favoured geometries for 5- and 6-ring chelates

Although much of the complexation criteria outlined have a profound affect on the thermodynamic stability, it should be remembered that it is kinetic stability and a rapid rate of formation of a complex which are the factors most relevant to radiopharmaceuticals (see above). Acid stability is especially important when considering local areas of low pH which may be encountered *in vivo* such as the stomach and bile.

Complementary ligands for technetium, rhenium and copper

Technetium and copper offer joint opportunities for the design and development of various radioparmaceuticals (with a choice of nuclear properties - see above) for SPET and PET imaging using a single class of ligand. This is due to some similarities in the coordination preferences of these metals, for example, borderline donor atom preferences and complex geometry (see below). Versatility of component parts would allow tailoring of characteristics, such as lipophilicity, required for specific applications. Complexation of the same system with rhenium also offers the potential for therapeutic radiopharmaceuticals. Therefore, these metals in particular provide the focus for the material presented in subsequent chapters.

Coordination chemistry

Copper has found useful applications for an estimated 7000 years. It is no stranger to biology as it is the third most abundant trace metal in the human body and is found in protein-bound forms. Its chemistry is dominated by two major oxidation states, Cu(I) and Cu(II), allowing a colourful range of coordination chemistry, characteristic of the transition metals, whilst uncomplicated by several oxidation states. Cu(III) is far less common, being easily reduced, although it is present transiently in the redox chemistry of the element.

Cu(II) has an electronic configuration of $[Ar]3d^9$ imparting paramagnetism and making regular complex geometries a rarity. Common coordination numbers are four, five and six arranged in square planar, tetragonally distorted octahedral or intermediate geometries as a result of Jahn-Teller distortion.[27] The unequal electron occupancy of the e_g set of the d^9 configuration leads to an elongation of the axial bonds in octahedral geometry, and in the extreme situation, complete loss of these two ligands to effectively produce square planar geometry. In practice, distorted octahedral, square planar or distorted tetrahedral geometries (Figure 1.12) are not sharply differentiated and many intermediate distorted geometries prevail.

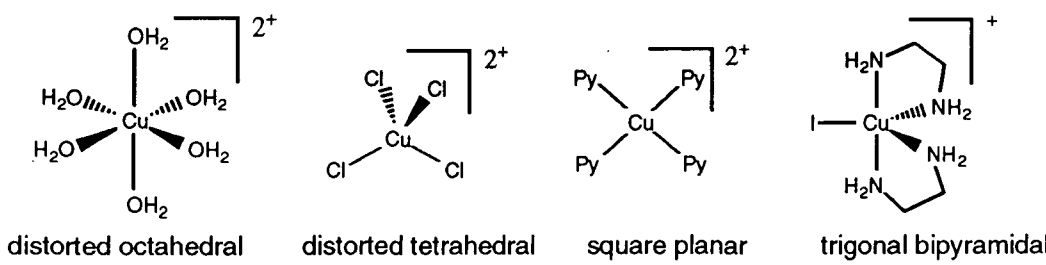

Figure 1.12 Examples of Cu(II) geometries

By contrast, Cu(I) is predominantly colourless or yellow in solution owing to its d^{10} configuration. Although commonly 4-coordinate and tetrahedral in geometry, coordination numbers of 2 and 3 are also known, giving linear and pyramidal

geometries respectively (Figure 1.13), in addition to binuclear bridged, polynuclear or chained structures.

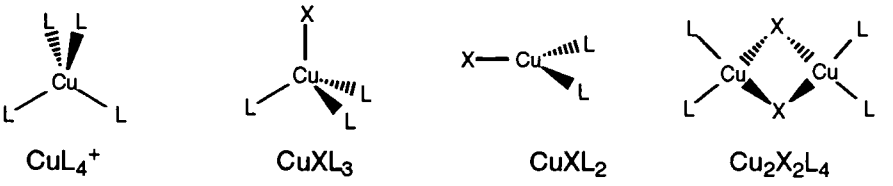

Figure 1.13 Examples of Cu(I) structures

In solution, Cu(I) is unstable with respect to disproportionation:

$$2Cu(I) \longrightarrow Cu(II) + Cu(s)$$

The redox couple, Cu(II) to Cu(I) (E° 0.153 V [H_2O, I=0.1, 298K]), also provides a useful means of initiating complex dissociation: a substitutionally inert Cu(II) complex may be readily reduced to a Cu(I) intermdiate and then undergo ligand exchange or dissociation. Such redox-catalysed ligand exchange can provide a useful biological trapping mechanism and a means of selective tissue targeting if the complex is tailored for this purpose.

As discussed above the choice of donor atom is critical to ligand design. Copper(II) is regarded as a 'borderline' cation according to the Pearson classification: a fact also evident from the natural occurrence of its major ores in the form of sulfides, oxides and carbonates. Fifty percent of all copper deposits are copper pyrite ($CuFeS_2$). Nitrogen and sulfur are well established in complexation of copper and there is a wealth of examples of complexes possessing these donor atoms. Copper(I), in particular, exhibits strong binding interactions with 'soft' polarisable ligands such as thioethers, nitriles, isonitriles, phosphines and thiolates. Hence the use of a 'softer' donor set should favour the reduction of a copper(II) complex to Cu(I). Conversely, reduction of Cu(II) could be blocked by using hard ligands, for example, in a targeted conjugate where complex stability is of greater importance.

As expected, the second and third row transition elements, technetium and rhenium, exhibit substantially similar coordination chemistry to each other. Their chemistry bears little resemblance to their first row counterpart, manganese, which is dominated by the oxidation state II. However, they have considerable chemistry in the IV and particularly, V oxidation states.[28,29] Oxo-compounds predominate and pertechnetate (TcO_4^-) and perrhenate (ReO_4^-) are especially useful. These ions are tetrahedral in geometry and stable in alkaline solution in contrast to their permanganate relation. Oxo

compounds are prevelant for the higher oxidation states of rhenium, in particular, V and VII. An important class of such complexes contain oxorhenium(V) centres with phosphine ligands. For example, $ReOX_3(PPh_3)_2$ is readily obtained[30] and the halide or ligand *trans* to the Re=O bond is labilised due to the *trans* effect (Scheme 1.1 and section 6.2).

$$ReOX_3(PPh_3)_2 \xrightarrow{EtOH} ReOX_2(OEt)(PPh_3)_2$$ **Scheme 1.1**

Three isomers of $ReOX_3(PPh_3)_2$ are possible although only two are observed (Figure 1.14).

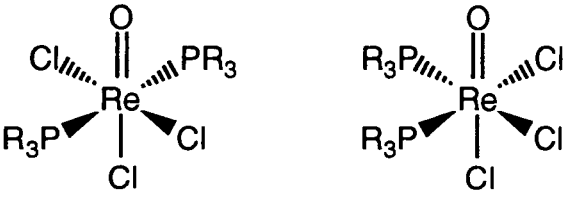

trans-isomer green — *fac*-isomer blue

Figure 1.14 Isomers of $ReOX_3(PPh_3)_2$

Complexes of rhenium(V) can also have a trans-dioxo core like technetium, for example, with pyridine as $[ReO_2py_4]$ (**3**) (see later Figure 1.16) and ethylenediamine $[ReO_2en_2]$. Nitrido complexes of rhenium(V) provide another series of stable complexes important to the metal in this oxidation state, such as $[Re(N)X_2(PR_3)_3]$.

The study of technetium coordination chemistry has taken place over the last fifty years since the discovery of the element.[31] There are no stable isotopes of technetium but full characterisation including X-ray structural analysis of technetium complexes has been achieved with the isotope ^{99}Tc ($t_{1/2}$=2.1 x 10^5 years) giving access to a useful array of structural information.[32,33] Coordination numbers vary from four to eight with six appearing the most regularly. In nuclear medicine, Tc(V) with an oxotechnetium (TcO^{3+}) core has proved the most amenable to the synthesis of well-defined small molecules that have sufficient stability in aqueous solution. Flexibility in their chemical make-up and properties is allowed by virtue of the choice of ligands. Five-coordinate complexes with an oxo-technetium core are typical, like rhenium, and attributed to the ability of the oxo species to quench the high formal charge of the metal in the +V oxidation state and labilise the *trans*-position of the complex to give an overall distorted square pyramidal geometry. Many Re(V) and Tc(V) complexes which contain an oxo-metal core are square-based pyramidal. The oxygen is at the apex and bidentate or tetradentate ligands occupy the basal positions, while the sterically demanding metal sits slightly above the basal plane (Figure 1.15).

Figure 1.15 Typical geometry for complexes with a TcO^{3+} core

The size of the chelate rings typically found in this class of complex are five-membered although some six-membered chelate rings are also successful. Other types of oxo core are also common such as $[O=Tc=O]^{+}$ and $[O=Tc\text{-}O\text{-}Tc=O]^{4+}$. The bisoxotechnetium core is important in the coordination chemistry of technetium(V), e.g. $[MO_2L_4]^{+}$, with its formation dependent upon the ability of the other coordinating ligands to donate negative charge to the metal. Such complexes bear strong relation to the oxo-rhenium complexes.

Neutral nitrogen donors tend to result in the formation of a bisdioxo (MO_2^{+}) core, like rhenium, as they are unable to deprotonate due to their relatively high protonation constants. As such, they are unable to offer any neutralisation of the high positive charge as demanded by the mono-oxo (MO^{3+}) core, and the bis-oxo complex predominates to aid the charge deficit and effect a mono-cationic complex. This similarity with rhenium is exemplified by characterisation of the analogous technetium complex with ethylenediamine[34] (**4**) and complexes with the macrocycle, 1,4,8,11-tetraazacyclotetradecane (cyclam)[35,36] (**5**) (Figure 1.16).

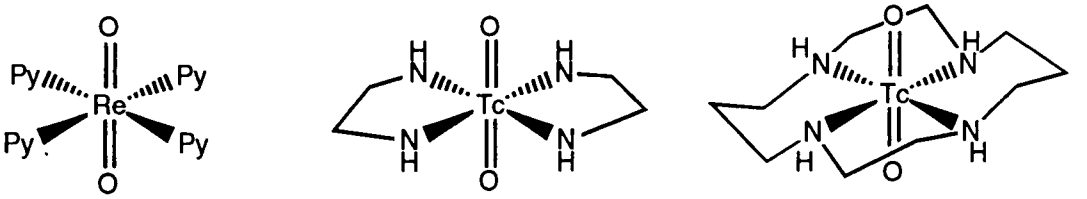

(**3**) $[TcO_2(Py)_4]^{+}$ (**4**) $[TcO_2(en)_2]^{+}$ (**5**) $[TcO_2(cyclam)]^{+}$

Figure 1.16 Examples of complexes with rhenium or technetium trans-dioxo cores

A range of donor atoms besides nitrogen are tolerated by technetium and rhenium, including oxygen, nitrogen and sulfur donors as well as phosphines and halides. Carbon donor ligands such as isonitriles form complexes with low oxidation state technetium. Athough rhenium and technetium in oxidation state (V) are regarded as 'soft' rather than 'hard',[37] they are known to bind 'hard' oxygen donors. Alcoholic or carboxylate forms of oxygen provide metal complexes which are amenable to ligand exchange, such as catechol[38] and tetrachlorocatechol (**6**),[39] and consequently provide good starting materials for nuclear medicine where relatively mild complexation conditions are

sought. Glycol, tartrate, citrate and glucoheptonate are similarly involved in the preparation of radiopharmaceuticals.[40]

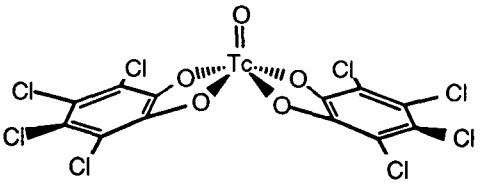

(6)

Sulfur donors are now extremely common in technetium and rhenium chemistry, having a high affinity for both metals, and forming well-defined mono-oxo species by satisfying the metal's positive charge. Although the metals can exhibit oxidation states from +I to VI, 'soft' sulfur donors promote Tc(V) and Re(V). This is especially true of negatively charged dithiolate ligand complexes, $[TcO(S_2)_2]^-$. Neutral S-donors such as thioethers and thiocarbonyls complex effectively with the metals and show a preference for oxidation states of less than five presumably due to their inability to satisfy the Tc(V) positive charge.[41]

The use of mixed donor groups in Tc and Re chemistry is widespread, with thio-amine systems proving particularly advantageous. Ligands possessing the N_2S_2 donor set were shown to form neutral lipophilic complexes of ^{99m}Tc as early as 1979.[42] For example, diamino-dithiols (DADT) ligands, [also known as bis(aminoethanethiol) (BAT)] (**7**) (Figure 1.17), form neutral complexes of $Tc(V)O^{3+}$ owing to the deprotonation of both thiols and one of the amines to neutralise the positive charge. The penicillamine complex of technetium (**8**) is an example of an N_2S_2 system prepared in strong acid solution to favour the amines remaining in their protonated form. One of the pendent carboxylate groups coordinates to fill the trans position, compensating for the charge of the core and rendering the complex 6-coordinate. The amine protons of DADT systems (**7**), are sufficiently basic for one of them to remain protonated upon complexation to give a charge neutral complex. In contrast, systems based upon ligands with a diamidedithiol (DADS) (**9**) backbone lose both amide-nitrogen protons in addition to the two thiols rendering the complex negatively charged as a result.[43,44,45,46] Neutral complexes of TcO^{3+} are formed by diamide-thiol-thioether ligands (**10**). The alkyl group forming the thioether side chain may be varied to allow the preparation of a versatile series of analogues or to tolerate conjugation to a targeting vector.[47]

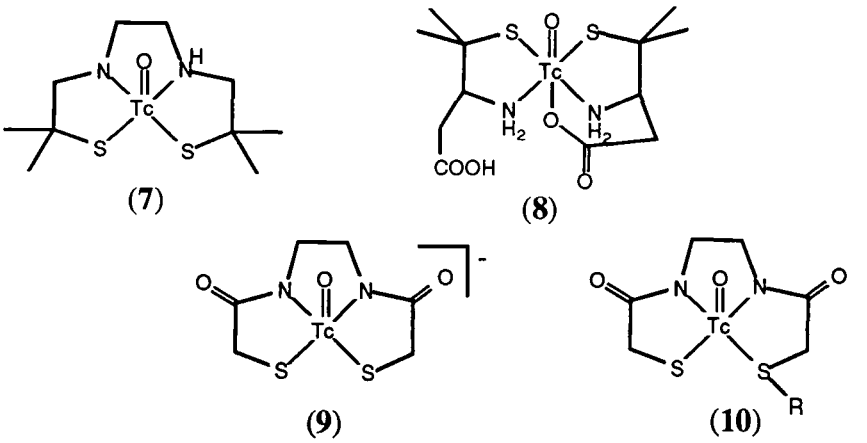

Figure 1.17 Oxo-technetium complexes with N_2S_2 donor systems

Mixed ligand sytems have recently increased in prominence because of the potential for easy modification of complex properties. Several possibilities are apparent in denticity and arrangement of ligands as illustrated (Figure 1.18). A tridentate amine ligand could form such a complex with, say, a thiol ligand filling the last coordination site and allowing further elaboration of the rest of the thiol moiety.

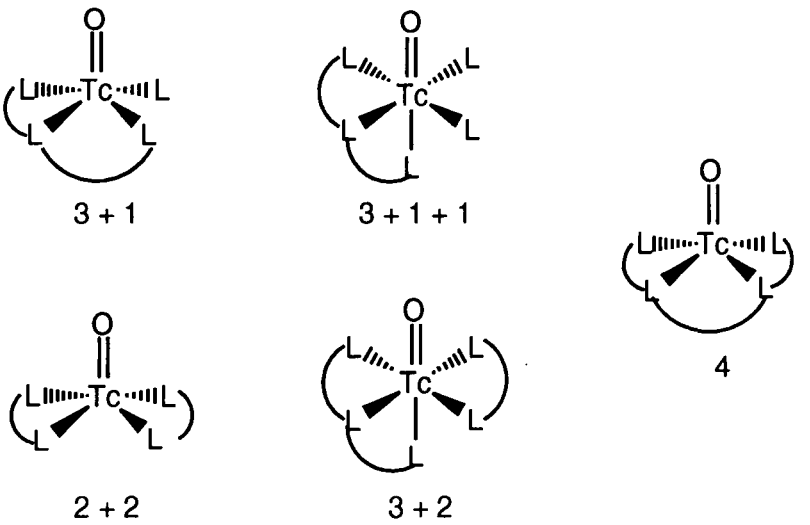

Figure 1.18 Possible arrangements of ligands around oxotechnetium

Tetradentate ligands offer the possibility of a mixed set of donor atoms with functional groups predisposed to binding and increased stability owing to an increase in the chelate effect.

1.6 Technetium, rhenium and copper complexes in nuclear medicine

There is a wide variety of technetium complexes in clinical use or undergoing pre-clinical and clinical research in nuclear medicine. Complexes which show promise for *in vivo* applications, but which are lacking in some quality necessary for imaging applications, can be derivatised and a series of analogues studied to find a more suitable

candidate. For example, more recent derivatives of DADT ligands (see above) were more lipophilic and the technetium complexes were able to penetrate the BBB as a result.[48] Successful research efforts have produced many well-defined Tc complexes for particular target organs, in particular, the brain and heart.[49,50,51,52]

This type of derivatisation was also employed to find a successful phosphine ligand. The ability of tertiary phosphine ligands to participate in synergic bonding enables them to form stable complexes with transition metals in a variety of oxidation states and geometries, for example, Tc (V), (III) and (I) form cationic complexes with 1,2-bis(dimethylphosphino)ethane (dmpe) (Figure 1.19). Subsequent studies and derivatisation of diphosphine ligands led to the synthesis of a promising myocardial imaging agent in the form of the *trans*-dioxotechnetium(V) complex of 1,2-bis(bis-ethoxyethyl)phosphino)ethane (**11**). The ether functionalities improve the clearance of the lipophilic tracer from non-target tissue.

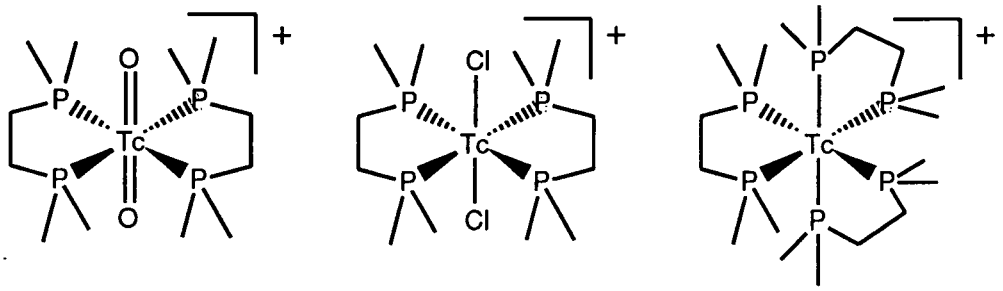

Figure 1.19 Technetium complexes with dmpe

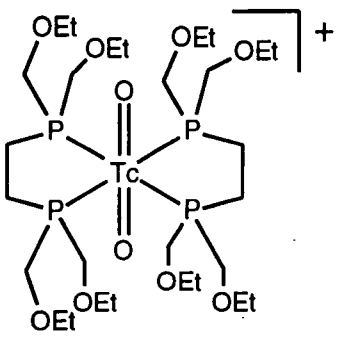

(**11**)

Ether functionalities are similarly exploited to increase hydrophilicity and reduce the protein binding *in vivo* in the ^{99m}Tc-furifosmin complex, (**12**). It is a technetium(III) complex with a mixed ligand system in which a tetradentate Schiff-base ligand, trans(1,2-bis[dehydro-2,2,5,5-tetramethyl-3-furanone-4-methylene-amino]ethane) occupies the equatorial sites, and the phosphine ligands occupy the two axial positions. Available as a heart imaging agent, ^{99m}Tc-furifosmin is formed in high radiochemical purity from a 'cold' kit containing the lyophilised ligand and accompanying components.

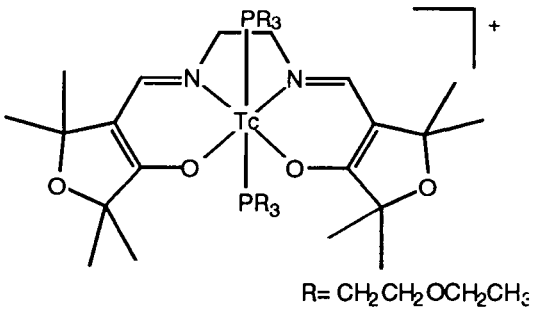

(12)

There are a number of commercially available radiotracers for brain imaging. Du Pont's Neurolite® utilises L,L-ethyl cysteinate dimer (L,L-ECD) (**13**) - a diamine-dithiol system with two ester functionalities on the carbon skeleton.[53] The esters have little hydrogen-bonding properties enabling radionuclide complexes of the ligand to penetrate the BBB. Many neutral complexes are able to penetrate the brain but are simply washed out. L,L-ECD is washed out of several species including mice, cats, dogs and monkeys but shows uptake in humans. The mechanism for retention is extremely elegant as only one ester is hydrolysed by endogenous esterase enzymes. The singly charged complex is then retained in the brain. Retention is also enantioselective as D,D-ECD diffuses back across the BBB and is obviously not a substrate for the esterase enzyme.[54]

Propyleneoxime (PnAO) derivatives[55] also form neutral complexes which show good cerebral extraction. Racemic hexamethyl propyleneoxime (d,l,-HMPAO) (**14**), available from Amersham International as Ceretec®, was the first approved ^{99m}Tc cerebral perfusion imaging agent for human applications.[56] The loss of two protons from two amines and one oxime renders the complex neutral. Once taken up into the brain, the racemic complex is retained and transformed (far more rapidly than the *meso* isomer) into a more hydrophilic species which is unable to diffuse back across the BBB. The selective retention mechanism is thought to involve intracellular glutathione, although the exact nature of the product species is not yet known. The conversion to the more hydrophilic species occurs within 30 minutes, hence imaging with d,l-HMPAO should be conducted as soon as the initial complex is formed.

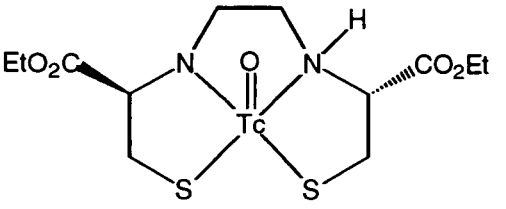

(**13**)Tc-ECD

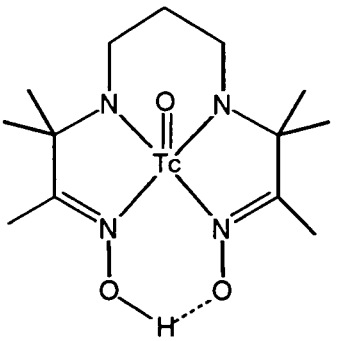

(**14**)Tc-HMPAO

Anionic complexes $[TcO(MAG_3)]^{2-}$ (**15**)[57] and the oxotechnetium complex of dimercaptosuccinic acid $[Tc(DMSA)_2]^-$ (**16**) are useful for renal imaging as the carboxylic acid functions aid renal excretion of the complexes, with the former marketed as TechneScan. The $[Tc(DMSA)_2]^-$ complex has three isomers due to the orientation of these acid groups in relation to the metal-oxygen core, similar to its rhenium counterpart (see below).

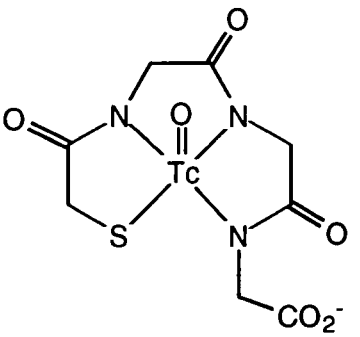

$[TcO(MAG_3)]^{2-}$

(**15**)

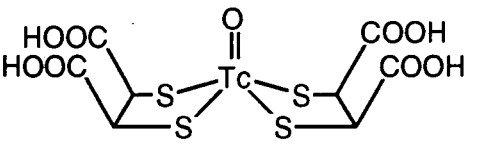

syn-endo

$[TcO(DMSA)_2]^-$

(**16**)

The production of rhenium-188 from a tungsten generator system has opened up the potential of this radionuclide in radiotherapy.[58] Although it forms a suitable therapeutic partner for technetium, rhenium is a great deal more difficult to substitute than its imaging counterpart. For example, Re-DTPA requires higher temperatures and a larger amount of the stannous reducing agent for complexation to occur. In contrast, Tc-DTPA forms instantly at room temperature. Radiopharmaceuticals of meso-1,2-dimercaptosuccinic acid (^{99m}Tc-DMSA) have found application in renal diagnosis. The complex also localises in medullary thyroid carcinoma, thus if labelled with β^--emitting ^{186}Re or ^{188}Re, a potential method of tumour therapy may be accessed. Again, the rhenium complexes require heating for formation (100°C, 30 mins for ^{186}Re)[59] while the technetium analogues are formed immediately at room temperature. With both metals, three isomers are formed, resulting from the orientation of the carboxylate groups on the backbone upon complexation. The isomers of $[Re(DMSA)_2]^-$ have been separated by HPLC[60] and elute in the order anti, syn-exo, syn-endo (Figure 1.20).

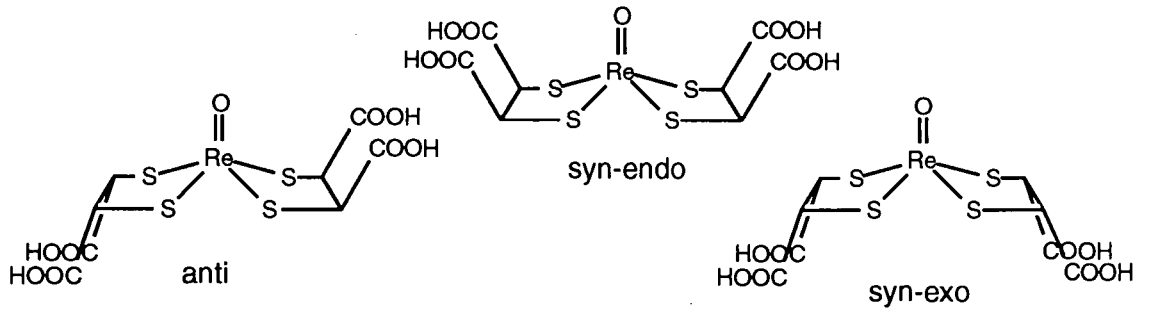

Figure 1.20 $[ReO(DMSA)_2]^-$ isomers

Another route to $[ReO(DMSA)_2]^-$ complex formation, which takes place at room temperature, has been reported by Lisic.[61] It utilises the precursor $ReOCl_3(PPh_3)_2$ complex in dichloromethane or chloroform.

The specificity of radionuclide imaging techniques has led to the design and synthesis of some extremely innovative coordination complexes as potential radiolabelled probes for steroid receptors with the imaging of receptor-positive tumours as their goal. The obvious approach may be conjugation of a suitable metal-complex to a steroid: the ambitious approach is the integration of the metal-complex with the steroid so that the whole molecule imitates the overall size and shape of the steroid. Katzenellenbogen and co-workers have produced several mimics of hormonal steroids[62,63] initially with the conjugated approach,[64] such as (**17**), and now concentrating upon an integrated approach. The conjugate (**17**) consists of a of a DADT complex and a progestin. One of its stereoisomers binds the progestin-receptor with three times the affinity of the natural hormone, but is, however, too lipophilic which resulted in non-specific binding. Less lipophilic analogues[65] still proved unsatisfactory for targeting due to their large mass and steric bulk.

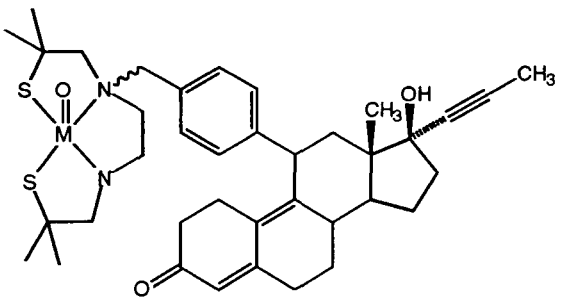

(**17**)

The less lipophilic conjugates did show some promise in terms of the relatively low polarity of the metal-complex. This promise led to the design of integrated systems where the metal could be incorporated into a steroid-like structure. Obvious challenges

of integrating a unit of the size of a metal-ligand complex are associated with compromising the binding affinity due to the added bulk. Computer modelling suggested that the complex (**19**) closely mimics the androgen, 5α-dihydrotestosterone (**18**) by replacement of the trans-decalin BC ring system with a bis(aminothiol) complex of oxotechnetium or oxorhenium for potential application in imaging prostatic carcinoma. Subsequent synthesis of the complex overcame some challenging stereochemical issues which could only be determined upon binding of the ligand to the metal. The Re=O bond is *anti* to the methyl and hydroxyl groups which is essential to the mimicry of the biological substrate. Another interesting issue is the successful formation of a heterodimeric complex of two different aminothiol ligands. Despite their successful synthesis, the complexes lacked stability and are degraded in water.[66] Recognition of the inferior stability of a bisbidentate complex compared to a tetradentate system has led to the synthesis of a tetradentate ligand for complexation and evaluation with oxotechnetium and oxorhenium cores.[67]

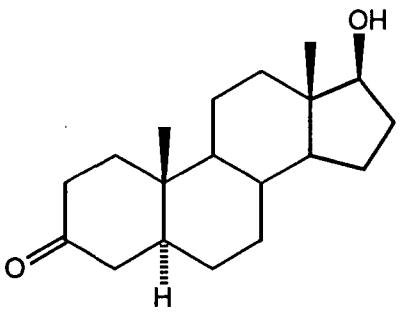

(**18**)
Natural Steroid - Dihydrotestosterone

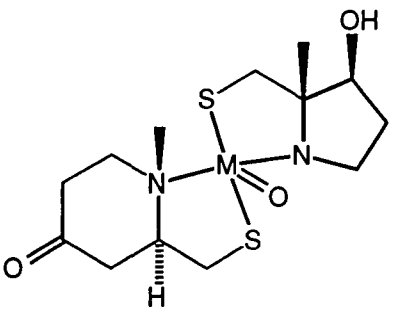

(**19**)
Steroid-Mimic Design

Figure 1.21 Steroid and complex mimic

Several complexes have been synthesised as mimics of estradiol (Figure 1.22) including (**20**) - a bis-bidentate complex. Attempts to make the tetradentate system (**21**) led to a tridentate (3+1) complex (**22**). Complex stability was enhanced by the derivation of a tetradentate ligand (**23**) with amine-amide-thioether-thiol N_2S_2 donor system and the rhenium complex was synthesised. However, it only showed micromolar affinity for the estrogen receptor.

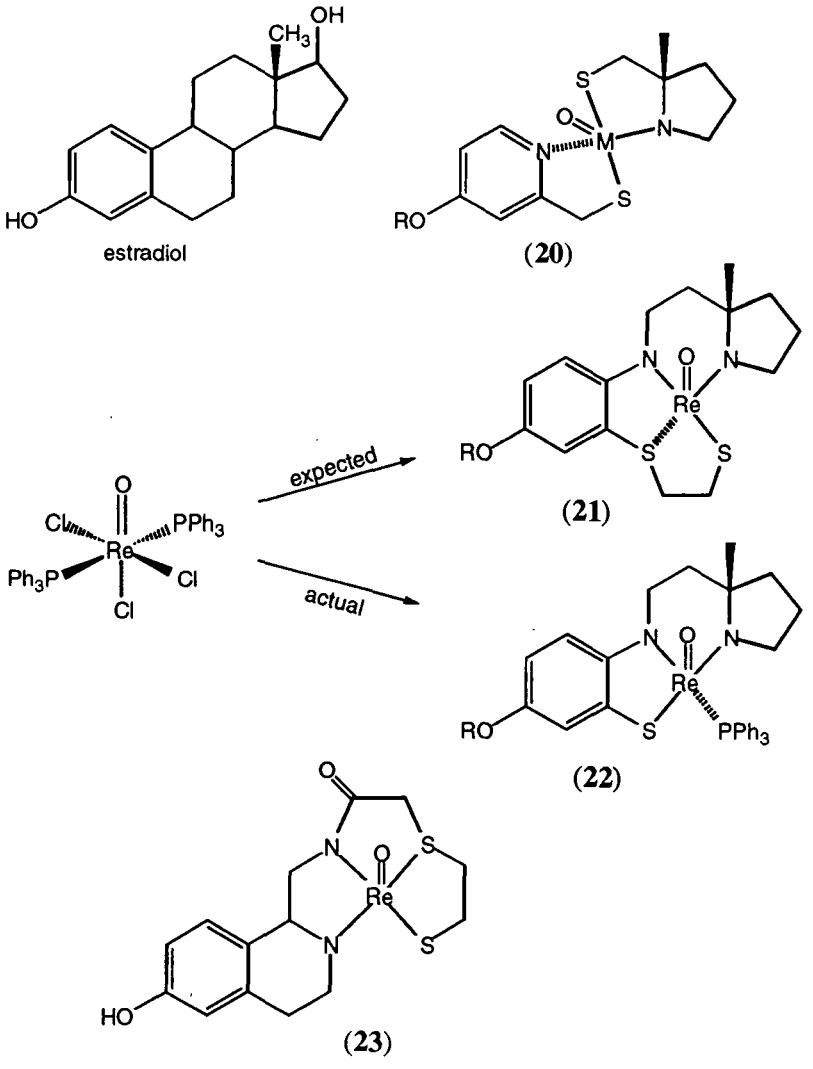

Figure 1.22 Estradiol and its steroid mimics

The 3+1 system (**25**) (Figure 1.23) was also synthesised by the same research group to mimic the structure of the non-steroidal estrogen, hexestrol (**24**). Although stable, its affinity for the estrogen receptor was also found to be low.[68]

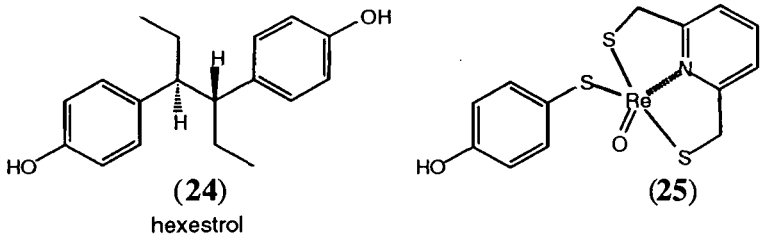

Figure 1.23 Hexestrol and its oxo-rhenium mimic

The availability of ^{62}Cu from the $^{62}Zn/^{62}Cu$ generator[69,70,71] has increased the potential application of this radionuclide in imaging. Copper bis(thiosemicarbazone) complexes are a very important class of radiopharmaceuticals. In particular, CuPTSM [PTSM=pyruvaldehyde bis(4-methiosemicarbazone)] (**26**) (Figure 1.24) has been studied extensively for use as a perfusion tracer in PET imaging. Two other derivatives,

PTS (**27**) and $PTSM_2$ (**28**), differing only in their degree of methylation were also examined and the PTS complex was shown to be inadequate to penetrate the BBB. The more lipophilic complexes (PTSM and $PTSM_2$) were able to diffuse into the brain, but $PTSM_2$ was rapidly cleared while PTSM was retained in the brain. The charge neutrality and lipophilicity of CuPTSM and its 'microsphere'-like distribution (rather than behaviour as a freely diffusible tracer) make it a good marker for perfusion measurement. This is desirable as a radiopharmaceutical that distributes as a microsphere would allow the quantitative study of blood flow. The trapping mechanism of Cu-PTSM was investigated by Green *et al*,[72] by studying a variety of Cu(II) bis(semicarbazone) complexes and measuring their reduction potentials. Cu-PTSM diffuses into cells where Cu(II) is reduced to Cu(I) by intracellular glutathione, making the previously neutral complex anionic and subject to intracellular binding. Cu-PTSM is taken up and and retained in most tissues and has the potential for myocardial and cerebral perfusion imaging in addition to regional blood flow to tissues.

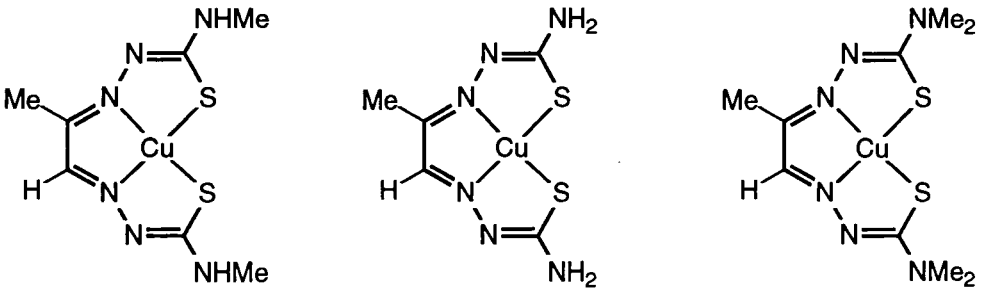

(**26**) CuPTSM (**27**) CuPTS (**28**) $CuPTSM_2$

Figure 1.24 Copper bis(thiosemicarbazone) complexes

Although Cu-PTSM is the best copper perfusion tracer to date, myocardial perfusion is underestimated at higher rates of flow. Uptake of the tracer is non-linearly proportional to blood-flow at higher flow rates and less tracer is extracted by the heart. This evidence in humans is contrary to the dog model and is an important example of interspecies variability which can often challenge radiopharmaceutical development. Consequently, more derivatives of Cu(II) bis(thiosemicarbazone) complexes have been prepared as the ligand system is known to be sensitive to substitution at the terminal carbon (C=S).[73] This time, two dissimilar thiosemicarbazone functions were incorporated (Figure 1.25). Thus the search for the perfect PET perfusion tracer continues.

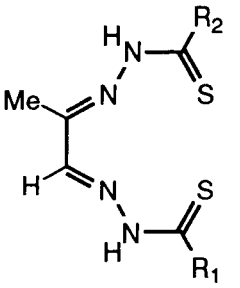

a) R_1= $NHCH_3$, R_2= NH_2
b) R_1= NH_2, R_2= $NHCH_3$
c) R_1= $NH(CH_3)_2$, R_2= NH_2
d) R_1= $NH(CH_3)_2$, R_2= $NHCH_3$

Figure 1.25 Further PTSM-type derivatives

A number of Schiff-base ligands have been synthesised and give rise to an $[N_2O_2]^{2-}$ core suitable for complexation with copper to form neutral, lipophilic molecules (Figure 1.26). Although some of the ^{62}Cu-radiolabelled complexes showed penetration of the BBB in rats, none of them were as effective as ^{62}Cu-PTSM.

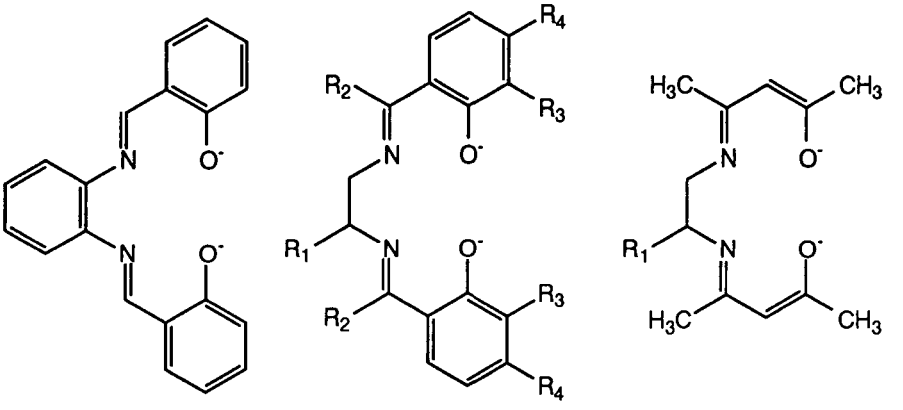

Figure 1.26 Examples of Schiff-base ligands for copper complexation

Copper radionuclides have also received much attention for their potential to form macrocyclic complexes conjugated to antibodies for radioimmunoscintigraphy.[74,75] The targeting of radiopharmaceuticals, in general, has been aided by the development of monoclonal antibodies which may be selectively functionalised by ligands for radionuclide complexation.[76] As the antibody has affinity for the antigens found on the surface of tumour cells, this protein can act as a carrier for the radionuclide and be used for both imaging and therapy[77,78] depending upon the nature of the radiation emitted (see section 1.5). In both instances, it is crucial that the complexes formed are substitutionally inert *in vivo* and suitable conjugates are known. Copper-64, copper-67 and technetium-99m have suitable half-lives for such applications. Both metals form thermodynamically stable and kinetically inert complexes with macrocycles like cyclam (Figure 1.16, section 1.6). Further application of stable complexes of nuclides like copper, with isotopes possessing suitable emissions, such as ^{64}Cu, may be found in targeted therapy and bifunctional complexing agents are under investigation for this purpose.[79] Several derivatives of cyclam bearing an appropriate pendent group allow

such protein conjugation. For example, the vinylpyridine group of (**29**) was conjugated to an antibody by conversion of the antibody lysine residue into a thiol and subsequent reaction of this functionality with the vinyl group. The study of other vehicles for the efficient and selective delivery of radiocopper is also in progress. Porphyrins are potentially suitable due to the high stability of copper-porphyrin complexes and the ease of porphyrin derivatisation for coupling.

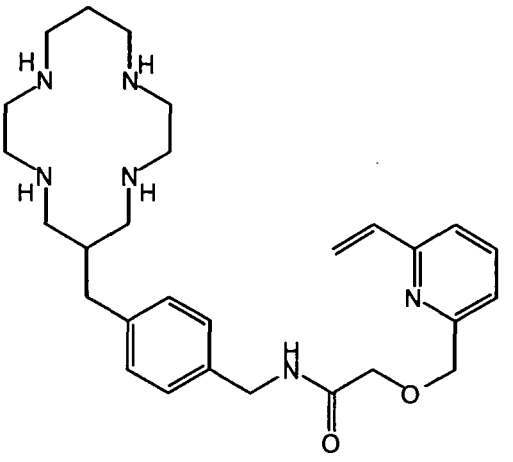

(**29**)

1.8 Scope of this work

ÍThis thesis is concerned with the synthesis of new ligand systems for radionuclide complexation, in particular, technetium, copper and rhenium.

Chapter 2 introduces a new tetradentate ligand system incorporating thiophosphinic acid and amine functional groups to offer an N_2S_2 donor atom array. The thiophosphinate functionality has several advantages including high acidity and a pentavalent site to tolerate further elaboration of the system. The overall system allows scope for variation of component parts and modification of complex lipophilicity, in addition to the possibility of conjugation to suitable targeting vectors. Difficulties in the synthesis of this ligand system and several alternative synthetic routes are discussed in addition to the complexation behaviour of the ligands with metal ions such as copper and rhenium.

Chapter 3 describes another new N_2S_2 tetradentate ligand system based on dihydrazide and dialkylthiophosphoryl functionalities. The ligand synthesis is described followed by the development of further ligands incorporating the dialkylthiophosphoryl functional group. The complexation behaviour of these systems is then addressed with particular attention to copper(I) and copper(II).

Chapter 4 considers ligand systems based upon the thiophosphinic acid group attached to more rigid skeletons. Difficulties in their synthesis are discussed together with several potential synthetic routes.

Chapter 5 describes the radiolabelling and preliminary evaluation of the ligands synthesised in chapters 2 and 3 with copper-64 and technetium-99m.

Chapter 6 details experimental procedures and general methods.

1.9 References and Notes

1. T. Jones, Eur. *J. Nucl. Med*, 1996, **23**, 207
2. R.J. Ott, M.A. Flower, J.W. Babich and P.K. Marsden, 'The Physics of Radioisotope Imaging', in *The Physics of Medical Imaging*, (ed. S. Webb), IOP Publishing 1988, Ch.6, pp142
3. A.H. Maurer, J-L,C. Urbain, L.S. Malmud, 'Radionuclide Imaging:General Principles', in *Diagnostic Radiology - A Textbook of Medical Imaging*, (eds R.G. Grainger and D.J. Allison) 3rd edition, Vol. 1, Pearson Professional Ltd, 1997
4. M.A. Green, 'Metal Radionuclides in Diagnostic Imaging by Positron Emission Tomography', in *Advances in Metals in Medicine*, (Eds. M.J. Abrams and B.A. Murrer), 1993, 1, pp75-114, JAI Press Inc.
5. P.H. Jarritt and P.D. Acton, *Nucl. Med Comm.*, 1996, **17**, 758
6. D.L. Bailey, F. Zito, M-C Gilardi, A.R. Savi, F. Fazio, T. Jones, *Eur. J. Nucl. Med.*, 1994, **21**, 381
7. T. Jones, *Eur. J. Nucl. Med*, 1996, **23**, 807
8. R.E. Boyd, *Int. J. Appl. Radiat. Isot.*, 1982, **33**, 801
9. V.J. Molinski, *Int. J. Appl. Radiat. Isot.*, 1982, **33**, 811
10. Although photons with energy greater than 80 keV can easily be detected, SPET usually requires gamma-rays in the energy range of 100-200 keV.
11. P. Richards, W.D. Tucker and S.C. Srivastava, *Int. J. Appl. Radiat. Isot.*, 1982, **33**, 793
12. G.B. Saha, W.J. MacIntyre and R.T. Go, *Seminars in Nuclear Medicine*, 1992, **22** (3), 150
13. K. Hamacher, H.H. Coenen and G. Stöcklin, *J. Nucl. Med.*, 1986, **27**, 235
14. J. Zweit, 'Medium half-life inorganic radionuclides for PET Imaging', in *Current Directions in Radiopharmaceutical Research and Development*, (ed. S.J. Mather), Kluwer Academic Publishers, 1996
15. R.T. Go, T.H. Marwick, M.J. MacIntyre, G.B. Saha, D.R. Neumann, D.A. Underwood and C.C. Simpfendorfer, *J. Nucl. Med.*, 1990, **31**, 1899

16. H.M. Chilton, S.W. Burchiel and N.E. Watson in '*Pharmaceuticals in Medical Imaging*', eds. D.P. Swanson, H. Chilton and J.H. Thrall, Macmillan, New York, 1990, 564
17. P.J. Blower, J.S. Lewis and J. Zweit, *Nucl. Med. Biol.*, 1996, **23**, 957
18. C.J. Anderson, S.R. Bergmann, *J. Nucl. Med.*, 1994, **35**(7), 1122
19. W.A. Volkert, W.F. Goeckeler, G.J. Ehrhardt and A.R. Ketring, *J. Nucl. Med.*, 1991, 32(1), 174
20. M.J. Abrams and B.A. Murrer, *Science*, 1993, **261**, 725
21. A. Aigner, S. Wolf and H.G. Gassen, *Angew. Chem. Int. Ed. Engl.*, 1997, **36**, 24
22. V.A. Levin, *J. Med. Chem.*, 1980, **23**, 682
23. G.B. Saha, W.J. MacIntyre and R.T. Go, *Seminars in Nulear Medicine*, 1994, **24** (4), 324
24. R.G. Pearson, *J. Am. Chem. Soc.*, 1963, **85** (22), 3533
25. N.N. Greenwood and A. Earnshaw, Chemistry of the Elements, Pergamon Press, 1984
26. R.D. Hancock and A.E. Martell, *Chem. Rev.*, 1989, 1893
27. M. Gerloch, *Inorg. Chem.*, 1981, **20**, 638
28. A. Davison and A.G. Jones *Int. J. Appl. Radiat. Isot.*, 1982, **33**, 875
29. A.G. Jones and A. Davison, *ibid*, 1982, **33**, 867
30. N.P. Johnson, C.J.L. Lock and G. Wilkinson, *J. Chem. Soc.*, 1964, 1054
31. The discovery of technetium was published by Emilio Segrè and Carlo Perrier in 1937; *Nature*, 1937, **140**, 193
32. E. Deutsch, K. Libson, S. Jurisson and L.F. Lindoy, Technetium Chemistry and Technetium Radiopharmaceuticals, *Progress in Inorg. Chem.*, (Ed. J.S. Lippard), 1983, **30**, 75
33. M. Melnik and J.E. Van Lier, *Coord. Chem. Rev.*, 1987, 77, 275
34. M.E. Kastner, M.J. Lindsay and M.J. Clarke, *Inorg. Chem.*, 1982, **21**, 2037
35. S.A. Zuckman, G.M. Freeman, D.E. Troutner, W.A. Volkert, R.A. Holmes, D.G. Van Derveer and E.K. Barefield, *Inorg. Chem.*, 1981, **20** (8), 2286
36. D.E. Troutner, J. Simon, A.R. Ketring, W. Volkert and R.A. Holmes, *J. Nucl. Med.*, 1980, **21**, 443
37. B. Johannsen and H. Spies, *Topics in Current Chemistry*, 1996, **176**, 77
38. A. Davison, B.V. De Pamphilis, A.G. Jones, K.J. Franklin, C.J.L. Lock, *Inorg. Chim. Acta.*, 1987, **128**, 161
39. M.J. Abrams, S.K. Larsen, J. Zubieta, *Inorg. Chem.*, 1991, **30**, 2031
40. L.L.Y. Hwang, N. Ronca, N.A. Solomon and J. Steigman, *Int. J. Appl. Radiat. Isot.*, 1985, **36**, 475
41. J.E. Smith, E.F. Byrne, F.A. Cotton and J.C. Sekutowsky, *J. Am. Chem. Soc.*, 1978, **100**, 5571

42. H.D. Burns, H. Manspeaker, R. Miller *et al, J. Nucl. Med*, 1979, **280**, 326
43. A. Davison, A.G. Jones, C. Orvig and M. Sohn, *Inorg. Chem.*, 1981, **20**, 1629
44. T.N. Rao, D. Adhikesavalu, A. Camerman and A.R. Fritzberg, *J. Am. Chem. Soc.*, 1990, **112**, 5798
45. S. Kasina, A.R. Fritzberg, D.L. Johnson and D. Eshima, *J. Med. Chem.*, 1986, **29**, 1933
46. D. Brenner, A. Davison, D. Lister-James and A.G. Jones, *Inorg. Chem.*, 1984, **23**, 2793
47. N. Bryson, J.C. Dewan, J. Lister-James, A.G. Jones, A. Davison, *Inorg. Chem.*, 1988, **27**, 2154
48. H.F. Kung, Y. Guo, C. Yu, J. Billings, V. Subramanyam and J.C. Calabrese, *J. Med. Chem.*, 1989, 32, 433
49. S. Jurisson, D. Berning, W. Jia and D. Ma, *Chem. Rev.*, 1993, **93**, 1137-1156
50. W.A. Volkert and S. Jurisson, *Topics in Current Chemistry*, 1996, **176**, 123
51. T.R. Carroll, 'Technetium heart and brain Brain Perfusion Imaging Agents', in *Advances in Metals in Medicine*, (Eds. M.J. Abrams and B.A. Murrer), 1993, 1, pp1-27, JAI Press Inc.
52. M. Nicolini, G. Bandoli and U. Mazzi, *Technetium in Chemistry and Nuclear Medicine*, 2, Cortina International, Verona, 1986
53. S.Z. Lever, K.E. Baidoo and A. Mahmood, *Inorg. Chim. Acta.*, 1990, **176**, 183
54. J. Leveille, G.Demonceau, M. DeRoo, R.A. Morgan, D. Kupranick and R.C. walovitch, *J. Nucl. Med.*, 1989, **30**, 1892
55. S. Jurisson, E.O. Schlemper, D.E. Troutner, L.R. Canning, D.P. Nowotrik and R.D. Neirinckx, *Inorg. Chem.*, 1986, **25**, 543
56. D.P. Nowotrik, L.R. Canning, S.A. Cumming, R.C. Harrison, B. Higley, G. Nechvatel, R.D. Picklett, I.M. Piper, V.J. Bayne, A.M. Forster, P.S. Weisner and R.D. Neirinckx; W.A. Volkert, D.E. Troutner and R.A. Holmes, *Nucl. Med. Commun.*, 1985, **6**, 499
57. A.R. Fritzberg, S. Kasina, D. Eshima and D.L. Johnson, *J. Nucl. Med.*, 1986, **27**, 111
58. K. Hashimoto and K. Yoshihara, *Topics in Current Chemistry*, 1996, **176**, 275
59. M.M. Bisunadan, P.J. Blower, S.E.M. Clarke, J. Singh an M.J. Went, *Appl. Radiat. Isot.*, 1991, **42**, 167
60. J. Singh, A.K. Powell, S.E.M. Clarke and P.J. Blower, *J. Chem. Soc. Chem. Commun.*, 1991, 1115
61. E.C. Lisac, S. Mirzadeh, F.F. Knapp Jr., *J. Labeled Compd Radiopharm*, 1993, **33**, 65
62. D.Y. Chi, J.P. O'Neil, C.J. Anderson, M.J. Welch and J.A. Katzenellenbogen, *J. Med. Chem.*, 1994, **37**, 928

63. J.P. O'Neil, K.E. Carlson, C.J. Anderson, M.J. Welch and J.A. Katzenellenbogen, *Bioconj. Chem.*, 1994, **5**, 182
64. J.P. DiZio, R. Fiaschi, A. Davison, A.G. Jones, J.A. Katzenellenbogen, *Bioconj. Chem.*, 1991, **2**, 353
65. J.P. O'Neil, S.R. Wilson and J.A. Katzenellenbogen, *Inorg. Chem.*, 1994, **33**, 319
66. R.K. Hom, D.Y. Chi, J.A. Katzenellenbogen, *J. Org. Chem.*, 1996, **61**, 2624
67. Y. Sugano and J.A. Katzenellenbogen, *Abstracts of 11th International Symposium on Radiopharmaceutical Chemistry, Vancouver, Canada,* 1996, 424
68. R.K. Hom, M.B. Skaddan, J.A. Katzenellenbogen, *Abstracts of 12th nternational Symposium on Radiopharmaceutical Chemistry, Uppsala, Sweden*, 1997, 510
69. Y.Fujibayashi, k. Matsumoto, Y. Yonekura, J. Konishi and A. Yokoyama, *J. Nucl. Med.*, 1989, **30**, 1838
70. G. Bormans, A. Janssen, P. Adriaens, D.Crombez, A. Witsenboer, J. De Goeij, L. Mortelmans and A. Verbruggen, Appl. *Radiat. Isot.*, 1992, **43** (12), 1437
71. J. Zweit, *Eur. J. Nucl. Med.,* 1992, **19**, 418
72. E.K. John and M.A. Green, *J. Med. Chem.*, 1990, **33**, 1764
73. J.K. Lim, C.J. Mathias and M.A. Green, *J. Med. Chem.*, 1997, **40**, 132
74. D. Parker, 'Imaging and Targeting' in *Comprehensive Supramolecular Chemistry*, (Eds. J.M. Lehn and D.N. Reinhoudt) 1996, **10**, pp 487, Elsevier Science Ltd, UK.
75. D. Parker, J.R. Morphy, K. Jankowski and J. Cox, *Pure and Appl. Chem.*, 1989, **61**, 1637
76. K.J. Jankowski and D. Parker, 'Diagnosis and therapy with antibody Conjugates of metal Radioisotopes, in *Advances in Metals in Medicine*, (Eds. M.J. Abrams and B.A. Murrer), 1993, 1, pp29-73, JAI Press Inc.
77. D.M. Goldenberg and S.M. Larson, *J. Nucl. Med*, 1992, **33**, 803
78. P.A. Schubiger, R. Alberto and A. Smith, *Bioconjugate Chem.*, 1996, 7, 165
79. D. Parker, *Chem. Soc. Rev.*, 1990, **19**, 271

Chapter Two

Aza-Thiophosphinic Acid Ligands

2. Aza-Thiophosphinic Acid Ligands

The design of a new class of ligands based upon aminothiophosphinic acids is presented. Key features of the architechture are examined with respect to the tailoring of radiopharmaceuticals (2.1), and the unique feature of the thiophosphinate functionality is related to aminocarboxylic acid and aminophosphinic acid analogues. The synthesis and difficulties experienced with different synthetic routes are explored and the successful synthesis of this ligand class is discussed (2.2). Complexation studies with rhenium and copper by techniques such as ESMS, HPLC and spectrophotometry are reported (2.3) and general conclusions are summarised (2.4).

2.1 Design of a New Ligand System

The range of radionuclear properties offered by the isotopes of copper, technetium and rhenium for their application in nuclear medicine provides the driving force for the design and synthesis of a new class of ligands to complex these metals and allow variation of the ligand component moieties to optimise the properties of the complex. Such versatility would allow the tailoring of the radiopharmaceutical lipophilicity by elaboration of the ligand, or alteration of radionuclear properties by substitution of a different radionuclide with similar coordination preferences. This may allow development of radiopharmaceuticals for different applications within nuclear medicine. Consideration of the desirable properties of a radiopharmaceutical reveals that a finite stability may in fact be advantageous (Ch.1). Rapid kinetics of complexation are essential and the complex should be sufficiently stable *in vivo* to reach the desired organs of the body and may encounter some areas of low pH in the process. However, degradation of the complex in some way, for example by dissociation or reduction of the metal, may provide a means of intracellular trapping and hence localisation of the radionuclide. These criteria together with analysis of the requirements of a ligand system for complexation of copper, technetium and rhenium radionuclides and consideration of observed trends in the coordination chemistry of these metals (Ch.1) led to the design of a new class of ligands with the general structure represented below (Figure 2.1).

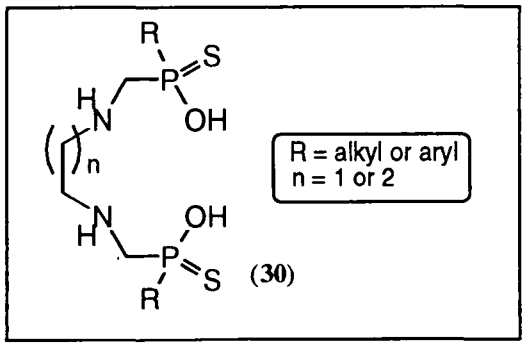

Figure 2.1 A new ligand system

Overall architecture

The overall structure of the ligand system is tetradentate with donor atoms arranged to form three 5-membered ring chelates or one 6-ring (n=2, Figure 2.1) with two 5-ring chelates. This offers the greater stability associated with ligands of higher denticity and optimum chelate ring size (see 1.6). Variation of the chelate ring-size may allow the optimum architecture for the particular metal to be assessed. Use of the N_2S_2 donor system should prove advantageous for copper, technetium and rhenium with their 'borderline' donor preferences. Neutral copper(II) complexes may be formed due to the combination of neutral amine donors with two negative sulfur donor atoms. Such donor atoms should favour the stabilisation of 'soft' Cu(I), which is potentially useful, as intracellular reduction of the Cu(II) complex (for example by glutathione) may lead to retention of the radionuclide. This could be due to the anionic nature of the reduced complex rendering it less able to diffuse back out of the cell, or because the Cu(I) complex is expected to be less stable to dissociation and hence may be retained following loss of copper from the complex. Neutral complexes may also be formed with technetium and rhenium in oxidation state (V) with an oxometal core (see examples in 1.6 and 1.7) by charge donation from the two negative sulfur donors and one deprotonated amine. The secondary amines may be easily deprotonated, hence a charge neutral complex may be formed by such ligands with a TcO^{3+} core, for example, ^{99m}Tc-ECD (**13**) (section **1.7**).

Tuning of Lipophilicity

Lipophilicity of radiopharmaceuticals is crucial to their activity *in vivo*, hence the ability to alter this characteristic without compromising other important properties is extremely advantageous. In the ligand design described above (Figure 2.1), it is possible to vary the lipophilicity of the complex without compromising the metal binding properties. The pentavalency at phosphorus allows control over complex lipophilicity and may also afford a means of conjugation to a suitable targeting vector through variation of the phosphorus alkyl or aryl substituents.[4] The ethanediamine or propanediamine backbone allows another option for further elaboration of the ligand. Substitution of this two-carbon or three-carbon backbone would also provide a means of alteration of complex lipophilicity or allow a tether to a targeting vector to be attached. For example, (**31**) shows a propylene backbone which can be derived from a malonate fragment.

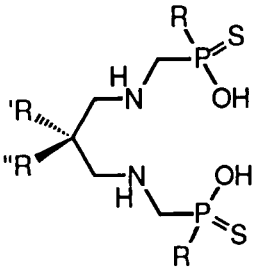

R', R"= H, alkyl

(31)

Acidity of thiophosphinic acids

The use of the thiophosphinate funtionality is a unique feature of this system. Thiophosphinic acids are more acidic than their corresponding phosphinic and carboxylic acid analogues, as demonstrated by the protonation constants for a series of acids (Table 2.1). Sequential replacement of the oxygen atoms by sulfur atoms decreases the protonation constants obtained.[1] This may enhance the stability of the metal complexes with respect to dissociation in acidic media.

Table 2.1 Decreasing trend in protonation constants for phosphorus acids

Ligand	pK_a
EtC(O)OH	4.87
$Et_2P(O)OH$	3.29
$Et_2P(O)SH$	2.54
$Et_2P(S)SH$	1.71

There is a tautomeric equilibrium between the two possible forms (Figure 2.2). With two different alkyl or aryl substituents at phosphorus, a stereogenic centre at phosphorus is formed which is not present in solution with the corresponding substituted phosphinic acids due to a similar tautomerism. With such phosphinates, however, a stereogenic centre is created at phosphorus when one of these phosphinate oxygens is bound to a metal.[2,3]

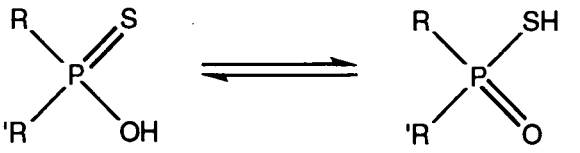

phosphinothionic acid phosphinothiolic acid

Figure 2.2

Corresponding amino-carboxylic and amino-phosphinic acids

Amino-carboxylic acids are ubiquitous in nature and have been greatly studied. However, they are generally unsubstituted at nitrogen and a higher denticity or array of linked donor atoms is preferable for use in coordination chemistry. Arguably, the most important ligand of this type is Schwarzenbach's EDTA (ethylenediamine-N,N,N,'N'-tetra-acetic acid)[4] (**32**), which gives an N_2O_4 donor set arranged to give 5-membered chelate rings upon metal complexation. Its relation, EDDA (ethylenediamine-N,N'-diacetic acid) (**33**),[5] has fewer donor atoms with an N_2O_2 donor set. Variations with a propylenediamine backbone, giving a 6-membered chelate ring have been exploited, as have macrocyclic arrays such as NOTA and DOTA.[6]

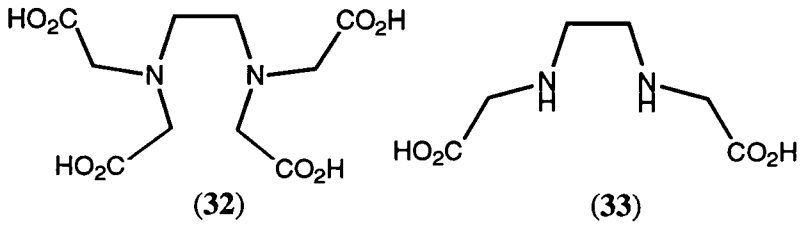

(32) (33)

Figure 2.3 EDTA and EDDA

Amino-phosphinic acids are generally similar in their properties to their carboxylic counterparts although the phosphinate oxygen is more difficult to protonate, as mentioned above, and a wealth of examples supporting this observation are documented.[7,8,9,10] Indeed, several azaphosphinate macrocyclic complexes are remarkably resistant to acid-catalysed dissociation.[11] Phosphinate analogues of EDTA and EDDA were reported by Martell[12] - EDTPi (ethylenediamine-N,N,N,'N'-tetra-phosphinic acid) (**34**) and EDDPi (ethylenediamine-N,N'-di-phosphinic acid) (**35**) (Figure 2.4). They show an increase in acidity (lower pK_a's) for P(O)OH deprotonation, as expected, and the basicity of the amine is lowered by the presence of the electron withdrawing groups. The ligands form 1:1 complexes with transition metals, although these are less thermodynamically stable than analogous carboxylate complexes.

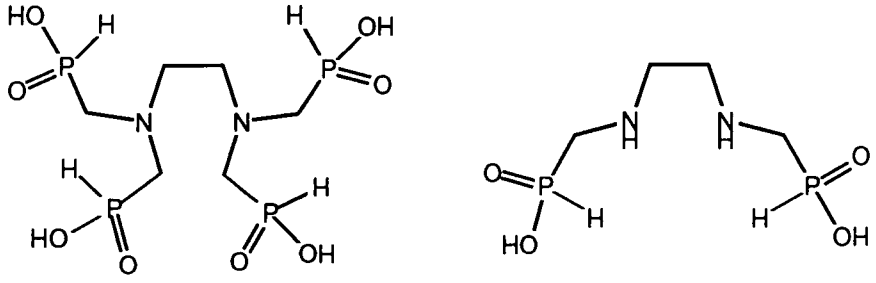

(34) (35)

Figure 2.4 EDTPi and EDDPi

The next stage in the development of such systems was substitution at phosphorus to yield ethylenediamine-tetrakis-[methylene(phenylphosphinic)] acid (H_4EDTMPPh), (**36**). Studies of the protonation behaviour of this ligand by Lukes[13,14] indicate that it shows greater similarity to EDTA than analogous phosphonic acids.

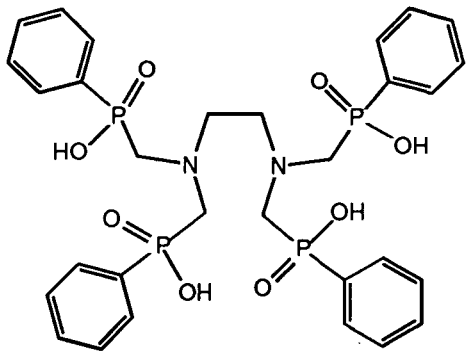

(36)

Although the most profound difference between the use of phosphinic acid groups in preference to carboxylic acids is an increase in acidity, there are other consequences of this change. The use of a phosphinic acid offers a larger chelate bite angle upon complexation than a carboxylic acid (Figure 2.5). The angle at the metal (<NMO) formed by the phosphinate is less acute than the angle produced by the carboxylate. Both the C-P and P-O bonds of the phosphinate (185 pm and 150 pm respectively) are longer than the corresponding C-C and C-O bonds of the carboxylate (154 pm and 125 pm respectively).[15]

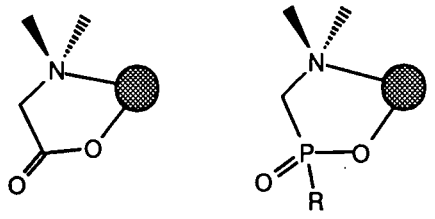

Figure 2.5 Chelate bite angles formed by aza-carboxylates and aza-phosphinates

Several acyclic tetradentate ligands incorporating substituted phosphinic acid functionalities were synthesised and their complexation behaviour was investigated by Parker *et al.*[16] The protonation constants for the methyl and phenyl P-substituted ligands was found to be very similar, while ligands with a diaminopropane skeleton gave higher protonation constants at nitrogen than the corresponding diaminoethane-based systems. The ligands were synthesised by the reaction of diaminoethane or diaminopropane with paraformaldehyde and the appropriate phosphorus (III) precursor to form the cyclic aminal diester (**37**) which was purified by column chromatography on alumina (Scheme 2.1). Subsequent hydrolysis by heating in 6M hydrochloric acid yielded the amino-phosphinic acid ligand (**38**).

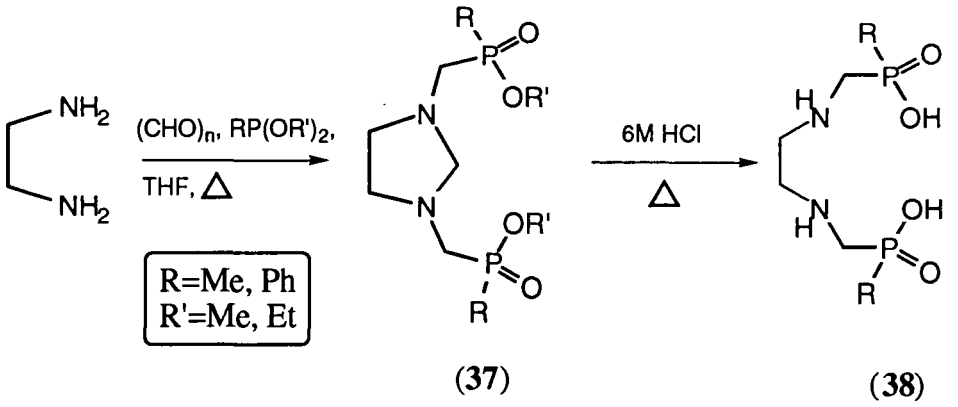

Scheme 2.1 Synthesis of substituted aza-phosphinic acids

^{31}P NMR

Another useful feature of both the phosphinic acid ligands and the proposed new thiophosphinic acid ligands is their amenability to ^{31}P NMR. This is an invaluable tool for monitoring the synthesis and complexation behaviour of new ligands. For example, a phosphinic acid with δ_P in the range of 20-30 ppm is in stark contrast to its thiophosphinic acid analogue with δ_P in the 60-80 ppm range - a difference in the region of 40-50 ppm. This is extremely diagnostic, since differentiation between sulfur and oxygen attached to phosphorus is much less apparent by a study of the neighbouring protons in the ^1H NMR spectra. Furthermore, the progress of a reaction can be studied simply by the temporary removal of a small sample and direct analysis by ^{31}P NMR since a deuterated solvent is not essential.

Ligand Series

Many variations upon this type of system (Figure 2.1) can be envisaged since a large number of alkyl or aryl substituents at phosphorus are possible. In order to allow evaluation of the coordination preferences of such aza-thiophosphinate ligands, a simple series of four ligands was proposed (Figure 2.6). For example, the use of a diaminoethane or diaminopropane moiety allows the effect of a five-membered chelate ring versus a six-membered chelate ring to be assessed with either a P-phenyl or a P-methyl substituent for each. The P-phenyl derivative with a diaminoethane backbone unit was addressed first, in order to establish a viable synthetic route.

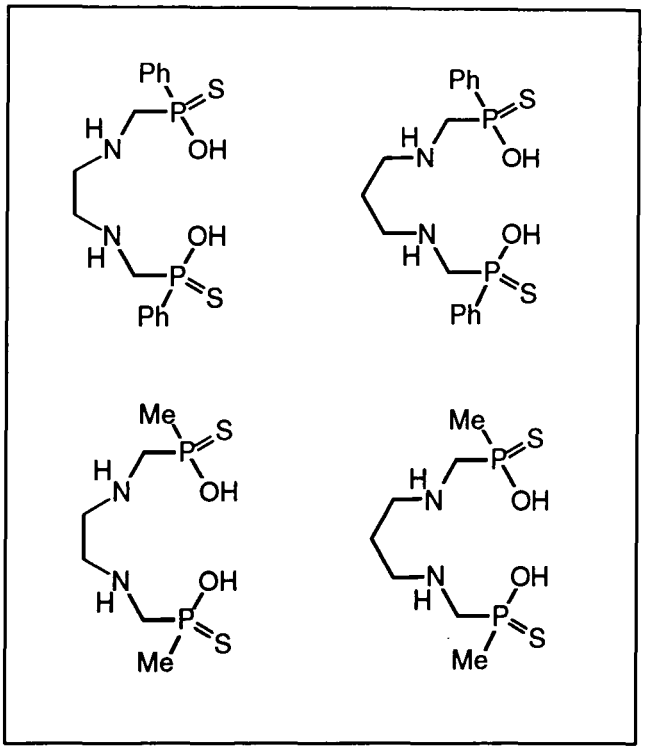

Figure 2.6 Amino-thiophosphinic acid ligand series

2.2 Synthesis

Initial P(III) route

A flexible, general synthetic route allowing a variety of different substituents at phosphorus was envisaged (Scheme 2.2) in an analogous manner to the synthesis of corresponding aza-phosphinic acids.[16] Therefore, the phosphorus(III) precursor required for this pathway was a monothioester of the type RP(OR')(SR") and had first to be prepared from a dichlorophosphine via a monosubstituted chloroethoxy intermediate.

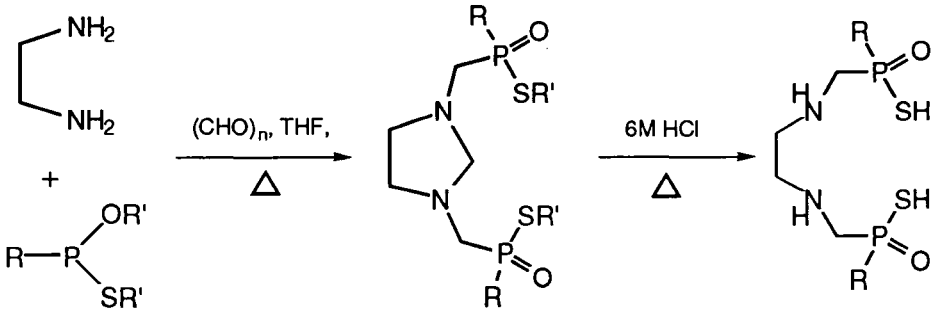

Scheme 2.2 Proposed synthesis of amino-thiophosphinic acid ligands

Preparation of chloroethoxyphenylphosphine, PhP(OEt)Cl, was initially attempted by addition of one equivalent of sodium ethoxide to dichlorophenylphosphine, $PhPCl_2$, in dry ether (Scheme 2.3). The reaction was followed easily by ^{31}P NMR, and more

sodium ethoxide was added until there was no dichlorophenylphosphine starting material remaining. The product mixture was filtered to remove the sodium chloride salt (removal of all traces of halide prior to Arbuzov reaction is crucial) to give a mixture of chloroethoxyphenylphosphine and diethoxyphenylphosphine.

Scheme 2.3

However, purification by vacuum distillation proved exceedingly difficult as both of the phosphorus (III) species are extremely sensitive to hydrolysis and very volatile. Use of higher temperatures induced the decomposition of both P(III) species. Therefore, a method was sought to prepare the phosphine more cleanly as this attempted purification proved too problematic. This was achieved by a metathetical reaction where equimolar amounts of dichloroethylphosphonite and dichlorophenyl phosphine were mixed at 0°C in an inert atmosphere to form chloroethoxyphenylphosphine cleanly (Scheme 2.4).[17]

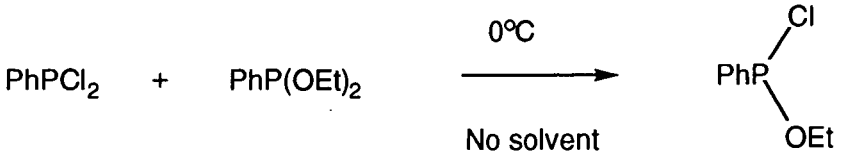

Scheme 2.4 Disproportionation reaction to give the pure product

The best result was obtained by carrying out the reaction in the absence of solvent, and ^{31}P NMR revealed that the monochloroethoxyphenylphosphine (δ_P +174 ppm) was the sole product. The mechanism by which this reaction occurs can be addressed by considering the relative nucleophilicities of the two different phosphorus species present. The more nucleophilic diethoxyphosphine may attack the dichlorophosphine and an intramolecular rearrangement may then occur to give only one product (Figure 2.7).

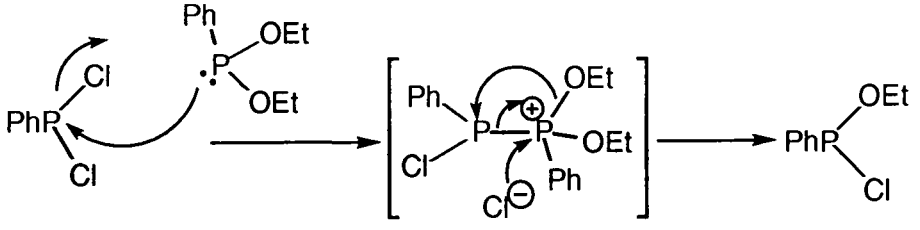

Figure 2.7

This procedure was also applied to an alkyl-substituted dichlorophosphine, in the form of an ethyl rather than methyl derivative due to the availability of the dichloroethyl starting material. The disproportionation reaction also worked well, producing the chloroethylethoxyphosphine after preparation of the other necessary starting material, diethylethylphosphonite, by addition of sodium ethoxide to dichloroethylphosphine in dry diethyl ether (Scheme 2.5).

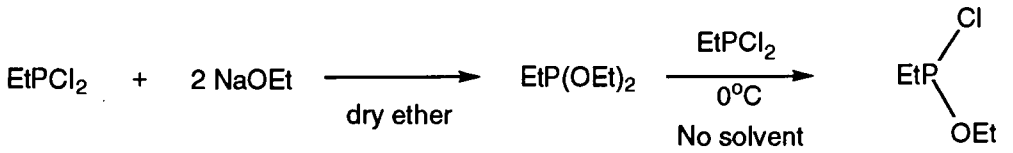

Scheme 2.5

Preparation of ethoxyphenyl-S-ethylphosphine, PhP(OEt)(SEt), was initially attempted by the addition of sodium ethanethiolate to the neat monochloro phosphine in order to displace the remaining chloride (Scheme 2.6). However, the reaction was observed to be too exothermic to allow effective heat dissipation from such a small reaction volume, and hence some solvents were considered for this step. Distilled toluene was found to be the best solvent for this reaction performed at -50°C. These conditions allowed the precipitation of the sodium chloride salt, enabling it to be removed effectively by filtration. ^{31}P NMR analysis indicated that the product, PhP(OEt)SEt, (δ_P +145.8 ppm) represented about 50% of the phosphorus species present. The chemical shifts of the other products were all much lower (~0-50 ppm), indicating that they were all P(V) species and that the only P(III) species present was PhP(OEt)SEt, although the overall purity of the sample was only 50%. However, the other products present were P(V) which have no effect upon the following Arbuzov reaction.

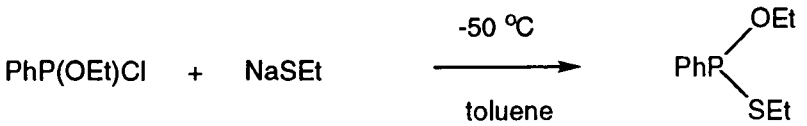

Scheme 2.6

The analogous dithiophosphine, $PhP(SEt)_2$ (δ_P +74.4 ppm) was prepared by the addition of two equivalents of sodium ethanethiolate to dichlorophosphine in dichloromethane at -30°C (Scheme 2.7). In an effort to prepare PhP(OEt)SEt more efficiently, a disproportionation reaction was attempted with $PhP(SEt)_2$ and $PhP(OEt)_2$ but perhaps unsurprisingly, no reaction was observed.

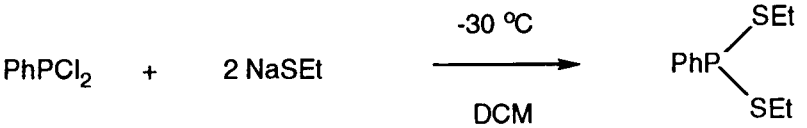

Scheme 2.7

Reaction of substituted thiophosphines

With the required PhP(SEt)OEt freshly prepared, the Arbuzov reaction was attempted by refluxing ethylene diamine and paraformaldehyde with the phosphine in dry THF using a Soxhlet apparatus with molecular sieves for 2 days, until only a little starting material remained visible by ^{31}P NMR. However, a mixture of several products had formed and a mass spectrum showed that none of the species present had a large enough mass to be consistent with the formation of the desired product. The largest mass observed, 230, was presumably the oxidised starting material - PhP(O)(OEt)(SEt) - which seemed to have formed competitively despite the inert gas atmosphere used. An analogous reaction was attempted with the less air-sensitive,[18,19] $PhP(SEt)_2$, but this failed to show any significant reaction.

Since the initial attempts to form the cyclic aminal diphosphinates from thiophosphines failed, consideration was then given to reactions with the oxygen analogue $PhP(OEt)_2$ to investigate if this reaction occurred readily, since it is known that the dimethoxyphosphines react effectively under identical conditions.[20] These results are summarised (Table 2.2) and indicate that a phenylphosphine with diethoxy substituents surprisingly does not exhibit the expected reactivity.

Table 2.2 Reactions with diethylphenylphosphonite

Amine	Aldehyde or Ketone	Result of reaction
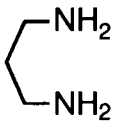	$(CH_2O)_n$ molecular sieves	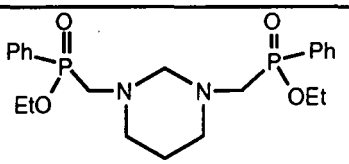 + hydroxymethylene
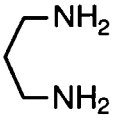	$(CH_2O)_n$ without sieves	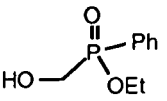 only hydroxymethylene
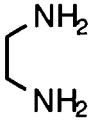	$(CH_2O)_n$	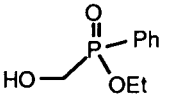 hydroxymethylene
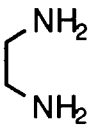		No reaction
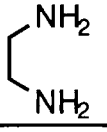		No reaction

Specificity problems of reactions with substituted phosphines

The problem with the failed reaction of the original scheme remained extremely curious as PhP(SEt)OEt and even $PhP(OEt)_2$ failed to react under these conditions when the analogous reaction is known with $PhP(OMe)_2$. A similar reaction was undertaken with $PhP(OMe)_2$, paraformaldehyde, and ethylenediamine under identical conditions. Purification of the products by chromatography and characterisation confirmed that the cyclic aminal bisphosphinate had formed readily, and the excess phosphine and paraformaldehyde had formed the hydroxymethylene species (Scheme 2.8).

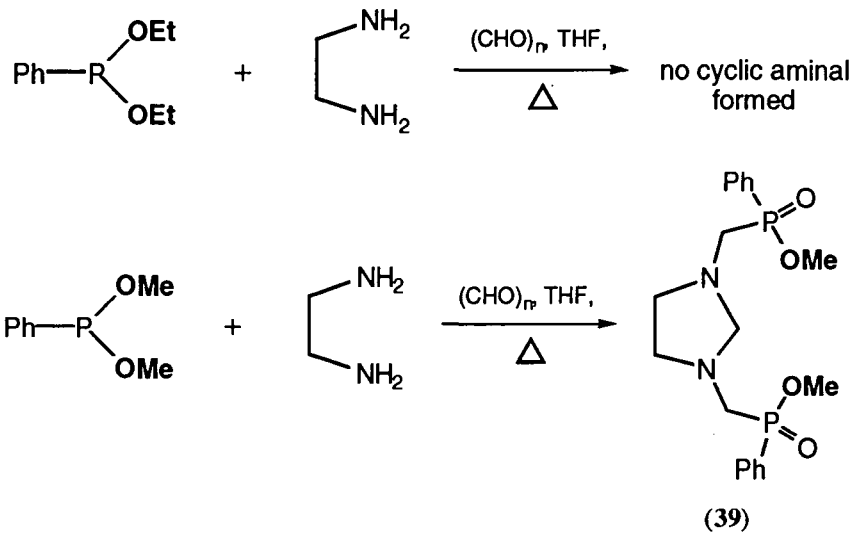

(39)

Scheme 2.8 Reactivity difference between methoxy- and ethoxyphosphines

It can be concluded that although reactions occur with diethoxyalkylphosphines, they do not proceed when the substituent is phenyl rather than alkyl. Greater reactivity is exhibited by dimethoxy-substituted phosphines as the reaction occurs even when the electron-withdrawing phenyl group is present.

With this knowledge, the original scheme was re-employed adopting dimethoxy phosphines in place of the diethoxy analogues. The original interchange reaction was attempted to prepare PhP(OMe)Cl . However, the reaction was much more vigorous and formed additional species presumably due to the release of a large amount of heat. The reaction was attempted in toluene at low temperature to give a greater volume to dissipate the heat of reaction. However, the reaction could not be carried out cleanly, as shown by ^{31}P NMR analysis. Formation of $PhP(SMe)_2$ was then attempted by addition of two equivalents of sodium methane thiolate to dichlorophenylphosphine, however, a mixture of products was obtained. The reaction itself was not visibly as instantaneous as its ethanethiolate counterpart.

In order to overcome the problem of decreased nucleophilicity of the phenyl substituted phosphines, an alkyl phosphine was utilised as the starting material in place of the

phenyl compound. Since the alkyl group is electron donating rather than delocalising, it should be more nucleophilic. Ethyldithioethylphosphine, $EtP(SMe)_2$, was prepared from dichloroethylphosphine by addition of sodium methanthiolate. The monothio-substituted product appeared to form reasonably rapidly (δ_P 166.6 ppm), and further portions of methanethiolate were added until conversion to the dithiomethyl species (δ_P 88.6) was complete. The product dithiophosphine was treated with diethylamine and paraformaldehyde under the usual conditions, as a test reaction, but it was found to merely oxidise to S,S-dimethylethylphosphodithiodic ester, $EtP(O)(SMe)_2$. Purification of $EtP(SMe)_2$ from slight P(V) impurities was attempted by distillation, but gave the same result - formation of $EtP(O)(SMe)_2$.

It is clear that the phosphine precursors are formed more readily with ethoxy and ethylthio substituted phosphines, but methoxy and methylthio substituted phosphines are required for the Arbuzov step. Furthermore, each phosphine with its particular substituents appears to have its own specific reactivity depending upon the choice of alkyl/aryl and alkoxy substituents rather than forming a series exhibiting general trends. Consequently, the planned route to these thiophosphinates is not at all versatile as had been initially hoped.

Another, though less immediate, problem with these thiophosphinate esters may be difficulties concerning their subsequent hydrolysis. The only literature examples to date detail the hydrolysis of activated thiophosphinate esters, (Figure 2.8) often requiring catalytic procedures with enzymes[21,22] or high pH.[23] This process is extremely slow and may not be achieved easily with the particular esters studied in this work.

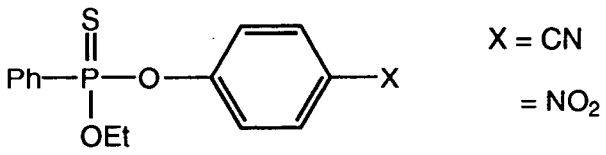

Figure 2.8 Activated phosphinate esters

With these difficulties in mind, alternative routes for the synthesis of aza-thiophosphinic acids were sought.

Conversion of P=O to P=S following cyclic aminal formation

Due to the failure of this initial route, attention was then directed towards a direct sulphur transfer to the oxygen analogues (P=O to P=S). This had been attempted in previous work by Eleanor Cole,[20] when it was found that a thiourea (**41**) formed on the bridge of the cyclic aminal (**40**) (Scheme 2.9).

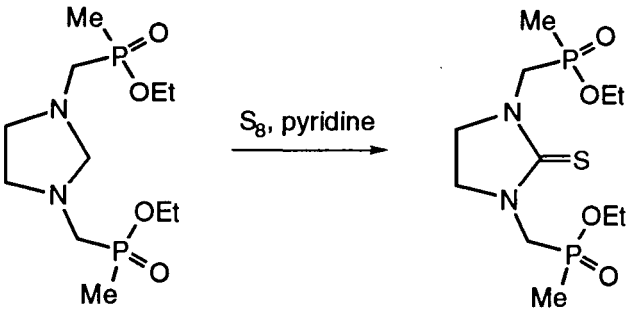

(40) **(41)**

Scheme 2.9

Since sulphur transfers to this position initially, the resulting thiourea was treated with phosphorus pentasulphide in a further attempt to transfer sulphur to the phosphonate esters (Scheme 2.10). ^{31}P NMR showed two major products had formed, δ_P 85.1 and δ_P 80.7, with the major mass intensity at 391 corresponding to the thiophosphinate adduct with ammonia (374 + 17). However, the proton NMR spectrum indicated the presence of the phosphorus methyl and ethoxy groups, but a great shift or disappearance of the N-$C\underline{H}_2$-P methylene protons. This pilot reaction was undertaken on a very small scale using an old sample from previous work and, clearly, further investigations are required here. However, the documented difficulty in the hydrolysis of such thiophosphinate esters provided sufficient motivation to investigate other routes which circumvented this anticipated problem.

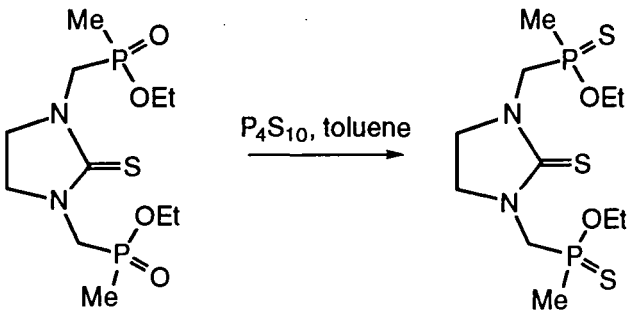

(41) **(42)**

Scheme 2.10

Alternative synthetic approaches

Sulphur transfer then amine addition

Consideration was therefore given to a number of alternative approaches. It is possible that the phosphinothiolic moiety can be created prior to the reaction with a tosylated amine. Hydrolysis of the esters and removal of tosyl groups may then be affected by HBr in glacial acetic acid (Scheme 2.11). One concern of this reaction may be the possibility of competing S-alkylation.[24] Nevertheless, if the mesylated

phosphinothiolate could be prepared without this interference, then the success of a subsequent reaction is a serious possibility.

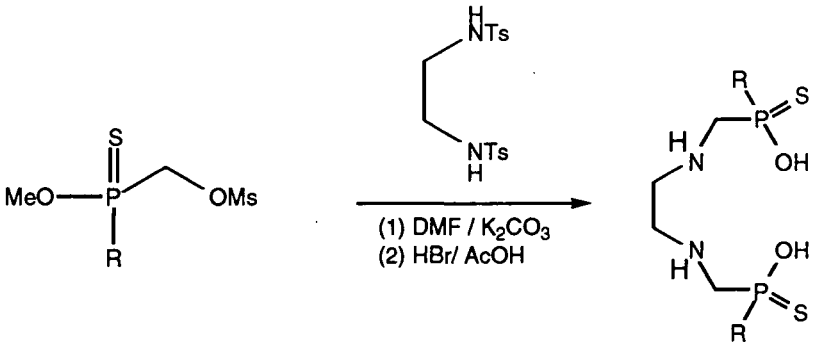

Scheme 2.11

The precursor could be prepared from a hydroxymethylene compound with a silicon group protecting the alcohol during the sulphur transfer (Scheme 2.12). Indeed, the silylation step was accomplished and the sulphur transfer was attempted, using ethyl[(hydroxymethylene) phenylphosphinate] which was isolated as a by-product from earlier reactions. The P=S compound sought was not initially isolable from the reaction mixture, and a parallel approach which showed more promise was pursued in preference.

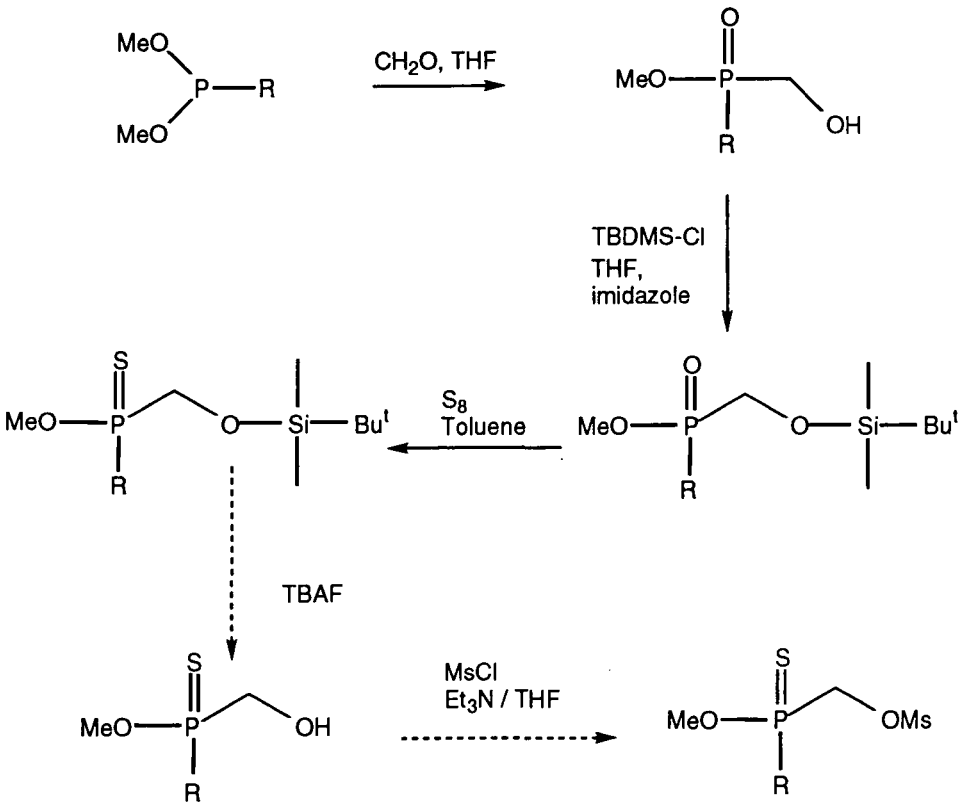

Scheme 2.12 Proposed synthesis of mesylated-thiophosphinate

Direct addition of sulfur

Attempts to transfer sulfur to a phosphinate ester have already been considered with regard to the aminal (see above). However, assuming this could be achieved, the question of hydrolysis of thiophosphinate esters remains unanswered. Hydrolysis of the phosphinate esters prior to sulfur transfer was thought to be a good solution as it may, in addition, be beneficial to the sulfur transfer step itself. This can be explained in terms of the relative ease of enolate formation (Figure 2.9). The NCH_2P methylene protons would not be so acidic and hence prone to sulfur insertion with an oxygen anion rather than a neutral ester.

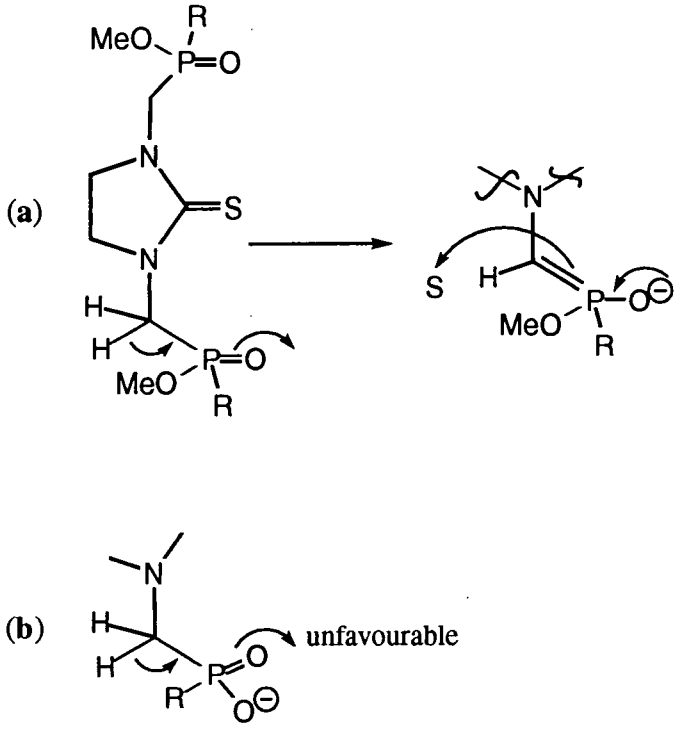

Figure 2.9 **a)** Possible problem with sulfur transfer
b) Methylene protons are less acidic with anion instead of ester

One possible route would require the cyclic aminal phosphinate esters as precursors which could then be treated with elemental sulfur to block the methylene bridge prior to removal of the esters with lithium hydroxide (Scheme 2.13). Sulfur transformation could then be achieved using P_4S_{10} for example, and finally, hydrolytic removal of the thiourea bridge would give the desired molecule. The replacement of P=O by P=S in such phosphinic acid derivatives has recently been reported by Harger. [25,26]

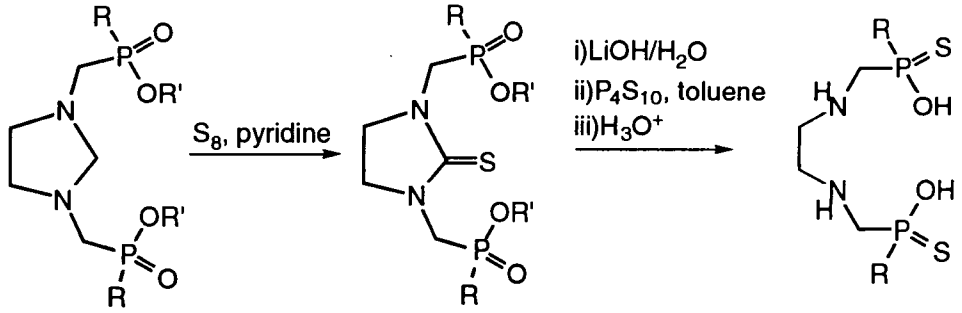

Scheme 2.13

Alternatively, the cyclic aminal phosphinate ester may be treated with DIBAL or sodium triethylborohydride to reduce the esters, allowing sulfur insertion into the P-H bond (Scheme 2.14).

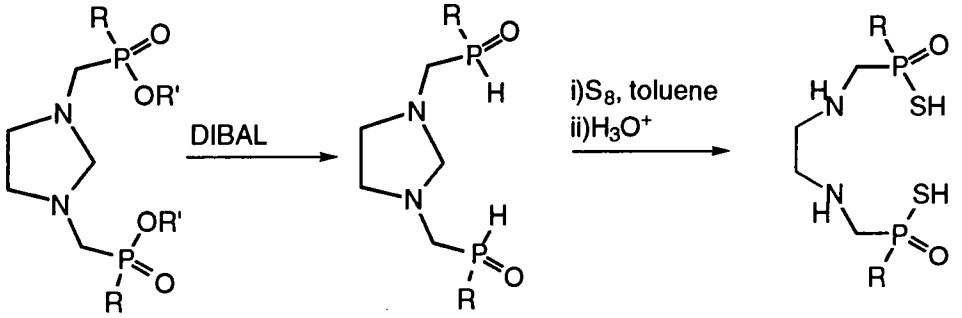

Scheme 2.14

Variations upon the route of phosphinic acid preparation/P=S conversion were envisaged. For instance, the methylene bridge of the aminal may be removed, and the amines protected prior to sulfur transfer by treatment with $PSCl_3$[25] or P_4S_{10} [26](Scheme 2.15).

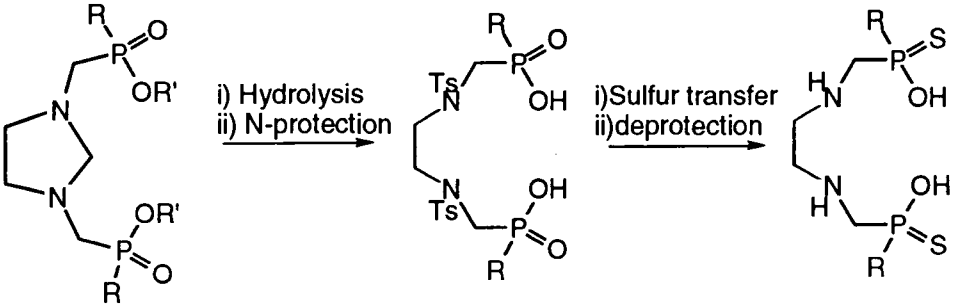

Scheme 2.15

This last proposed route was concentrated upon because, on paper at least, it looked the most accessible although all of these last three suggested routes avoid the possible problem of thiophosphinate ester hydrolysis at the final stage of synthesis.

The successful route - from P(O)OH to P(O)SH

The phosphinate ester (**39**) was prepared by reaction of ethane-1,2-diamine with freshly sublimed paraformaldehyde and $PhP(OMe)_2$ in dry tetrahydrofuran as described by Parker *et al.*[16] Purification by chromatography on alumina gave the ester as a colourless oil in 72% yield; in addition, methyl [(hydroxymethylene)phenylphosphinate] was isolated as a by-product. Hydrolysis in 6M hydrochloric acid with heating at reflux for 16 hours yielded the precursor amino-acid (**43**). Protection of the amine functionalities was effected by tosylation in aqueous sodium hydroxide solution, maintaining the pH around 10 by further additions of sodium hydroxide, to give (**44**) (Scheme 2.16). The pH was critical to the success of the reaction as basic conditions were required for the solubility of the amino-acid while very high pH conditions (>pH 11) merely served to convert tosyl chloride to the acid, leaving less tosyl chloride to react with the amino acid. Therefore, the optimum conditions required pH 8-10 with heating to 40°C as the reaction proceeds only very slowly. Isolation of the product ditosylamide in 65% yield with high purity was facilitated by precipitation with 4M hydrochoric acid to pH 2.

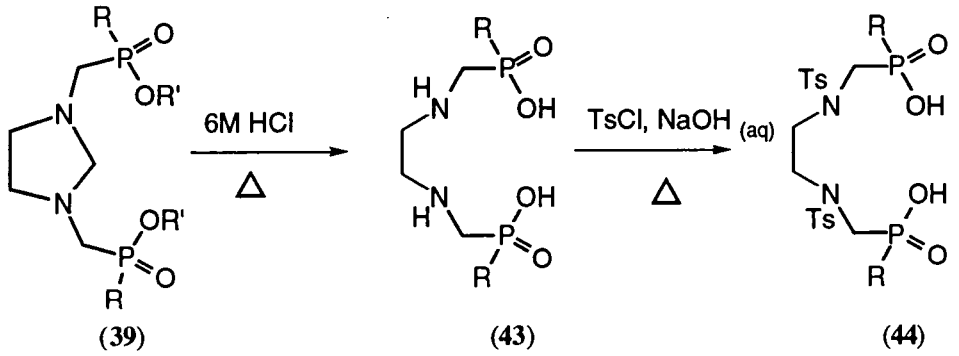

(39) (43) (44)

Scheme 2.16

Before the sulfur transfer could be attempted, the phosphinic chloride of the ditosylamide (**44**) had to be formed. The phosphinic chloride (**45**) was prepared in quantitative yield (^{31}P NMR analysis) as a 1:1 mixture of RR/SS and RS diastereoisomers by treatment with oxalyl chloride of a suspension of the ditosylamide in dichloromethane (Scheme 2.17), giving a clear solution. This was observed by ^{31}P NMR (δ_P 46.8 and 47.0) (Figure 2.10). The solvents and excess oxalyl chloride were removed under reduced pressure and the product was kept under high vacuum for 3-4 hours to ensure complete removal of all traces of the reagent prior to the P=O to P=S transformation.

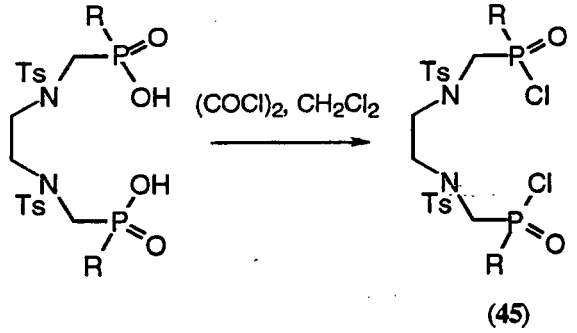

(45)

Scheme 2.17

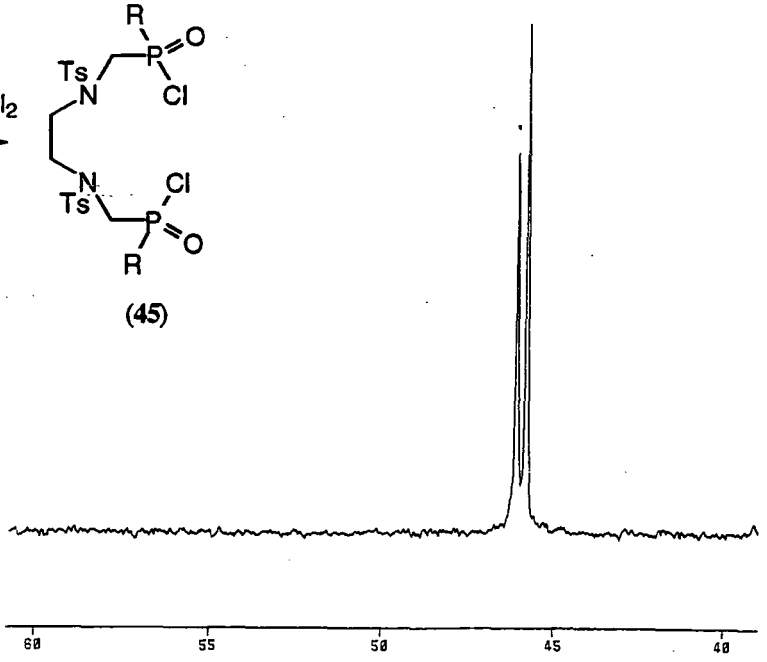

Figure 2.10 ^{31}P NMR shows diastereoisomers of (**45**)

Subsequent exchange of oxygen for sulphur gave the thiophosphinic chloride (**46**) in 94% yield, by heating in $PSCl_3$ with a catalytic amount of dimethylformamide as originally described by Coogan and Harger.[26] The ^{1}H NMR spectrum of the thiophosphinic chloride (**46**) showed an interesting, if somewhat complicated, splitting pattern (Figure 2.11/over). Although the unusual pattern shown between 3 and 5 ppm could be assigned to the methylene protons between nitrogen and phosphorus ($NC\underline{H}_2P$), there was initial difficulty in the absolute interpretation as the pattern was expected to account for the diastereoisomerism, phosphorus splitting and vicinal coupling (Figure 2.12a). ^{31}P NMR analysis showed a 1:1 mixture of diastereoisomers was present (Figure 2.12b). Complete assignment of the couplings shown in the ^{1}H NMR spectrum required acquisition of the spectrum at a higher frequency to spread out the shifts of the diastereoisomers (Figure 2.12c), and a ^{31}P decoupled ^{1}H spectrum in order to identify the phosphorus splitting (Figure 2.12d) by comparison. The result was surprising as the coupling to phosphorus was absent or too small to be observed for the proton resonating at higher frequency.

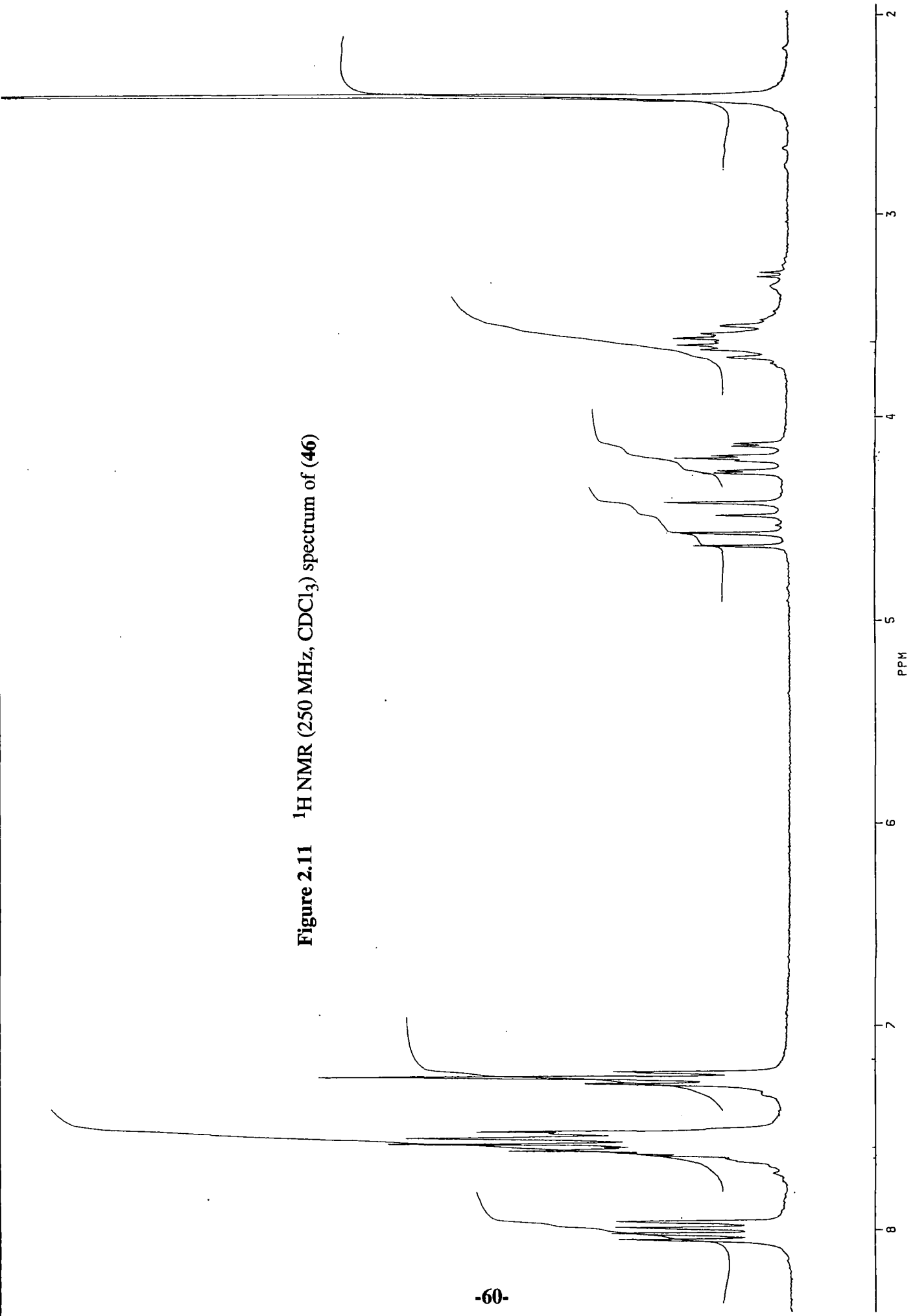

Figure 2.11 ^{1}H NMR (250 MHz, $CDCl_3$) spectrum of (**46**)

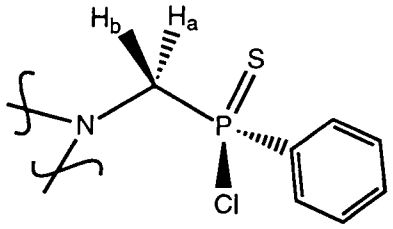

Figure 2.12a The chiral centre at phosphorus generates an ABX spin system for the diastereotopic methylene protons

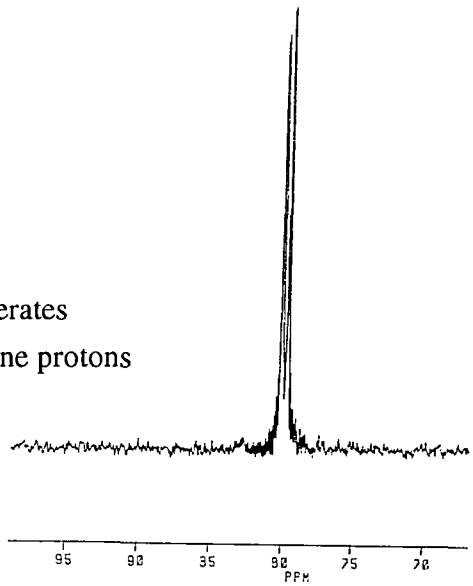

Figure 2.12b
^{31}P NMR spectrum showing two diastereoisomers

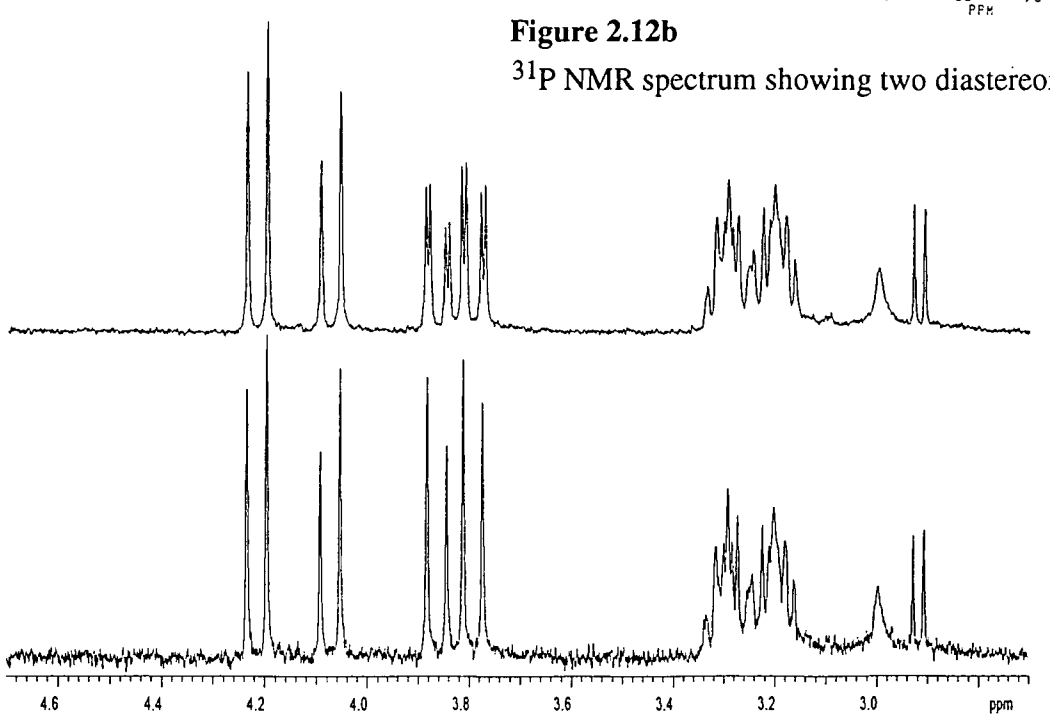

Figure 2.12c ^{1}H NMR (400 MHz, $CDCl_3$) spectrum of (**46**) showing $NC\underline{H}_2P$ protons

Figure 2.12d ^{1}H $\{^{31}P\}$ NMR (400 MHz, $CDCl_3$) spectrum of (**46**) showing $NC\underline{H}_2P$ protons

Having successfully synthesised the aminothiophosphinic chloride in high yield and purity, the conversion of the chloride to the acid and subsequent detosylation were expected to be trivial manipulations. However, the P-Cl bond of (**46**) showed remarkable stability with respect to hydrolysis and several unsuccessful attempts were made using a variety of conditions (Table 2.3) before complete hydrolysis to the thiophosphinic acid (**47**) was achieved in near quantitative yield by heating the thiophosphinic chloride (**46**) with 5M potassium hydroxide for 16h.

Table 2.3 Attempted hydrolysis of thiophosphinic chloride to thiophosphinic acid

Reaction conditions	Result
(**46**) dissolved in CH_2Cl_2, stirred vigorously with NaOH (pH 11), heated for 2 days.	no reaction
(**46**) dissolved in CH_2Cl_2, stirred vigorously with NaOH + phase transfer catalyst (cetyltrimethylammonium bromide), heated for 2 days.	no reaction
(**46**) added to HBr/acetic acid/phenol, heated 100°C	mixture of many species
(**46**) added to CH_3COONa/CH_3COOH at 25°C	P=S reverted to P=O
Solid (46) stirred in KOH (5M), 100°C, 16 h	**Quantitative yield of acid**

Detosylation of the protected thiophosphinic acid ligand was attempted under standard method of heating to reflux in hydrobromic acid/acetic acid with phenol. However, these conditions proved far too harsh and merely facilitated C-P and N-C(P) cleavage. Neither treatment with dissolved sodium metal in liquid ammonia under Birch conditions nor the use of samarium (II) iodide[10] with DMPU led to satisfactory detosylation. The ditosylated aza-phosphinic acid (**44**) was used to as a model for the sulfur-containing ligand in order to find a successful method of deprotection. Successful detosylation of the phosphinic model and the thiophosphinic ligand (**47**) to give (**48**), required gentle heating at 40°C in HBr/acetic acid in the presence of a ten-fold excess of phenol over a period of two days. The desired ligand precipitated from the reaction mixture as a pale yellow solid (77% yield) which was characterised as the dihydrobromide salt.

The overall synthetic route is summarised in Scheme 2.18

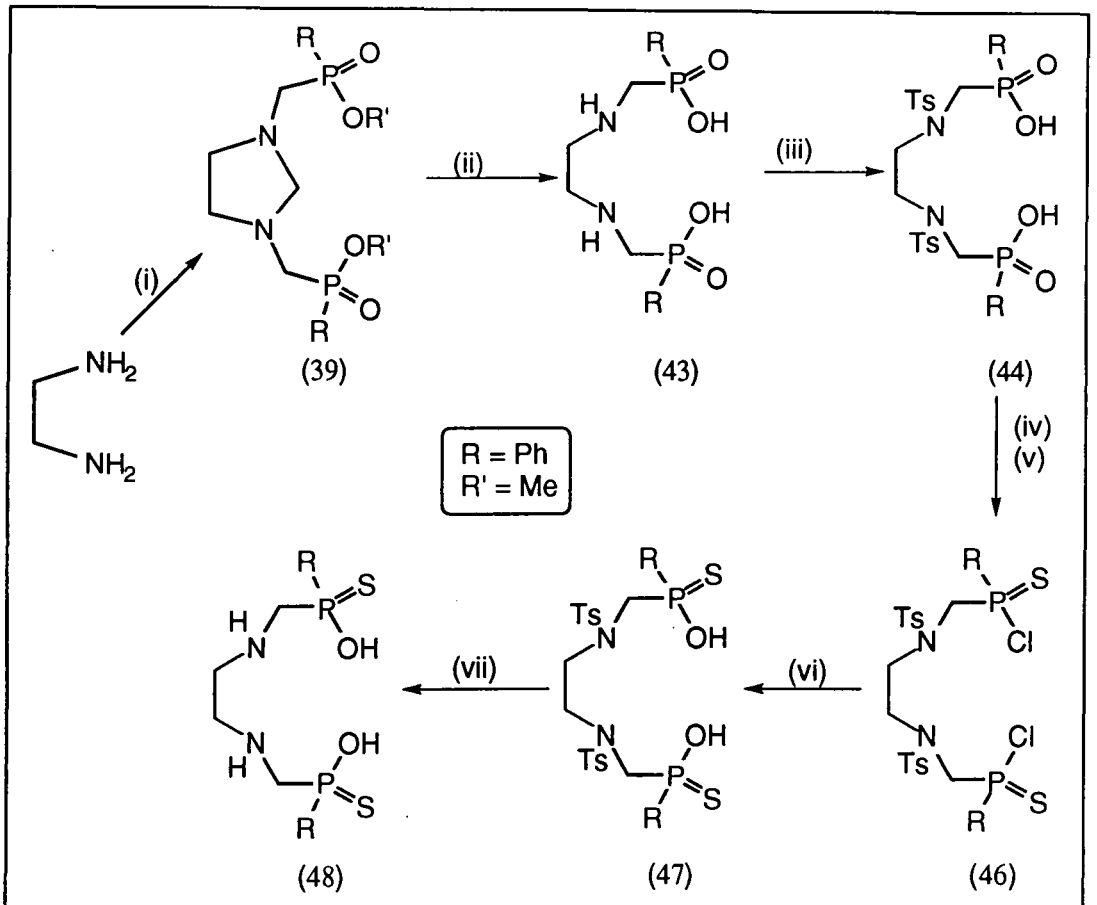

Scheme 1 (i) $(CHO)_n$, $RP(OR')_2$, THF (ii) 6M HCl, 100°C (iii) TsCl, $NaOH_{(aq)}$ pH10, 40°C, (iv).$(COCl)_2$, CH_2Cl_2 (v) $PSCl_3$, cat. DMF 110°C (vi) $KOH_{(aq)}$ 100°C (vii) HBr/CH_3CO_2H, phenol, 40°C

Scheme 2.18 Synthesis of aza-thiophosphinic acid ligands

With a feasible synthetic route proven for the phenyl-substituted thiophosphinic acid (**48**), the synthesis of the other proposed members of the series (from Figure 2.6 above) was then attempted. Preparation of the precursor phosphinates (**49**), (**50**) and (**51**) was achieved via analogous syntheses employing 1,3-diaminopropane or the dialkylphosphine, $RP(OR')_2$ [R=Ph, R'=Me; R=Me, R'=Et] starting materials. Hydrolysis in hydrochloric acid (6M) gave the desired phosphinic acids in near quantitative yield (Scheme 2.19). Tosylation of these acids proceeded under basic conditions (pH 8-10) as before, although the isolation of the P-methyl-substituted ditosylamides proved more difficult than their P-phenyl analogues due to their greater solubility in water. As a result, they did not precipitate from the reaction mixture with the addition of hydrochloric acid but remained in solution. After removal of the solvents, sparing amounts of cold water were required to wash the P-methyl ditosylamides and isolate them from the salts of *p*-toluenesulfonic acid. This procedure resulted in a lowering of the isolated yield for the P-methyl compounds.

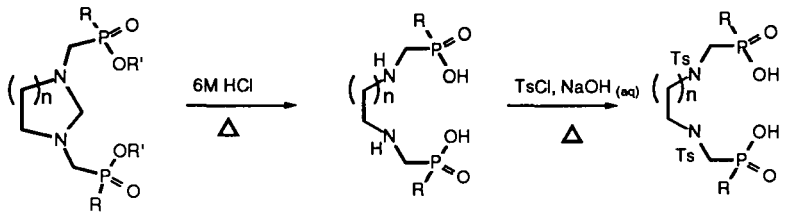

(**49**), R=Ph, R'=Me, n=2
(**50**), R=Me, R'=Et, n=1
(**51**), R=Me, R'=Et, n=2

(**52**), R=Ph, n=2
(**53**), R=Me, n=1
(**54**), R=Me, n=2

(**55**), R=Ph, n=2
(**56**), R=Me, n=1
(**57**), R=Me, n=2

Scheme 2.19

Preparation of the corresponding phosphinic chlorides was effected as described for (**45**) and sulfur transfer to phosphorus was achieved analogously with thiophosphoryl chloride and DMF catalyst. Although each analogue was successfully converted to its thiophosphinic derivative, none of the thiophosphinic chlorides could be produced in as high a yield or purity as the original phenylthiophosphinic chloride, (**46**). The P-methyl-substituted analogues were the most difficult to convert, although the diaminoethane derivative, (**59**) (Scheme 2.20), precipitated from the $PSCl_3$ solution and was isolated in high purity by filtration.

^1H NMR of these subsequent thiophosphinic chloride derivatives showed similar splitting patterns to (**46**).

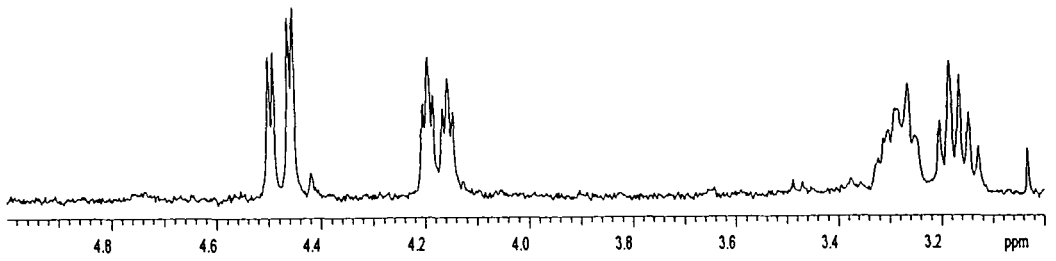

Figure 2.13a ^1H NMR (400 MHz) spectrum of (**58**) showing $NC\underline{H}_2P$ protons

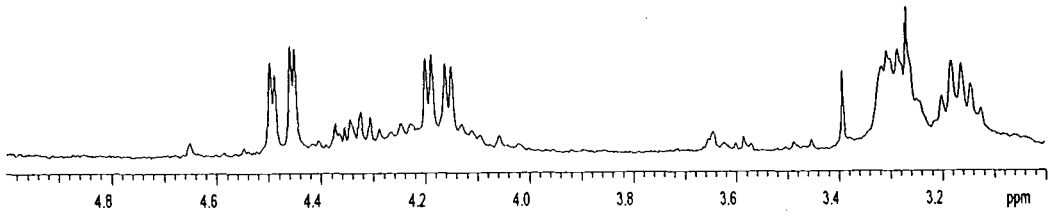

Figure 2.13b ^1H $\{^{31}P\}$ NMR (400 MHz) spectrum of (**58**) showing $NC\underline{H}_2P$ protons*

* Minor signals due to impurities are present in the ^1H $\{^{31}P\}$ NMR spectrum only, as this decoupling experiment was performed at a later date with a less pure sample than the original (a).

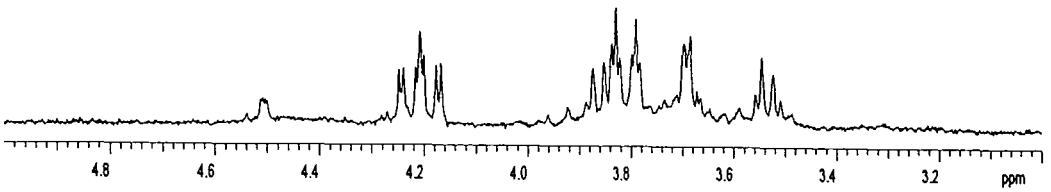

Figure 2.14a $^{1}H\{^{31}P\}$ NMR (400 MHz) spectrum of (**59**) showing $NC\underline{H}_2P$ protons

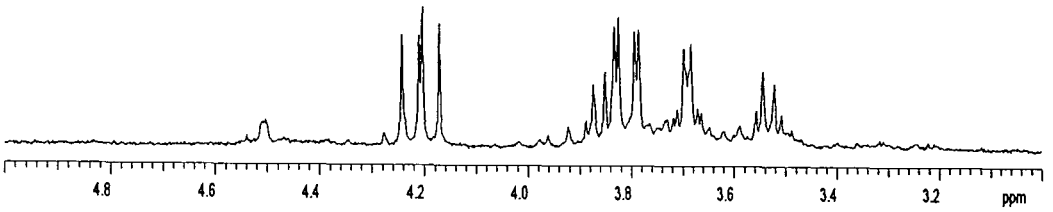

Figure 2.14b $^{1}H\{^{31}P\}$ NMR (400 MHz) spectrum of (**59**) showing $NC\underline{H}_2P$ protons

Similar stability of the P-Cl bond with respect to hydrolysis was observed for all subsequent derivatives (**58**) to (**60**), as the use of lower concentrations of potassium hydroxide or lower temperatures resulted in incomplete hydrolysis. Deprotection of the ditosylamides (**61**)-(**63**) was achieved by the same 'mild' reaction conditions with HBr/ acetic acid and phenol at 40-50°C for 2-3 days. The aminothiophosphinic acids (**64**) and (**66**) were isolated by dropping the reaction mixture into diethyl ether prior to isolation following centrifugation while a small amount of (**65**) precipitated from the HBr/acetic acid reaction mixture as the ligand-dihydrobromide salt in an analogous manner to that of (**48**). The ligands and intermediates gave ^{1}H NMR, ^{13}C NMR, ^{31}P NMR spectra, mass spectra and elemental analyses which were consistent with the structures shown.

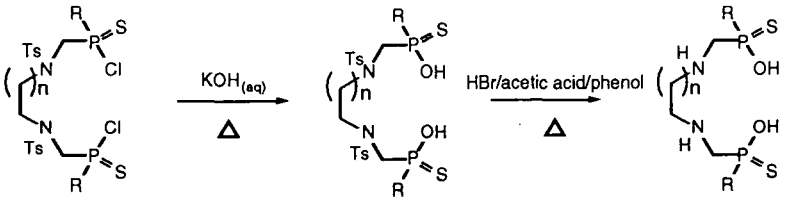

(**58**), R=Ph, n=2
(**59**), R=Me, n=1
(**60**), R=Me, n=2

(**61**), R=Ph, n=2
(**62**), R=Me, n=1
(**63**), R=Me, n=2

(**64**), R=Ph, n=2
(**65**), R=Me, n=1
(**66**), R=Me, n=2

Scheme 2.20

All four ligands were synthesised as a 1:1 mixture of RR/SS and RS diastereoisomers, which was evident both by ^{31}P NMR and ^{1}H NMR as exemplified by the P-methyl ligand (**65**) (Figure 2.15).

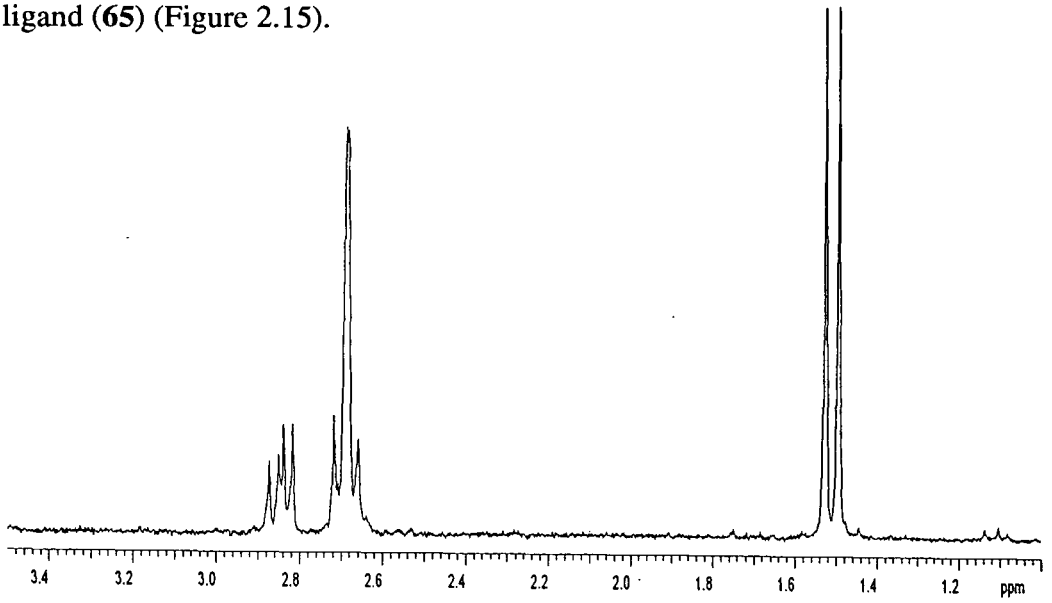

Figure 2.15a ^{1}H NMR (400 MHz) spectrum of (**65**)

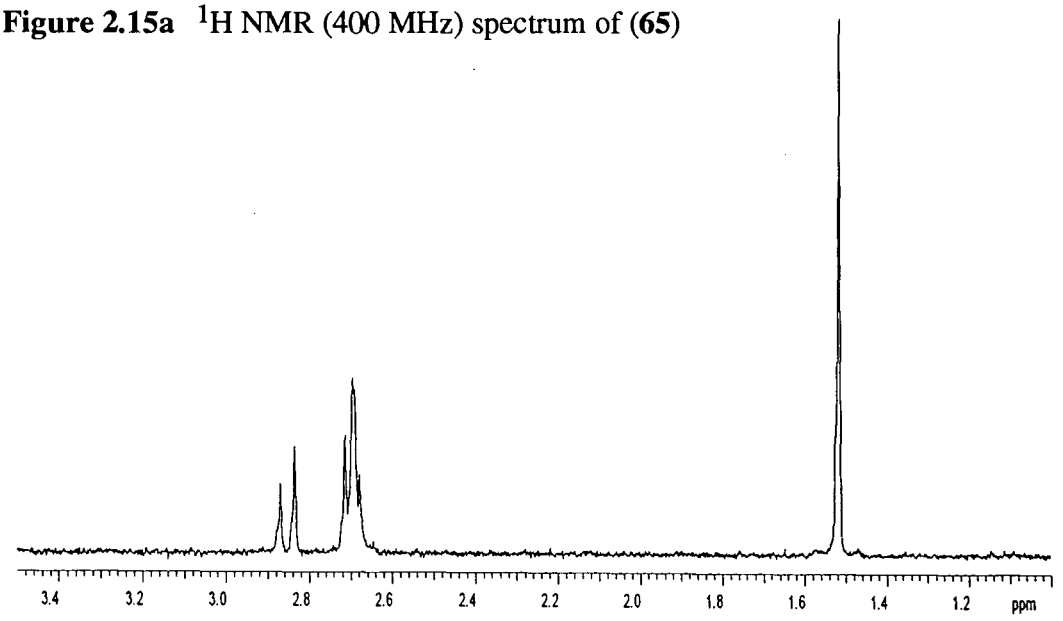

Figure 2.15b $^{1}H\ \{^{31}P\}$ NMR (400 MHz) spectrum of (**65**)

N-substituted aza-thiophosphinic acid ligands

A potentially useful extension to this ligand series could be ligands substituted at nitrogen. For example, methylation at nitrogen could affect the overall stability of the metals complexes formed with this type of ligands. Alkylation may render the nitrogen donors more electron-donating and offer more rapid formation or greater stability of the metal complexes formed. However, this type of substituent could also cause some destabilising interactions by the associated diaxial steric strain, in a similar manner to tetramethyl $12N_4$, where the diaxial interactions between methyl groups decrease complex stability.[27] Synthesis of such a ligand, (**67**), was investigated in order to gain more of an insight into the behaviour of this new class of ligand.

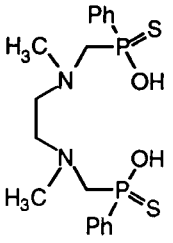

(67)

Reductive methylation of the thiophosphinic acid, (**48**), was attempted with formaldehyde and formic acid (Scheme 2.21) as described by Pine and Sanchez.[28] The volatility of the other reagents makes isolation of the product simple. Although N-methylation was successful, the thiophosphinic acid functionality was lost by replacement of sulfur by oxygen, yielding (**68**), which is, itself, a new aza-phosphinic acid ligand.

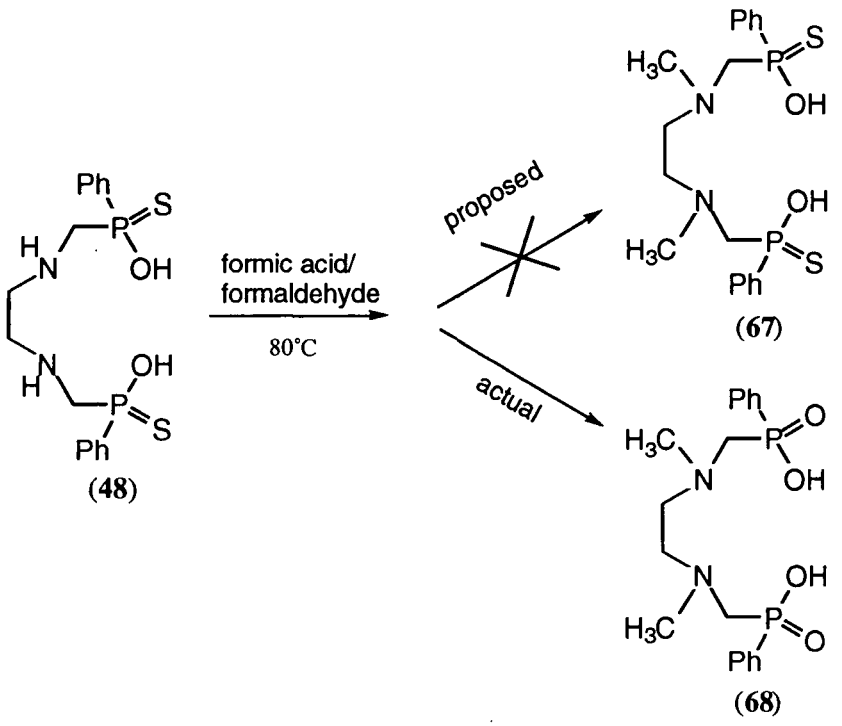

Scheme 2.21 Reductive methylation of aza-thiophosphinic acid ligand

Sulfur transfer to reform the thiophosphinic acid of this new N-methylated ligand, (**68**), was attempted under the previous conditions using thiophosphoryl chloride and a catalytic amount of DMF. However, ^{1}H NMR analyis revealed that some other undesirable process had taken place as the spectrum showed a mixture of products and lacked any remnants of recognisable features such as the NCH_2P protons. The only difference between this reaction and previous sulfur transfer reactions performed under identical conditions is the substituent on nitrogen. Therefore, it is reasonable to

conclude that successful employment of the N-protecting toluenesulfonyl groups in the original reaction scheme prevented the nitrogen lone pair from interfering in the subsequent reactions at phosphorus. In contrast, the N-methyl substituents have a detrimental effect by allowing attack of the nitrogen nucleophile at the electrophilic phosphorus centre.

It was apparent that sulfur transfer would not prove easy following methylation and another method of N-methylation of the thiophosphinic acid was sought. A milder route was then attempted utilising a procedure described by Hemo and Charles,[29] involving treatment of the thiophosphinic acid (**48**) with aqueous formaldehyde at 60°C for 30 minutes and subsequent reduction with sodium borohydride. However, the result was identical: N-methylation of the ligand was accompanied by the replacement of sulfur by oxygen.

Corresponding dithiophosphinic acids

It is possible that similar ligand systems may be synthesised incorporating the dithiophosphinic acid moiety, that is, RR'P(S)(SH). This would have the effect of lowering the pKa further than the mono-thio systems and removing the chiral centres from the ligands which give rise to diastereoisomers prior to complexation. However, the absolute stability of such systems is uncertain as the analogous thiophosphinic acids have a tendency to revert to phosphinic acids under certain conditions, and dithio systems may be even less stable.[30]

An attempt was made to synthesise the dithiophosphinic analogue of (**48**) by treating the appropriate thiophosphinic chloride (**46**) with excess sodium thiolate in aqueous solution with heating over several hours. However, the reaction mixture contained none of the desired ligand.

2.3 Solution Complexation Behaviour

Electrospray Mass spectrometry

Complexation was first investigated by electrospray mass spectrometry (ESMS) because it is a soft ionisation technique which allows detection of intact metal complexes without the fragmentation observed with many other mass spectroscopy techniques. The major isotope patterns are presented and the software allows the modelling of the isotope pattern expected for a particular molecular formula which is a particularly useful diagnostic tool when studying metal complexes. Many metals, such as copper and rhenium, have more than one major stable isotope each with a different

relative abundance, and modelling allows a clearer indication of the validity of the 'envelope' of the major peak(s) observed experimentally.

Complexation of all four ligands with copper was initially investigated by ESMS. The negative ion mode of operation produced the best results, showing the copper complexes as bromide adducts and isotope patterns which correlate with these structures (Figure 2.16). The ESMS spectra were consistent with the formation of neutral copper(II) complexes picking up bromide in the negative ionisation process.

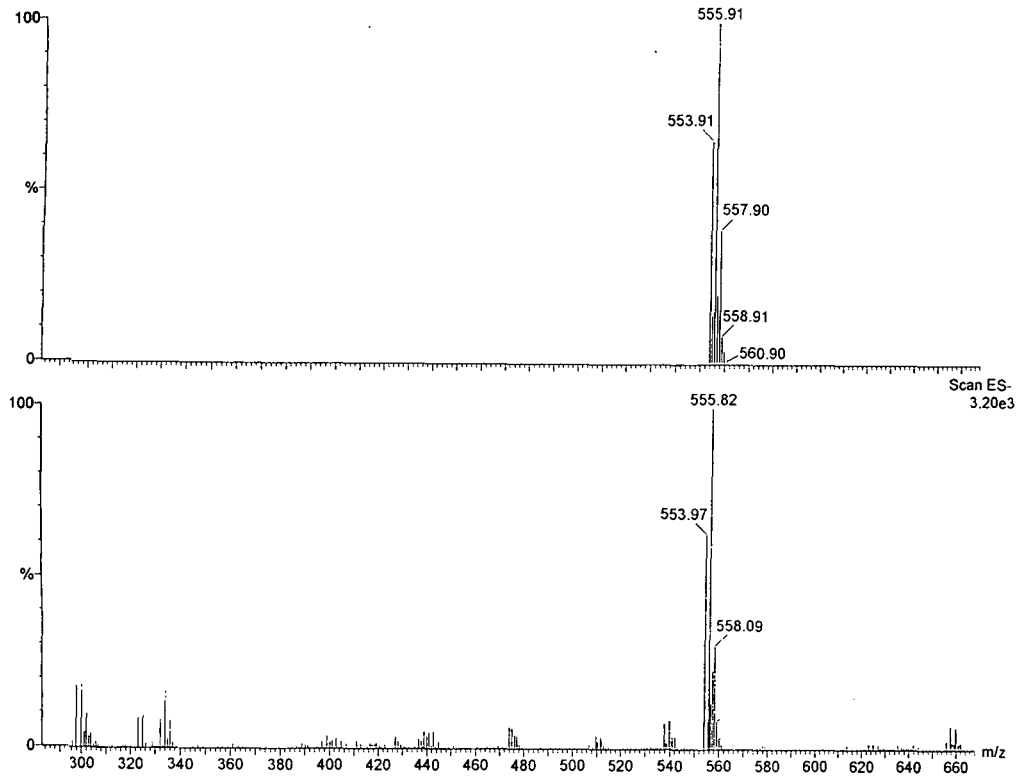

Figure 2.16 ESMS$^-$ spectrum of [Cu(**64**)Br$^-$] (bottom) with isotope model (top)

Complexation with rhenium

Before ligand complexation with rhenium could be attempted, a precursor rhenium complex in the correct oxidation state (V) with an oxo-rhenium core had to be prepared due to the inherent difficulties associated with rhenium substitution. The favoured complex for this task is normally [$ReOCl_3(PPh_3)_2$] (Ch.1, 1.6 & 1.7) which was duly prepared according to the method of Wilkinson.[31] The documented difficulty with the labile axial position *trans* to Re=O (section 1.6) was also experienced as the reaction solvent, ethanol, was found to occupy this position upon characterisation of the complex as $Re(O)Cl_2(EtOH)(PPh_3)_2$. Due to this lability, the substitution was easily reversed by dissolving the greeny-brown dichloro complex in dichloromethane and stirring vigorously with 6M hydrochloric acid. The desired trichloro derivative precipitated from the mixture as a yellow-green solid. Due to the low solubility of the oxorhenium precursor, it was suspended in benzene prior to complexation, and the

ligand (**48**) was added as a solution in methanol. After heating the mixture under reflux for 16 hours, the complex was isolated as a deep pink solid (Scheme 2.22).

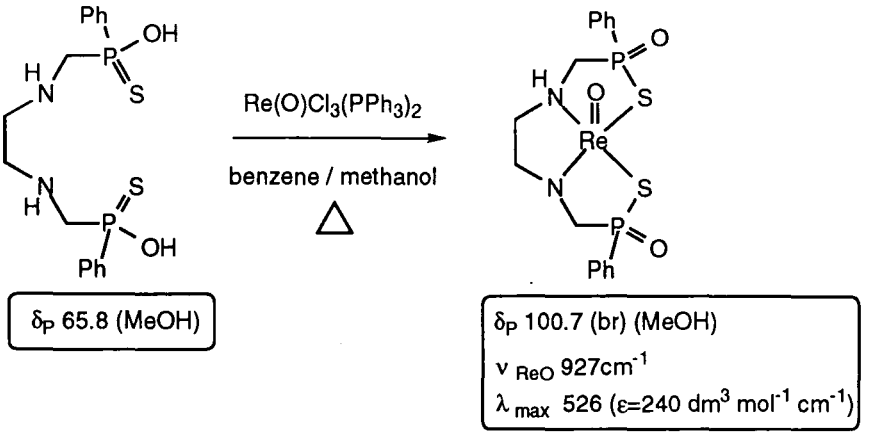

Scheme 2.22 Complexation of ligand (**48**) with oxorhenium

Further evidence for this complex was given by the electrospray mass spectrum and the excellent correlation with the isotope model (Figure 2.17). The two stable isotopes of rhenium (185 and 187) are observed in their expected relative abundances as oxorhenium complexes of the ligand (**48**). The peaks correspond to the formation of a neutral complex (that is, deprotonation of one amine N-H) with the loss of a further proton occurring in the electrospray ionisation process with the negative ion mode.

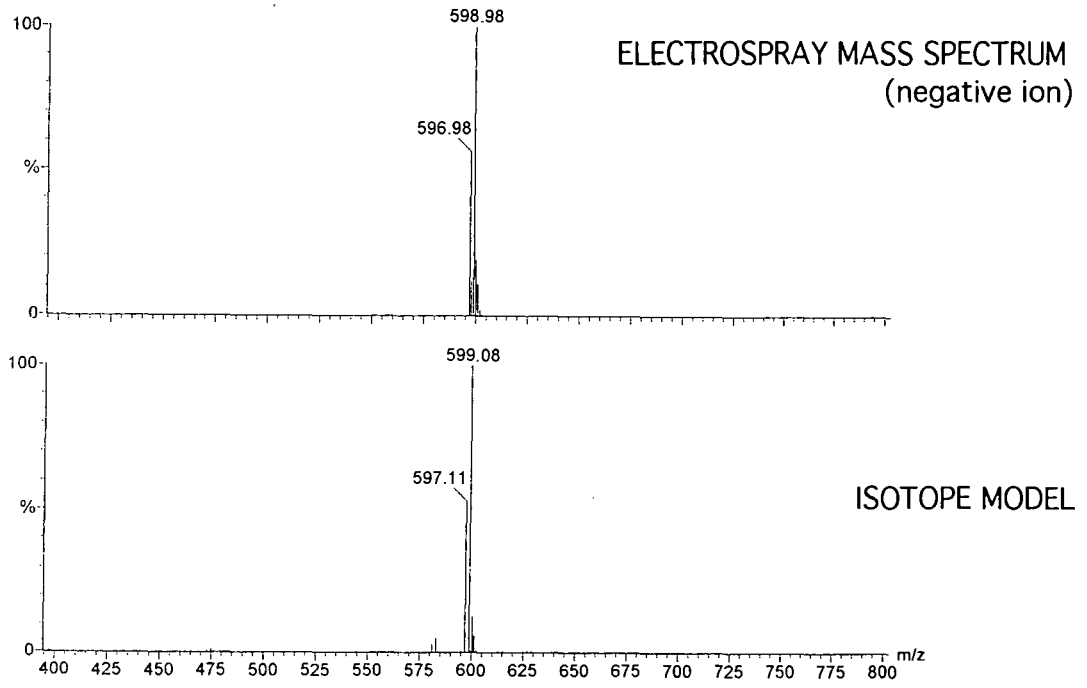

Figure 2.17 ESMS$^-$ spectrum of [Re(O)(**48**)] shows excellent correlation with model

Preparation of the analogous oxorhenium complex with the propylene ligand, (**64**), was attempted under identical conditions. However, the resulting black oil proved difficult to purify and characterise.

Isolation of the copper complexes

Addition of equimolar amounts of ligand (**48**) and Cu^{2+} in the form of a triflate, perchlorate or tetrafluoroborate salt in methanol led to the precipitation of a dark green solid. Attempts to redissolve the solid after its isolation were unsuccessful, even in DMF or DMSO. Heating in DMF did, however, result in solvation but the compound reprecipitated upon cooling only slightly. The deep green colour showed that some type of complex was present, but its lack of solubility in any solvent suggests that it is oligomeric in nature rather than a discrete molecule.

A similar result was obtained when the ligand was treated in the same manner with zinc(II) triflate, nickel(II)chloride and cadmium(II) triflate which yielded colourless, pale green and colourless solids respectively. The infrared spectra of these oligomeric complexes showed some similar features to one another. Combustion analysis confirmed the n:n (n=integer) stoichiometry of the compounds formed with (**48**) and each of these metals.

The isolation of the discrete complexes proved difficult due to this oligomerisation in methanol but was possible in dilute methanol solution (< 5 mmol dm^{-3}). Analysis by ESMS confirmed the 1:1 stoichiometry and the formation of discrete rather than oligomeric species. Complexation occurred readily in aqueous solution and the products remained in solution. The ligand, however, exhibited a low solubility in water which led to only dilute solutions being employed for complexation.

HPLC analysis

Further investigation of the solution complexation behaviour of the ligands with copper was undertaken by HPLC analysis since this method of quality control is often used in radiopharmaceutical development. A study of the 'cold' complexation using HPLC as a quality control may be directly analogous to preparation of radiotracers of these ligands and radiocopper. Both P-phenyl substituted ligands were studied as their phenyl chromophore allows UV detection (λ_{abs}=254 nm). HPLC analysis of a methanol solution of the free ligand (5 mmol dm^{-3}), a 1:1 ligand-copper solution, and a 2:1 ligand-copper solution was undertaken for both ligands, (**48**) and (**64**).

The HPLC trace for the free ligand (**48**) showed a single peak with a retention time of around 4-5 minutes, confirming the high purity of the complex. For the 1:1 complex, a retention time of 11 minutes was observed while another, albeit minor, peak was present in the chromatogram of both the 1:1 and 2:1 ligand/metal preparations with a retention time of 8 minutes (Figure 2.18). Neither variation of the ligand/metal ratio nor the concentration of the solution appeared to affect the formation of this unknown species.

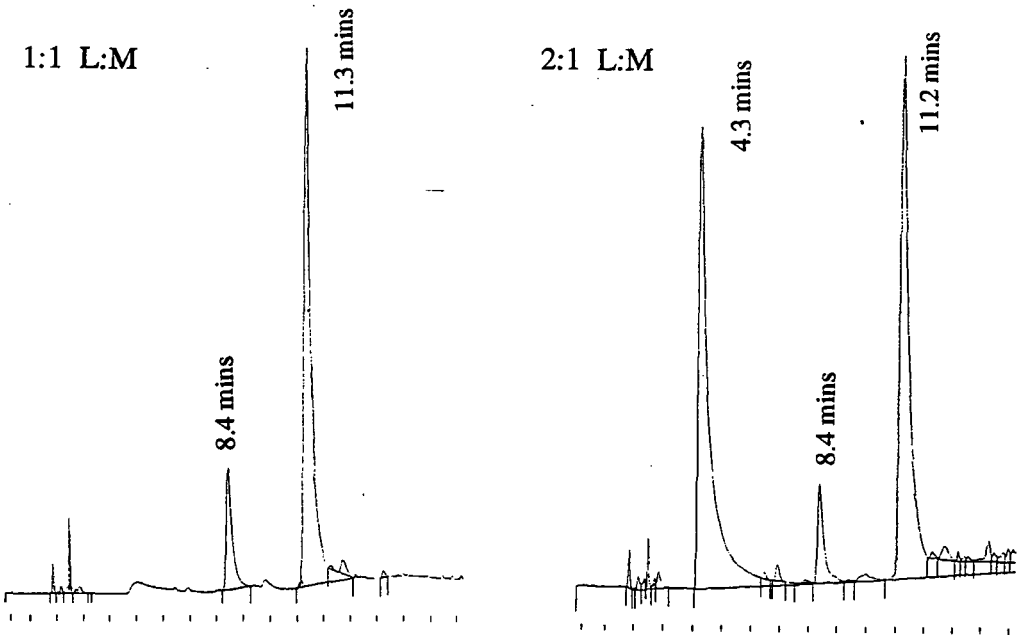

Figure 2.18 HPLC traces of Cu(II)(**48**)

An analogous result was observed for copper complexation by ligand (**64**): complexation was immediate, little or no unbound ligand was observed with a 1:1 L/M solution, and a further, unknown species was observed at a shorter retention time (7.7 minutes) than the copper complex of the ligand (at 12.5 minutes).

Table 2.4 Summary of HPLC analysis of Cu(II) complexation with (**48**) and (**64**)

	Retention Time / minutes (% species)		
Preparation	free ligand	unknown impurity	Cu complex
free ligand (**48**)	4.7		
1:1 L/Cu (**48**)	little oberved	8.4 (14%)	11.3 (82%)
2:1 L/Cu (**48**)	4.3 (39%)	8.4 (5%)	11.2 (48%)
free ligand (**64**)	4.2		
2:1 L/Cu (**64**)	little observed	7.7 (11%)	12.5 (21%)

Attempts were made to identify the unknown species produced by copper(II) and ligand (48) with a retention time at around 8 minutes. Less than one milligram of the compound was isolated by preparative HPLC, and ESMS analysis of this sample showed none of the Cu(**48**) complex but some species with a mass corresponding to the ligand with two sulfur atoms replaced by oxygens.

The absolute stability of ligand (**48**) in methanol solution was also shown by the absence of change in its HPLC profile over a period of 6 hours, and the observation of an unchanged ^{31}P NMR spectrum over five days at room temperature.

Ultraviolet and Visible Photospectroscopy of Ligands with Copper

The UV-visible spectra gave data that was consistent with the formation of 1:1 complexes with copper (from $[Cu(BF_4)_2]$) in water. The wavelengths and extinction coefficients of absorption maxima in the visible region were compared with the values obtained for the analogous substituted aza-phosphinic acid ligands with copper in previous work by Eleanor Cole.[20] The aza-thiophosphinic acid ligands formed green complexes as reflected in the values given (Table 2.5).

Table 2.5 Comparison of λ_{max} (nm) and extinction coefficients for copper(II) complexes with P(O)OH and P(O)SH ligands in H_2O

Ligand		λ_{max} / nm (H_2O)	ε/dm^3 mol^{-1} cm^{-1}	λ_{max} / nm (H_2O)	ε/dm^3 mol^{-1} cm^{-1}
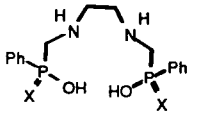	X=O[a]	710	40		
	X=S[b]	598	300	332	8300
	(48)				
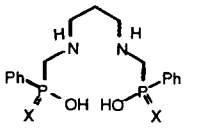	X=O[a]	774	20		
	X=S[b]	628	350		
	(64)				
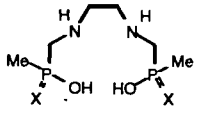	X=O[a]	725	40		
	X=S[b]	598	150	334	10 000
	(65)				

a From reference 20

b This work

Comparison of the general trends shows that the thiophosphinate complexes absorb around 600 nm while the analogous phosphinate complexes absorb at over 700 nm. Within each ligand series, the trends appear similar: the phosphorus substituent has little effect, while the change from a five- to six-membered chelate ring shows a pronounced difference. The ligands incorporating a propanediamine unit have slightly higher λ_{max} values compared to the ethylenediamine ligands, suggesting that they engender a weaker ligand field. Further evidence for this is given by the disappearance of this absorption band from the spectrum of Cu(**64**) with time (several days). The solution turned colourless with time, indicating that Cu(II) had been reduced to Cu(I). The corresponding ethylenediamine-based complex, Cu(**48**), showed only a slight loss of colour intensity over the same period. The similarity of the λ_{max} values for Cu(**48**) and Cu(**65**) - differing only in phenyl and methyl phosphorus substituents respectively - is consistent with the metal binding remaining unaffected by the substituent at phosphorus.

NMR titrations

In an attempt study the metal binding of the ligands, NMR titrations were performed by adding small increments of a solution of the metal (0.1M) to a sample of the ligand (0.01M) and monitoring any shift in the NMR spectrum. Since the Cu(II) ion is paramagnetic, an attempt was made to determine the stability constant of the Cu(I) complex using $[Cu(CH_3CN)_4BF_4]$ in a solution of acetonitrile/water (1:1) followed by ^{31}P NMR.

After only 4 values had been measured with Cu(I) corresponding to M/L=0.4, a small but sharp peak was observed in the ^{31}P spectrum at δ_P 18.6 ppm. After two further additions of metal (M/L=0.6), the phosphinate peak was even more pronounced and some precipitate had formed. The solution in the NMR tube was green, indicating that some Cu(II) species had been created in addition to the desulfurisation of the ligand to give its phosphinate analogue.

Attention then turned to zinc as a tetrahedral model without the redox chemistry of copper. The same procedure was carried out using zinc triflate in the same solvent system at the same concentration. The difference in the change of shift was noted and the results plotted as M/L with change in the chemical shift. However, a large scatter in the points was observed as well as a continuing increase rather than reaching a plateau. This behaviour is consistent with only very weak binding of the metal, under these conditions.

Protonation constants

The protonation constant for the thiophosphinic acid ligand was determined using potentiometric titrations (by Hayati Sari at the University of Newcastle) followed by an iterative least-squares analysis carried out by Dr Ritu Kataky at the University of Durham. Titrations were carried out in a thermostatted cell at 25°C at an ionic strength of 0.1 mol dm^{-3} tetramethylammonium nitrate, using tetramethylammonium hydroxide (0.05 mol dm^{-3}) as the base. The latter solution was calibrated by titration against a standard solution of hydrochloric acid (0.02 mol dm^{-3}). Incremental additions to the cell containing the ligand in the background electrolyte were controlled by a computer which allowed the volume added and time between the additions to be adjusted. The results are tabulated and presented together with pK_a values for similar ligand systems (Table 2.6).

Table 2.6 Nitrogen protonation constants for disubstituted ligands

Ligand	pK_1	pK_2
en[a]	9.89	7.08
EDDA[a]	9.57	6.48
EDDPi[b]	8.08	4.98
(**53**)[c]	8.35	5.33
(**54**)[c]	8.91	7.00
(**43**)[c]	8.63	4.34
(**48**)[d]	8.19	5.09

[a] Data from reference 9 [c] Data from reference 16

[b] Data from reference 12 [d] This work

The values shown are the constants for protonation of the nitrogen atoms (Figure 2.19), as the thiophosphinic acid oxygens have lower protonation constants which could not be evaluated by this method.

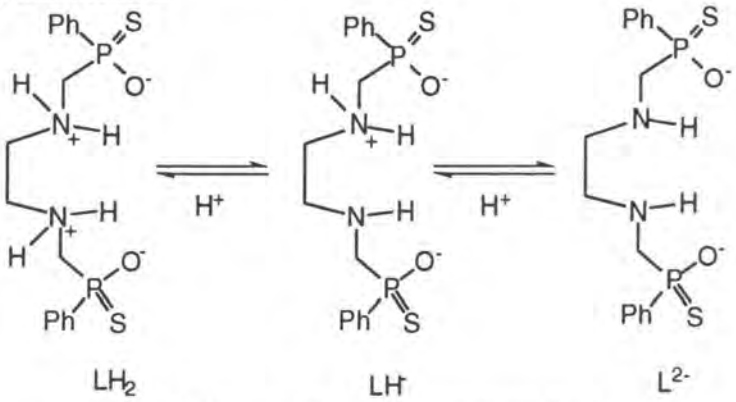

Figure 2.19 Protonation constants for (**48**)

The speciation diagram (Figure 2.20) shows the percentage of these ligand species present in solution at a given pH. For example, at pH 3 only the LH_2 species is present, whereas, at just above pH 8, there is a 50% mixture of the free ligand and LH species, showing the pK_a.

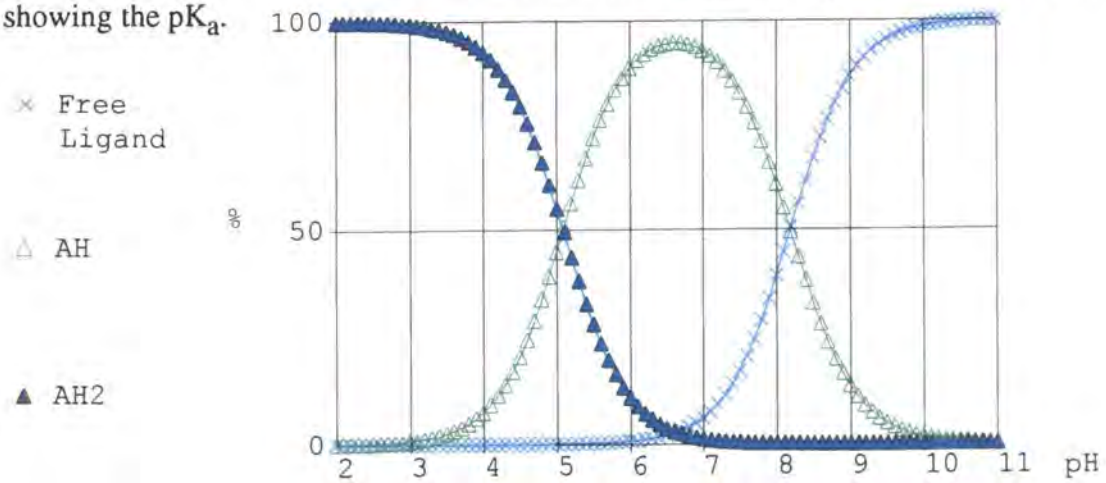

Figure 2.20 Speciation diagram for the variation of protonation behaviour of ligand (**48**) with pH.

Inspection of Table 2.6 shows that the effects of a different phosphorus substituent upon the protonation behaviour for the phosphinic acid ligands are negligible. The second pK_a for (**43**) is slightly lower than that of the corresponding methylphosphinate (**53**) due to the electron withdrawing effect of the phenylphosphinate group rendering the amine less basic.

Stability constants for copper complex formation

The stability constant for the formation of Cu(II)(**48**) was determined and analysed, again by Ritu Kataky, using a similar pH-potentiometric procedure to the method used for the determination of the protonation constants for the pure ligand (**48**) above. A 1:1 ratio of the ligand and copper(II) solutions in an electrolyte background of tetramethylammonium nitrate (0.1M) was stirred in a thermostatted cell at 25°C and tetramethylammonium hydroxide was used as the titrant.

The metal-ligand and protonated metal-ligand species were observed (Scheme 2.22) and their formation constants were determined using a non-linear least squares analysis. Formation of some $MLOH^-$ was also observed although the formation constant was small. The values are tabulated with those of the corresponding aza-phosphinic acid ligands for comparison (Table 2.7).

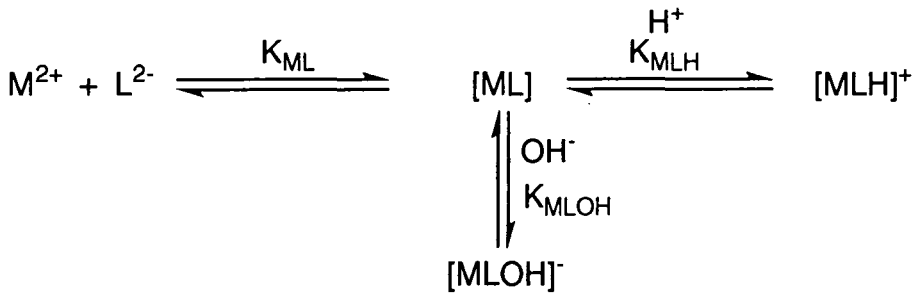

Scheme 2.22 Solution complexation equilibria

Previous work[16,20] showed that the 1:1 complexes formed with substituted aza-phosphinic acid ligands were relatively weak and bound only through the nitrogen donors while the oxygens did not appear to contribute to the overall binding of the complex. The $\log\beta_{ML}$ value obtained for the thiophosphinic acid ligand (**48**) is higher, as expected, and is consistent with the visible spectrophotometric data which indicated that binding to copper takes place through both sulfur and nitrogen.

Table 2.7 Formation constants for copper complex formation of (**43**), (**53**), (**54**), and (**48**) (298K, I=0.1 mol dm^{-3} NMe_4NO_3)

Compound	log β CuL	CuLH	CuLOH
(**53**)[a]	8.03		
(**54**)[a]	7.43		
(**43**)[a]	6.56		
(**48**)[b]	10.13	13.85	0.1

[a] Data from reference 16 [b] This work

X-ray analysis

Attempts were made to obtain a crystal of the Cu(**48**) complex for X-ray analysis. Solutions of different concentrations containing equimolar amounts of ligand and Cu^{2+} were left to stand. However, only colourless crystals formed and were found to be the amino-phosphinic acid ligand (**43**), providing further evidence for the desulfurisation of the ligands with time after complexation with copper. The disappearance of the green colour was consistent with the reduction of Cu(II) to Cu(I) with, possibly, concomitant ligand oxidation to form the phosphinic acid from the thiophosphinic acid.

The X-ray structure was solved by Janet Moloney (Figure 2.21a and Appendix A). The ligand is present as its zwitterionic form, with two protons positioned on each nitrogen and the phosphinate oxygens entirely deprotonated. The amine protons were actually located rather than modelled. The hydrogen bonding interactions between the phosphinate oxygen and the amine protons of another ligand molecule are extremely strong (Figure 2.21b). For example, the distance O1-H(3)N is only 1.84(5) Å or H(2)N-O3 is 1.83(5) Å for these linear interactions (see Figure 2.21 and Appendix A) while a similar hydrogen bond interaction which is non-linear, O1-H(4)N, is longer (2.52(4) Å). The incredible packing diagram along the a-axis shows how these strong interactions (distance ~ 1.8Å) govern the stacking of the molecules in their dimers (Figure 2.22). Each ligand has three water molecules of crystallisation associated.

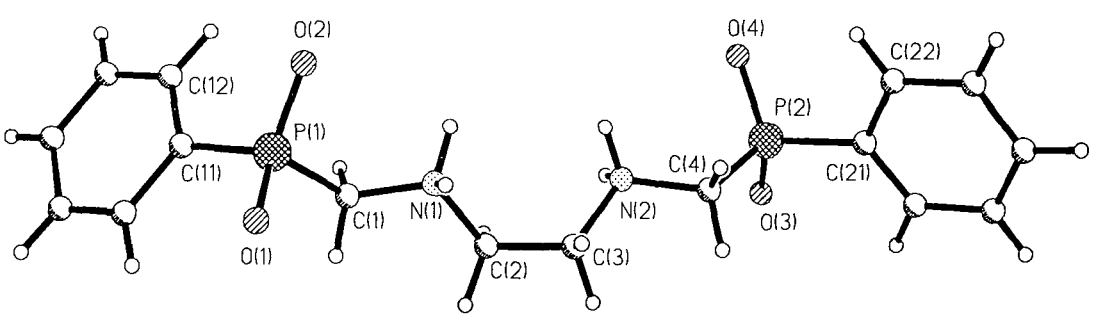

Figure 2.21a X-ray crystal structure and numbering system of (**43**)

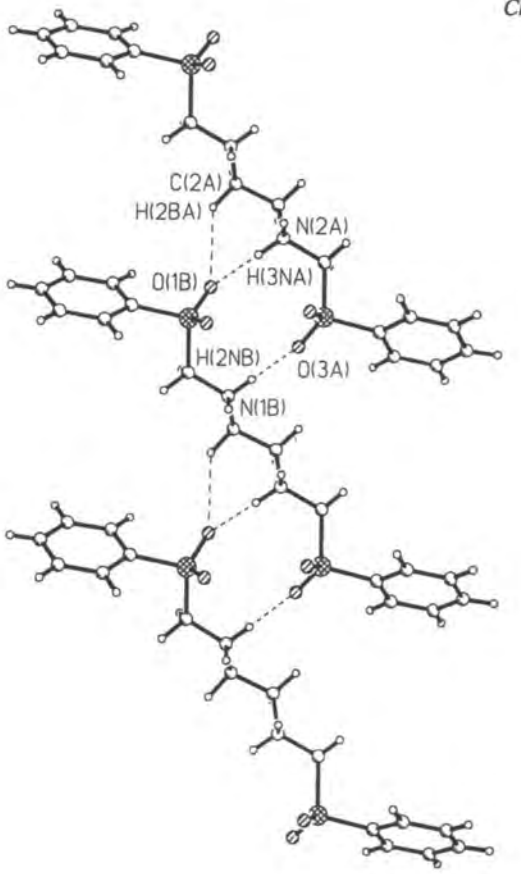

2.21b Packing diagram in the X-ray crystal structure of (**43**) viewed along the **c** axis

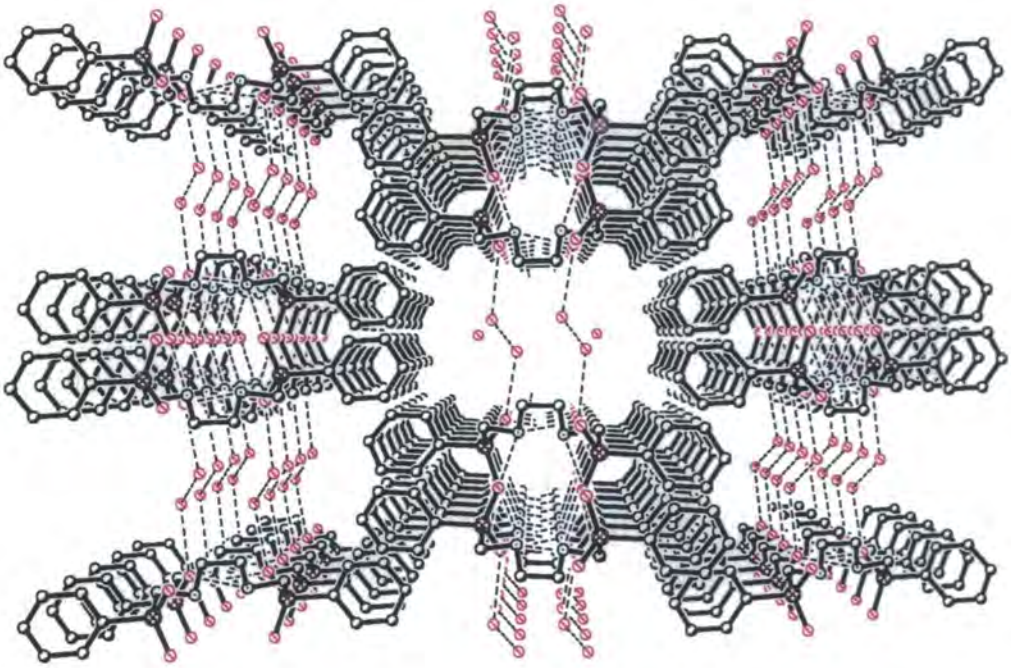

Figure 2.22 Packing diagram in the X-ray crystal structure of (**43**) viewed along the **a** axis. Hydrogen atoms are omitted for clarity

Square Wave Voltammetry

In an effort to gain more of an insight into the redox behaviour of the ligand (**48**) upon copper(II) complexation, square wave voltammetry was carried out by Dr Ritu Kataky at the University of Durham. The current passing through the electrolyte was monitored as a function of the applied stepped voltage by this technique. An aqueous solution of the thiophosphinic acid ligand (**48**) (0.001 mol dm^{-3}) was prepared with the addition of one molar equivalent of a standard sodium hydroxide solution (to neutralise one of the ligand protons) and a background electrolyte of tetramethylammonium nitrate (0.1 mol dm^{-3}). A solution of copper(II) nitrate (0.01 mol dm^{-3}) was similarly prepared in the aqueous electrolyte. The peaks observed correspond to the electroactive species present and the peak height relates directly to the concentration of the species.

The samples of the background (containing an equimolar amount of sodium bromide with the ligand above), a second background containing copper, and unbound ligand in the electrolyte, showed no evidence of any electroactive species present in the voltage range (0-1 V) (Figure 2.23). With the ligand and copper(II) salt present, the oxidation of a single species was observed at 0.9 V with concomitant precipitation of a small amount of a pale green solid from the electrolysed solution. This species is likely to be a dimer or oligomer as described above. The electroactive species observed at 0.9 V is also consistent with the formation of a dimer or an oligomeric species as the redox behaviour characteristic of copper(II) normally occurs at a lower potential than that of the species observed (in the region of +300 to -200 mV).[32]

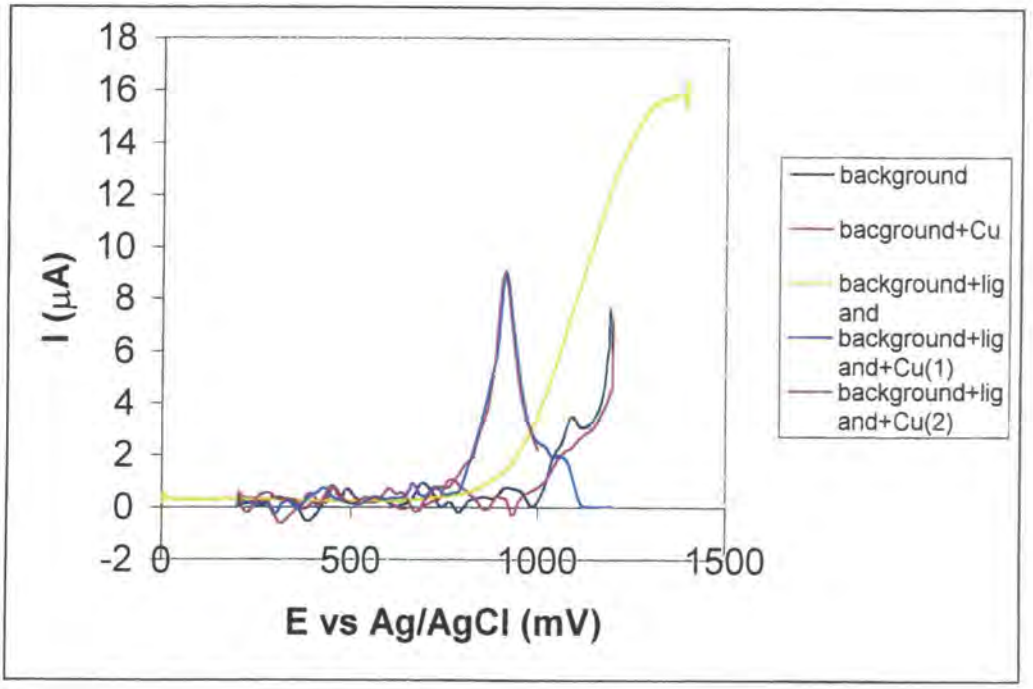

Figure 2.23 Square wave voltammogram of (**48**), Cu^{2+}, and Cu(**48**) in tetramethylammonium nitrate/NaBr background

Molecular Modelling

Modelling of the copper complexes of the ligand series was performed by Christopher Edlin using the Sybyl 6.3 programme (Tripos UK Ltd) at Zeneca Specialties, Blackely. The charge distribution of the complexes was calculated using MNDO (minimum neglect at differential overlap) force field routine, and the structures were then minimised using an AM1 force field (Figure 2.24 and 2.25). The models are consistent with the above results and discussion as they show that the phosphorus substituent has little effect upon the metal binding, while the size of the chelate rings does affect the overall geometry. The complexes of the ethanediamine-based systems with three 5-membered chelate rings show a distorted square planar geometry, while the propanediamine systems incorporating a 6-membered chelate ring tend more to a distorted tetrahedral arrangement. These models are in agreement with observations that the copper complex of ligand (**64**) tends to Cu(I) more easily than the copper complex of ligand (**48**).

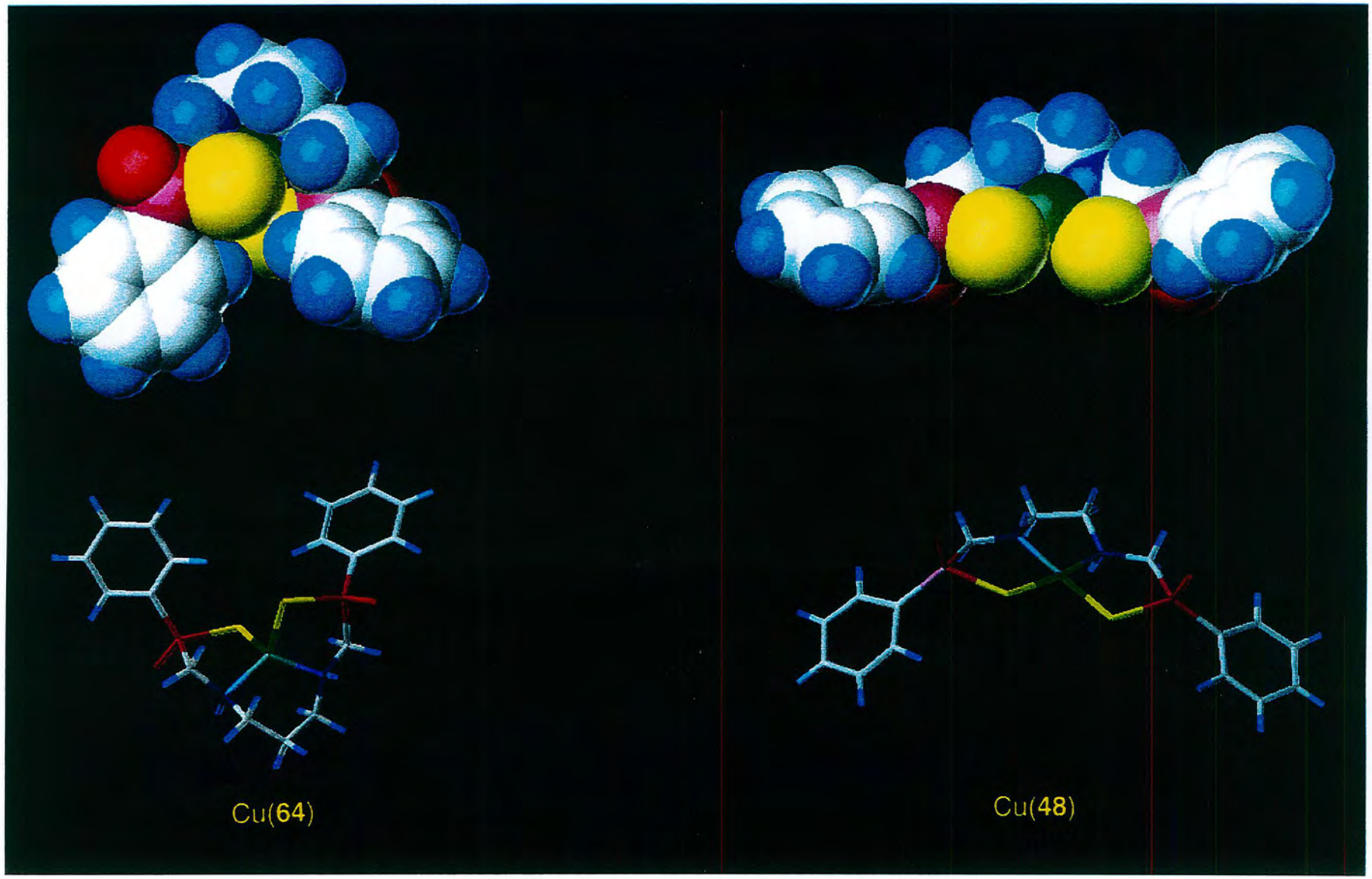

Figure 2.24 Molecular models of copper complexes

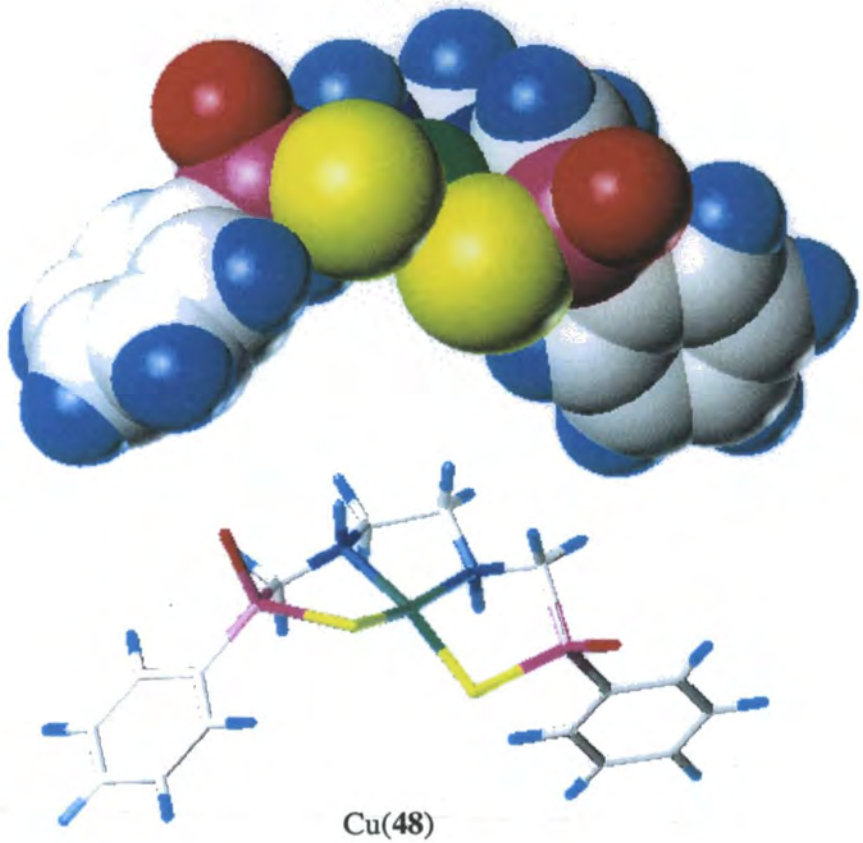

Cu(**48**)

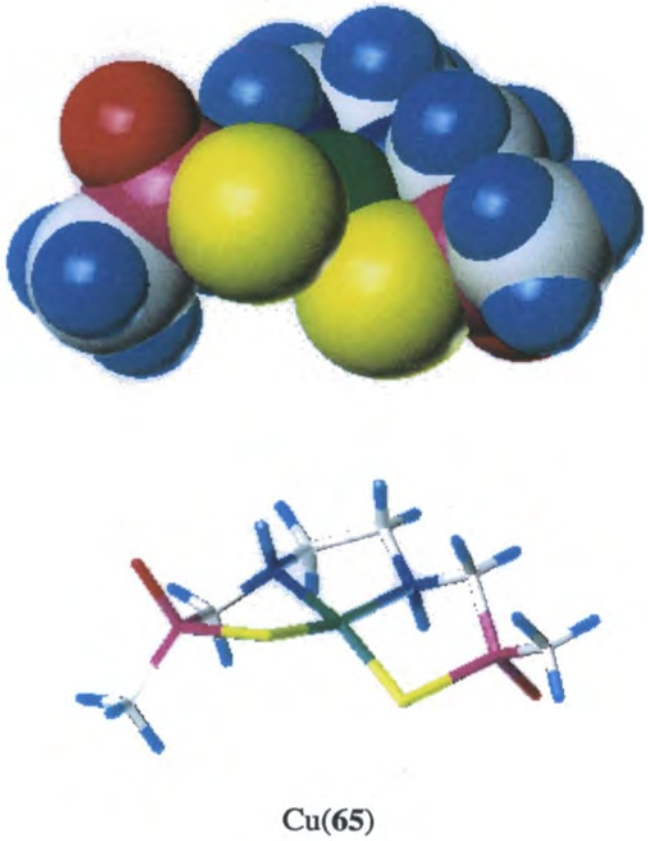

Cu(**65**)

Figure 2.25 Molecular models of copper complexes

2.4 Conclusions

A viable synthesis of this new class of ligand - amino-thiophosphinic acids - has been established, which allows variation of substituents and component parts. This proven synthetic route may allow many other such derivatives to be prepared. The failure of the sulfur transfer step following N-methylation was, however, disappointing for its wider implications, for example, the facile synthesis of future systems such as a tetrathiophosphinic acid analogue of EDTA.

Characterisation of the oxorhenium and copper complexes of the new ligands synthesised shows promise for successful radiolabelling with radionuclides of these metals and technetium. The solution stability of the copper complexes, in particular, appears to be finite and may thereby offer potential for a cellular trapping mechanism. Clearly, the ligands are suitable candidates for radiolabelling studies (see Chapter 5).

2.5 References

1. Corbridge, D.E.C., '*Phosphorus: An Outline of its Chemistry, Biochemistry and Technology*', 4th Ed., Elsevier (1990), Ch. 4 & 7
2. S. Aime, M. Botta, D. Parker and J.A.G. Williams, *J. Chem. Soc. Dalton Trans.*, 1995, 2259
3. D. Parker, P.K. Pulukkody, T.J. Norman, A. Harrison, L. Royle and C. Walker, *J. Chem. Soc., Chem. Commun.*, 1992, 1441
4. G. Swarzenbach, *Helv. Chim. Acta.*, 1952, **35**, 2344
5. S. Chaberek Jr. and A.E. Martell, *J. Am. Chem. Soc.*, 1952, **74**, 6228
6. K.P. Pulukkody, T.J. Norman, D. Parker, L. Royle and C.J. Broan, *J. Chem. Soc. Perkin Trans. 2*, 1993, 605
7. P. Baylis, C.D. Campbell, J.G. Dingwall, *J. Chem. Soc. Perkin Trans 1*, (1984) 2845
8. J.G. Dingwall, J. Ehirenfreund, R.G. Hall, *Tetrahedron*, 1989, **45**, 3787
9. A.E. Martell, R.M. Smith, 'Critical Stability Constants', Plenum Press,1974, **1**; 1975, **2**
10. H.L.M.N. Irving and L.D. Pettit, *J. Chem. Soc.*, 1963, 3051
11. A.S. Craig, I.M. Helps, K.J. Jankowski, D. Parker, N.R.A. Beeley, B.A. Boyce, M.A.W. Eaton, A.T. Millican, K. Millar, S.K. Rhind, A. Harrison and C. Walker, *J. Chem. Soc., Chem Commun.*, 1989, 794
12. R.J. Motekaitis, I. Murase, A.E. Martell, *J. Inorg. Nucl. Chem.*, 1971, **33**, 3353
13. I. Lukes, K. Bazakas, P. Hermann, P. Vojtisek, *J. Chem. Soc. Dalton Trans*, 1992, 939

14. I. Lukes, P. Hermann, P. Pech, *Collect. Czech. Chem. Commun.*, 1989, **54**, 653
15. D. Parker, 'Imaging and Targeting', Ch. 17, *Comprehensive Supramolecular Chemistry*, Eds. J.M. Lehn, D.N. Reinhoudt, Pergamo, Oxford, 1996
16. G.B. Bates, E. Cole, D. Parker and R. Kataky, *J. Chem. Soc., Dalton Trans.*, 1996, 2693
17. D.E.C. Corbridge, *'Phosphorus: An Outline of its Chemistry, Biochemistry and Technology'*, 4th Ed., Elsevier (1990), p329
18. E.A. Krasil'nikova, A.M. Potapov, A.I. Razamov, *Zh.Obshch Khim*, 1968, **38** (3), 609-13, Engl. 587
19. B.A. Arbuzov, N.I. Rizpolozhensky, M.A. Zvereva, *Izv. An SSSR, OKhn*, 1957, 184, (Engl. 189)
20. E. Cole, *Complexation Behaviour of Aza-Phosphinic Acids*, Ph.D. Thesis, University of Durham, 1993
21. P.K. Danikhel and Purnanand; *Indian J. Chem.*, Sect. A., 1990, 29 (A) (9) 256
22. R. Honeycult, L. Ballantine, H. Le Baron, D. Paulson, V. Sein, C. Ganz, G. Milad, *ACS Symp Ser* , 1984, **259**, 343; *Chem. Abs.* 101 : 224809n
23. W. Steurbaut, W. Dejonckheere and R.H. Kips, *Meded. Fac. Landbouwnet Rijksuniv Gent,* 1980, **45** (4) 943; Chem. Abs. 94 : 78413x
24. E.A. Krasil'nikova, *Russian Chem. Revs.*, 1977, **46** (9), 861
25. A. Chaudhry, M. Harger, P. Shuff and A. Thompson, *JCS, Chem. Commun.*, 1995, 83
26. M.P. Coogan, M.J.P. Harger, *J. Chem. Soc., Perkin Trans. 2,* 1994, 2101
27. R.M. Smith and A.E. Martell, 'Critical Stability Constants', Plenum Press, London
28. S.H. Pine and B.L. Sanchez, *J. Org. Chem.*, 1971, **36**, 829
29. B.L. Sondengam; J.H. Hemo, G. Charles, *Tetrahedron Lett.*; 1973; **3**, 261
30. W.A. Higgins. P.W. Vogel and W.G. Craig, *J. Am. Chem. Soc.*, 1954, **77**, 1864
31. N.P. Johnson, C.J.L. Lock and G. Wilkinson, *J. Chem. Soc.*, 1964, 1054
32. Reduction of copper(II) complexes in aqueous media may occur up to 700 mV depending upon the nature of the complex.

Chapter Three

Dialkylthiophosphoryl Ligand Systems

3. Dialkylthiophosphoryl Ligand Systems

The design of a new class of ligands which incorporate the dialkylthiophosphoryl functional group is presented. The scope for variation of component parts is considered in tandem with the ligand architechture with respect to the tailoring of radiopharmaceuticals (3.1). Synthetic routes to these ligands are discussed and the design and synthesis of further ligands of this class are explored (3.2). Complexation studies with rhenium and copper by techniques such as ESMS, HPLC and UV-visible spectrophotometry are reported (3.3) and general conclusions are summarised (3.4).

3.1 Design of New Dialkylthiophosphoryl Ligands

The importance of the copper complex, Cu-PTSM (**26**) has been highlighted previously (Ch. 1, section 1.7) as an imaging agent for use in Positron Emission Tomography as it is one of the best perfusion tracers to date. Despite this promising performance, Cu-PTSM is by no means a perfect PET perfusion tracer (see section 1.7) and the search for improved derivatives continues.[1] With this in mind, new ligands analogous to PTSM may be formed by replacement of C=S by P=S (Figure 3.1) and allow further scope still for substitution at phosphorus and consequent variation of lipophilicity. As with the design of the thiophosphinate series (Ch.2), the pentavalency at phosphorus may also provide a tolerant site for the attachment of a tether. Similarly, substitution of the backbone allows further means of elaboration of the ligand and, hence, of the metal complexes.

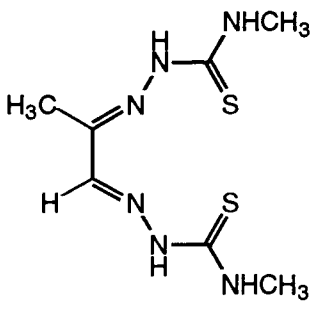

(**26**) PTSM

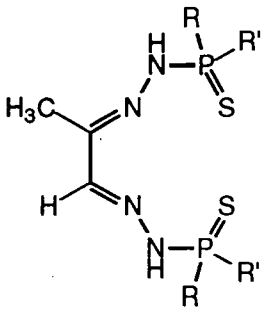

(**69**) thiophosphoryl analogue

Figure 3.1 Possible PTSM-analogues containing disubstituted thiophosphoryl groups

This design of a new thiophosphoryl ligand may be generalised to allow various substituents on the carbon skeleton and at phosphorus (**70**), (Figure 3.2). This new ligand system was designed and pursued concurrently with the thiophosphinic acid ligand series (Ch. 2). It incorporates much of the same overall architecture in terms of the choice of donor atoms and size of chelate rings which has already been discussed (sections 1.6 and 2.1). The ligand system should form three 5-membered chelate rings

upon complexation and also has two nitrogen and two sulfur donor atoms although the latter are present as neutral rather than anionic donors.

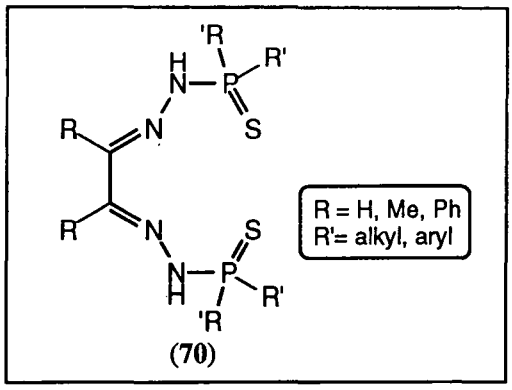

(70)

Figure 3.2 A new ligand system

However, neutral copper complexes may form by deprotonation of the nitrogens adjacent to phosphorus which make up the chelate ring (**71**) in an analogous process to the formation of Cu-PTSM (section 1.7). This type of amide N-H deprotonation also occurs in peptide complexes of copper above pH 5.[2] A similar complexation process occurring with oxorhenium(V) or oxotechnetium(V) may lead to the formation of cationic species or complexes with a dioxo core to satisfy the high positive charge of the metal.

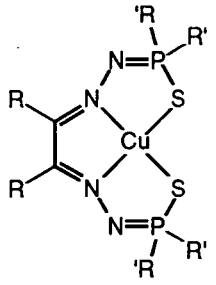

(71)

The incorporation of hydrazine and hydrazide moieties within phosphorus-containing ligands has proved useful for the development of new systems for coordination in transition metal and organometallic chemistry.[3] Although diverse, many of these systems possess similar structural motifs, (**72**) or (**73**).

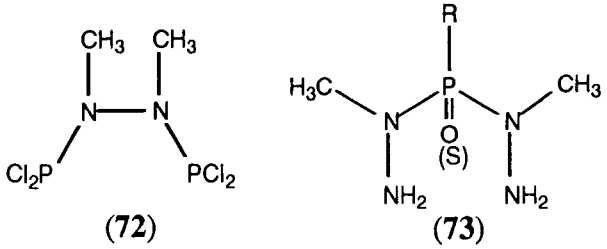

(72) (73)

Figure 3.3 Typical structures of P(III) and P(V) hydrazides

Some phosphorus hydrazide ligands have been shown to form complexes with ^{99m}Tc for the development of new potential radiopharmaceutials, for example, $^{99m}Tc(V)$ phenylbis(hydrazide)phosphine (**74**).[4] Indeed, hydrazine moieties continue to find application as nitrogen-based ligands in the complexation of both early and late transition metals.[5] Furthermore, they can be elaborated into a flexible ligand framework due to the versatile reactivity of the terminal hydrazido groups in many reactions. This allows the incorporation of other donor atom sites or another hydrazide fragment to impart greater stability to metal centres. Ligands with the structure (**75**) have also been reported for complexation of palladium(II), copper(I) and cobalt(I).[6]

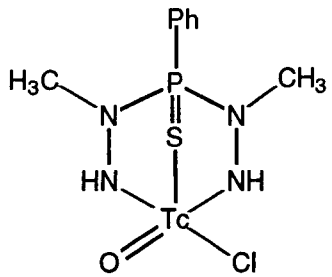

(**74**)

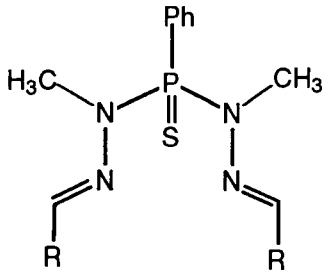

(**75**)

Dialkylthiophophoryl groups

Many disubstituted phosphonothioic halides are known and some examples of these are given in Figure 3.4. Although derivatives with alkyl ($C_{1\text{-}20}$), cycloalkyl ($C_{5\text{-}6}$), aryl, bromide and chloride substituents are known, some syntheses require very harsh conditions of extremely high temperatures and give a mixture of the $R_2P(S)X$ and $RP(S)X_2$.[7] There are, however, systems which are more accessible, such as $Me_2P(S)Br$ and $Ph_2P(S)Br$ or their chlorides[8] via their respective bi(phosphine sulfide) derivatives (see section 3.2 below).

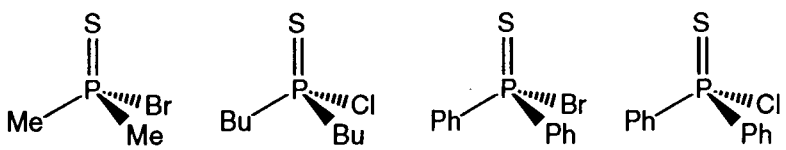

Figure 3.4 Examples of disubstituted phosphonothioic halides

3.2 Ligand Synthesis

The general synthetic route envisaged for these bisdialkylthiophosphoryl ligands was by reaction of an appropriate dihydrazide with a suitable thiophosphorus compound (Scheme 3.1).

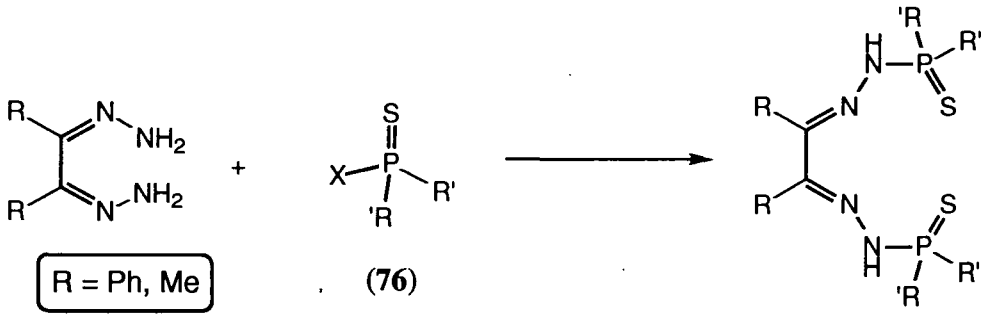

Scheme 3.1 Synthetic route to new bis(dialkylthiophosphoryl) ligands

Preparation of the thiophosphoryl moiety

There are many potential sources of dialkyl or diaryl thiophosphoryl functionalities, as mentioned above. Dimethylthiophosphoryl bromide [(**76**) R'=Me, X=Br] was chosen for this purpose due to its relative ease of preparation and an initial preference for methyl substituents of the ligand as they are not bulky or too lipophilic. This thiophosphoryl bromide was prepared very simply by addition of a molar equivalent of bromine to the corresponding substituted diphosphine disulfide (**77**) (Scheme 3.2).[9] The preparation of the latter precursor (**77**), although facile, was not as simple due to the extreme vigorousness of the reaction. A solution of thiophosphoryl chloride in diethyl ether was added very slowly and carefully to a stirred solution of methylmagnesium bromide in diethyl ether at around -15°C. After a short induction time, the reaction proceded quite vigorously and the temperature was maintained at -20 to -10°C. Maintaining the temperature within this range was extremely important: if the reaction is not cooled, then it proceeds almost explosively; and if it is cooled too much, then it hardly reacts at all, until the mixture has warmed up and the whole amount of both reagents react violently at once rather than being added together in a controlled manner. With this addition successfully accomplished, the reaction mixture containing the white precipitate formed was poured carefully onto crushed ice prior to washing with sulfuric acid and water. Recrystallisation from ethanol gave long colourless needle-like crystals which could be stored until the subsequent thiophosphoryl bromide was required.

Usually the thiophosphoryl bromide was freshly prepared and used *in situ* as a solution in carbon tetrachloride by addition of a molar equivalent of bromine in carbon tetrachloride to a stirred suspension of the bisphosphine (**77**) at 0°C.[10] Although a portion of dimethylthiophosphoryl bromide was isolated by distillation of the solvent at atmospheric pressure and subsequent purification by vacuum ditillation to give a colourless solid, the best results were obtained by the *in situ* reaction of this material.

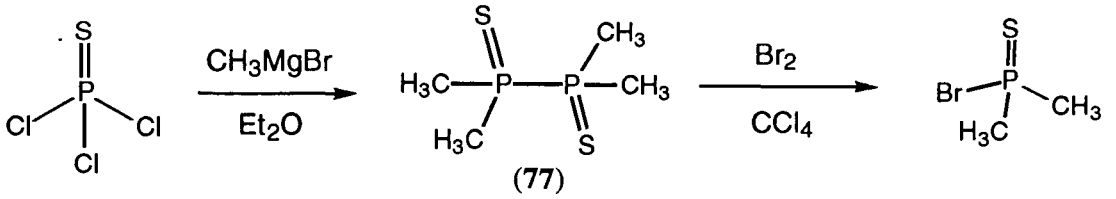

Scheme 3.2 Preparation of dimethylthiophosphoryl bromide

Dihydrazone synthesis

For the synthesis of the dihydrazone moiety, an appropriate α-diketone was required. There are many such ketones commercially available, such as phenylgyloxal, benzil, pyruvic aldehyde, butanedione and isomers of hexanedione, constituting suitable starting materials. Initially, phenylglyoxal was treated with hydrazine hydrate in ethanol in an attempt to synthesise the precursor (**78**) required for the ligand (**79**) (Scheme 3.3) which is unsymmetrical in its substitution like PTSM.

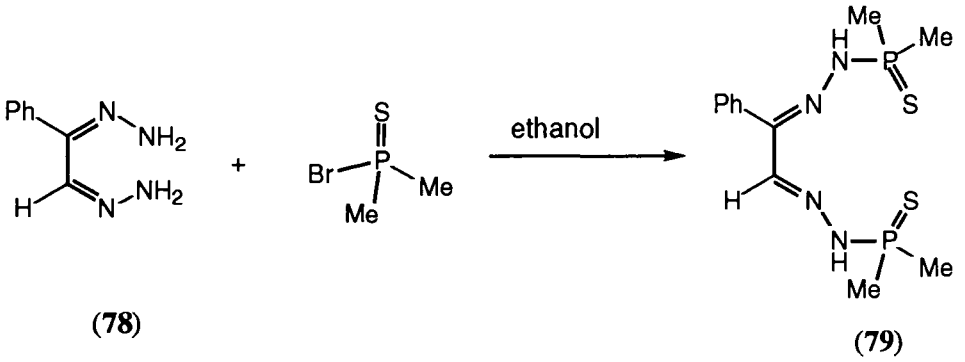

Scheme 3.3 Proposed synthesis of a 'PTSM-type' ligand

A white solid precipitated from the reaction mixture but a mass spectrum (DCI) of the solid showed a mass of 293. The reaction which had taken place was not the formation of the dihydrazone (**79**), but formation of a dimeric species of the constitution (**80**). The synthesis was repeated by dropping the phenyl glyoxal into an excess of hydrazine hydrate in an attempt to form the dihydrazone. However, the solid product (**80**) was again formed and its structure was confirmed by full characterisation. The synthesis of the disubstituted analogues was then addressed since the preparation of di-substituted di-hydrazones was expected to be less problematic.[11]

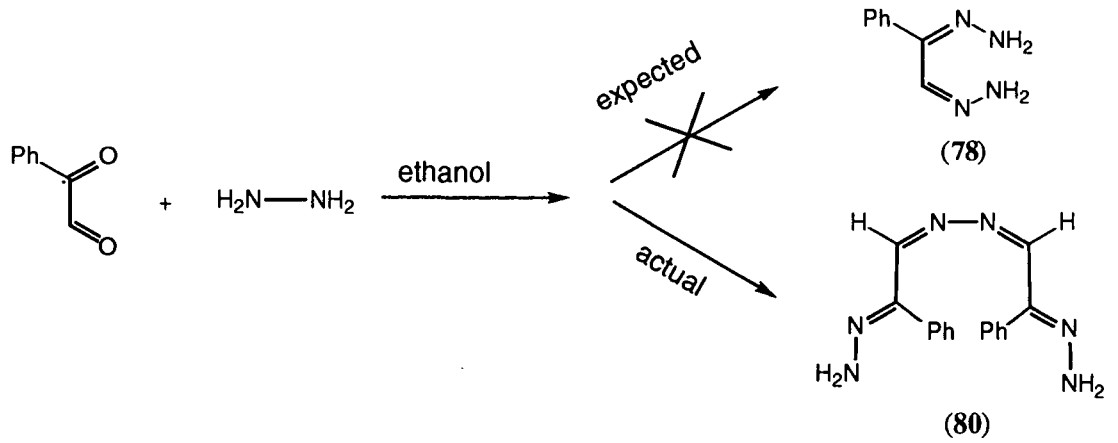

Scheme 3.4 Attempted preparation of phenylglyoxal dihydrazone

The diphenyl substituted dihydrazone (**81**) was conveniently prepared from benzil and hydrazine hydrate in *n*-butanol solution (Scheme 3.5), following the standard procedure of Cope.[12] After heating under reflux for 48 h, the dihydrazone crystallised from the solution upon cooling. The methyl substituted analogue (**82**) was similarly prepared from butane-2,3-dione.

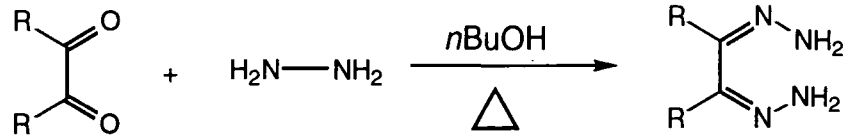

(**81**) R = Ph
(**82**) R = Me

Scheme 3.5 Preparation of substituted dihydrazones

Initially, the synthesis of corresponding diphenyl ligand (**70**)[R=R'=Ph] was undertaken by the addition of benzildihydrazone (**81**) to a stirred solution containing two molar equivalents of freshly prepared dimethylthiophosphoryl bromide. However, no trace of the ligand or starting material was present in the mixture of products. Mass spectroscopy (DCI) confirmed that the predominant species had a mass 412 (MH^+, 413) corresponding to the cyclic dimer (**83**) (Scheme 3.6) and no evidence for the formation of even a mono-substituted dihydrazone was found. This observation is consistent with the synthesis of (**83**) (3,4,7,8-tetraphenyl-1,2,5,6-tetrazocine) and several analogues which were reported by Schlesinger via condensation of benzildihydrazone with an aromatic substituted diketone such as benzil.[13]

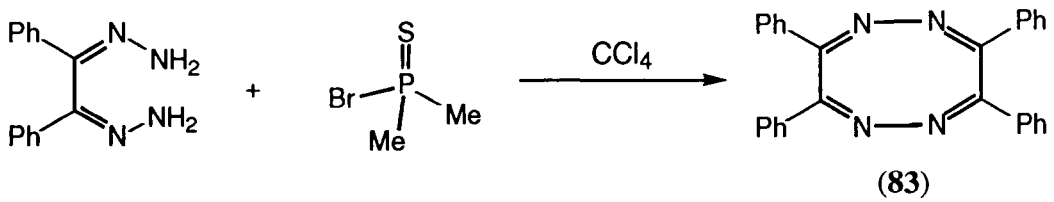

(**83**)

Scheme 3.6 Unexpected formation of the tetraphenyltetrazocine

The same reaction was then carried out in the presence of an organic base. The dihydrazone (**81**) was added to a freshly prepared solution of thiophosphoryl bromide in carbon tetrachloride with two equivalents of triethylamine (Scheme 3.7). The reaction was followed by ^{31}P NMR analysis and after several hours, the triethylamine salts precipitated allowing their removal. Evaporation of the solution left a residue which was taken up into diethyl ether. Large yellow-orange coloured crystals of the ligand (**84**) formed in 70% yield upon standing. On occasions when crystallisation did not occur spontaneously, an aqueous work-up was performed on the ether solution to remove any impurites and the organic phase was evaporated to give (**84**) as a pale orange powder.

The methyl analogue (**82**) reacted analogously under identical conditions with dimethylthiophosphoryl bromide, only a different work-up was required. The product (**85**) co-precipitated from the reaction solution with the triethylamine salts and was isolated by filtration and washed with water to remove the salts. The ligand (**85**) was obtained in 89% yield as a pale yellow powder.

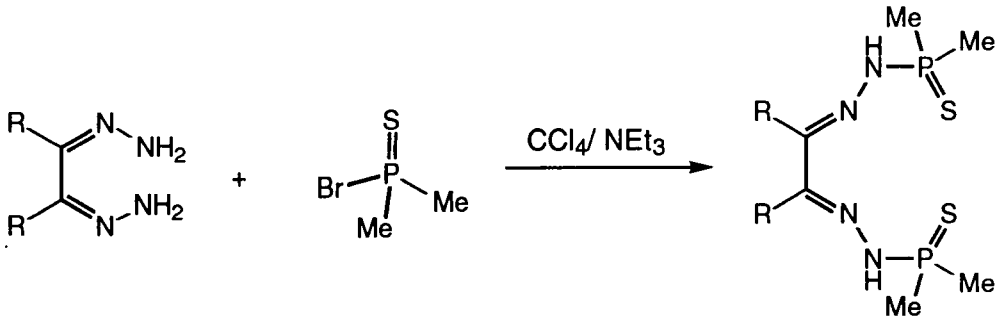

(**84**) R = Ph
(**85**) R = Me

Scheme 3.7 Synthesis of disubstituted bis[(dimethylthiophosphoryldihydrazides)]

Amino-pyridine type ligands

A bidentate ligand (**86**) (Scheme 3.8) based upon this dialkylthiophosphoryl functionality and amino-picoline was also considered. The incorporation of the pyridine nitrogen donor with the neutral sulfur donor gives an NS donor set. Two of these ligands may coordinate to metals, such as copper, giving an N_2S_2 array of donor atoms in an ML_2 complex. The methyl substituent on pyridine (position 6) was incorporated in the ligand to restrict the number of possible coordination geometries. Its presence disfavours an octahedral or trigonal bipyramidal coordination geometry because of the steric effect of the methyl group. Indeed, it may tend to favour Cu(I) by stabilising a tetrahedral geometry in preference to the square planar or square pyramidal geometry characteristic of copper(II).

Synthesis was achieved by the reaction of three molar equivalents of 2-amino-6-picoline (available commercially) in a stirred solution of freshly prepared dimethylthiophosphoryl bromide in carbon tetrachloride where the excess amino-picoline acted as the base. The product (**86**) co-precipitated with the amine picolinic hydrobromide salts and was extracted into diethyl ether and allowed to crystallise. Large colourless crystals were formed in 82% yield. When only two equivalents of the aminopicoline were used, the product yield was lowered due to the formation of a species with disubstitution at nitrogen (**87**). This species is similar to another disubstituted amine (**88**) reported in 1968 which was arguably the first ligand of this class to be synthesised.[14]

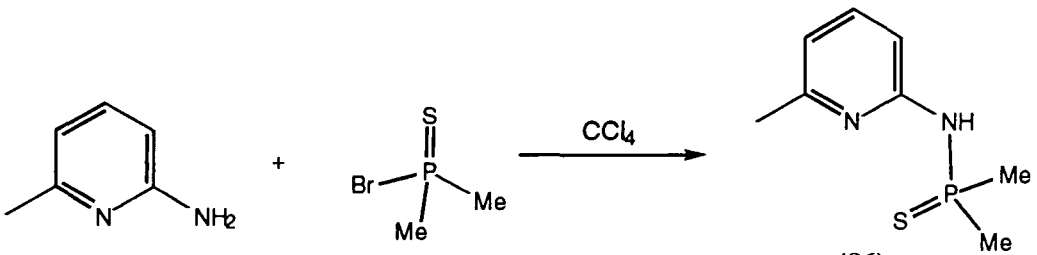

(**86**)

Scheme 3.8 Synthesis of the bidentate ligand

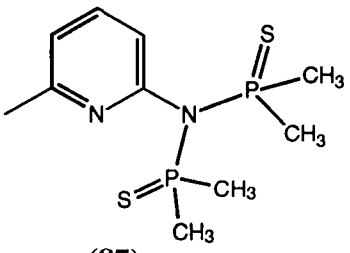

(**87**)

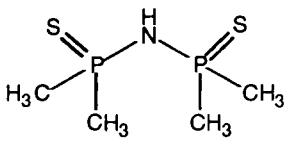

(**88**)

A similar reaction was undertaken with 2,6-diaminopyridine with excess thiophosphoryl bromide in the presence of triethylamine to give the disubstituted ligand (**89**). This new tridentate ligand was designed to incorporate an NS_2 donor set in order to form two 6-membered chelate rings upon complexation to a metal. This ligand would therefore require another single monodentate ligand to make up the fourth coordination site[15] (3 + 1 system, section 1.6) if its application were attempted in this context. It may, however, find application in the complexation of other metals preferring a lower coordination number such as Au^+ or transition metals with a preference for an octahedral geometry, in an ML_2 complex.

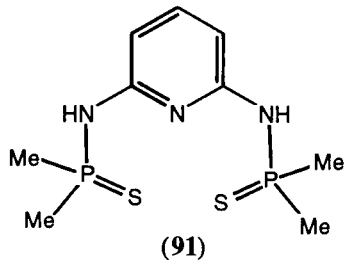

(91)

Variation of the dihydrazide system

Many variations within this class of ligand were originally envisaged, with particular respect to the tetradentate system, in terms of the wealth of possible substituents at phosphorus and on the C-C backbone. Further extensions were proposed to alter the chelate ring size or enforce some rigidity. For example, instead of a 1,2-diketone arrangement of the precursor, a 1,3 spacing would allow the 5-ring chelate to become 6-ring. However, pentane-2,4-dione could not simply replace butane-2,3-dione in the above synthesis (Scheme 3.7) as the central methylene protons are extremely acidic (pK_a ~9) due to the two adjacent carbonyls. These positions had, firstly, to be blocked. The mono-methylated material, 3-methyl-2,4-pentanedione (**90**) was obtained commercially as a mixture of tautomers and formed a suitable starting compound for the proposed synthesis. Treatment of (**90**) with sodium hydride in tetrahydrofuran followed by methyl iodide (Scheme 3.9) as described in the literature,[16] gave the 3,3-dimethyl derivative (**91**) as a colourless oil.

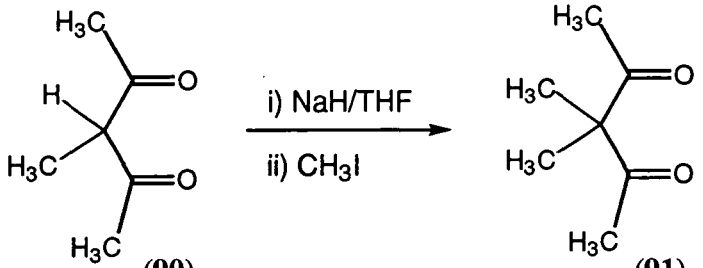

(90) **(91)**

Scheme 3.9 Methylation of 3-methyl-2,4-pentanedione

Preparation of the pentanedihydrazone (**92**) was then attempted with the dimethylated diketone (**91**) using the conditions described previously (Scheme 3.5). However, the ^1H NMR spectrum of the products indicated that although two different environments of methyl proton were present in equal proportions, no amine protons were observed. In the mass spectrum ($ESMS^+$), the molecular ion at 147 (MH^+) was in agreement with the formation of the isopyrazole (**93**)[17] (Scheme 3.10). Despite further efforts to effect the formation the desired product by slow dropwise addition of the diketone to an excess of hydrazine, the same white solid (**93**) was recovered as the major product.

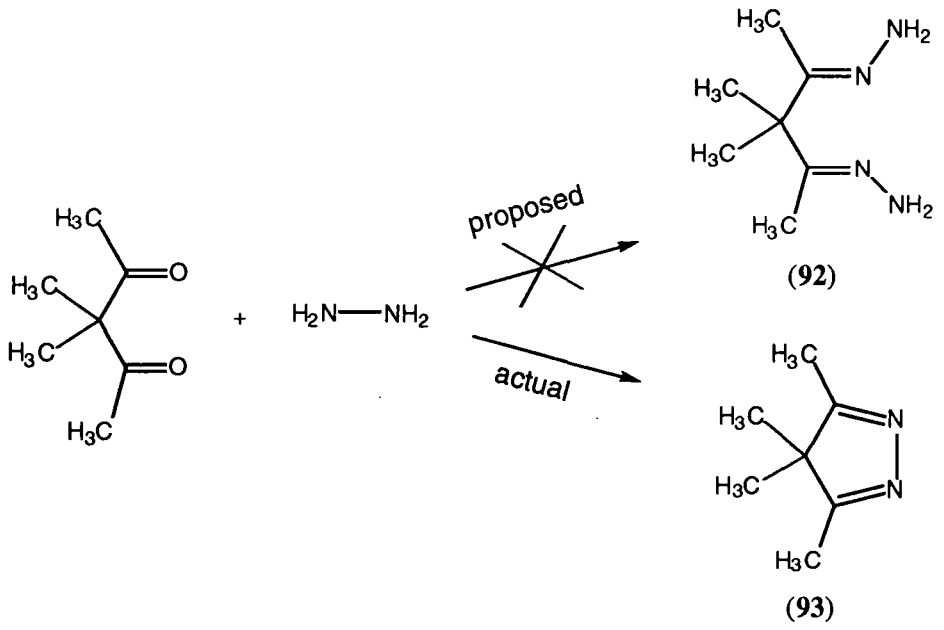

Scheme 3.10 Treatment of the 1,3-diketone with hydrazine hydrate

Another tetradentate ligand in this dialkylthiophosphoryl series was designed to include a rigid backbone (**94**). Use of a cyclopentane or a cyclohexane unit in this manner was proposed to allow less flexibility in the orientation of the thiophosphorylhydrazide units and perhaps render greater predisposition to metal binding. Although cyclopentane offers greater rigidity, the cyclohexyl system was investigated first, due to the commercial availability of cyclohexane-1,2-dione as a suitable starting material.

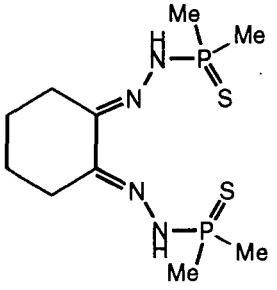

(**94**)

This time, a different retrosynthesis was envisaged, given some of the above problems with formation of the appropriate dihydrazones. Synthesis of a thiophosphorylhydrazine unit was proposed first, followed by reaction of the hydrazine moiety with any diketone in an attempt to eliminate the complications which arose from two neighbouring dihydrazone functions (Scheme 3.11).

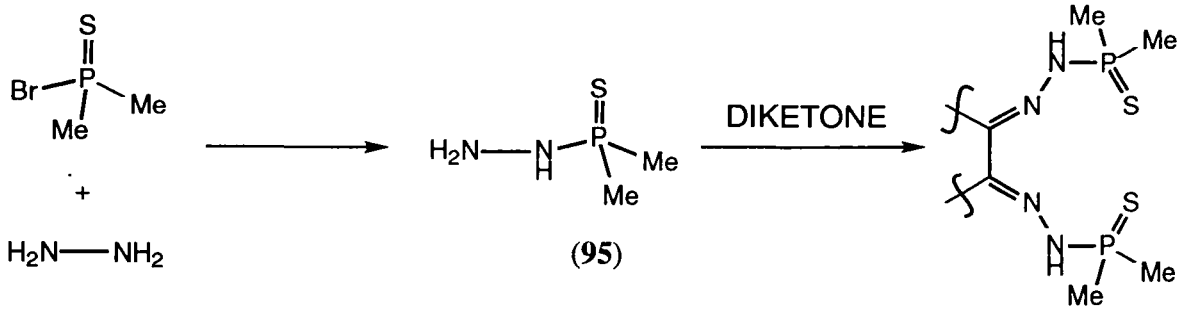

Scheme 3.11 An alternative flexible synthesis

Dimethylthiophosphorylhydrazine (**95**) was prepared by the dropwise addition of dimethylthiophosphoryl bromide (freshly prepared as before but concentrated by distillation of carbon tetrachloride at atmospheric pressure) to an excss of hydrazine hydrate. After stirring at room temperature for 4 hours, the product (**95**) was extracted into chloroform and isolated as a colourless oil. Treatment of the cyclohexane dione with dimethylthiophosphoryl hydrazine (**95**) failed to show any reaction and the starting material was recovered from the reaction mixture.

In order to investigate whether this failure to react was specific to the cyclohexane dione or typical behaviour for these systems, a control experiment was undertaken. This alternative route of hydrazine-ketone condensation as the second step was applied to the benzil ligand (**84**) previously synthesised by the initial method (Scheme 3.7). Dimethylthiophosphorylhydrazine (**95**) was added to a stirred solution of benzil in butanol and heated under reflux for 20 hours. Upon cooling the reaction mixture, a white precipitate formed which was identified by ^{1}H NMR analysis as benzildihydrazone (**81**). Clearly, the P-N bond had cleaved as no phosphorus signal was detected in the sample by ^{31}P NMR analysis and the dihydrazone had formed. Although the reaction was repeated using milder conditions of 25°C, the result was the same.

Clearly, synthesis via condensation of the diketone with a substituted thiophosphorylhydrazine was not as generally applicable as the original synthesis via formation of the corresponding dihydrazones. In view of this evidence, synthesis of the cyclohexyl ligand (**94**) was attempted using the original scheme. Cyclohexane dione was treated with hydrazine hydrate in *n*-butanol under reflux for 40 hours. Upon cooling the reaction mixture, no precipitation occurred and the solvents were evaporated to give a brown oil. ESMS analysis of the residue indicated that the dihydrazone was indeed present, and its preparation and recrystallisation are described in the literature.[18,19] However, purification of the compound was not pursued at that time due to the limited time available for the pursuit of other systems described below and complexation study of the ligands synthesised above.

The synthesis of further systems based upon the pyridine ligand (**86**) was also envisaged in parallel with the work described above, since this system only has one thiophosphorus functionality and avoids the synthetic problems of reacting two sites simultaneously. The original pyridine ligand (**86**) and an analogous system containing a substituted thiophosphinic acid (**96**) (see also Ch.2), rather than the dialkylthiophosphoryl functionality, may provide an interesting comparison. This new system would also allow the formation of neutral complexes without deprotonation of the amide N-H due to the much lower pK_a expected for the thiophosphinic acid proton.

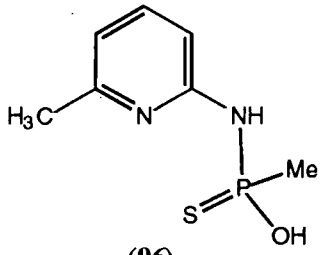

(**96**)

A synthetic route to this ligand (Scheme 3.12) was proposed and attempted. The required precursor, chloroethoxyphenylphosphine, was prepared as previously described (section 2.2) and added dropwise to a stirred solution of excess amino-picoline in dichloromethane. ^{31}P NMR analysis showed the formation of a single P(III) species at δ_P 104, confirming that chloroethoxyphenylphosphine (δ_P 174) was no longer present. The phosphine (**97**) was then treated with trimethylsilyl bromide under an inert atmosphere for 30 minutes prior to the addition of water. ^1H NMR analysis revealed the loss of the distinctive N-H coupling to phosphorus and suggested that P-N bond cleavage had occurred. This was not altogether surprising considering the acid lability of the phosphorus-amine bond.

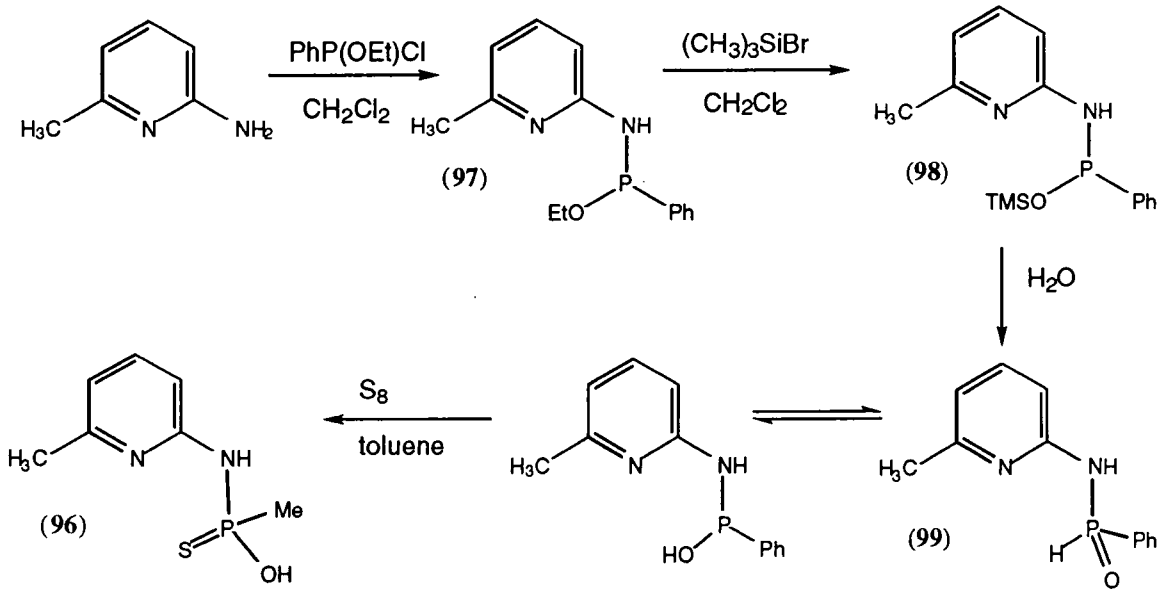

Scheme 3.12 Proposed synthesis of a thiophosphinate analogue of the pyridine ligand

An alternative route was proposed and attempted (Scheme 3.13) which involves the preparation of the amino-picoline-N-ethoxyphenylphosphine (**97**) from chloroethoxyphenyl phosphine and excess 2-amino-6-picoline in a similar procedure to the above, using acetonitrile as the solvent. The amino-picoline hydrochloride salt was removed by filtration and the solvent was evaporated from the filtrate. The residue (δ_P 104) was then stirred in 6M hydrochloric acid for 16 hours at room temperature to hydrolyse the P(III) ester (**97**) to (**99**). Removal of the solvent yielded the colourless solid product (δ_P 22). Elemental sulfur was the chosen sulfonating reagent for the next step as the tautomeric eqilibrium of the phosphinous acid with its P(III) form (see Scheme 3.12) allows reaction by nucleophilic attack of phosphorus. Crushed, dry sulfur was added to a stirred solution of the phosphinous acid (**99**) in acetonitrile and heated at 45°C for 16 hours. However, ^{31}P NMR analysis revealed that the compound (**99**) was the only phosphorus-containing species present and that no reaction with sulfur had taken place. Aluminium trichloride was added to the reaction mixture, in an attempt to activate the S_8, and the reaction was heated at reflux for 20 hours. The result was identical: no reaction being observed by ^{31} P NMR analysis.

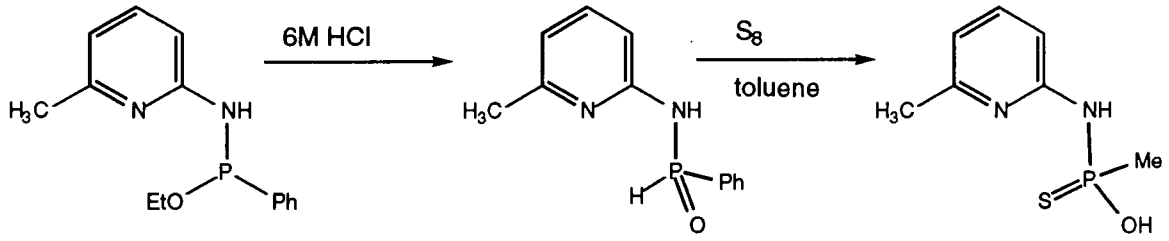

(**97**) (**99**) (**96**)

Scheme 3.13 Possible alternative synthesis of the thiophosphinate pyridine ligand

Due to the failure of these attempts to synthesise the ligand (**96**) the design was modified slightly in order to render the ligand synthetically more accessible. The design of the dithiophosphinate ligand (**100**) was based upon the reaction envisaged between 2-amino-6-picoline and the cyclic thiophosphinic anhydride (**101**) known as Lawesson's reagent (LR) (Scheme 3.14).

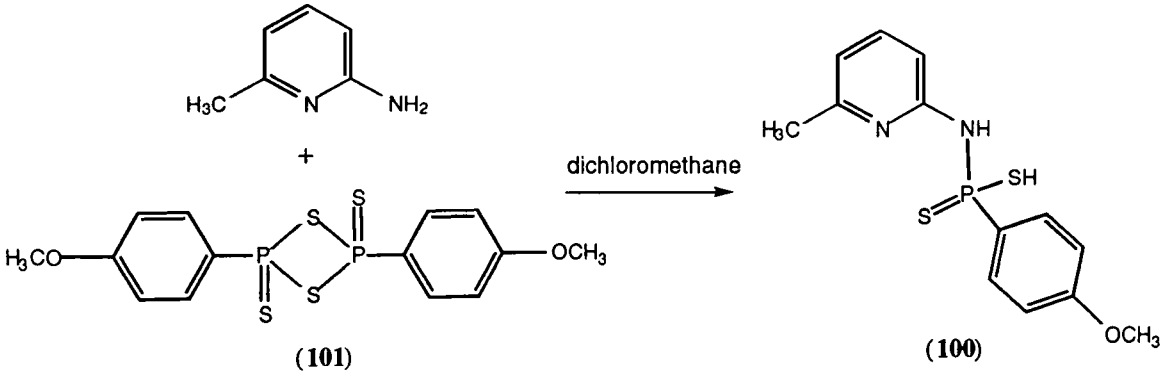

(**101**) (**100**)

Scheme 3.14 Synthesis of dithiophosphinate ligand

The latter compound (**101**) is the dimeric anhydride of methoxyphenyldithiophosphinic acid which is well known as an extremely effective thionating reagent.[20] It has been used extensively in the synthesis of thioamides, thioketones, thioesters, thiopeptides and sulfur-containing heterocycles. Another use is its application to other transformations in organic synthesis where mild conditions are sought, such as the conversion of an ester to the corresponding ether via the intermediate thioester and subsequent removal of sulfur with Raney nickel. The preparation of alkyl(aryl)dithiophosphonic acids and their derivatives are known by the reaction of different nucleophiles such as primary and secondary amines[21]with LR.[22] For example, carboxylic acids attack at phosphorus of LR to open up the dithiaphosphetane ring resulting in the formation of mixed anhydrides as useful intermediates for further synthesis (Scheme 3.15).[23,24]

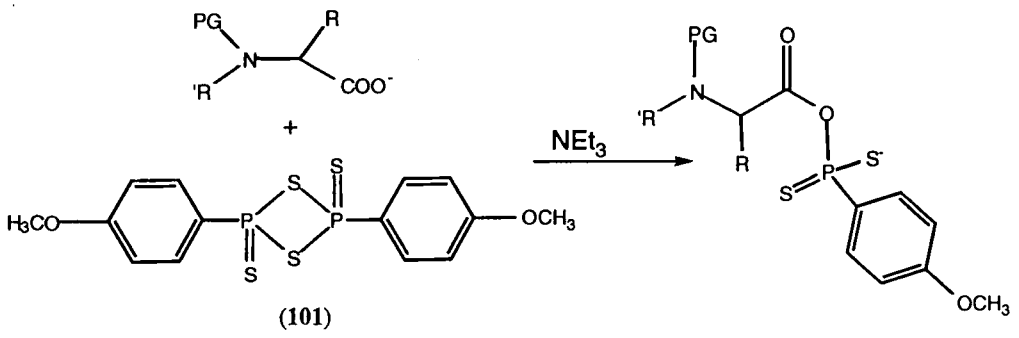

Scheme 3.15 Nucleophilic attack at Lawesson's reagent

It was this type of nucleophilic attack which was envisaged by the amino-picoline on LR to form the ligand (**100**). 2-Amino-6-picoline was added to a stirred suspension of Lawesson's reagent in dichloromethane, and a solution was formed immediately. After 10 minutes, the suspension reappeared, but analysis by ^{1}H NMR confirmed that some starting material and another species were present and that the reaction was still in progress. After 18 hours, the product was extracted into water and lyophilised to give a white solid. Despite the evidence of ^{1}H, ^{13}C and ^{31}P NMR analysis (δ_P 72) in addition to combustion analysis which gave data consistent with the structure (**100**), the mass spectrum of the product was inconclusive as it did not show the expected mass of 310 -only several lower masses. This led to concern that the structure was a 1:1 salt rather than a single molecule since ESMS is the softest mass spectroscopy technique, least likely to fragment the molecule. It was also noted in the laboratory handling of the product, that it reacted with trace amounts of ethanol stabilisers in chloroform, suggesting a that the nature species was labile. Hence, further studies of this system were not pursued as P-N bond was perhaps too labile with such an acidic function. At this point, the evaluation of the potential for metal complexation of the systems successfully synthesised and fully characterised above was deemed more important before further derivatives were proposed.

X-ray structural analysis of ligands

Crystalline samples of the tetradentate ligand (**84**) and bidentate ligand (**86**) of suitable quality for X-ray analysis were easily obtained from diethyl ether solution and without further recrystallisation. A small sample of the tetradentate ligand (**85**) was recrystallised from diethyl ether, and small pale yellow crystals formed. X-ray crystal structures of the tetradentate ligands (**84**) and (**85**) were solved by Dr. Andrei Batsanov and Christian Lehmann respectively (Figures 3.5 and 3.6 and Appendix B).

In both structures, (**84**) and (**85**) the amino nitrogen atoms have planar (sp^2) bonding geometry within experimental error. However, their molecular conformations are quite different. The backbone of (**84**) adopts a 'curled' conformation, being twisted by approximately 72° around the central C(1)-C(2) bond and by a smaller degree around the other single bonds (see Table 3.1). The structure of (**85**) possesses a crystallographic inversion centre (Figure 3.6). All non-H atoms (save the P-methyl carbons) are coplanar (with a maximum deviation of 0.07 Å and the mean one of 0.03 Å). The absence of signifigant hydrogen bonding in both structures is noteworthy. In (**84**) the intramolecular contacts N(2)-H...N(3) and N(4)-H...N(1) exhibit H...N distances of 2.55(2) and 2.53(2) Å with N-H-N angles of 116(2) and 119(2)°. They may be regarded as electrostatic interactions rather than hydrogen bonds, since the direction of the contacts do not correspond to the lone pair sites on N(1) and N(3).

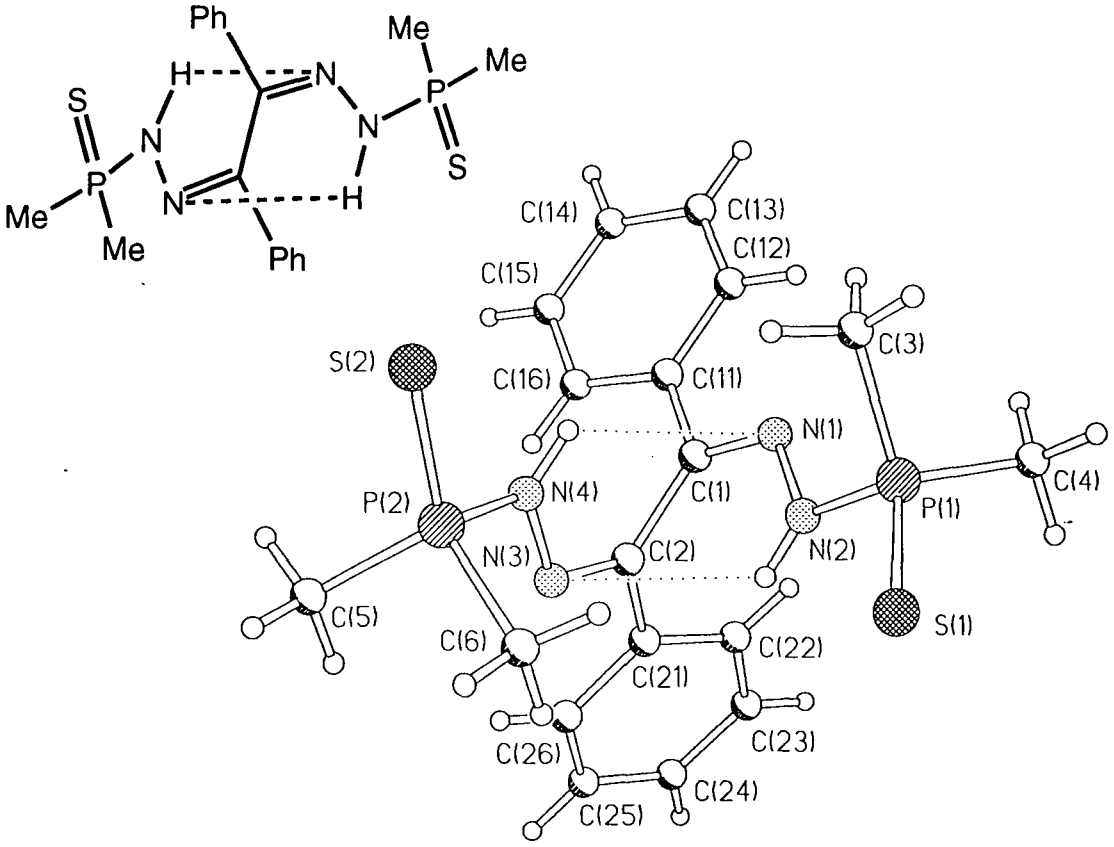

Figure 3.5 X-ray crystal structure of ligand (**84**)

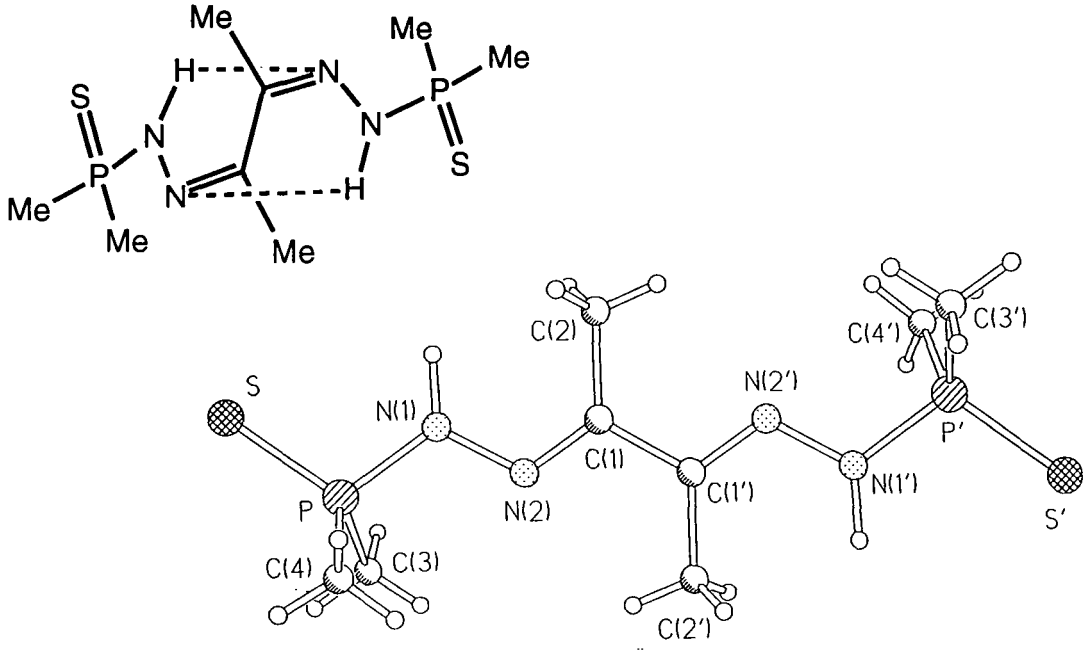

Figure 3.6 X-ray crystal structure of (**85**)

The structure of ligand (**86**) was also solved by Dr Batsanov (Figure 3.7) and shows inversion-related molecules linked by intermolecular hydrogen bonding of the amines to sulfur (N(2)-H...S'), lying practically in the same plane.

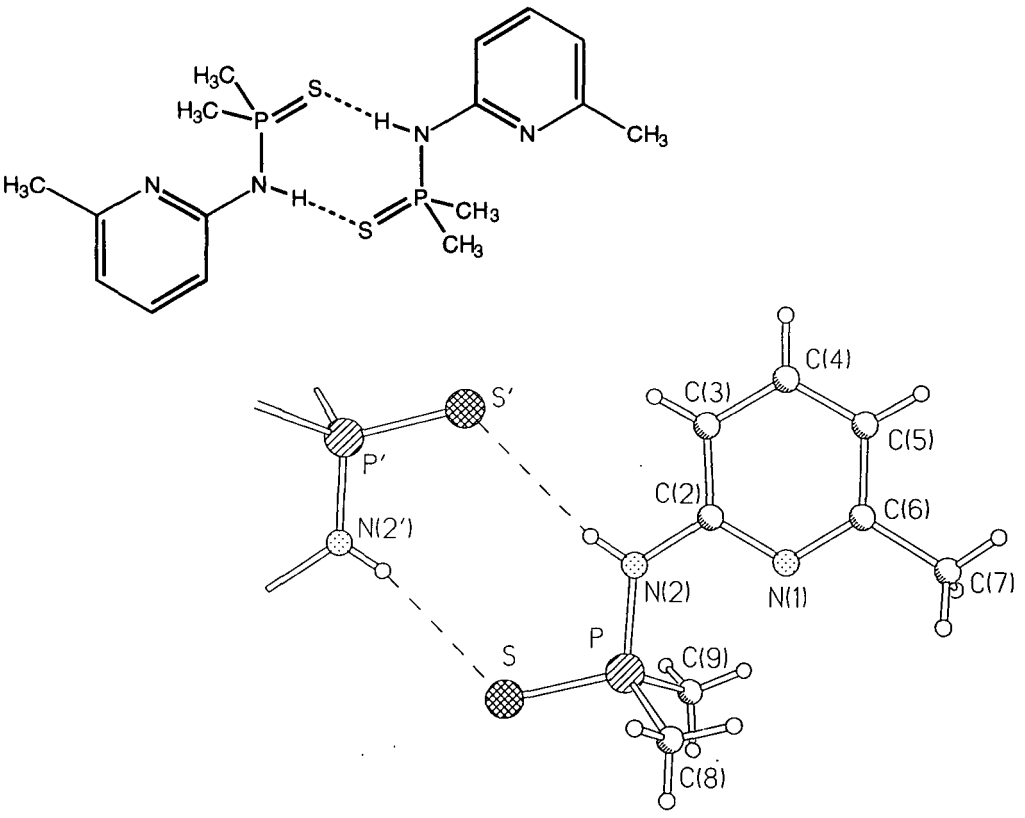

Figure 3.7 X-ray crystal structure of ligand (**86**), showing intermolecular hydrogen bonds. Inversion-related atoms are primed.

Table 3.1 Selected bond distances (Å), bond and torsion angles (°)

Structure (**84**)			
P(1)-S(1)	1.935(1)	P(2)-S(2)	1.947(1)
P(1)-N(2)	1.680(2)	P(2)-N(4)	1.689(2)
N(1)-N(2)	1.376(2)	N(3)-N(4)	1.380(2)
C(1)-N(1)	1.292(2)	C(2)-N(3)	1.291(2)
C(1)-C(2)	1.506(2)	P-C mean	1.786(5)
N(4)...N(1)	3.156(2)	N(2)...N(3)	3.139(2)
N(1)C(1)C(2)N(3)	71.9		
S(1)P(1)N(2)N(1)	167.4(1)	N(3)N(4)P(2)S(2)	-177.1(1)
P(1)N(2)N(1)C(1)	-168.7(1)	C(2)N(3)N(4)P(2)	-165.6(1)
Structure (**85**)			
P-S	1.955(1)	P-N(1)	1.676(1)
N(1)-N(2)	1.383(1)	C(1)-N(2)	1.296(2)
C(1)-C(2)	1.478(2)	P-C mean	1.801(2)
Structure (**86**)			
P-S	1.966(1)	P-N(2)	1.677(1)
N(1)-N(2)	1.400(2)	P-C mean	1.798(2)
N(2)...S'	3.544(2)	N(2)H(2)...S'	166(1)
SPN(2)C(2)	176.2(1)	PN(2)C(2)N(1)	7.2(2)

3.3 Complexation Studies

The ligands (**84**), (**85**), (**86**) and (**89**) prepared above displayed extremely poor aqueous solubility. However, the ligands were found to be soluble to varying degrees in common solvents such as acetonitrile and methanol. This did not deter studies with a view to future radiolabelling of these ligands, since the complexation of Cu-PTSM itself takes place with the aid of ethanol to dissolve the ligand rather than under purely aqueous conditions.[25] Initial studies were performed by electrospray mass spectrometry, as for the previous ligand series (Ch. 2).

Electrospray Studies

Complexation and electrospray analysis was carried out with (**84**), (**85**), (**86**) and (**89**) using the divalent metal ions of copper, nickel and zinc as their perchlorate salts (warning - perchlorate salts are explosive). Analysis of complexation with Cu(I) was also undertaken with $[Cu(I)(CH_3CN)_4]BF_4$ which was prepared from copper(I) oxide in acetonitrile in a similar manner to $[Cu(I)(CH_3CN)_4]PF_6$ prepared by Kubas.[26] Stock solutions of the ligands and metals with concentrations of the order of 10^{-4}M were

prepared. Although not quantitative, the $ESMS^+$ studies gave a preliminary insight into the coordination preferences of the ligand.[27]

Butane-2,3-bis[(dimethylthiophosphoryl)hydrazide (85)

Equimolar amounts of ligand (**85**) and copper(II) perchlorate in acetonitrile gave a clean spectrum of the ML complex only with the major mass (100%) at 359.94 corresponding to the loss of two protons from the ligand on positive ion mode. The isotope model with the major intensity at 359.98, showed close correlation with the observed mass ($C_8H_{18}N_4P_2S_2Cu$ requires 359.98, ES^+). When a similar analysis was performed using Cu(I) as the initial source of copper, the major mass (100%) was observed at 360.78, corresponding to the loss of one proton (Figure 3.8), and correlating with an isotope model intensity at 360.99 ($C_8H_{19}N_4P_2S_2Cu$). This suggests that neutral complexes of the ligand are formed with both Cu(II) and Cu(I). The nickel complex also gave a strong signal corresponding to the 1:1 complex, Ni(**85**). Complexation also occurred with zinc, but other species including a very small amount of $Zn(\mathbf{85})_2$ were also observed.

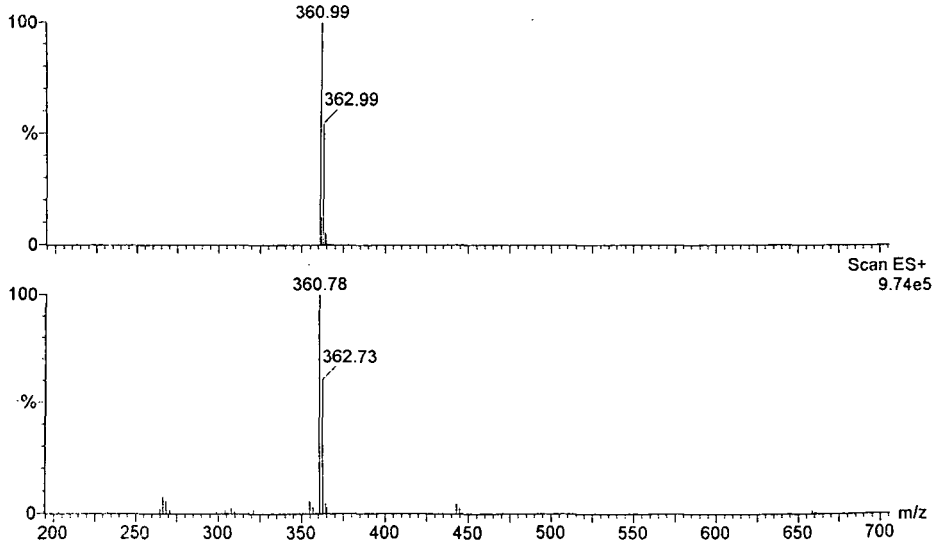

Figure 3.8 $ESMS^+$ spectrum of Cu(I)(**85**) showing loss of one ligand proton

1,2-Diphenylethane-1,2-bis[(dimethylthiophosphoryl)hydrazide (84)

Equimolar amounts of the ligand (**84**) and copper(II) perchlorate produced ML and ML_2 species, at 484.74 and 906.27 respectively. The major mass (100%) at 484.74 corresponds to the loss of one proton from the ligand (using positive ion mode), suggesting that a neutral copper(I) complex had formed. The isotope model with the major intensity at 485.02, showed close correlation (within the calibration of the instrument) with the observed mass ($C_{18}H_{23}N_4P_2S_2Cu$ requires 485.02, ES^+). The ML_2 complex at 906.27 corresponds to copper complexation of two ligands with the

loss of two protons overall, suggesting that this species is a copper (II) complex. Complexation with zinc produced a similar result, as both Zn(**84**) and Zn(**84**)$_2$ species were observed in the spectrum, in addition to a peak at the ML half-mass (corresponding to the doubly-charged complex) and a perchlorate adduct of ML. Again, nickel produced a similar spectrum, with ML, ML_2 and the half-mass peak of ML predominating.

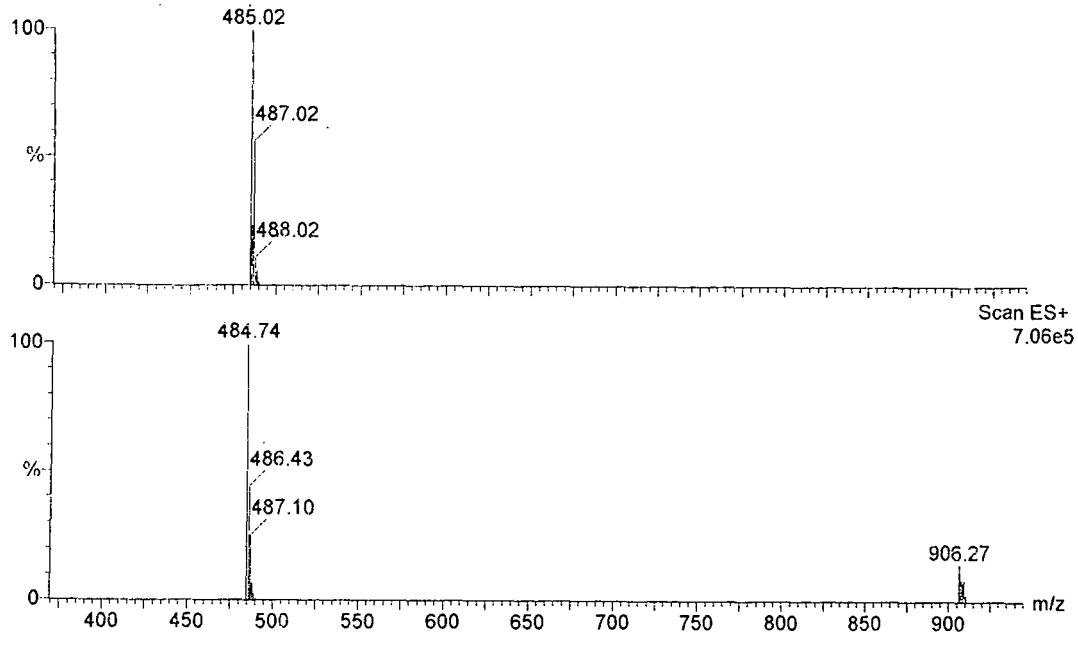

Figure 3.9 ESMS$^+$ spectrum of Cu(**84**), showing a Cu(I)L complex predominantly and a Cu(II)L_2 complex.

2-Dimethylthiophosphorylamino-6-picoline (86)

Since the expected coordination preference of copper(II), nickel(II) and zinc(II) with the ligand (**86**) involved the formation of bis-bidentate complexes, separate electrospray studies were carried out using both 2:1 and 1:1 equivalents of ligand to metal. The 2:1 Cu/L solution gave a spectrum containing Cu(**86**)$_2$ at 100% intensity in addition to smaller peaks due to some ML complex and unbound ligand. The 1:1 solution again showed the ML_2 species was dominant although L and ML were observed. Spectra for both nickel and zinc complexes (1:1 M/L) gave intense peaks consistent with the formation of ML_2 species and the remaining uncomplexed ligand, while the respective ML species were visible as only small peaks. The CuL and CuL_2 species at 262.98 and 462.95 respectively, showed the loss of one ligand proton in both species, suggesting that copper(I) complexes had formed.

ESMS analysis of 2:1 solutions of the ligand with zinc and nickel showed the unbound ligand as the major mass intensity and an ML_2 species as the only complex present, as expected. All of these observations suggest that ML_2 complexes are preferred and that copper is bound more avidly than either nickel or zinc.

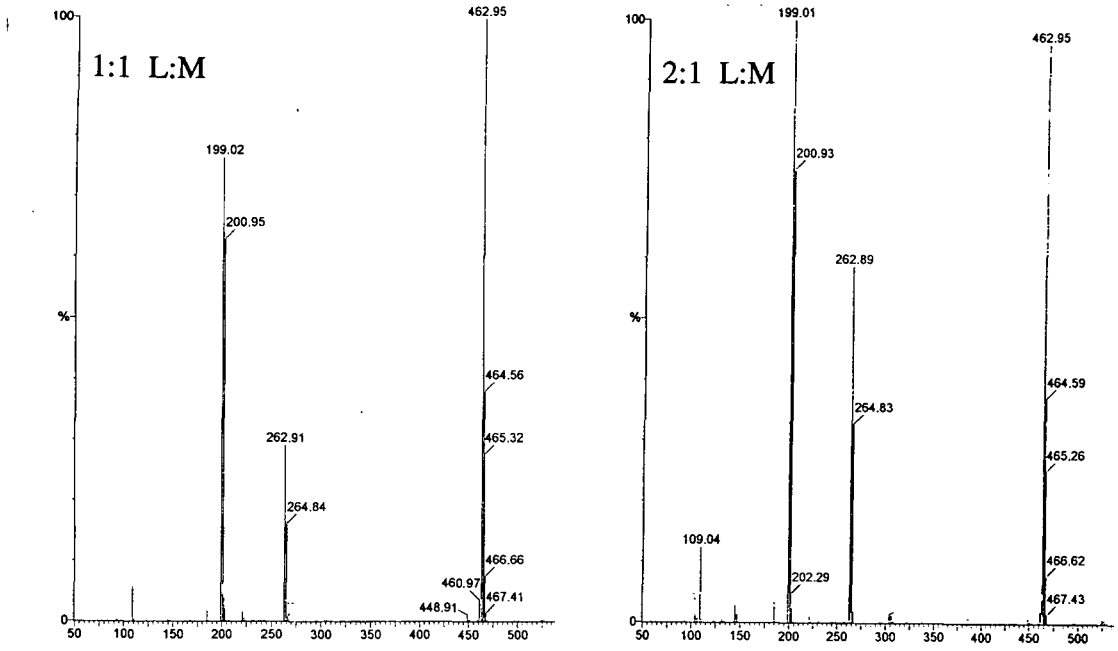

Figure 3.10 ESMS$^+$ spectrum of (**86**) + Cu^{2+} prepared as 1:1 ratio and a 2:1 ratio

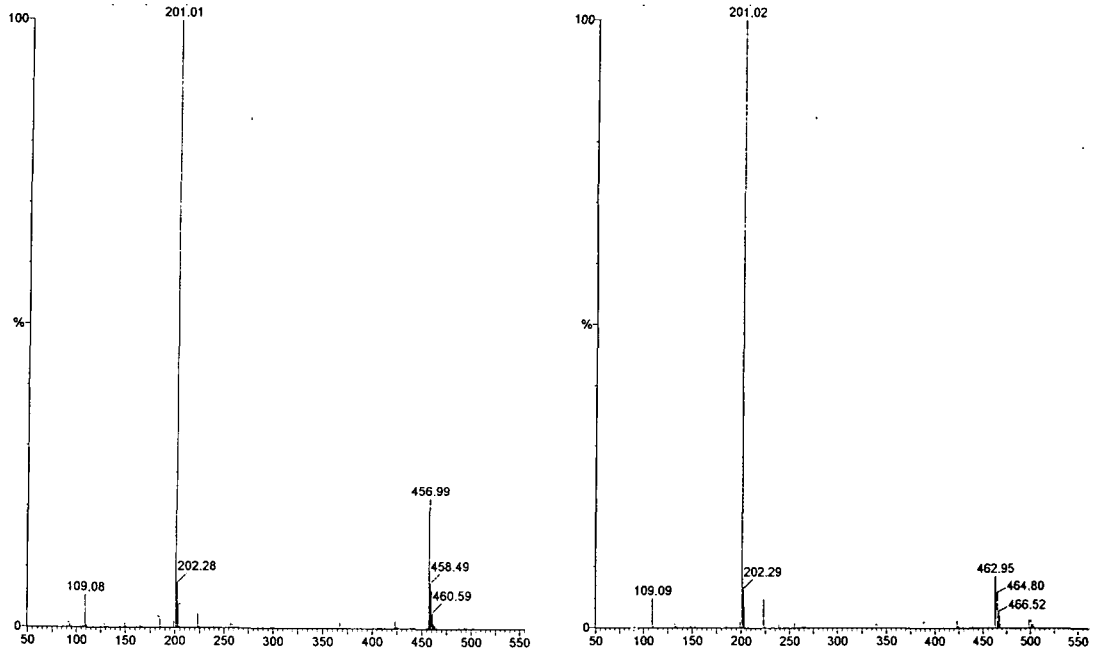

Figure 3.11(a)ESMS$^+$ spectra (**86**) + Zn^{2+} prepared as a 2:1 ratio

(b)ESMS$^+$ spectra (**86**) + Zn^{2+} prepared as a 2:1 ratio

2,6-Bis(dimethylthiophosphorylamino)pyridine (89)

The spectrum of the 1:1 complex of copper showed an extremely clean spectrum of Cu(**89**) only and no unbound ligand (Figure 3.12) with the major mass intensity at 355.81 corresponding to the single deprotonation of the ligand, consistent with the formation of a copper(I) species. By contrast, electrospray analysis of the nickel and zinc species formed upon complexation with ligand (**89**) showed that several species were present in each sample. With nickel, the most intense peak was due to the free ligand, then ML (349.9) and ML_2 (642.7), as well as peaks at 449.8 and 742.5 which

indicated the presence of perchlorate adducts of ML and ML_2 respectively. The formation of all of these species was mirrored by the spectrum of the ligand with zinc: peaks due to L, ML, ML_2 and their perchlorate adducts were present.

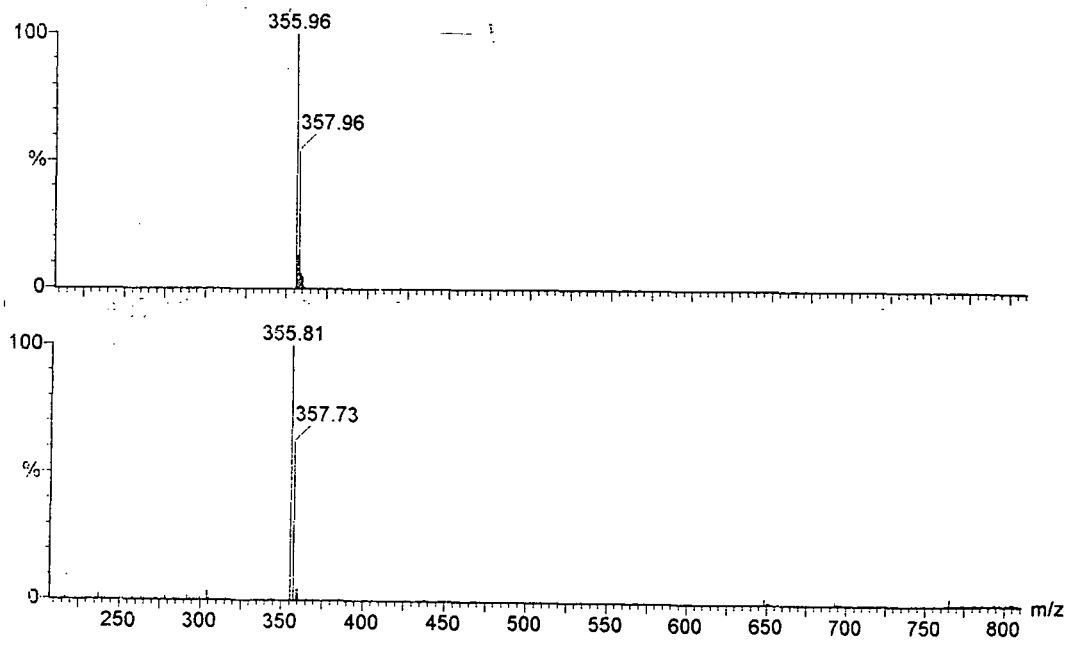

Figure 3.12 $ESMS^+$ spectrum showing Cu(**89**) and isotope model (above)

Another interesting observation was that nickel and zinc ML peaks corresponded to the mass of the metal plus ligand, minus two protons. The same calculation with copper corresponded to the loss of only one amine proton, which suggests that copper is present as copper(I).

At this stage it was unclear if the reduction to Cu(I) occurred upon ligand complexation or during the electrospray ionisation process.

Ultraviolet and visible photospectroscopy of ligands with copper(I) and (II)

The UV-visible spectra provided further evidence which was consistent with the formation of complexes with copper. The λ_{max} values for the free ligands (Table 3.2) and their copper complexes were measured in acetonitrile using copper(II) triflate and tetrakis (acetonitrile)copper(I) tetrafluoroborate as sources of Cu^{2+} and Cu^+ ions respectively (Table 3.3).

Table 3.2 λ_{max} values of dimethylthiophosphoryl ligands

Ligand	λ_{max} / nm	ε / $dm^3\ mol^{-1}\ cm^{-1}$
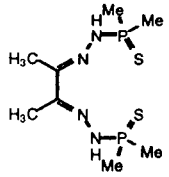 **(85)**	274 (C=N : π-π^*)	31 000
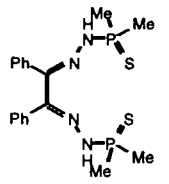 **(84)**	276	31 000
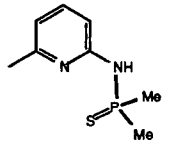 **(86)**	232 286	11 000 4 000
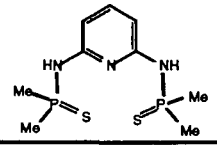 **(89)**	244 300	8 000 6 000

Table 3.3 λ_{max} values of 1:1 complexes formed from $Cu(CF_3SO_3)_2$ and $[Cu(I)(CH_3CN)_4BF_4]$ in acetonitrile at 293K

Ligand	COPPER(II) ADDED		COPPER(I) ADDED	
	λ_{max} / nm	ε / $dm^3\ mol^{-1}\ cm^{-1}$	λ_{max} / nm	ε / $dm^3\ mol^{-1}\ cm^{-1}$
(85)	206	19 600	204	40 000
	302	12 500	274	35 000
	392	4 700	430	2 000
	636	210		
(84)	208	shoulder		
	280	50 000	280	78 000
(86)	232	49 300	232	18 500
	286	15 200	286	62 500
(89)	240	shoulder	240	18 400
	302	8 800	302	12 000
	326	5 700		

Comparison of the results in the presence of added Cu(II) and Cu(I) clearly shows that only ligand (**85**) forms a Cu(II) complex while ligands (**84**), (**86**) and (**89**) reduce copper(II) to copper(I). The values given for the complexation of these three ligands with the two sources of metal are very similar. In contrast, the λ_{max} values for ligand (**85**) with copper(I) and copper(II) are quite different, indicating an entirely different geometry. The obvious difference amongst the ligands is that (**85**) does not contain any

aryl group whereas the other ligands form conjugated systems which include a pyridyl or phenyl aromatic rings.

Measurements were also carried out upon the complexes formed with copper (II) and the same ligands in methanol to check for any evidence of a solvent dependence (Table 3.4). Again, the methyl dihydrazide ligand (**85**) formed a dark green solution showing a weak d-d band (λ_{max} 638 nm, ε 150 dm^3 mol^{-1}) consistent with the formation of a copper(II) complex. The complex formed with the phenyl dihydrazide ligand in methanol showed more colour than the corresponding species in acetonitrile. The former species showed an extra band, a metal to ligand charge transfer band (λ_{max} 404 nm, ε 180 dm^3 mol^{-1}), giving rise to the yellow colour.

Table 3.4 λ_{max} values of dimethylthiophosphoryl ligands in methanol

Ligand	COPPER(II) λ_{max} / nm	ADDED ε / dm^3 mol^{-1} cm^{-1}	complex colour
(**85**)	208	16 500	dark green
	310	15 400	
	388	7 600	
	638	150	
(**84**)	206	40 100	greeny-yellow
	280	26 000	
	404	180	
(**86**)	232	28 200	colourless
	286	10 100	
(**89**)	240	13 800	pale yellow
	310	6 100	

Upon standing for five days, the methyl ligand copper(II) complex Cu(II)(**85**) showed different behaviour in the two solvents. In acetonitrile, the dark green Cu(II) complex remained whereas, in methanol, the formerly dark green solution had turned very pale yellow in colour, indicating that the Cu(II)(**85**) complex had been reduced to the corresponding Cu(I)(**85**) complex.

NMR titrations

A similar procedure to the method used for the metal binding study of the thiophosphinic acid ligands (Ch. 2, section 2.3) was adopted. NMR titrations were attempted with both zinc and copper(I). Ligand (**84**) showed only minor changes in the shift of the phosphorus signal followed by ^{31}P NMR analysis during the incremental addition of the metal. However, for the formation of a 1:1 complex, the shift expected upon addition of excess metal (M/L >1) would be much less than any initial shift due to

binding of the ligand. These continuous minor shifts provided evidence of only weak bindingwith Cu(I). However, several ^1H NMR spectra were obtained (in CD_3CN) during the incremental addition process, and a change in the chemical shift and coupling constant of the P-methyl substituents were observed, although only qualitatively, due to the proximity of the protonated solvent peak. The coupling constant increased from 4 Hz to 19 Hz over the metal addition process. With the addition of zinc ions the phosphorus chemical shift hardly changed at all, as expected from the ESMS analytical evidence above, of only very weak formation of a zinc complex.

The ligands (**84**) and (**85**) themselves, were studied for N-H/N-D exchange in CD_3OD. The proton NMR spectrum of a sample of each ligand in $CDCl_3$ showed the distinctive phosphorus-coupled broad doublet at ~6 ppm (J~21 Hz) characteristic of these ligands. Two drops of CD_3OD were added to each sample, and proton NMR spectra were re-aquired. The spectrum of the methyl ligand (**85**) showed that the N-H signal had disappeared completely, while the analogous spectrum of the phenyl ligand (**84**) showed an N-H signal, but its integral was reduced by greater than 50%. These observations indicate that N-H/N-D exchange occurs with both ligands and that the rate of N-H/N-D exchange is more rapid for the methyl ligand (**85**). At an infinite time point, the ^1H NMR specrum of $CDCl_3/CD_3OD$ sample of the phenyl ligand (**84**) showed that the integral of the N-H proton was very small (« 0.5H). Obviously there is an equilibration process taking place between the acidic H and D of the ligand and the excess CD_3OD, indicating a similarity in the pK_a values of the species. Hence the acidity of the ligand N-H may be estimated to be somewhat less than that of CD_3OD (the dissociation constant of methanol is 15.92).

HPLC analysis

HPLC analysis was performed with tetradentate phenyl-substituted ligand (**84**) and copper(II) acetate in methanol as a prelude to possible radiolabelling studies. The chromatogram of the ligand (**84**) confirmed the purity of the compound and gave a single peak with a retention time of 13 minutes. Analysis of a solution containing a 1:1 mixture of (**84**) and Cu^{2+} (as copper(II) acetate) revealed that very little complex was present, and only the ligand along with another very minor small peak corresponding to a minor impurity were observed in the chromatogram. Preparation of the complex with the addition of 2:1 equivalents sodium methoxide to ligand followed by the addition of copper showed an improvement in the amount of complex formed. The chromatogram still showed some ligand (R_t 13 minutes, 28%) but a higher proportion of the copper complex was observed with a retention time around 15 minutes (44%) in addition to a minor species with a retention time of 16 minutes (8%). This sample was also analysed by ESMS which confirmed that the major species formed were CuL and CuL_2.

Isolation of solid complexes

Crystallisation of the copper complexes was attempted in order to obtain suitable crystals for structural elucidation in the solid state by X-ray analysis. Initial attempts focussed upon ligand (**85**) since it formed complexes with both Cu(I) and Cu(II) and solid state structures of both complexes would have allowed comparison of the copper geometries. However, upon cooling (-5°C) and standing, the deep green solution of Cu(II)(**85**) in acetonitrile yielded only small amounts of colourless suspensions and the complex appeared to degrade rather than form crystals with time. The Cu(I) complex of ligand (**85**) was prepared by the addition of a solution of $[Cu(CH_3CN)_4]BF_4$ to a solution of the ligand. An orange solid precipitated immediately and was isolated and characterised by elemental analysis and ESMS as the neutral Cu(I)(**85**) complex. Crystals were formed by allowing a solution of the complex in acetonitrile to stand and undergo slow evaporation of the solvent, but characterisation of the colourless crystals which formed, showed that these were $[Cu(CH_3CN)_4]BF_4$. This suggests that the complex has a limited stability and dissociates with time.

Similarly, solutions of a 1:1 complex of (**85**) and Cu(II) and a 2:1 complex of Cu(**86**)$_2$ which instantly reduced Cu(II) to Cu(I) (deduced from the yellow and colourless solutions respectively) failed to yield any crystals but produced very small amounts of a colourless solid powder. Attempts to induce crystallisation by the addition of diethyl ether or tetrahydrofuran and by changing the counter ion to perchlorate or hexafluorophosphate failed to give any suitable crystals.

Attempted complexation with oxorhenium (V)

Preparation of the oxorhenium derivatives of ligands (**84**) and (**85**) was attempted using $[Re(O)Cl_3(PPh_3)_3]$ in an analogous manner to that described previously (Ch. 2, section 2.3). The phenyl ligand (**84**) gave a dark brown solid which was only sparingly soluble in solvents such as methanol and acetonitrile. The ESMS$^-$ spectrum obtained in methanol gave a rhenium isotope pattern at 249 and 251 in relative abundances corresponding to perrhenate and the other major intensity at 389 correspondng to the ligand with two sulfurs replaced by oxygen. ^{31}P NMR analysis showed a single phosphorus species at δ_P 47.32 (MeOH) - a chemical shift more characteristic of P=O species - in agreement with the above observations. Combustion analysis of various samples of the solid product failed to give consistent results, indicative of a mixture rather than a well-defined single species. A dark brown solid also formed with the methyl ligand (**85**) and combustion analysis similarly failed to give consistent results.

Attempted complexation of the ligands with oxorhenium(V) was also performed in dichloromethane but similar dark brown solutions were obtained. From the above observations, it appears that some redox processes occur at the P-S bond in the

thiophosphoryl ligand allowing transformation to its phosphoryl analogue with concomitant electron transfer to and from the rhenium centre.

Molecular Modelling

Models of the copper complexes of the bis[(dimethylthiophosphoryl)hydrazide] ligands (**84**) and (**85**) were created by Christopher Edlin at Zeneca Specialties using the method as described previously (Ch.2, section 2.3). The models (Figure 3.13) show copper with a distorted tetrahedral geometry suggesting that the ligands may stabilise Cu(I) and destabilise Cu(II). This correlates with the observations that the ligands have a tendency to stabilise Cu(I) although the phenyl-substituted ligand (**84**) performs the Cu(II)/(I) reduction instantaneously whereas the corresponding methyl ligand (**85**) does not behave in this manner as discussed above. These simple models do not account for the behaviour of the metal with the specific ligand system but give a good insight into the possible preferred geometry of the metal.

3.4 Conclusions

The synthesis of new dimethylthiophosphoryl ligands is relatively simple provided that the appropriate dihydrazone can be prepared. The synthesis of the dihydrazide ligands via disconnection of the P-N bond proved to be more general in scope than condensation of the corresponding diketone with a substituted thiophosphorylhydrazine. Although all of the thiophosphoryl derivatives considered above were dimethyl substituted, a range of substituents may be accessible via the bi(phosphine sulfide) compounds, including those containing two different alkyl groups at phosphorus.[28]

Analysis of the copper, nickel and zinc complexes by electrospray mass specrometry shows, that although all four ligands formed complexes with these metals, the copper complexes appeared to form the most avidly and cleanly for each ligand. Furthermore, visible photospectroscopy of all four ligands with Cu(II) and Cu(I) confirms that reduction of Cu(II) to Cu(I) is strongly favoured in both acetonitrile and methanol.

Characterisation of the copper complexes of the ligands (with the metal present in either Cu(II) or Cu(I) oxidation state) looks promising for the formation of neutral complexes and suggsts that the radiolabelling of these ligands should be investigated.

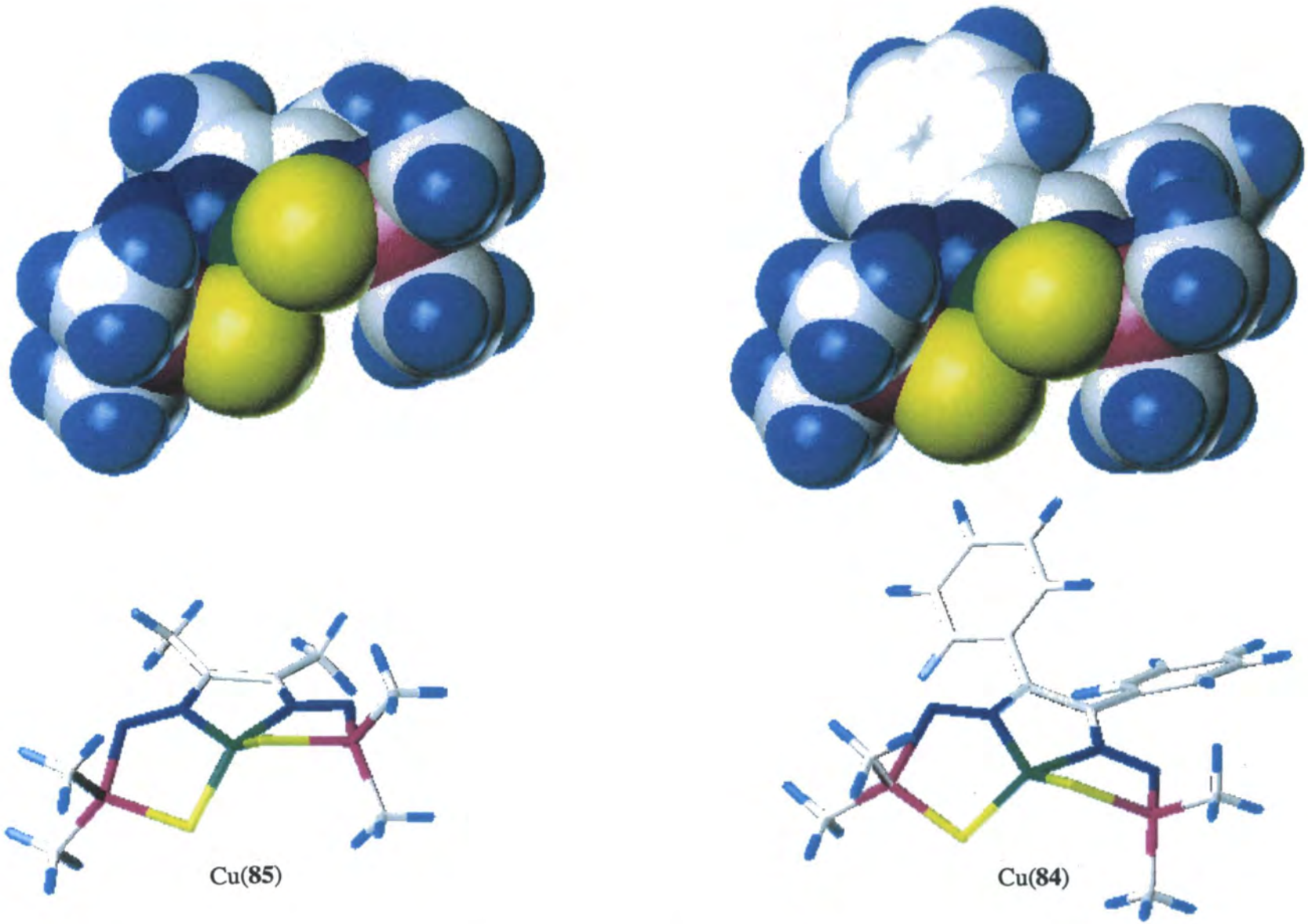

Figure 3.13 Molecular models of copper complexes

3.5 References

1. J.K. Lim, C.J. Mathias and M.A. Green, *J. Med. Chem.*, 1997, **40**, 132
2. L.D. Pettit, I. Steel, G. Formicka-Kozlowska, T. Tatarowski and M. Bataille, J. *Chem. Soc. dalton Trans.*, 1985, 535
3. K.V. Katti, V.S. Reddy and P.R. Singh, *Chem. Soc. Rev.*, 1995, 97
4. W.A. Volkert, P.R. Singh, A.R. Ketring, K.V. Katti and K.K. Katti, *J. Labl. Comp. Radiopharm.*, 1993, **32**, 15
5. P.R. Singh, H. Jimenez, K.V. Katti, W.A. Volkert and C.L. Barnes, *Inorg. Chem.*, 1994, **33**, 736
6. K.V. Katti, P.R. Singh and C.L. Barnes, *Inorg. Chem.*, 1992, **31**, 4588
7. A.D.F. Toy and E.G. Uhing, U.S. Patent 4,076 (Cl. 260-543P; CO7F9/04), 28 Feb. 1978, Appl 502,702
8. K.A. Pollart and H.J. Harwood, *J.Org.Chem.*, 1962, **27**,4444
9. H. Reinhardt, D. Bianchi and D. Mölle, *Chem. Ber.*, 1957, 1656-1660
10. W. Kuchen and H. Buchwald, *Agnew. Chem*, 1959, **4**, 162
11. J. Tsuji, H. Kezuka, Y. Toshida, H. Takayangi and K. Yakamoto, *Tetrahedron* , 1983, **39** (20), 3279
12. A.C Cope, D.S. Smith and R.J. Cotter, *Org.Synthesis Coll.*, 1963, **4**, 377
13. H. Schlesinger, *Angew. Chem.*, 1960, **72**, 563
14. A. Schmidpeter and J. Ebeling, *Chem. Ber.*, 1968, **101**, 815
15. I.C. Pirmettis, M.S. Papadopoulos and E. Chiotellis, *J. Med. Chem.*, 1997, **40**, 2539
16. J.J. Bloomfield, *J. Org. Chem.*, 1961, 26, 4112
17. K. Beck and S. Hunig, *Chem. Ber.*, 1987, **120**, 447
18. N.A. Domin and N.S. Glebovskaya, *J. Gen. Chem. USSR.*, 1957, **27**, 656
19. G. Wittig and A. Krebs, *Chem. Ber.*, 1961, 3261
20. R.A. Cherkasov, G.A. Kutyrev and A.N. Pudovik, *Tetrahedron*, 1985, **41**, 2567
21. E. Fluck and R.M. Reinisch, *Chem. Ber.*, 1962, **45**, 1388
22. E. Fluck and H. Binder, *Z. Anorg. Chem.*, 1967, **354**, 113
23. U. Pederson, M. Thorsen, E.E. A.M. El-Khrisy, K. Clausen and S.-O. Lawesson, *Tetrahedron*, 1982, **38**, 3267
24. U. Pederson, M. Thorsen, K. Clausen, M. Thorsen and S.-O. Lawesson, *Tetrahedron*, 1982, **38**, 3267
25. I.D. Baerga, R.P. Maikel and M.A. Green, *Nucl. Med. Biol.*, 1991, **19**, 697
26. G.J. Kubas, *Inorg. Synth.*, 1979, **19**, 90; *ibid*, 1990, **28**, 68
27. M. Goodall, P. Kelly, D. Parker, K. Gloe and H. Stephan, *J. Chem. Soc., Perkin Trans. 2*, 1997, 59
28. H.J. Harwood and K.A. Pollart, *J. Org. Chem.*, 1963, **28**, 3430

Chapter Four

Systems with more Rigid Skeletons

4. Aza-Thiophosphinate Systems with More Rigid Skeletons

The accessibility of further new amino-thiophosphinate ligands by the incorporation of more rigid (aromatic) units in the overall skeleton is discussed (4.1). Possible synthetic routes and the difficulties encountered towards the preparation of such systems are presented (4.2), together with suggestions for further systems and plausible synthetic pathways (4.3).

4.1 Extending the Thiophosphinic Acid Series - Design of two new systems

A useful extension to the aza-thiophosphinate ligand series was envisaged by altering the chelate ring system and including some rigid spacers. Added rigidity may have the effect of favouring a particular geometry and disfavouring undesired geometries such as tetrahedral and octahedral, thus increasing the selectivity for a particular metal ion (see section 3.2). In the thiophosphinate series described earlier (Ch.2), the ligands are disposed to form three five-membered chelate rings (5,5,5) or two five-membered and one six-membered chelate rings (5,6,5) upon metal complexation. The methylene linkers between the nitrogen donors and their adjacent thiophosphinate funtionality of the previous aza-thiophosphinate ligands (**30**) (Ch. 2) could each be replaced by an aromatic ring to increase the chelate ring size from five-membered to six-membered, giving a (6,5,6) ring system overall (Figure 4.1).

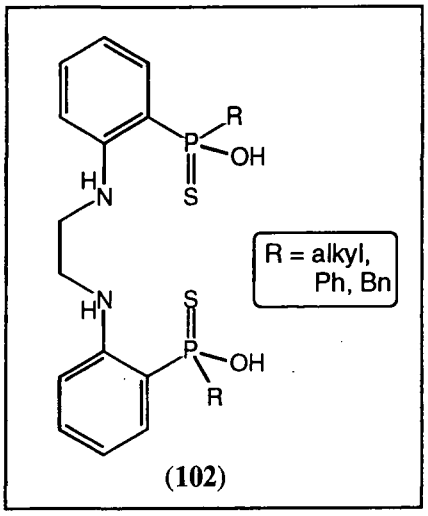

(102)

Figure 4.1 New ligand design with 6,5,6 chelate rings.

The incorporation of an aromatic ring as part of the skeleton in the design of (**102**) may find further advantage as the nitrogen donor atoms of the ligand should be less readily protonated in acidic media. This is particularly attractive for oxotechnetium(V) and oxorhenium(V) complexes which require the deprotonation of one of the amines in addition to the thiophosphinate donors, in order to achieve charge neutrality. The

deprotonation of such aromatic nitrogen donor atoms upon formation of the oxo-technetium complex is known for highly delocalised, unsaturated electron-rich ligands, such as *o*-phenylenediamine (pda).[1] Reduction of pertechnetate with sodium dithionite in the presence of excess phenylenediamine results in the formation of an anionic complex with a $TcON_4^-$ core, whereas the absence of a reducing agent results in the formation of the tris-bidentate complex with a TcN_6^- core. In both complexes, the amines are deprotonated and act as negative nitrogen donor atoms.

Another system, based on a 1,10-phenanthroline moiety (**103**), is also an attractive backbone to support the thiophosphinate functionality. With two suitably spaced nitrogen donor atoms capable of forming 5-membered chelates, it has already been used to form the basis of several ligands which bind many metals. The increasing application of phenanthroline-based systems to coordination chemistry results from their predisposition to metal binding which is manifested by their entropic advantage. The two nitrogen donor atoms of 1,10-phenanthroline ligands are held in the same plane which has considerable advantage over ethylenediamine systems (**104**). The phenanthroline unit offers similar donor atoms and chelate ring size, but unlike ethylenediamine, there is no rotation about the C-C and C-N sigma bonds (Figure 4.2). This advantage also holds over bipyridyl (bpy) systems (**105**) where rotation may occur around the central bond depending on whether both nitrogen atoms are cooperatively engaged in binding a proton in acidic media.

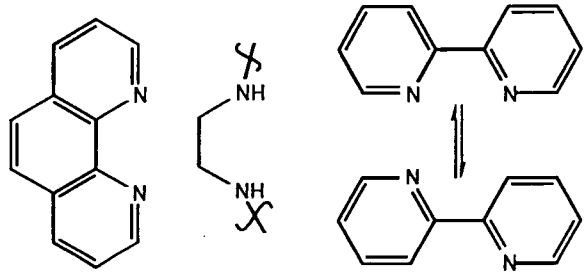

(**103**) (**104**) (**105**)

Figure 4.2

Examples of 1,10-phenanthroline ligands in coordination and analytical chemistry are widespread and include applications in ionic and self-assembling systems[2] and potentiometric sensors.[3] Systems based upon 2,9-substituted phenanthrolines have been generally applied to the coordination chemistry of many metals.[4] Copper(I) generally adopts tetrahedral geometry by phenanthrolines and there are a variety of examples of 2,9-dimethyl-1,10-phenanthroline (neocuproine) complexing this metal ion as an $[ML_2]^+$ complex (**106**).[5,6]

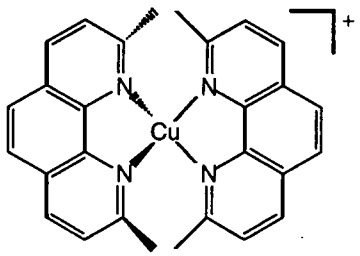

(106)

A series of acyclic tetradentate phosphinic acid ligands based on 1,10-phenanthroline (Figure 4.3) was synthesised by George Bates.[7] The subsequent study of these N_2O_2 ligands showed that the hard phosphinate donors bound zinc(II) and nickel(II) ions and enhanced the stability of their phenanthroline complexes, while copper(II) was, unsurprisingly, bound only through nitrogen.

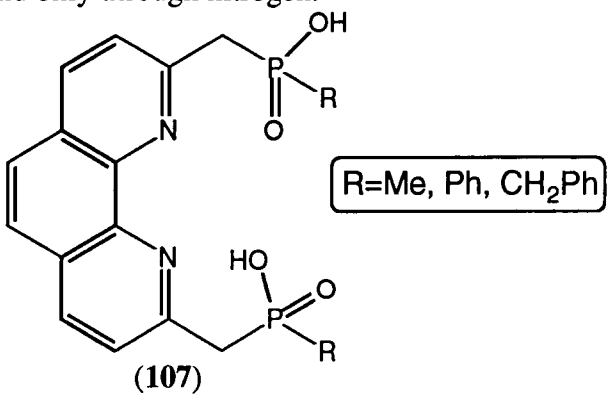

(107)

Figure 4.3 Phosphinate phenanthroline ligand system

Analogous thiophosphinic acid ligand systems were proposed herein (**108**) (Figure 4.4), as an extension of the original thiophosphinate ligand series (Ch. 2) incorporating the phenanthroline unit for predisposition to metal binding. Use of sulfur donors should enable all four donor atoms to bind to copper, unlike the 'hard' phosphinate ligands, and the incorporation of the longer P=S and S-M compared with the P=O systems may give a geometry favourable for copper(II).

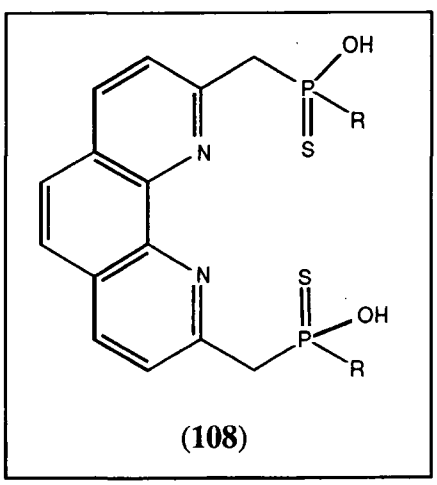

(108)

Figure 4.4 Design of new phenanthroline thiophosphinate ligands

4.2 Synthesis

4.2.1 Phenylene aza-thiophosphinate system

An additional advantage of the design of (**102**) was foreseen in the ligand synthesis, as disconnection between the aromatic ring and phosphorus may be possible giving an aromatic bromide skeleton and the appropriate phosphonous ester as the synthons in a palladium(0) coupling reaction (Scheme 4.1). Such couplings have been described by Xu and Huang[8] and Hirao[9] where palladium(0) in the form of $[Pd(PPh_3)_4]$ effectively catalyses the reaction between aromatic bromides and phosphonous esters - RP(O)H(OR) types. This coupling reaction is extremely tolerant of the presence of other functional groups.

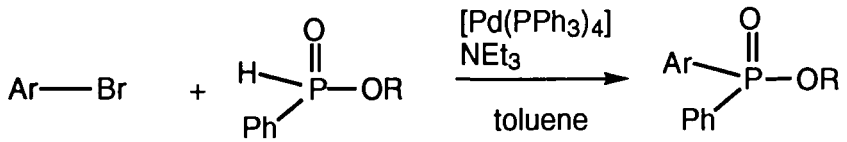

Scheme 4.1 Pd(0) coupling

The synthesis was designed with 2-bromoaniline as the starting compound for the preparation of the carbon skeleton (**109**) prior to the introduction of a phosphorus functionality (Scheme 4.2). Treatment with tosyl chloride at room temperature in pyridine gave the tosylated bromoaniline in 93% yield. Subsequent reaction with 1,2-bis(*p*-toluenesulfonato)ethane in DMF and caesium carbonate in an analogous procedure to that reported by Parker,[10] required heating under reflux for 18 hours to give the product mixture as an oil. Crystallisation of the residue from ethyl acetate / light petroleum (40-60) afforded the aromatic bromide (**109**) as a colourless powder.

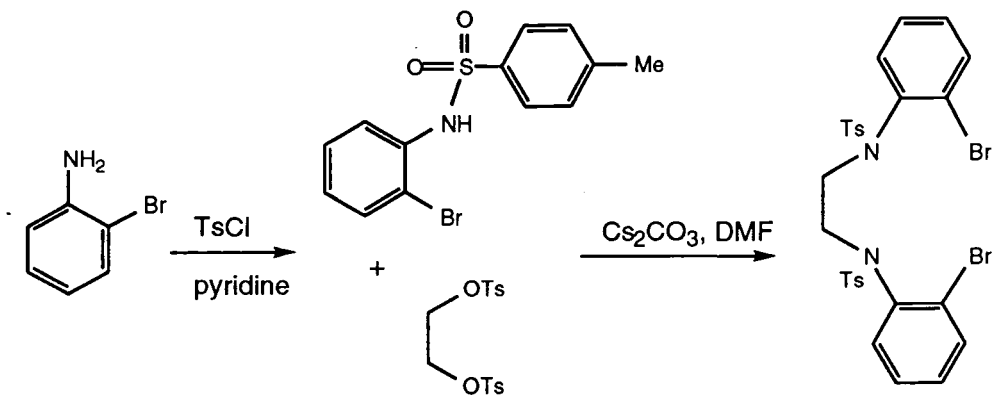

(**109**)

Scheme 4.2 Synthesis of the ligand skeleton

The rest of the ligand synthesis was proposed (Scheme 4.3), and the next step was the carbon-phosphorus bond-forming reaction (see above) by treatment of the aromatic bromide (**109**) with the appropriate phosphonous ester.

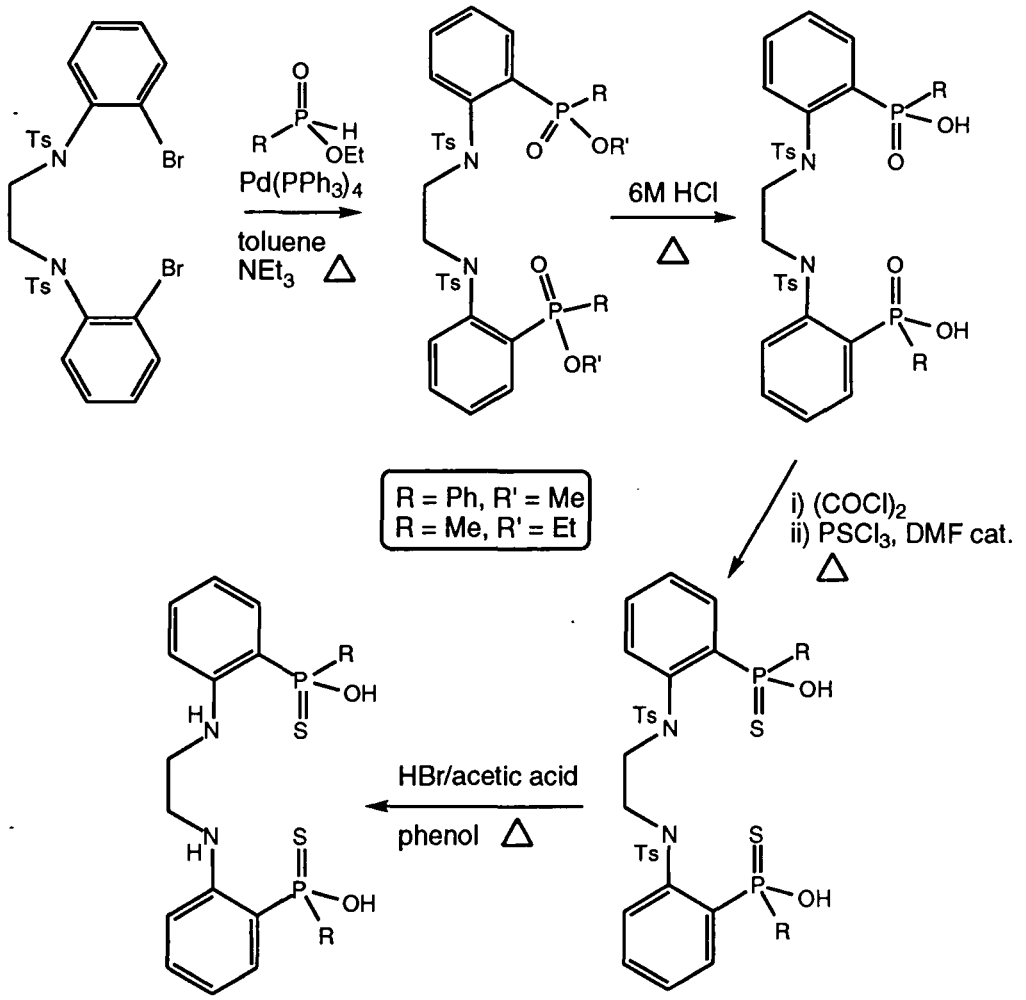

Scheme 4.3 Proposed synthesis of aromatic thiophosphinate ligands

Although the phenyl phosphonous ester was available commercially, the methyl analogue had first to be prepared. The synthesis of MeP(O)(H)OEt was carried out according to literature methods,[11,12] using dichloromethylphosphine and ethanol as a reagent in a solvent free procedure (Scheme 4.4).

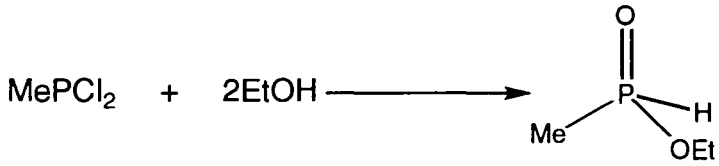

Scheme 4.4 Preparation of methylethylhydrogen phosphonite

The palladium coupling was then attempted with methylethyl phosphonite [MeP(O)H(OEt)] using the conditions described.[9] The aromatic bromide (**109**), triethylamine and phosphonous ester were placed in dry toluene and the mixture was degassed using a freeze-thaw cycle under vacuum. A catalytic amount of $Pd(PPh_3)_4$ was added to the mixture which was degassed again and heated under an inert atmosphere for 20 h. However, analysis of the products by ^{31}P and ^{1}H NMR showed

that the phosphorus-carbon bond had failed to form and the aromatic bromide had been converted to its protonated form (**110**). This reaction was attempted several times with both ethylphenylphosphonite, [PhP(O)H(OEt)] as well as the methyl compound - using fresh catalyst, freshly distilled solvents and samples of the aromatic bromide (**109**) which had been dried *in vacuo* for several hours. Under all the conditions described, neither of the desired phosphinate esters was observed by ^{31}P NMR, ^{1}H NMR or ESMS.

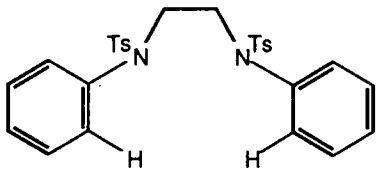

(110)

Consideration was therefore given to the mechanism,[9] represented schematically below (Scheme 4.5). This involves oxidative addition of the Pd(0) species and aromatic bromide which results in the intermediate Pd(II) species prior to attack by the phenyl phosphonite.

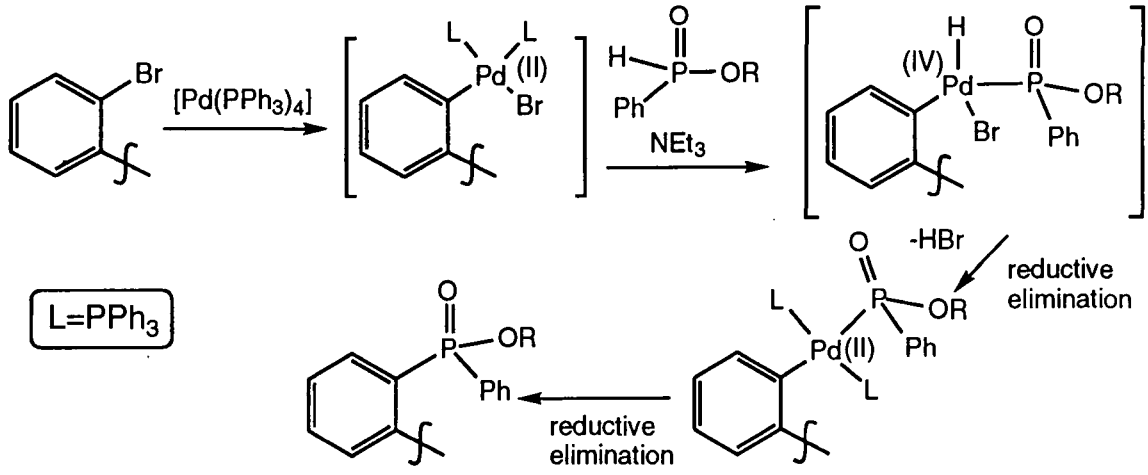

Scheme 4.5 Reaction of the phosphinous ester to give the desired P-aromatic bond

The reaction product (**110**) suggests that elimination of HBr from the palladium complex (Figure 4.5) does not occur and instead, elimination of H-aryl unexpectedly takes place. There is no obvious reason for this occurrence, but speculation may involve steric arguments.

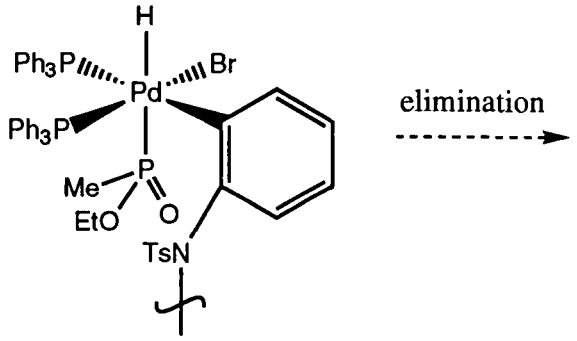

Figure 4.5 Representation of the putative Pd(IV) intermediate

Other Aryl-Phosphorus bond-forming reactions

Literature methods of forming phosphorus-carbon bonds from suitable aromatic and phosphorus starting materials were investigated, and another method of performing this type of transformation was considered. The nickel-catalysed Arbuzov reaction of diethyl methylphosphonite with *o*-iodotoluene was reported by Grabiak to give the aryl phosphinate in excellent yield.[13,14] High temperatures were required and the preparation of anhydrous nickel chloride was achieved by drying under vacuum at 200°C. Another method involving irradiation of diethyl methylphosphonite with substituted *o*-iodobenzylamide was also reported by Grabiak[14] to give the corresponding phosphinate ester. Nickel catalysed Arbuzov reactions have also been reported for 1-substituted-5-bromonaphthalenes using nickel bromide and diethyl methylphosphonite.[15] A more mild method of achieving such phosphorus substitution of an aryl system using diethyl methylphosphonite as a substrate was reported by Cadogan via nucleophilic displacement of a nitro group.[16] This reaction was reported to occur with several substituted phosphonites in acetonitrile without heating (Scheme 4.6) and the aryl substrate required was 1,2-dinitro-benzene. Despite the apparent limitation imposed upon this reaction by the prerequisite nitro group, an extremely versatile precursor was foreseen simply by reduction of this nitro substituent to an amine. This concept led to the design of a whole new synthetic scheme based upon this mild reaction as the initial step (Scheme 4.7).

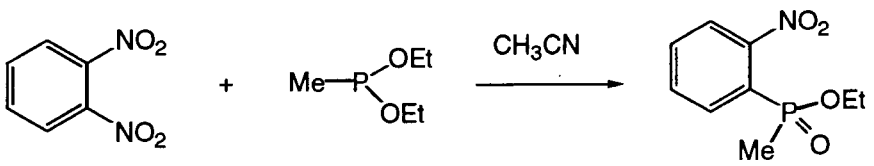

Scheme 4.6 Substitution of a nitro group by phosphorus

Alternative synthetic route requiring the arylphosphinate as starting material

Consequently, an alternative synthesis was proposed involving the formation of the aryl carbon-phosphorus bond prior to elaboration of the structure and formation of the overall ligand skeleton (Scheme 4.7).

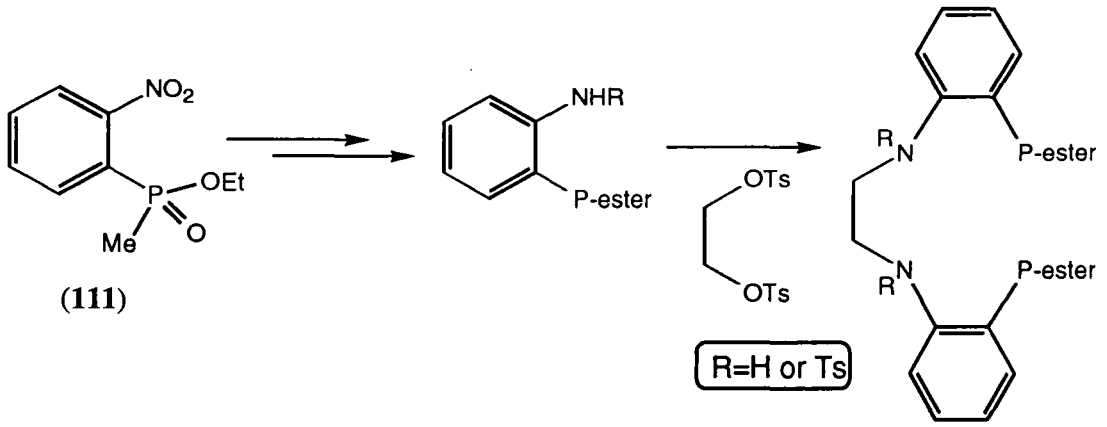

Scheme 4.7 Basis of alternative towards the synthesis of (**102**)

First, P-methyl-o-nitrophenylphosphinate was prepared by the reaction of methyldiethoxyphosphine with dinitrobenzene in dry acetonitrile at room temperature as described previously.[17] The pure product was obtained by vacuum distillation in 83% yield as an orange oil which crystallised upon cooling. Reduction of this material to the P-methyl-*o*-aminophenylethylphosphinate was carried out as described by Kyba and Clubb using iron powder in aqueous ammonium chloride and heating the mixture at reflux for 16 hours[17] to give the product (**112**) in 82% yield following an aqueous work-up (Scheme 4.8).

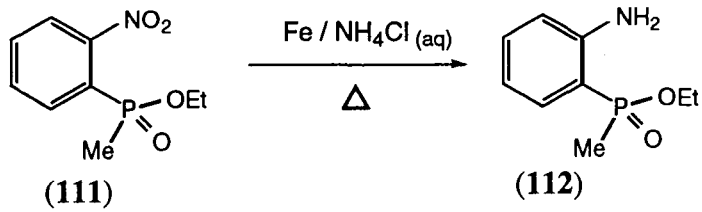

Scheme 4.8 Reduction of the nitro group to an amine

Amide refinement

At this point, the original design (**102**) was refined to incorporate amide rather than amine nitrogens (**113**) (Scheme 4.9). It was envisaged that the amide nitrogen lone pairs may be sufficiently tied up in the amide bond that N-protection prior to the eventual sulfur-transfer step may not be required. The amide carbonyl groups could remain as part of the new ligand, similar to diamidodithiol (DADS) systems used for radionuclide complexation (see section 1.7), or be removed in the final step by some form of reduction to achieve the original system (**102**) proposed.

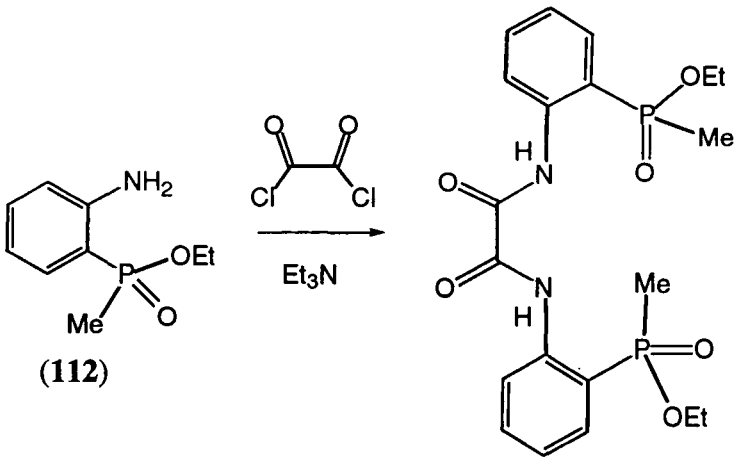

(112) (113)

Scheme 4.9 Synthesis of an amido ligand skeleton

Preparation of the diamide (**113**) was initially attempted by the addition of diethyloxalate to a stirred solution of two molar equivalents of the amine (**112**) and triethylamine in dichloromethane. Despite heating for 18 hours, no reaction was observed by tlc analysis. The amido compound (**113**) was sucessfully prepared by the addition of oxalyl chloride to two equivalents of P-methyl-o-aminophenylethylphosphinate (**112**) and triethylamine in dichloromethane. Aqueous work-up gave the product which was recrystallised from ethyl acetate/diethyl ether to give (**113**) as a white solid in 84% yield. The propane analogue (**114**) was also prepared in good yield using malonyl dichloride in place of oxalyl chloride in this procedure. This analogue would lead to a ligand with three 6-membered chelate rings in addition to the original ligand with a 6,5,6-ring system. The oxalyl ligand (**113**) was treated with lithium hydroxide (4M) at room temperature to hydrolyse the ethylphosphinate diester to the diacid (**115**).

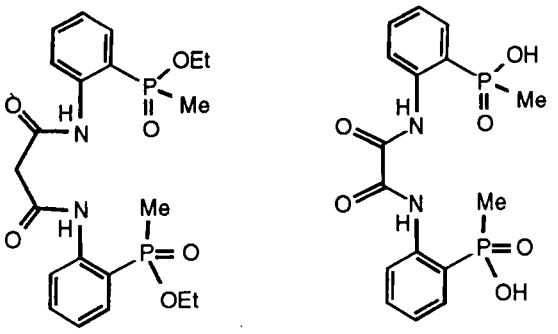

(114) (115)

Preparation of the phosphinic chloride was necessary prior to the sulfur transfer step, and was attempted using oxalyl chloride in dichloromethane as described previously

(section 2.2). However, the phosphinic acid (**115**) proved insoluble in the solvent, unlike the systems prepared previously in this manner where the initial suspension formed a clear solution. Sulfur transfer was attempted in $PSCl_3$ which is also a chlorinating agent capable of forming the phosphinic chloride prior to sulfur transfer. However, ^{31}P NMR analysis showed that no species with a chemical shift greater than 50 ppm were present, suggesting that no disubstituted thiophosphinic chloride species were present. Another method of transforming P=O to P=S was attempted by treatment of the phosphinic acid with PCl_5 in carbon tetrachloride as described by Grabiak[15] followed by Lawesson's reagent (see section 3.2) but to no avail. Part of the problem perhaps lies with the lack of stability of the diamide system towards acidic conditions which dictated the base hydrolysis of the phosphinate ester, and from the formation of a 6-membered chelate ring involving the amide N-H and the phosphinate. Attempts to free the phosphinate (**115**) from its lithium salt (to make the ligand more organically soluble by protonation) by careful addition of 0.1M hydrochloric acid to pH7 resulted in amide hydrolysis (ESMS analysis). The original design (**102**) incorporating the ethane backbone with synthesis proceeding via the ditosylamide appeared to be a more favourable option at this stage.

Attempted synthesis with an ethane backbone

The synthetic route to couple of aromatic amine (**112**) with an ethane backbone from 1,2-bis(paratoluenesulfonato)ethane was attempted (Scheme 4.7, above). The amine (**112**) was dissolved in acetonitrile and stirred with disodium orthophosphate as the base and a solution of 1,2-bis(paratoluenesulfonato)ethane was added. No reaction was observed (monitored by ^{31}P NMR and ESMS analysis) even when the reaction mixture was heated under reflux for 24 h. Reaction of the two substrates was then attempted in dimethylformamide with caesium carbonate in a similar procedure to that described above for the preparation of the aromatic bromide skeleton (**109**). Despite heating at reflux for two days, there was still no reaction observed by mass spectrometry (DCI) and ^{31}P NMR analysis. The only remaining pathway to attempt was the tosylation of the aromatic amine starting material prior to attempting the above reaction again (Scheme 4.10). Although tosylation would appear to make the amine more hindered, it would also make the remaining amine proton more acidic and more likely to be removed, allowing a more favourable starting material for treatment with 1,2-bis(*p*-toluenesulfonato)ethane.

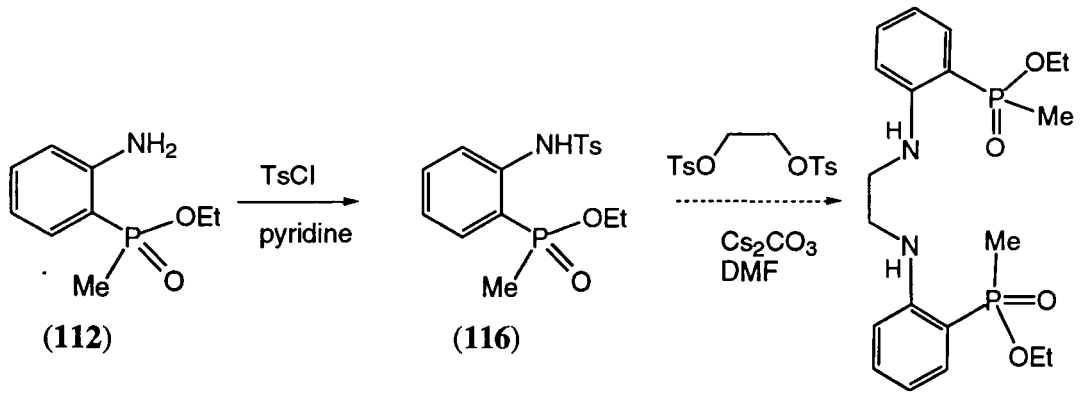

(112) (116)

P-Methyl-o-aminophenylphosphinate was tosylated in pyridine with tosyl chloride in an analogous reaction to the tosylation of bromoaniline described above for (**109**). The crude product (**116**) was used without further purification for the subsequent reaction owing to the limited time available. A solution of 1,2-bis(paratoluenesulfonato)ethane in DMF was added dropwise to a stirred solution of the tosylamine (**116**) in DMF with caesium carbonate and the mixture was heated under reflux for 20 h. Only the starting materials were observed by ^{31}P and ^{1}H NMR analysis. This single attempt to react (**116**) with the ethane derivative was not repeated or attempted under different conditions due to the limited time available. This reaction may be possible, analogous to the above reaction of the tosyl-bromo-aniline to form (**109**) (Scheme 4.2) which did not proceed readily at the first attempt.

4.2.2 Systems based on 1,10-Phenanthroline

The target ligand of this design initially chosen was the P-methyl substituted system (**117**), in order to keep the molecular weight of the ligand fairly low for potential radiopharmaceutical applications. One drawback to this choice was the relatively poor yield reported for the methylphosphinic ester derivative required (2.5% to 47%), in comparison to the yields of the phenyl and benzyl substituted analogues.[8] Nevertheless, the synthesis was embarked upon.

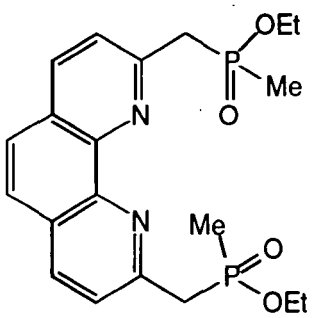

(117)

The dihydrobromide salt of the dibromide (**119**) was synthesised by George Bates according to Scheme 4.11, and and stored for several months at -5°C. The first two

steps of the synthesis used literature reactions to form the alcohol (**118**),[18] while conversion to 2,9-dibromo-1,10-phenanthroline was achieved by treatment with 48% v/v HBr/acetic acid at 100°C.[19]

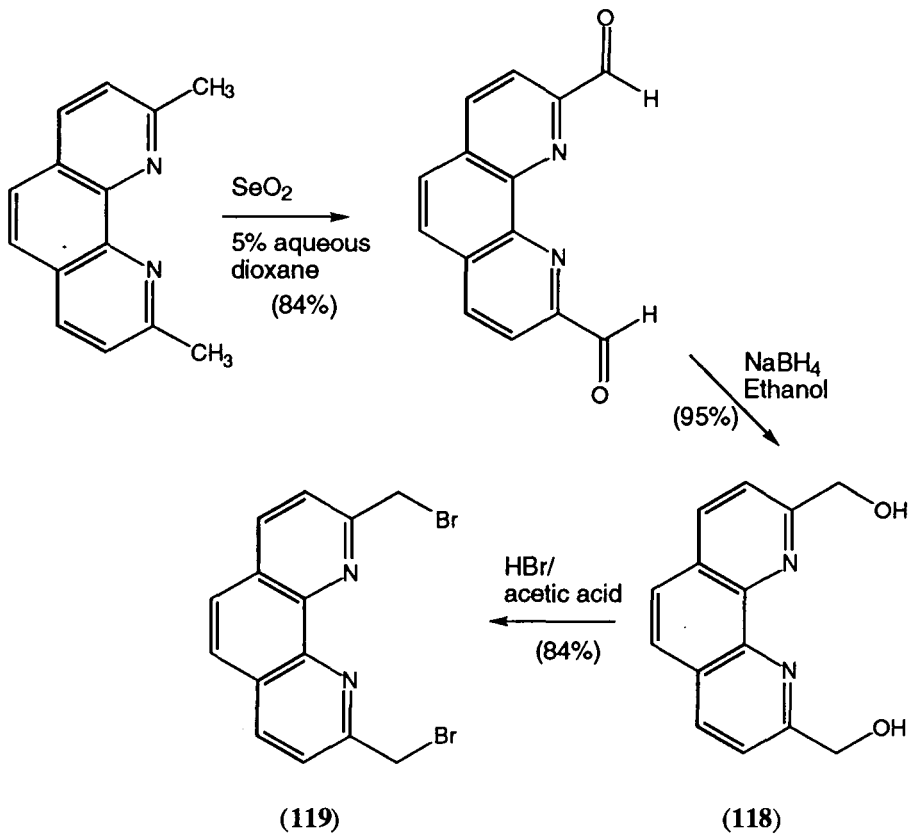

(**119**) (**118**)

Scheme 4.11 Synthesis of the dibromophenanthroline

When required, the hydrobromide salt of (**119**) was neutralised with aqueous sodium carbonate and extracted into chloroform to give the pure dibromo-phenanthroline (**119**) as an orange solid prior to immediate reaction. The methylphosphinate ester (**117**) was prepared in the manner described earlier and was isolated and purified in approximately 15% yield. Competitive halophilic abstraction by $MeP(OEt)_2$ may occur to generate the intermediate ylide which gives a methyl group upon protonation (Scheme 4.13) and hence reduce the yield of the Arbuzov product (Scheme 4.12).

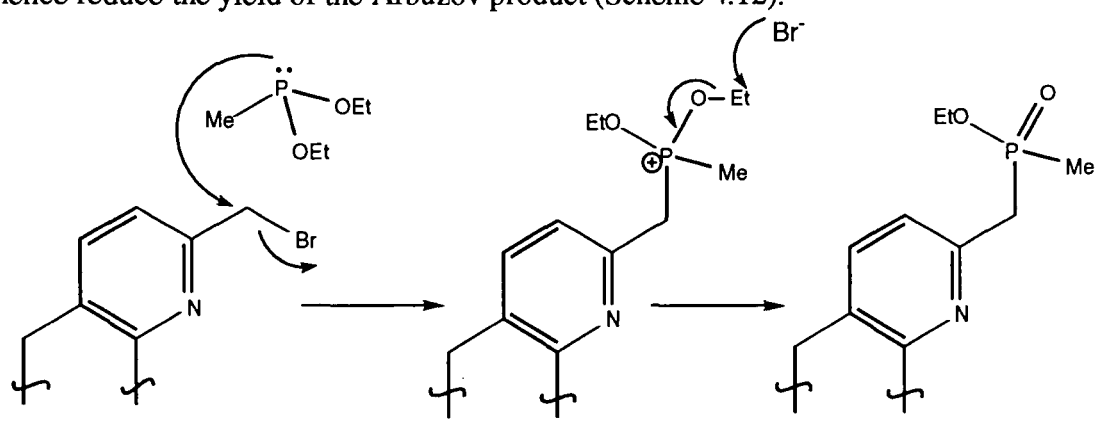

Scheme 4.12 Desired Arbuzov reaction

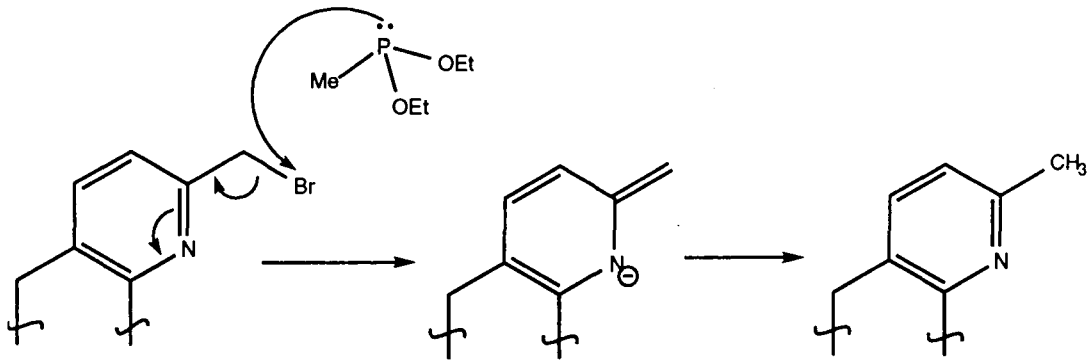

Scheme 4.13 Competing process

There are literature examples of the latter process occurring with chloro and bromo ketones. Triphenylphosphine abstracts the halogen in the above manner to give an enolate which picks up a proton to form the methyl substituent of the ketone.[20,21,22] Ohta[23] found that this process also occurred for the reaction of bromoacetophenone with triphenylphosphine in an attempt to prepare the corresponding phosphonium salt. The major product was acetophenone (Scheme 4.14), and the intended product formed in only 3% yield. However, when a catalytic amount of triethylamine was added, the desired phosphonium salt (**120**) was formed in 92% yield. These observations may be rationalised by consideration of the of the triethylamine as a better leaving group and also a far less favourable group than bromide to be abstracted by the phosphine (Scheme 4.15).

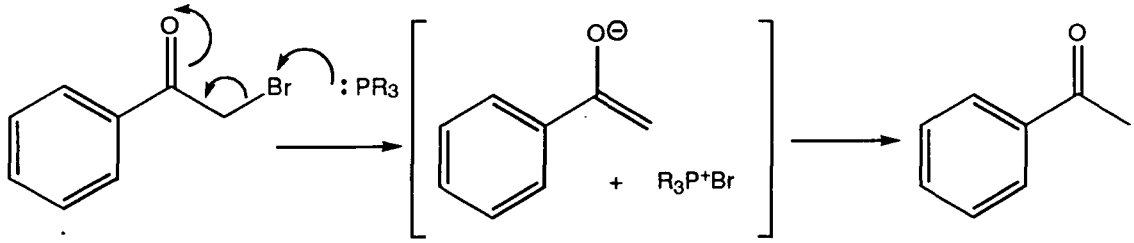

Scheme 4.14 Without triethylamine

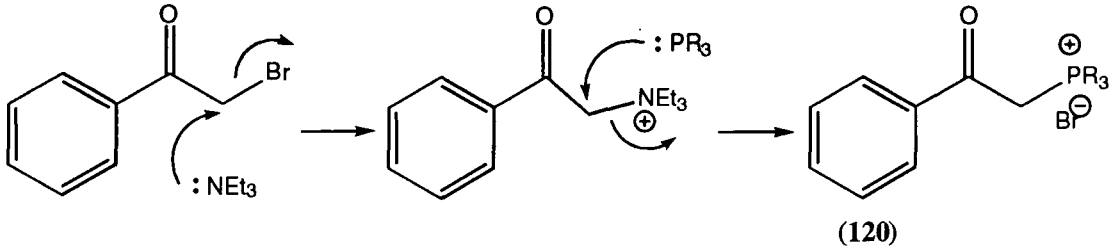

(120)

Scheme 4.15 With a catalytic amount of triethylamine

Due to the similarity of the competing chemical mechanisms in the above work (Scheme 4.14) and the Arbuzov reaction undertaken herein (Scheme 4.11), this catalytic procedure was applied to the synthesis of phenanthroline phosphinate system. Diethylmethylphosphonite was added to a stirred suspension of the dibromide (**119**) in

dry acetonitrile and a catalytic amount of triethylamine was added. The reaction mixture was heated for 18 hours, the solvent was evaporated and the product was purified by chromatography on alumina to give (**117**) as a yellow oil in 70% yield (Scheme 4.15). Hydrolysis of the phosphinate ester in 6M hydrochloric acid as described,[20] gave the phosphinic acid (**121**).

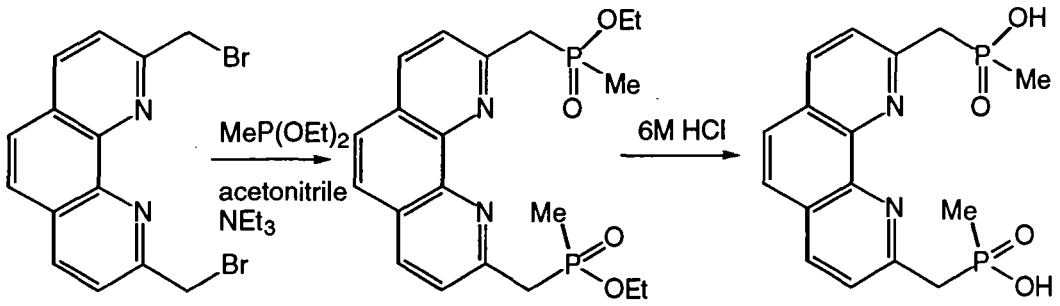

(**119**) (**117**) (**121**)

Scheme 4.15 Synthesis of the phenanthroline-2,9-bis(methylenemethylphosphinic acid)

Conversion to the thiophosphinic chloride was expected to be facile from the phosphinic acid, since no tosylation/detosylation steps were required which also lowered the overall yields of the thiophosphinate ligands previously synthesised (section 2.2). The methylphosphinic acid (**121**) was stirred in dichloromethane and oxalyl chloride was added. After only a few minutes, the reaction mixture had changed in appearance from a golden coloured solution to a deep green suspension, suggesting that some process other than the one desired had taken place. The intractable green solid was difficult to handle and ^{31}P NMR analysis of the chloroform-soluble material gave no phosphorus signal. A similar procedure was undertaken by very slow, dropwise addition of oxalyl chloride to a stirred solution of the phosphinic acid, but to no avail. Other chlorinating procedures such as treatment with thionyl chloride failed to give the desired phosphinic chloride. Treatment of the ester (**117**) directly with PCl_5 in toluene was also attempted and initially looked promising as it gave one phosphorus peak by ^{31}P NMR analysis, shifted +8ppm from the starting ester. However, heating the material in $PSCl_3$ under reflux for 20 hours gave no trace of any disubstituted P=S species by ^{31}P NMR analysis.

One possible reason for the failure of this step especially in view of its success with similar systems may be derived from the greater acidity of the methylene protons as they are flanked by two electron withdrawing groups. If this were the case, then blocking the methylene position via methylation (**122**) may alleviate the problem and the corresponding methylated-methylene methylthiophosphinic acid may be accessed. The conversion of the methylene diester (**117**) to its tetramethylated analogue was attempted using sodium ethoxide in ethanol followed by addition of iodomethane, then repetition of the sequence. ^{1}H NMR analysis revealed that the methylene protons were

still present in the same ratio as the starting compound. Another attempt was made using LDA in THF followed by iodomethane. Again, the methylene protons remained intact which was surprising given their ability to undergo H-D exchange in CD_3OD as documented.[20]

A lack of time prevented a more thorough investigation of this situation and further attempts to transform the phosphinate ester (**117**) or phosphinic acid (**121**) to the desired thiophosphinate compound. The possibility of exploring the behaviour of an analogue of (**117**) with a different substituent at phosphorus, such as a phenyl group, in the above thiophosphorylating attempts was considered. Substituent-specific behaviour of many phosphorus compounds was described in chapter 2. However, in the other reported substituted-phosphinic acid phenanthroline analogues, the rate of H-D enolate exchange was found to be phenyl > benzyl ≈ methyl,[20] thus any detrimental effect caused by these protons may be augmented further.

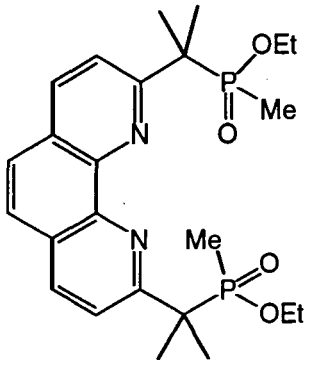

(**122**)

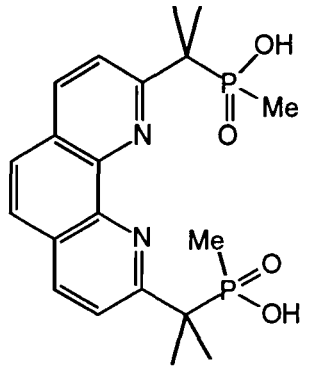

(**123**)

4.3 Future Synthetic Work

Although the work described above has not yielded the target ligands yet, some synthetic steps have been accomplished and some versatile intermediates have been prepared. A successful conclusion may be possible with more time to explore the remaining pathways discussed above from the compounds already prepared.

There are many other similar ligand systems possible, based upon the new classes of ligands described in this chapter and the previous two chapters. For example, the dialkylthiophosphoryl functionality described previously (Ch. 3) could be combined with an amino-substituted phenanthroline skeleton (**124**). The aromatic system would render the amine proton quite acidic and hence liable to deprotonation upon complexation, as well as including a rigid structural unit described above (section 4.1).

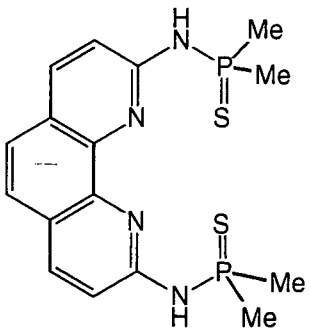

(124)

Alteration of the phosphorus substituents in this and other dialkylthiophosphoryl systems should have a tremendous impact upon the complexation behaviour of these ligands. For example, replacement of the P-methyl substituents of systems such as (**84**), (**85**) and (**86**) (Ch. 3) with methoxy groups should increase the donor ability of sulfur towards the metal cation without a significant alteration in the overall lipophilicity of the system. The scope for new ligands is enormous.

4.4 References

1. T.I.A. Gerber, H.J. Kemp, J.G.H. du Preez, G. Bandoli and A. Dolmella, *Inorg. Chim. Acta.,* 1992, **202**, 191
2. J-M. Lehn, *Angew. Chem., Int. Ed. Engl.*, 1988, **27**, 89; *ibid*, 1990, **29**, 1304
3. C.J. Chandler, L.W. Deady and J.A. Reiss, *J. Heterocycl. Chem.*, 1986, **23**, 1327
4. J. Lewis and T.D. O'Donoghue, *J.Chem.Soc., Dalton Trans.*, 1980, 736
5. G. Frederick Smith and W.H. McCurdy Jr., *Anal. Chem.,* 1952, **24**, 371
6. G. Stephens, H.L. Felkel Jr. and W.M. Spinelli, *Anal. Chem.*, 1974, **46**, 692
7. G. B. Bates, Ph.D. Thesis, University of Durham, 1995
8. Y. Xu, Z. Li, J. Xia, H. Guo and Y. Huang, *Synthesis*, 1983, 377
9. T. Hirao, T. Masunaga, Y. Ohshiro and T. Agawa, *Synthesis*, 1981, 56
10. D. Parker, 'Macrocycle Synthesis: A Practical Approach', Oxford university Press 1996
11. B.A. Arbuzov and N.I. Ripolozhensky, *Izv. An. SSSR, OKhn.,* 1952, 843
12. V.G. Gruzdev, K.V. Karavanov and S.Z. Ivin, *Zh. Obs. Khim.*, 1968, **38** (7), 1548
13. J.A. Miles, R.C. Grabiak and M.T. Beeny, *J. Org. Chem.*, 1981, **46**, 3486
14. J.A. Miles, R.C. Grabiak and M.T. Beeny, *J. Org. Chem.*, 1982, **47**, 1677
15. L. Horner and H.W. Flemming, *Phosphorus Sulfur*, 1984, **19**, 345
16. J.I.G. Cadogan, D.J. Sears and D.M. Smith, *J. Chem. Soc (C)*, 1969, 1314
17. E.P. Kyba and C.N. Clubb, *Inorg. Chem.*, 1984, **23**, 4766-4768
18. C.J. Chandler, L.W. Reiss, *J. Het. Chem.*, 1981, **18**, 599

19. G.B. Bates, E. Cole, D. Parker and R. Kataky; *JCS Dalton Trans*, 1996, 2693
20. A.J. Kirby, S.G. Warren, 'The Organic Chemistry of Phosphines', Elsevier, 1967, pp117
21. A.J. Spezlate and L.J. Taylor, *J. Org. Chem.*, 1966, **31**, 2451
22. R.D. Partos and A.J. Spezale, *J. Am. Chem. Soc.*, 1965, **87**, 5068
23. M. Ohta, K.K. Fuku, R. Sudo and M. Masuke, *J. Org. Chem.*, 1968, **33**, 3504

Chapter Five

Radiolabelling

5. Radiolabelling

Consideration is given to the tactics employed for radiolabelling (5.1), followed by an investigation of radiolabelling the aza-thiophosphinic acid ligands with technetium-99m (5.2). The source of the less readily available copper-64 radionuclide is related to the radiolabelling process together with the search to find a means of assessing the degree of complexation (5.3). In vitro *characterisation of the copper-radiolabelled complexes is addressed and conclusions drawn.*

The"... chemist should be the designer of a tailor-made suit around technetium in such a way that it will last, at least for the duration of the wedding ceremony, that is, for clinical analysis."

G. Bandoli, 1986[1]

The suits have now been fashioned and cut. How well will they fit technetium or copper?

5.1 General considerations

Complexes of a ligand and a radionuclide must be formed rapidly, preferably at room temperature and in good radiolabelling yield and radiochemical purity in order to be clinically useful. Radiochemical purity provides a measure of the desired radiolabelled species as a percentage of the total amount of radioactivity present in a sample. Radiochemical impurities are therefore other forms of the radioactivity which are undesired. Another term, radionuclide purity, refers to the presence of radionuclides other than the one of interest which may form a complex with the ligand(s) present. Excess ligand is commonly used in the development of radiopharmaceuticals in order to asses how well the trace amount of radionuclide complexes with the particular ligand.

The starting point for the synthesis of ^{99m}Tc complexes is the eluant from the $^{99}Mo/^{99m}Tc$ generator, i.e. pertechnetate in physiological saline solution,[2] which is the starting material for all ^{99m}Tc compounds in nuclear medicine. The anion TcO_4^- is then reduced (usually by the stannous ion)[3] in the presence of the ligand to be labelled.[4] For copper radiolabelling, generator-produced ^{62}Cu ($t_{1/2}$ 9.8 min) has a comparatively short half-life for studies in the development of new radiopharmaceuticals. Therefore ^{64}Cu with a half-life of 12.7 hours is suitable for this type of study in the form of its dichloride salt in aqueous solution.

5.2 Radiolabelling with Technetium-99m

The following work with ^{99m}Tc was undertaken at Amersham International with the assistance of Dr. Alex Gibson. The radiolabelling of the thiophosphinic acid ligands (**48**), (**64**), (**65**) and (**66**) (Figure 5.1) was studied with ^{99m}Tc eluted from the generator system in the presence of the standard reducing agent $SnCl_2$ in saline solution. Standard radio-HPLC and TLC methods were used to assess the species formed as the other technetium species normally competing in the radiolabelling process are pertechnetate [TcO_4^-] and reduced hydrolysed technetium (RHT) (or colloid) [TcO_2], and it is essential to identify these.

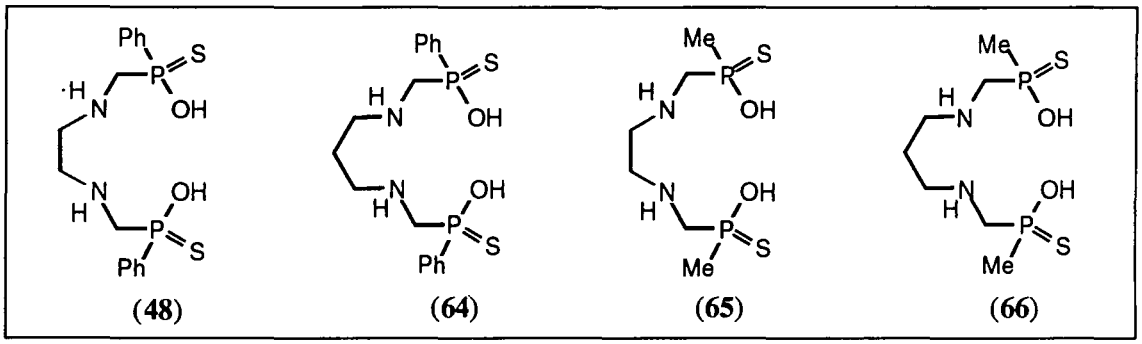

Figure 5.1 Thiophosphinic acid ligands for radiolabelling with ^{99m}Tc

Results and discussion

Ligand (**48**) labels extremely rapidly at room temperature at pH 8 to give predominantly two species, presumably isomers of ^{99m}TcO(**48**) as shown by radio-HPLC (Figure 5.2). The UV trace shows only the excess unbound ligand and the radiochromatogram shows the radiolabelled species and clear evidence that the ligand radiolabels in high yield and radiochemical purity. The amount of TcO_2 and TcO_4^- observed by tlc was reasonably small (in the order of 5% and 30% respectively). The radiolabelling efficacy is affected by the labelling conditions as shown by the formation of small amounts of other species when the complex is prepared at pH6 (Figure 5.3). The free ligand (**48**) was subjected to the labelling conditions in the absence of TcO_4^- which demonstrated that the ligand was indeed stable under these conditions. However, it is the stability of the complex which is questionable as it appeared to degrade after a period of roughly six hours. No assessment of the kinetic stability and dissociation time of the complex has yet been undertaken.

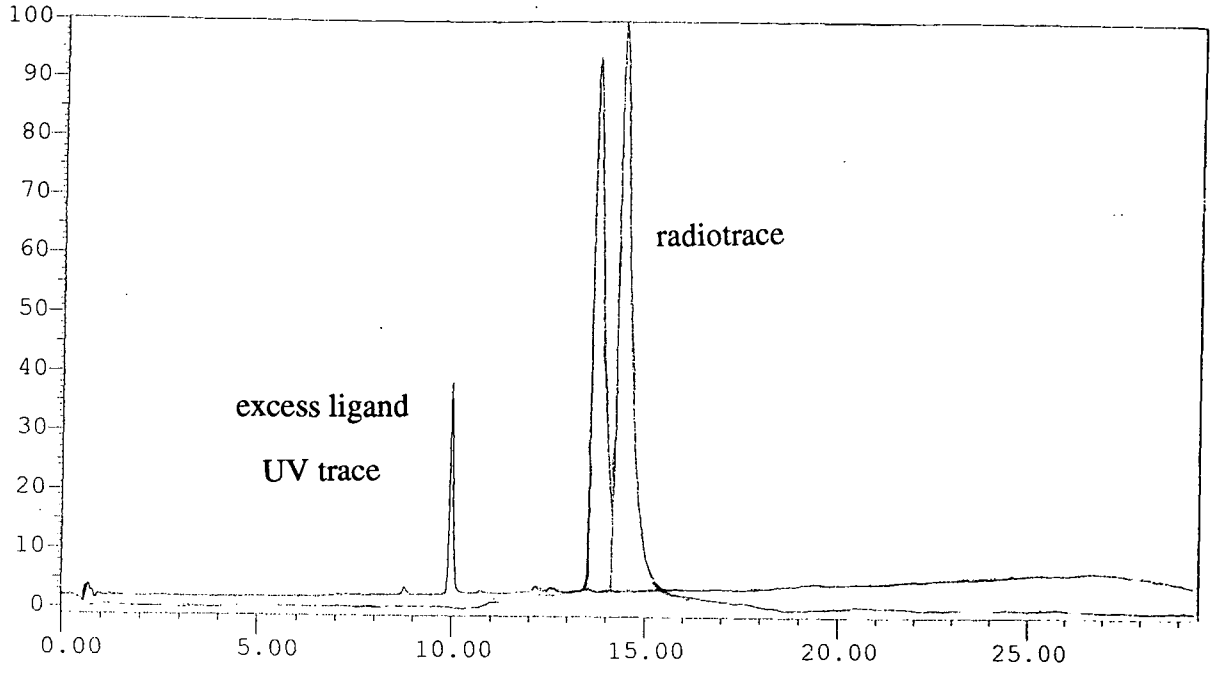

Figure 5.2 Radiochromatogram of ^{99m}TcO(**48**) prepared at pH8

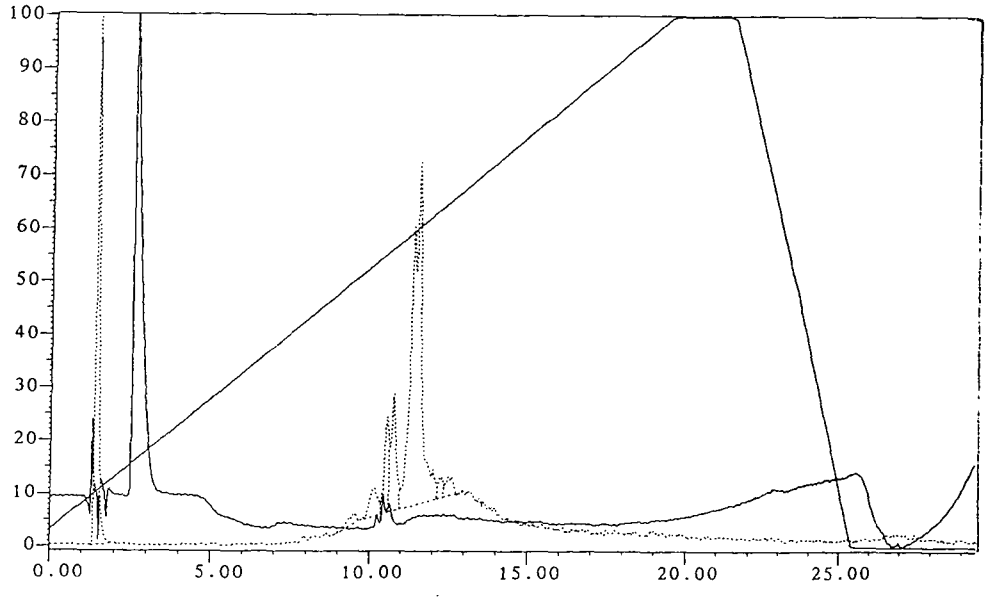

Figure 5.3 Radiochromatogram of ^{99m}TcO(**48**) prepared at pH6

The complex is likely to be cationic or neutral, in a similar manner to diaminodithiol (DADT) ligands[5,6,7] (see section 1.6), depending upon the deprotonation of one of the amines upon coordination of the metal (Figure 5.4). The two major species observed in the radiochromatogram of ^{99m}TcO(**48**) in a 1:1 ratio are due to two stereoisomers (meso and d,l) which arise from the two phosphorus stereogenic centres manifest in the ligand as diastereoisomers RS, RR/SS at phosphorus.

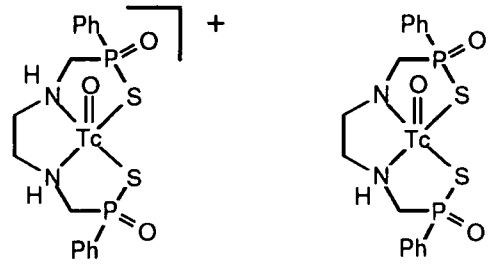

Figure 5.4 Possible structures of cationic or neutral complexes of TcO(**48**)

The radiolabelling of the other ligands was undertaken with the same conditions at pH8. Some labelling of ligand (**65**) was observed although the labelling yield was low. Ligand (**64**) labels well but seemed to give many species. This behaviour may be a reflection of slight sulfur-containing impurities present in the ligand sample although these should not bind technetium themselves. Similarly, ligand (**66**) gives many species but the sample of the ligand used was only about 70% pure, as judged by ^{31}P NMR analysis.

Conclusions

Ligand (**48**) labels very efficiently with technetium-99m while ligands (**64**)-(**66**) show varying degrees of radiolabelling but extremely poor radiochemical purity. This may simply result from the fact that optimal conditions for their labelling were not found due to the limited time available. Their radiolabelling was only attempted under the conditions determined using ligand (**48**). Another contributory factor may be the small impurities present in the ligand samples (**64**)-(**66**) having some adverse affect upon the labelling process. The apparent lack of stability of ^{99m}TcO(**48**) should not be a deterrent from further studies and the subsequent development of this radiopharmaceutical as the stability of a radiopharmaceutical can be finite as long as it is stable for enough time to achieve its function. For example, Amersham's own commercially available system, Ceretec (^{99m}TcHMPAO) suffers from limited stability.[8,9] It must be prepared with freshly eluted technetium (no more than 2 h old) and the radiopharmaceutical used within 30 minutes of its preparation. It is possible that fresh eluant may also be required for the successful radiolabelling of ligands (**64**)-(**66**).

5.3 Radiolabelling with Copper-64

The following work with ^{64}Cu was carried out at the MRC Cyclotron Unit, Hammersmith Hospital with the assistance of Dr. Jamal Zweit. Firstly, a stock of ^{64}Cu for the radiolabelling experiments was prepared. No carrier added (NCA) ^{64}Cu was produced by the ^{64}Ni(d, 2n)^{64}Cu reaction[10] on 96% enriched ^{64}Ni and complete oxidation of the irradiated target to nickel(II) and copper(II) was achieved by heating in

a solution of hydrochloric acid with aqueous hydrogen peroxide. The salt $^{64}CuCl_2$ was separated from the nickel(II) and trace quantities of cobalt(III) isotopes by anion exchange chromatography. Subsequent studies were carried out over four days, during which time the radioactive concentration of the stock solution of copper-64 fell from 450 MBq ml^{-1} to 9.6 MBq ml^{-1} due to the decay ($t_{1/2}$=12.7 h) of the radionuclide. The radiolabelling of the series of amino thiophosphinic acid ligands (**48**), (**64**), (**65**) and (**66**) (as above) and the tetradentate dialkylthiophosphoryl ligands (**84**) and (**85**)(Figure 5.5) were studied using this stock solution of copper-64. Suitable radiolabelling conditions, taking account of both ligand and complex solubility, as well as a method for assessing complex formation had first to be found.

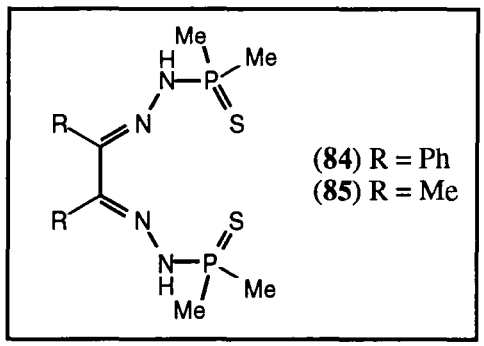

Figure 5.5 Dialkylthiophosphoryl ligands for radiolabelling investigations

Initial investigations focused on ligand (**48**) as there was a more plentiful supply. By analogy with the 'cold' copper complexes (Ch.2), aqueous or methanol solutions of (**48**) were used initially for tracer preparation. Typical preparations of the copper-64 radiolabelled complex were undertaken using an excess of ligand (**48**) dissolved in pure (MilliQ) water (with the addition of sodium hydroxide solution giving ca. pH 3). This was added to a solution of $^{64}CuCl_2$ buffered with sodium acetate solution giving an overall pH of 5.5. After thorough mixing of this preparation, the products were examined by thin layer chromatography (TLC) on silica with ethyl acetate as the mobile phase. This method of quality control has been used extensively for studies with complexes such as Cu-PTSM[11] as the free copper ions remain on the baseline while the complex moves up the plate. However, γ-detection of the 'hot' spots on the silica plate of the ^{64}Cu(**48**) preparation revealed that all forms of ^{64}Cu remained on the baseline. Alternative conditions of analysis were then sought. Precipitation occurred when the above preparation was carried out with a solution of the ligand in ethanol (ethanol is biologically preferable to methanol). However, precipitation also occurred by merely adding an equivalent volume of water to an ethanol solution of the ligand. Several other solvent systems such as methanol, acetonitrile/water, were considered for TLC but allowed no differentiation between unbound $^{64}CuCl_2$ and complexed copper-64. Partitioning of the ^{64}Cu(**48**) mixture in octanol/water (see below) gave a log P value of 0.65 showing that a complex had indeed been formed (as free $^{64}CuCl_2$ gives a negative

value as it remains in the water layer) and suggested that another method of quality control should be sought.

The use of a radio-HPLC isochratic system with equal ratios acetonitrile/water or 40% acetonitrile/water also failed to separate the different forms of the copper-64 radioactivity as both the ligand (UV detection) and the radioactive species were detected simultaneously. Clearly the same HPLC conditions used to analyse the 'cold' complexes employing gradient elution (Ch.6) were required. Successful analysis of ^{64}Cu(**48**) and subsequent preparations of the other radiolabelled ligands was achieved in this manner. Analytical HPLC was not only advantageous for the detection of the radiolabelled complexes but also allowed the collection of the pure species as it came off the HPLC column. The amino-thiophosphinate ligands (**64**), (**65**) and (**66**) were radiolabelled with ^{64}Cu in a similar manner, using water to dissolve the P-methyl substituted ligands (**65**) and (**66**), and methanol for the other P-phenyl substituted ligand, (**64**). Slight variations in the amount of activity (MBq) and the quantity of ligand used for each radiotracer preparation were found to have no effect upon complex formation.

Results and Discussion

HPLC analysis of a pure $^{64}CuCl_2$ solution showed a retention time of 2 minutes. A very small peak at 2 minutes - corresponding to unbound copper-64 - was observed in the radiochromatogram of ^{64}Cu(**48**) (Figure 5.6) in addition to a large peak at 10 minutes assigned to the radiopharmaceutical itself and a small peak at 7 minutes. These results correspond directly to the HPLC chromatogram of the 'cold' copper complex of (**48**) (Ch2), in that another minor ^{64}Cu-labelled species was observed with a similar retention time in addition to the major species that was the copper-ligand complex under the HPLC conditions defined.

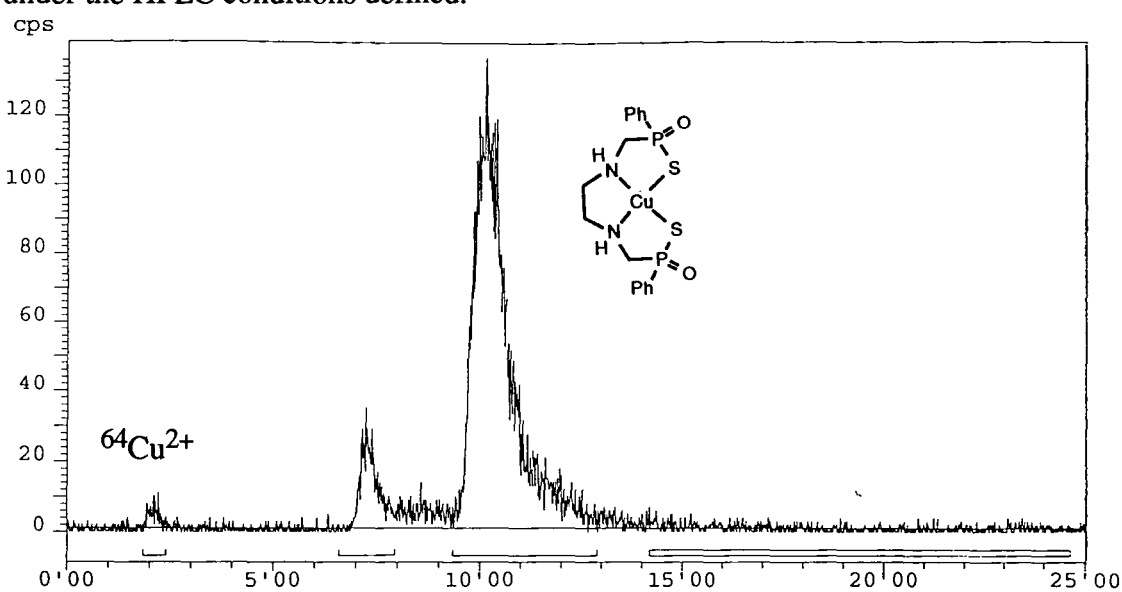

Figure 5.6 Radiochromatogram of ^{64}Cu(**48**)

Integration of these three peaks gave the area of each in terms of radioactivity from which the radiolabelling efficacy and radiochemical purity could be established quantitatively. Radiolabelling yields were calculated as the total amount of complexed ^{64}Cu as a percentage of the total amount of ^{64}Cu present. For example, from the chromatogram of ^{64}Cu(**48**) the counts under peak 3 (R_t=10 minutes) are expressed as a percentage of the total counts of peaks 1+2+3. Radiochemical purity was expressed as a percentage of radioactivity from the desired ^{64}Cu-ligand complex of the total radioactivity detected in the radiochromatogram. Repetition of the preparation and HPLC analysis of ^{64}Cu(**48**) gave consistent results of 98% radiolabelling yield and a radiochemical purity of 87% prior to HPLC purification. It should be noted that this does not account for the excess ligand present. The radiolabelling of the other thiophosphinate ligands (**64**)-(**66**) and the dihydrazide ligand (**84**) was assessed in a similar manner. The results of ^{64}Cu radiolabelling of the ligands are summarised in Table 5.1.

Table 5.1 Summary of Radiolabelling Analysed by HPLC

Species	Conditions	Retention Time / minutes	Radiolabelling Yield / %	Radiochemical Purity of crude preparation*/ %
$^{64}CuCl_2$	diluted in H_2O	2.0	-	-
^{64}CuL(**48**)	CH_3OH	10.1	98	85
	complex pH 5	10.1	99	89
		10.2	97	87
^{64}CuL(**65**)	H_2O	2.5	94	94
	complex pH 5			
^{64}CuL(**64**)	CH_3OH	7.4	95	95
^{64}CuL(**66**)	H_2O	6.5	62	62
^{64}CuL(**84**)	CH_3CN/NEt_3	17.1	100	73

*Radiochemical purity of the HPLC-eluted Cu-complexes was assumed to be 100%

The dimethylthiophosphoryldihydrazide ligands (**84**) and (**85**) were briefly examined in the rather limited time available. Owing to their poor solubility in methanol, acetonitrile was used to dissolve the compounds. Ligand (**84**) showed no evidence of any radiolabelling when a solution in acetonitrile was treated with a solution of aqueous $^{64}CuCl_2$. However, when the ligand solution was first treated with a little triethylamine prior to the addition of aqueous $^{64}CuCl_2$, the ligand radiolabelled very well. A large peak due to the radiotracer complex was observed at 17 minutes while no free copper-64 was observed at 2 minutes. Some impurites - presumably adducts of copper-64 with triethylamine - appeared as broad peaks with very low peak intensity between 4 and 10 minutes (Figure 5.7). Again, the pure complex, ^{64}Cu(**84**), was collected as it eluted

the column. Complexation of ligand (**85**)was attempted under these basic conditions but there was no evidence for radiolabelling. Due to the structural similarities between ligands (**84**) and (**85**) (only the substituents on the carbon backbone are different) analogous metal-binding could be expected. Therefore, successful radiolabelling of this ligand may be possible if the appropriate conditions can be established.

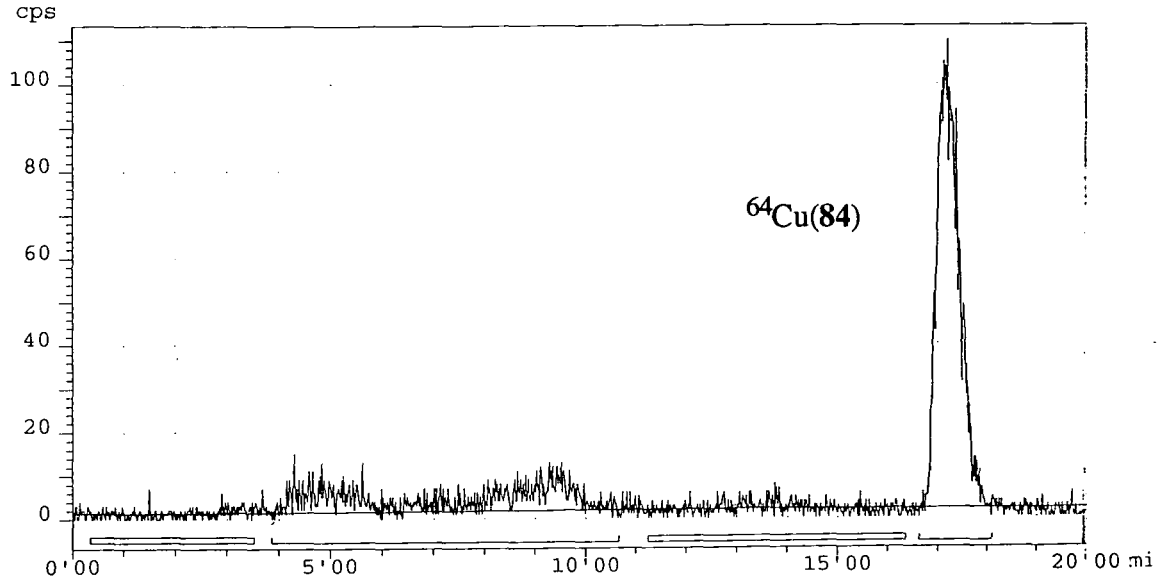

Figure 5.7 Radiochromatogram of ^{64}CuL(**84**)

Characterisation of ^{64}Cu Labelled complexes *in vitro*

Lipophilicity Measurements

Lipophilicity reflects the lipid solubility of a complex and hence its ability to penetrate the blood-brain barrier and diffuse through cell membranes, as discussed earlier (Ch.1). Measurement of lipophilicity is important when evaluating the suitability of a new radiopharmaceutical. The partition coefficients of the new radiotracers were measured between octanol and water (summarised schematically in Figure 5.8) as a measure of complex lipophilicity (assuming that the complex does not dissociate). The amount of radioactivity in each layer gives the partition coefficient according to the relationship:

$$\log_{10}P = \log_{10} [\gamma\text{-counts in octanol} / \gamma\text{-counts in water}]$$

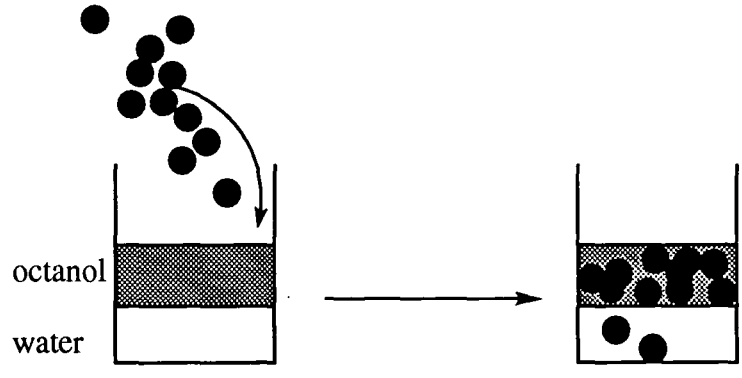

Figure 5.8 Schematic diagram of lipophilicity measurement

Figure 5.8 Schematic diagram of lipophilicity measurement

Measurements were carried out in duplicate on each radiolabelled complex and are summarised in Table 5.2. As expected, the P-phenyl substituted thiophosphinate ligands show a higher propensity to accumulate in the organic phase than their P-methyl counterparts. The values found for samples which were taken directly from the radiotracer reaction mixture were found to be higher than for their HPLC-purified counterparts. This is surprising as the values of the 'crude' complex preparations should be slightly lower than the actual value due to the small percentages of unbound copper-64 present in the sample. This anomaly may be a consequence of instability in the purified complexes which had been evaporated to near dryness under vacuum centrifugation with heating.

Table 5.2 LogP values of ^{64}Cu-ligand complexes

Complex	log P (prep)	log P (HPLC purified)*
^{64}Cu(**48**)	0.73 (MeOH) 0.65 (aqueous pH5.5)	0.46
^{64}Cu(**65**)	-0.96 (H_2O)	-2.42
^{64}Cu(**64**)	0.37	-1.22
^{64}Cu(**66**)	-1.48 (H_2O)	-1.57
^{64}Cu(**84**)	0.99 (CH_3CN/NEt_3)	
$^{64}CuCl_2$	-2.06	

* values may be affected by complex degradation during the solvent evaporation process

Plasma-Protein Binding Studies

Gel permeation chromatography was used to study the behaviour of the radiolabelled complexes ^{64}Cu(**48**), ^{64}Cu(**65**) and ^{64}Cu(**64**) in human or rat plasma. This technique assesses whether there is any protein-bound radioactivity present after incubation of the copper-64 complex in plasma. The radiolabelled complex was incubated in plasma prior to loading onto a buffered gel permeation column that had been preconditioned with human serum albumin. The product was eluted with the same buffer solution and around fifteen fractions of 0.5 ml were collected and γ-counted. The results are presented graphically in Figures 5.9 to 5.11.

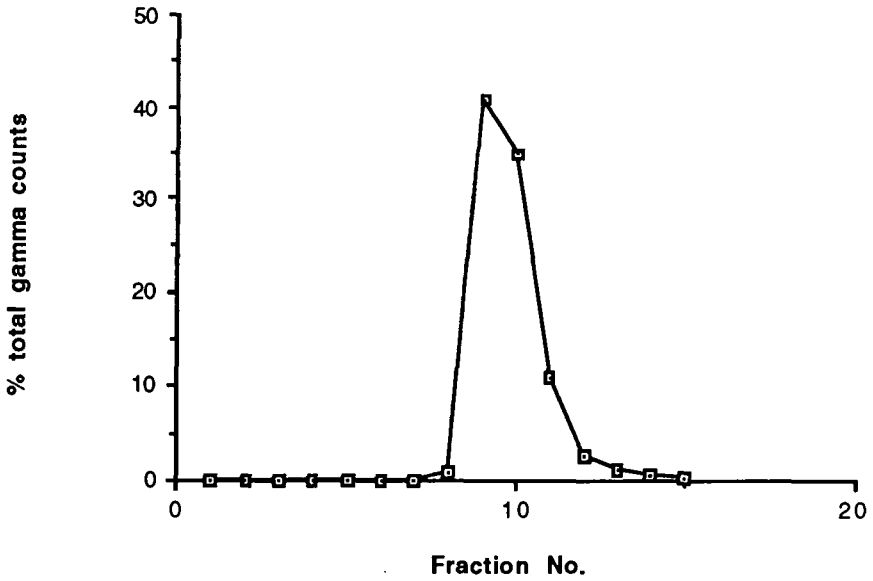

Figure 5.9 Gel permeation profile of ^{64}Cu(**48**) incubated in human plasma for 1 h.

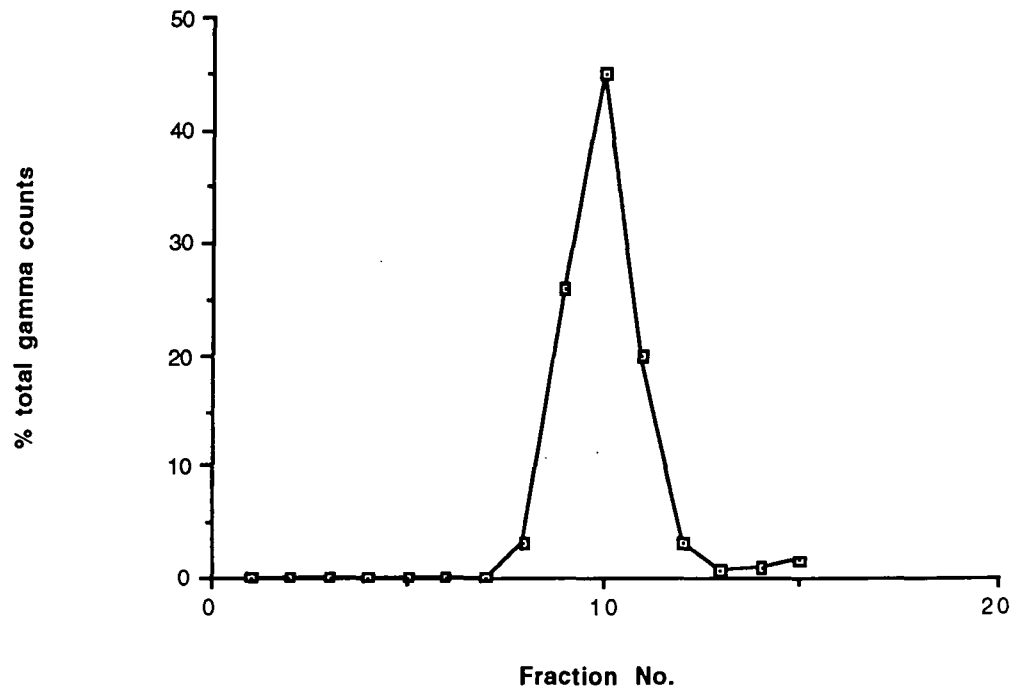

Figure 5.10 Gel permeation profile of ^{64}Cu(**65**) incubated in human plasma for 1 h.

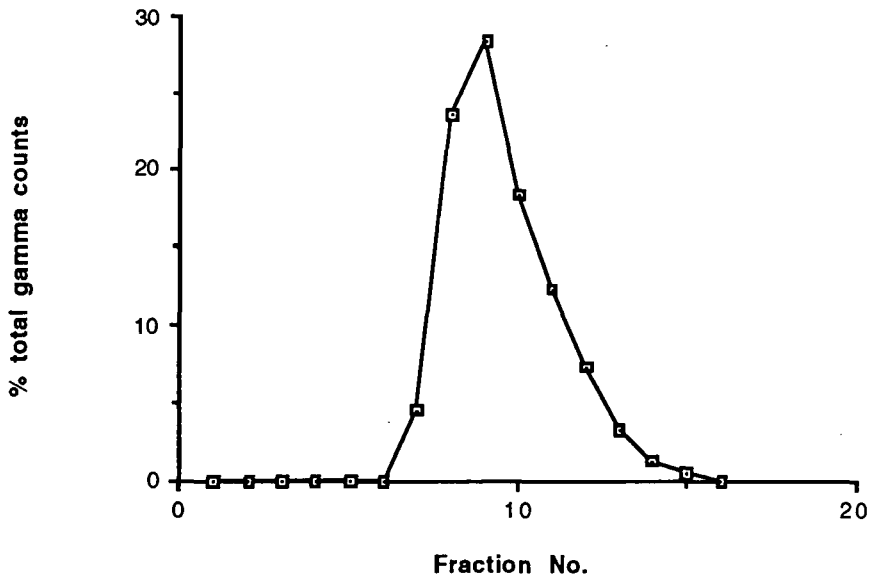

Figure 5.11 Gel permeation profile of ^{64}Cu(**64**) incubated in human plasma for 1 h.

The gel permeation profiles show that the active species elute in the later fractions where low molecular weight species are found. There is no radioactivity due to protein -bound species as ^{64}Cu that has become bound to protein in serum elutes almost immediately (i.e. in fractions 1-3) while low molecular weight species take longer to elute. Therefore any ^{64}Cu liberated as a result of complex degradation in human serum would be detected as the metal would rapidly bind to human serum albumin and show a similar elution to that of uncomplexed copper-64 which does bind to protein. This indicates that there is no non-specific binding of the complexes to serum proteins and confirms the stability of the complexes in plasma over the time period of 1 hour.

Partitioning of ^{64}Cu-Complexes Between Plasma and Red Blood Cells

The uptake of the radiotracers into red blood cells with time was assessed by partitioning samples of the radiolabelled complexes which had been incubated in whole blood. Aliquots were removed after different time points - 10, 15, 30 and 60 minutes - in duplicate and were separated into layers of plasma and red blood cells (RBC) for γ-counting. The resulting γ-counts are expressed as a percentage uptake in red blood cells and plasma at the various time points. Studies focused on ^{64}Cu(**48**) and ^{64}Cu(**64**) which appeared the most promising in terms of lipophilicity: the results are summarised in Table 5.3.

Table 5.3 Summary of Blood-Plasma Partitioning Results for ^{64}Cu(**48**) and ^{64}Cu(**64**)

	POST-MIXING TIME / minutes						
SYSTEM* / % counts	10	15	15	30	30	60	60
^{64}Cu(**48**) plasma	93	90	72	81	87	88	86
^{64}Cu(**48**) red blood cells	7	10	28	19	13	12	14
^{64}Cu(**64**) plasma		86	87	78	82	81	
^{64}Cu(**64**) red blood cells		14	13	22	18	19	

* studies using whole human blood

^{64}Cu(**65**) was studied in a similar manner with whole rat blood with time points of 15 and 30 minutes and γ-counts were recorded as percentages (Table 5.4)

Table 5.4 Summary of Blood-Plasma Partitioning Results for ^{64}Cu(**65**)

	POST-MIXING TIME / minutes					
SYSTEM* / % counts	15	15	15	30	30	30
^{64}Cu(**65**) plasma	93	91	92	53	54	52
^{64}Cu(**65**) red blood cells	7	9	8	47	46	48

* studies using whole rat blood

^{64}Cu(**48**) and ^{64}Cu(**64**) only show a slight increase of RBC uptake between 15 and 30 minutes. ^{64}Cu(**65**) shows high association with the plasma fraction up to 15 minutes. By 30 minutes the RBC uptake has increased significantly which may reflect an intracellular trapping mechanism of the ^{64}Cu(**65**) complex. This may be due to some mechanism which may involve dissociation of the complex, possibly by intracellular reduction of the complex to the Cu(I) species, or by desulfurisation of the thiophosphinate to its 'hard' oxygen analogue. This behaviour follows a similar pattern of behaviour to the findings of Mathias[12] for Cu-PTSM. This may indicate that ^{64}Cu(**48**) and ^{64}Cu(**64**) are less susceptible to intracellular redox trapping compared to ^{64}Cu(**65**). Alternatively this difference may simply result from interspecies variation,[13]

as human blood was used for the former studies and rat blood was used for the latter studies.

Aqueous Stability

The absolute stability of the purified radiolabelled complexes ^{64}Cu(**48**) and ^{64}Cu(**65**) in aqueous solution over 24 hours was assessed by analytical radio-HPLC. The radiochromatogram of the ^{64}Cu(**48**) (Figure 5.12) had a similar appearance to that of the original crude preparation (Figure 5.6). By integration of the peaks, it was calculated that 70% of the total amount of activity detected was due to radiolabelled species, with the desired tracer now accounting for about 60% of the total activity present, corresponding to dissociation of about 40% over 24 h.

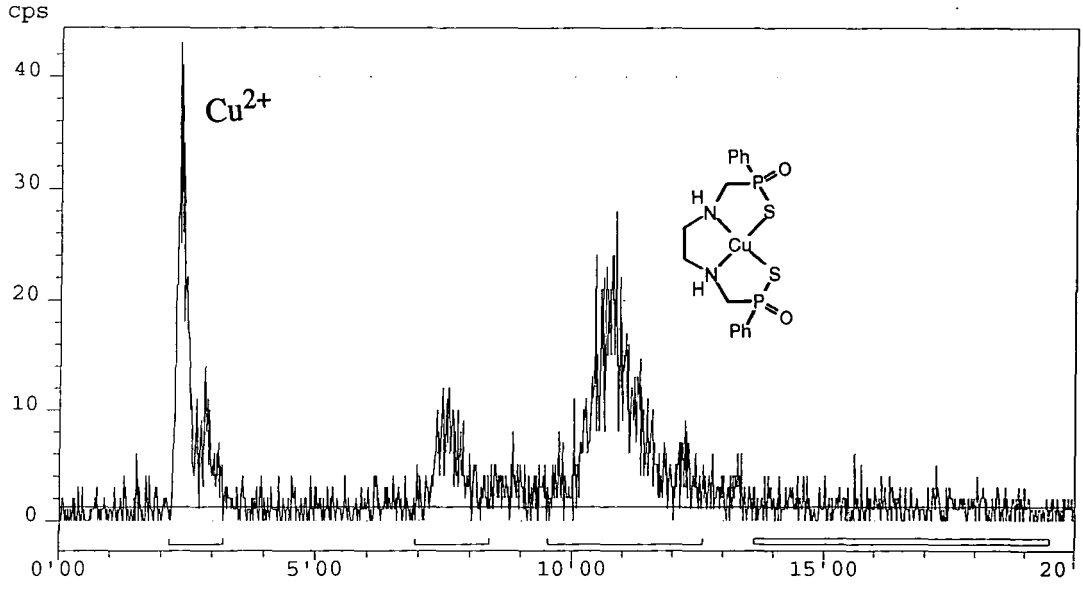

Figure 5.12 Radiochromatogram of ^{64}Cu(**48**) 24 h after complexation/purification

The radiochromatogram of ^{64}Cu(**65**) showed no evidence of any free^{64}Cu and only one species with a retention time corresponding to the complex. Therefore this complex was judged to be stable with respect to dissociation over the 24 hour period (ca. 2 half-lives).

Conclusions

The amino thiophosphinic acid ligands (**48**), (**64**), (**65**) and (**66**) form complexes with copper-64 extremely rapidly in water or methanol solution at room temperature. Although good radiolabelling yields and radiochemical purity were achieved, these could be optimised by further investigation of the radiolabelling conditions such as variation of solvents and pH. Indeed, a dramatic effect upon complexation with a small change in the conditions was displayed by ligand (**84**). An excess of ligand to copper-64 was used in all of the above studies to be consistent with current radiolabelling methodology. However, HPLC studies with UV detection of the 'cold' copper

complexes (Ch.2) suggest that it may be possible to reduce the amount of ligand to copper-64 to as little as 1:1, although the rate may be slower. This would be advantageous preventing any unnecessary toxic effects that may be associated with administration of the free ligand with studies of the radiopharmaceutical *in vivo*. The use of a smaller amount of ligand is secondary, as the amounts of ligands used for this application are very small.

It is not yet known whether the complexes investigated possess sufficient lipophilicity to enable them to cross the BBB. The highest log P value was around 1.0 (Cu(**84**)) whereas, a value nearer 2.0 would be more favourable. However, compounds with log P values between 0.9 and 2.5 have been reported to freely diffuse accross the BBB.[14] Lipophilicity is not the only factor which determines diffusion across the BBB as other factors such as molecular weight and charge are important (section 1.6). Furthermore, it is possible to modify the basic structure of the ligands, and their metal complexes (sections 2.1 and 3.1) by the choice of substituents at phosphorus and on the carbon skeleton. The preparation of a series of more lipophilic derivatives would allow the assessment of the best candidate - a process which has proved fruitful in the discovery of Cu-PTSM.[15]

In answer to the initial question: the suits fit both copper and technetium - some of them very well indeed. The question remaining is, 'for how long can they be worn?'

5.4 References

1. G. Bandoli, U. Mazzi, A. Moresco, M.Nicolini, F. Refosco, F. Tisato, Technetium complexes containing tridentate and bidentate Schiff-base type ligands, in *Technetium in Chemistry and Nuclear Medicine*, (Eds M.Nicolini, G. Bandoli, U. Mazzi) Cortina International, Verona, 1986, **2**, 73
2. P. Richards, W.D. Tucker and S.C. Srivastava, *Int. J. Appl. Radiat. Isot.*, 1982, **33**, 793
3. S. Jurisson, D. Berning, W. Jia and D. Ma, *Chem. Rev.*, 1993, **93**, 1137
4. W.C. Eckelman and P. Richards, *J. Nucl. Med.*, 1970, **11**, 761

5. T.R. Carroll, 'Technetium heart and brain Brain Perfusion Imaging Agents', in *Advances in Metals in Medicine*, (Eds. M.J. Abrams and B.A. Murrer), 1993, **1**, pp1-27, JAI Press Inc.
6. W.A. Volkert and S. Jurisson, *Topics in Current Chemistry*, 1996, **176**, 123
7. B. Johannsen and H. Spies, *Topics in Current Chemistry*, 1996, **176**, 77
8. R.D. Neirinckx, J.F. Burke, R.C. Harrison, A.M. Forster, A.R. Andersen and N.A. Lassen, *J. Cereb. Blood Flow Metab.*, 1988, **8**, S4
9. J.C. Hung, M. Corlija, W.A. Volkert and R.S. Holmes, *J. Nucl. Med.*, 1988, **29**, 1576
10. J. Zweit, A.M. Smith, S. Downey and H.L. and H.L. Sharma, *Appl. Radiat. Isot.*, 1991, **42**, 193
11. M.A. Green, C.J. Mathias, M.J. Welch, A.H. McGuire, D. Perry, F. Fernandez-Rubio, J.S. Perlmutter, M.E. Raichle and S.R. Bergmann, *J. Nucl. Med.*, 1990, **31**, 1989
12. C.J. Mathias, S.R. Bergmann and M.A. Green, *Nucl. Med. Biol.*, 1993, **20**, 343
13. C.J. Mathias, S.R. Bergmann and M.A. Green, *J. Nucl. Med.*, 1995, **36**, 1451
14. D.D. Dischino, M.J. Welch, M.R. Kilbourn and M.E. Raichle, *J. Nucl. Med.*, 1983, **24**, 1030
15. E.K. John and M.A. Green, *J. Med. Chem.*, 1990, **33**, 1764

Chapter Six

Experimental Methods

6 Experimental Methods

6.1 General

All reactions were performed under an argon atmosphere in apparatus which had been oven dried and cooled under argon. Merck grade four molecular sieves were used, which were activated prior to use by heating while under high vacuum. Chromatography was performed using silica (Merck Kieselgel 230-400 mesh) and alumina (Merck Alumina activity II-III) that was soaked in ethyl acetate at least 24 h prior to use. In some cases, characterisation of a P(III) precursor is limited to ^{31}P NMR data due to practical difficulties which include air-sensitivity and stench of phosphorus species produced. However, this is sufficient to show the homogeneity of the sample, since often the only species studied are phosphorus-derived. All solvents were dried by distillation from the appropriate drying agent and water was purified by the PURITE system.

Instrumentation

Analytical and preparative HPLC were performed on a Varian Vista 5500 or a Varian Star 5065 instrument fitted with a reverse phase column, using gradient elution with water (0.1% TFA) and acetonitrile (0.1% TFA) at a flow rate of 1.4 ml min^{-1}.

All ^{31}P NMR were recorded on a Bruker AC250 spectrometer operating at 101 MHz. ^{1}H and ^{13}C NMR spectra were obtained with a Bruker AC 250 operating at 250.13 MHz and 62.9 MHz respectively, Varian Gemini 200 operating at 200 and 50 MHz respectively, Varian VXR operating at 200 MHz or a Varian VXR 400s operating at 399.96 MHz and 100.58 MHz respectively. Spectra are described in ppm to higher frequency and downfield shift from TMS and reported consecutively as position (δH and δC), relative integral, multiplicity [singlet (s), doublet (d), doublet of doublets (dd), triplet (t), quartet (q), quintet (qnt), multiplet (m), broad (b)] and coupling constants (J Hz) if applicable. Infrared spectra were recorded on a Perkin-Elmer 1600 FT-IR spectrometer as a thin film, KBr disc or with a Graseby-Specac 'Golden Gate' diamond ATR accessory, and absorbance maxima are given in wavenumbers (cm^{-1}). Ultra-violet and visible spectra were recorded on a UVIKON 930 spectrometer using a 1 cm pathlength cell. Absorbance maxima are quoted in nm.

Mass spectra were recorded on a VG 7070E, operating in FAB, EI^{+} or DCI ionisation modes as stated and electrospray ionisation mass spectra were obtained on a VG platform-II (Fisons Instruments). Major ions are quoted as a percentage of the base peak intensity, and, for some electrospray species, isotope patterns were modelled

using Mass Lynx software. Accurate mass spectroscopy was performed by the EPSRC Mass Spectroscopy service at Swansea.

Combustion analysis was performed using an Exeter Analytical Inc CE440 elemental analyser. Metal concentration was determined by atomic absorption spectroscopy using a Perkin Elmer 5000 atomic absorption spectrophotometer.

Melting points were determined on a Kofler block melting point apparatus and are uncorrected.

NMR Titrations.

NMR titrations were carried out in a single 5 mm oven dried tube. A solution of the ligand was prepared (typically 0.01M) in a suitable solvent (undeuterated where only the phosphorus shift is studied by ^{31}P NMR) and a known amount (0.5-0.75 ml) of the solution transfered to the tube by Gilson pipette. A solution of the metal triflate was also prepared in the same solvent (typically 0.1M). The metal solution was then added in increments of known volume to the ligand solution and the shift of a given proton or phosphorous resonance monitored as a function of the M/L ratio. Typically the M/L ratios examined were 0.25, 0.5, 0.75, 1.0, 1.5, 2.0, 2.5, 3.0, 4.0, 5.0. The change in shift of the given resonance is then plotted against the M/L ratio and the curve analysed using a least squares procedure[1] to give an estimate of the effective stability constant, K.

Speciation analysis by electrospray mass spectrometry.

A stock solution of the ligand was prepared (typically 0.3 mmol) in freshly distilled methanol, a stock solution of the metal triflate or perchlorate was also prepared (typically about 1 mmol) in methanol. To a sample of the ligand solution (1ml) and methanol (1ml) was added the appropriate volume of metal triflate solution to make a 1:1 or 1:2 metal to ligand ratio. Using 10 µl of the test solution mass spectra were obtained with the ionisation mode (+ or -) stated.

HPLC analysis of copper complexes

HPLC analysis of the ligands containing an aromatic group for UV detection at λ=254 nm was carried out to determine their retention times prior to analysis of their copper complexes. Solutions containing 1:1 and 2:1 ratio of ligand to copper with concentrations of the order of 5 mmol dm^{-3} were investigated as a preliminary study for radiolabelling to determine the number of species present and their retention times.

6.2 Synthesis

Chapter 2

***Chloroethoxyphenylphosphine*[2] (125)**

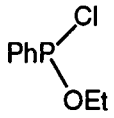

Dichlorophenylphosphine(0.98 ml, 7 mmol) was added to diethylphenylphosphonite (1.37 ml, 7 mmol) at 0°C under an inert atmosphere with stirring to give a colourless liquid in quantitative yield, **^{31}P NMR** ($CDCl_3$) δ_P 174; **^{1}H NMR** (250.13MHz, $CDCl_3$) δ_H 1.46 (3H, td, J_H=7 Hz, J_P=1.1 Hz, P-O-$CH_2\underline{C}H_3$), 4.1 (2H, m, P-O-$C\underline{H}_2CH_3$), 7.6 (3H, br m, *o*-, *p*-, phenyl), 7.89 (2H, m, m-phenyl), **^{13}C NMR** (62.9 MHz, $CDCl_3$) δ_C, 16.43 (P-O-$CH_2\underline{C}H_3$), 64.90 (d, J_P=8.7 Hz, P-O-$CH_2\underline{C}H_3$), 128.49 (d, J=4.8 Hz, *m*-Ph), 129.72 (d, J=25.7 Hz, *o*-Ph), 132.3 (*p*-Ph)

***Ethoxyphenyl-S-ethylphosphine* (126)**

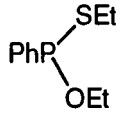

Sodium ethanethiolate (1.36 g, 15.4 mmol) was stirred in toluene at -50°C under an inert atmosphere. Chloroethoxyphenylphosphine (2.87 g 14 mmol) was added to the reaction mixture which was left to warm up to room temperature and stirred for 2 h. The solution was filtered and the solvent evaporated to leave a pale yellow oil (1.71 g, 57% with ~50% purity), **^{31}P NMR** ($CDCl_3$) δ_P 145.8

***Phenyl-bis-S-ethylphosphine* (127)**

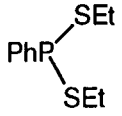

The above method described for (**126**) was employed using sodium ethanethiolate (660 mg, 7.4 mmol) in dichloromethane (4 ml) at -30°C with dichlorophenylphosphine (0.46 ml, 3.39 mmol) to give a pale yellow oil (324 mg, 42%); **^{31}P NMR** ($CDCl_3$) δ_P 74.4

***Attempted preparation of Diethyl-tetrahydroimidazole-N,N'-bis(methylenedithiophenylphosphinate)* (128)**

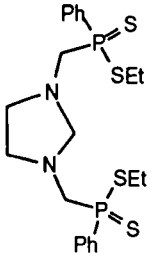

Ethylenediamine (0.26 ml, 3.9 mmol) and paraformaldehyde (0.71 g, 23.4 mmol) were stirred in dry THF (50 ml) and heated to reflux at 100°C using a Soxhlet apparatus filled with molecular sieves (4Å) under an inert atmosphere. Freshly prepared $PhP(SEt)_2$ (**127**) (2.24 g, 9.75 mmol) was added to the mixture, which was maintained under reflux for 48 h. ^{31}P NMR analysis of the reaction mixture showed that little or no reaction had taken place.

Ethyl[(t-butyl dimethylsiloxy methylene)phenylphosphinate] **(129)**

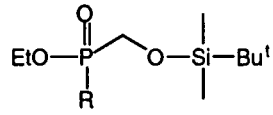

Ethyl[(hydroxymethylene)phenylphosphinate] (1.53 g, 7.65 mmol), *t*-butyl dimethylsilylchloride (8.4 mmol, 8.4ml of 1M solution in THF) and imidazole (1.14 g, 16.8 mmol) were stirred in DMF (50ml) under an inert atmosphere for 3h at room temperature. The solvents were removed *in vacuo* leaving an oily residue which was dissolved in dichloromethane (40 ml), washed with sodium carbonate solution (10%, 3 x 40ml), dried (Na_2SO_4) and the solvent evaporated under reduced pressure to give a pale yellow oil (1.5g, 62%); **^{31}P NMR** ($CDCl_3$) δ_P 37.7; **^1H NMR** (250 MHz, $CDCl_3$) δ_H -0.36 (6H, d, J=10.1 Hz, $Si(C\underline{H}_3)_2tBu$), 0.81 (9H, s, $C(C\underline{H}_3)_3$), 1.34 (3H, t, J=7 Hz, $OCH_2C\underline{H}_3$), 3.97 (4H, b s, $PC\underline{H}_2OH$, $OC\underline{H}_2CH_3$), 7.45 (3H, m, *o*-,*p*-PhH), 7.85 (2H, m, *m*-PhH); **m/z** (CI) 315 (60%, MH+), 201 (100, MH_2^+-$Si(Me)_2tBu$).

Attempted preparation of ethyl[(t-butyldimethylsiloxymethylene) phenylphosphinthiolate] **(130)**

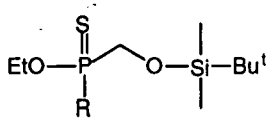

Ethyl[(*t*-butyldimethylsiloxymethylene)phenylphosphinate] (**129**) (150 mg, 0.48 mmol) was stirred in toluene (15 ml) with di-phosphorus pentasulphide (0.25 g, 0.56 mmol) for 1 h at room temperature under an inert atmosphere. ^{31}P NMR analysis revealed a mixture of species, and the reaction was stirred until no further change in the ^{31}P NMR spectrum was detected (now several signals). The product mixture was filtered and the solvent removed under reduced pressure to leave a yellow oil (100 mg, 63%); **^{31}P NMR** ($CDCl_3$) δ_P 37.2, 37.6, 79.9, 80.3, 83.6, 84.0 (mixture of species); **^1H NMR** (250 MHz, $CDCl_3$) δ_H 0.30 (6H, m, $Si(C\underline{H}_3)_2tBu$), 0.83-0.96 (9H, m, $C(C\underline{H}_3)_3$), 1.33-1.37 (3H, m, $OCH_2C\underline{H}_3$), 4.05-4.75 (4H, bm, $PC\underline{H}_2OH$, $-OC\underline{H}_2CH_3$), 7.52 (3H, m, *o*-,*p*-PhH), 7.96 (2H, m, *m*-PhH) consistent with the proposed structure but lacking resolution.

***Dimethyltetrahydroimidazole-1,3-diyldimethylenebis(phenylphosphinate)]*[3] (39)**

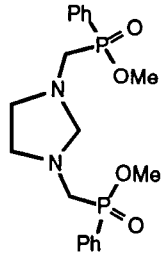

Synthesis of the title compound was carried out according to the procedure of Parker *et al.*[3] 1,2-Diaminoethane (1.44 g, 24 mmol) and paraformaldehyde (1.2 g, 40 mmol) were stirred in THF (120 ml) under reflux for 30 mins under an inert atmosphere. Phenyldimethoxyphosphine (12.2 g, 11.3 ml, 72 mmol) was added to the reaction mixture and heating was continued for a further 18 h. The solvent was removed under reduced pressure and the residue purified by chromatography on alumina with gradient elution (dichloromethane to 2% methanol-dichloromethane) to give the colourless oil (7.1 g, 72%); **^{31}P NMR** ($CDCl_3$) δ_P 40.8; **^{1}H NMR** (250.13 MHz, $CDCl_3$) δ_H 2.83 (4H, s, $NC\underline{H}_2C\underline{H}_2N$), 3.05 (4H, d, ^2J=9.1 Hz, $PC\underline{H}_2N$), 3.46 (2H, d, ^4J_P=3.1 Hz, $NC\underline{H}_2N$), 3.63 (3H, d, J_P=11 Hz, $POC\underline{H}_3$), 3.64 (3H, d, J_P=11 Hz, $POC\underline{H}_3$),.7.45-7.60 (6H, m, *m*-, *p*-Ph), 7.75-7.83 (4H, m, *o*-Ph); **^{13}C NMR** (62.9 MHz, $CDCl_3$) δ_C 51.37 (d, J=6 Hz, $POC\underline{H}_3$), 53.88 (d, ^2J_P=120 Hz, $NC\underline{H}_2P$), 53.99 (d, J=7.4 Hz), 79.17 (t, J=9.7 Hz, $NC\underline{H}_2N$), 128.50 (d, J_P=12.6 Hz, *m*-Ph), 129.71 (d, J_P=124 Hz, PPh), 131.98 (d, J=9 Hz, *o*-Ph), 132.6 (d, J=4 Hz, *p*-Ph); **m/z** (DCI) 409.89 (100%, MH^+).

***Ethylenediiminodimethylenebis(phenylphosphinic) Acid*[3] (43)**

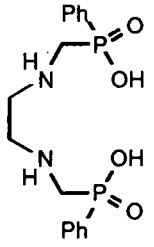

Dimethyltetrahydroimidazole-1,3-diyldimethylenebis(phenylphosphinate), (**39**), (5.5 g, 13 mmol) was heated under reflux for 16 h in hydrochloric acid (6M, 100 ml). The solvent was removed under reduced pressure to give a white solid (5.2 g, 99%); **m.p.** > 250°C (lit.[3] 276-278°C); **^{31}P NMR** (D_2O, pD14) δ_P 27.16; **^{1}H NMR** (250.13 MHz, D_2O, pD14) δ_H 1.57 (4H, d, J=2 Hz, $NC\underline{H}_2C\underline{H}_2N$), 1.86 (4H, d, J=11 Hz, $PC\underline{H}_2N$), 6.59 (6H, m, *o*-, *p*-Ph), 6.77 (4H, m, *m*-Ph); **^{13}C NMR** (62.9 MHz, D_2O, pD14) δ_C 48.53 (d, J=11 Hz, $NC\underline{H}_2C\underline{H}_2$), 48.80 (d, ^1J_P=103 Hz, $NC\underline{H}_2P$), 128.23 (d, ^3J=11.5 Hz, *m*-Ph), 130.64 (d, ^2J=9 Hz, *o*-Ph), 131.11 (s, *p*-Ph), 135.14 (d, ^1J_P=123 Hz, PPh); **m/z** (ESMS$^-$) 367.1 (100%, M-2H$^+$); Found C, 51.8; H, 6.02; N, 7.28 $C_{16}H_{22}N_2O_4P_2$.HCl requires C, 52.2; H, 6.02; N, 7.61%.

N,N'-*Bis*-p-*toluenesulfonyl*-N,N'-*bis[methylene(phenylphosphinic)acid)]-1,2-diaminoethane* (44)

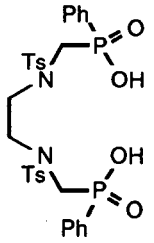

Ethylenediiminodimethylenebis(phenylphosphinic) acid, (**43**) (5.7 g, 14.1 mmol) was suspended in water (30 ml) and sodium hydroxide (4M) was added with stirring until the solids dissolved at pH 10. Tosyl chloride (5.91 g, 31 mmol) was added as a solid and the reaction mixture heated to 40 °C for 36 h, maintaining a pH range of 8-10 by further additions of sodium hydroxide. The excess tosyl chloride was removed by filtration upon completion of the reaction. A fine solid was precipitated from the filtrate by addition of hydrochloric acid to pH2 and the remaining liquor was decanted after centrifugation. The solid was recrystallised from boiling water then filtered and dried to give a white solid (6.5 g, 65%); **m.p.** 294-296 °C (decomp.); **^{31}P NMR** (D_2O, pD14) δ_P 25.02; **^{1}H NMR** (250.13 MHz, D_2O, pD14) δ_H 1.65 (6H, s, $C\underline{H}_3$), 2.35 (4H, s, $NC\underline{H}_2C\underline{H}_2N$), 2.88 (4H, d, ^2J_P=7.1 Hz, $PC\underline{H}_2N$), 6.55 (4H, d, ^{3}J=8 Hz, Ts$\underline{H}$), 6.77 (4H, d, ^{3}J=8 Hz, Ts$\underline{H}$), 6.86 (6H, m, Ph$\underline{H}$), 7.13 (4H, m, Ph$\underline{H}$); **^{13}C NMR** (62.9 MHz, D_2O, pD14) δ_C 20.56, (s, $\underline{C}H_3$), 45.33 (s, $N\underline{C}H_2\underline{C}H_2N$), 47.87 (d, ^1J_P=109 Hz, $N\underline{C}H_2P$), 126.78 (s, Ts), 128.10 (d, ^{3}J=11 Hz, *m*-Ph), 129.52 (s, Ts) 131.07 (s, *p*-Ph), 131.33 (d, ^{2}J=8.7 Hz, *o*-Ph), 134.24 (s, Ts), 134.65 (d, ^1J_P=127 Hz, PPh), 144.11 (s, Ts); **m/z** (ESMS $^-$, CH_3OH) 674.9 (100%, M-2H$^+$); **IR** ν_{max} 3423 br, 2360, 1620 br, 1345, 1160, 1129, 1043, 823, 739, 698, 625, 549, 525 cm^{-1}; Found 51.8, 4.82, 4.03; $C_{30}H_{34}N_2O_8P_2S_2.H_2O$ requires C, 51.9; H, 5.22; N, 4.03%.

N,N'-*Bis* -p-*toluenesulfonyl* -N,N'-*bis[methylene(phenylthiophosphinic) chloride]-1,2-diaminoethane* (46)

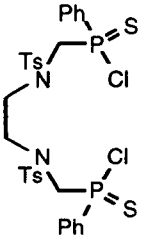

N,N'-Bis-*p*-toluenesulfonyl-*N,N'*-bis[methylene(phenylphosphinic)acid)]-1,2-diaminoethane, (**44**), (2.13 g, 3.0 mmol) was dissolved in dry dichloromethane (50 ml) and oxalyl chloride (2.5 ml, 28 mmol) was added. The solution was stirred at room temperature under an inert atmosphere for 20 mins to give the intermediate acid chloride as a mixture of diastereoisomers ($\delta_{P[CH_2Cl_2]}$ 46.8 and 47.0). The solvent was removed under reduced pressure and further portions of dichloromethane (2 x 25 ml)

were added and pumped off to remove any traces of unreacted oxalyl chloride. The crystalline solid was dried thoroughly *in vacuo.*

Excess thiophosphoryl chloride (40 ml) was added to the solid followed by a catalytic amount of DMF and the reaction mixture was stirred at 110 °C for 16 h. The solvent was removed under reduced pressure and dichloromethane (3 x 5 ml) was added and removed under reduced pressure to remove any volatile material leaving a yellow crystalline solid (2.2 g, 94%), **m.p.** 42-44°C; **^{31}P NMR** ($CDCl_3$) (two diastereoisomers observed) δ_P 79.75, 80.16; **^{1}H NMR** (399.96 MHz, $CDCl_3$) (two diastereoisomers observed) δ_H 2.33 (3H, s, Ts-C$\underline{H}_3$), 2.34 (3H, s, Ts-C$\underline{H}_3$), 3.49 (4H, m, NC$\underline{H}_2$C$\underline{H}_2$N), 4.09 (1H, dd, $^{2}J_{HaHb}$=15.2 Hz, J_{HaP}=3.2 Hz, PC$\underline{H}_2$N), 4.16 (1H, dd, $^{2}J_{HbHa}$=15.2 Hz, J_P=3.2 Hz, PC$\underline{H}_2$N), 4.37 (1H, dd, $^{2}J_{HaHb}$=15.2 Hz, PC$\underline{H}_2$N), 4.51 (1H, dd, $^{2}J_{HaHb}$=15.2 Hz, PC$\underline{H}_2$N), 7.17 (4H, m, Ts$\underline{H}$), 7.44-7.48 (6H, m, *m*-, *p*-Ph$\underline{H}$), 7.50-7.54 (4H, m, Ts$\underline{H}$), 7.92 (4H, m, *o*-Ph$\underline{H}$); **^{13}C NMR** (62.9 MHz, $CDCl_3$) δ_C 22.29 (s, Ts-$\underline{C}H_3$), 48.67 (s, N$\underline{C}H_2\underline{C}H_2$N), 57.87 (d, J_P=107 Hz, N$\underline{C}H_2$P), 59.06 (d, J_P=107 Hz, N$\underline{C}H_2$P), 128.46 (Ts), 129.35 (d, ^{3}J=14 Hz, *m*-Ph), 130.50 (Ts), 131.48 (Ts), 132.72 (d, J=24 Hz, PPh), 134.08 (s, *p*-Ph), 135.27, (d, J_P=5 Hz, *o*-Ph), 145.62 (Ts); **m/z** (ESMS $^-$, CH_3CN) 744.6 (100%, M^-); **IR** ν_{max} 1700, 1600 w, 1440, 1340-1260, 1155 s, 1090, 1000-900 br, 810-830, 740-690 m, 650-610 s, 550 s, 500-470 br, cm^{-1}; Found: C, 44.8, H, 4.27; N, 3.52; $C_{30}H_{32}Cl_2N_2O_4P_2S_4.CH_2Cl_2$ requires C,44.8; H, 4.13; N, 3.37%

N,N'-*Bis*-p-*toluenesulfonyl*-N,N'-*bis[methylene(phenylthiophosphinic) acid] -1,2-diaminoethane* (47)

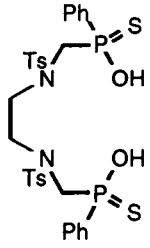

Compound (**46**) (3 g, 4.0 mmol) was heated under reflux in a solution of potassium hydroxide (5M, 50 ml) for 12 h. The solution was acidified to pH2 with hydrochloric acid (4 M) and the aqueous phase decanted leaving an extremely viscous oily residue. This was washed with water (2 x 20 ml) and dried (Na_2SO_4) to give a yellow crystalline solid in quantitative yield; **m.p.** 96-100°C; **^{31}P NMR** ($CDCl_3$) δ_P 58.1, 58.26; **^{1}H NMR** (250.13 MHz, $CDCl_3$) δ_H 2.33 (6H, s, Ts-C$\underline{H}_3$) 3.15-3.51 (4H, br m, NC$\underline{H}_2$C$\underline{H}_2$N), 3.51-3.88 (4H, br m, PC$\underline{H}_2$N), 7.06 (4H, d, J=7.5 Hz, TsH), 7.16 (6H, br, m, *m*-, *p*-Ph$\underline{H}$), 7.39 (4H, t, J_P=9 Hz, Ts$\underline{H}$), 7.85 (4H, q, *o*-Ph$\underline{H}$); **^{13}C NMR** (100.51 MHz, $CDCl_3$) (two diastereoisomers observed) δ_C 21.50 (s, Ts-$\underline{C}H_3$), 49.99 (N$\underline{C}H_2$C$\underline{H}_2$N), 50.55 (N$\underline{C}H_2$C$\underline{H}_2$N), 56.23 (d, J_P=80 Hz, N$\underline{C}H_2$P), 56.72 (d, J_P=80 Hz, N$\underline{C}H_2$P), 127.62 (s, *m*-Ts), 128.48 (d, ^{3}J=13 Hz, *m*-Ph), 129.96 (s, *o*-Ts) 131.37 (d, ^{2}J=6 Hz, *o*-Ph), 131.48 (d, ^{2}J=6 Hz, *o*-Ph), 131.69 (d, $^{1}J_P$=108 Hz, PPh), 132.46 (d, ^{3}J=7 Hz, *p*-Ph), 133.23 (s, NTs), 144.50 (s, STs); **m/z** (ESMS$^-$, CH_3CN) 707.2 (100%,

M - H^+); **IR** ν_{max} 2930 br, 1600 (Ar-H), 1440, 1340-1260, 1150 s, 1090, 900, 820, 720-690, 650 cm^{-1}; Found: C, 48.7; H, 4.70; N, 3.85; $C_{30}H_{34}N_2O_6P_2S_4$ .HCl requires C, 48.4; H, 4.73; N, 3.76 %.

Ethylenediiminodimethylenebis(phenylthiophosphinic acid) (**48**)

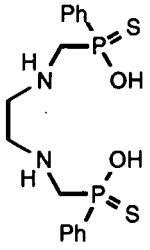

The ditosylamide, (**47**), (1.06 g, 1.5 mmol) was added portionwise to a solution of phenol (1.4 g, 15 mmol) in HBr in glacial acetic acid (45%, 30 ml). The mixture was stirred at 40 °C for 3 days and the resulting precipitate was separated from the liquor after centrifugation. The solid was washed with ether (4 x 35 ml) to remove the remaining phenol and dried to give the dihydrobromide salt of (**48**) as a pale yellow solid (650 mg, 77%); **m.p.** 183-185°C; **^{31}P NMR** (D_2O/NaOD, pD14) δ_P 62.79; **^{1}H NMR** (250.13 MHz, D_2O/NaOD, pD14) δ_H 2.09 (4H, s, $NC\underline{H}_2C\underline{H}_2N$), 2.96 (4H, dd, $^2J_{HaHb}$=12 Hz, $^2J_{HaP}$=5.9 Hz, $PC\underline{H}_2N$), 7.49 (6H, m, *m*-, *p*-ArH), 7.74-7.82 (4H, m, *o*-ArH); **^{13}C NMR** (62.9 MHz, D_2O/NaOD, pD14) δ_C 50.98 (d, ^{3}Jp=9.7 Hz, $NC\underline{H}_2C\underline{H}_2N$), 57.52 (d, Jp=77 Hz, $NC\underline{H}_2P$), 131.17 (d, ^{2}J=11Hz, *o*-Ar), 133.04 (d, ^{3}J=9.1 Hz, *m*-Ar), 133.87 (s, *p*-Ar), 141.09 (d, ^{1}Jp=96.1 Hz, PPh); **m/z** (ESMS$^-$, CH_3OH) 421 (100%, M-2H^+ + Na^+); **IR** ν_{max} 2970 br, 2750 br, 1440 s, 1110-1000, 900 s, 730-690, 620 br cm^{-1}; Found: C, 33.9; H, 4.24; N, 4.81; $C_{16}H_{22}N_2O_2P_2S_2$. 2HBr requires C, 34.2; H, 4.30; N, 4.98%.

Dimethylhexahydropyrimidine-1,3-diyldimethylenebis(phenylphosphinate)[3] (**49**)

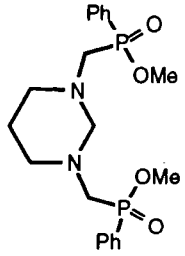

Using the same procedure as (**39**),[3] 1,3-diaminopropane (1.74 g, 24 mmol) was treated with paraformaldehyde (2.8 g, 93 mmol) and phenyldimethoxyphosphine (11.34 ml, 72 mmol) in dry tetrahydrofuran (170 ml). Purification of the crude product by chromatography on alumina, with gradient elution (dichloromethane to 2% methanol-dichloromethane) gave a colourless oil (4.5 g, 44%); **^{31}P NMR** ($CDCl_3$) δ_P 40.73; **^{1}H NMR** (250.13 MHz, $CDCl_3$) δ_H 1.51 (2H, t, ^{3}J=5 Hz, $NCH_2C\underline{H}_2$), 2.67 (4H, m, $NC\underline{H}_2CH_2$), 2.85 (4H, d, ^{2}J=9 Hz, $PC\underline{H}_2N$), 3.34 (2H, d, ^4J_P=5.4 Hz, $NC\underline{H}_2N$), 3.61 (3H, d, ^3J_P=4 Hz, $POC\underline{H}_3$), 3.65 (3H, d, ^3J_P=4 Hz, $POC\underline{H}_3$), 7.41 (6H, m, PhH), 7.73 (4H, m, PhH); **^{13}C NMR** (62.9 MHz, $CDCl_3$) δ_C 21.33 (s, $NCH_2C\underline{H}_2$), 51.59 (d, J=6

Hz, PO$\underline{C}H_3$), 52.10 (d, J=6 Hz, PO$\underline{C}H_3$), 53.10 (d, J=120 Hz, N$\underline{C}H_2$P), 77.75 (s, N$\underline{C}H_2$N), 129.08 (d, J_P= 12 Hz, *m*-Ph), 132.35 (d, J_P=129 Hz, PPh), 132.67 (d, J=9 Hz, *o*-Ph), 132.98 (s, *p*-Ph); **m/z** (DCI) 423 (100%, MH^+); **IR** ν_{max} 2600-3100 br (C-H), 1590, 1450 w (PPh), 1440 m (POMe), 1170-1300 br s (tertiary amine and P=O), 1120 br (POMe), 800-700 cm^{-1} (POMe).

Propylenediiminodimethylenebis(phenylphosphinic) Acid[3] **(52)**

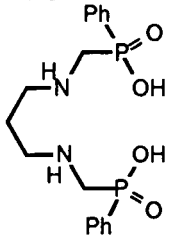

Dimethylhexahydropyrimidine-1,3-diyldimethylenebis(phenylphosphinate) (**49**) (2 g, 4.7 mmol) was hydrolysed as described for (**43**) to give a white solid in quantitative yield (1.98 g); **m.p.** > 250°C; **^{31}P NMR** (101.26 MHz, D_2O/NaOD, pD14) δ_P 20.26; **^{1}H NMR** (250.13 MHz, D_2O/NaOD, pD14) δ_H 1.99 (2H, t, J=8 Hz, NCH$_2\underline{C}H_2$), 3.07 (4H, t, J=8 Hz, N$\underline{C}H_2CH_2N$), 3.30 (4H, d, ^3J_P=12.8 Hz, PC$\underline{H}_2$N), 7.57 (6H, m, *m*-, *p*-Ph$\underline{H}$), 7.74 (4H, m, *o*-Ph$\underline{H}$); **^{13}C NMR** (62.9 MHz, D_2O/NaOD, pD14) δ_C 21.6 (s, NCH$_2\underline{C}H_2$), 45.81 (d, N$\underline{C}H_2CH_2$, ^{4}J=7 Hz), 46.59 (d, ^2J_P=81 Hz, N$\underline{C}H_2$P), 128.65 (d, ^{3}J=12 Hz, *m*-Ph), 130.96 (d, ^{2}J=9 Hz, *o*-Ph), 133.20 (d, ^1J_P=130 Hz, PPh), 134.24 (s, *p*-Ph$\underline{H}$); **m/z** (ESMS$^+$, CH_3OH) 409.36 (75%, M+Na^+), 382.96 (100%, MH^+); **IR** ν_{max} 3000 br, 2780 br, 1590, 1440, 1200-1180, 1130-1100, 960-880, 810, 740, 690, 540 cm^{-1}.

N,N'*Bis*-p-*toluenesulfonyl*-N,N'-*bis[methylene(phenylphosphinic) acid]-1,2-diaminopropane* (55)

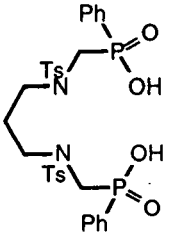

Ligand (**52**) (2.3 g, 5.5 mmol) was treated with tosyl chloride (2.3 g, 12 mmol) following the same procedure as for (**44**). A fine solid was precipitated by addition of hydrochloric acid (4 M) to pH 2.5, and was isolated by filtration and dried to give a white solid (2.3 g, 58%); **m.p.** 190-192°C; **^{31}P NMR** (D_2O, pD14) δ_P 25.32; **^{1}H NMR** (250.13 MHz, D_2O/NaOD, pD14) δ_H 1.03 (2H, m, NCH$_2\underline{C}H_2$), 2.35 (6H, s, Ts$\underline{C}H_3$), 2.50 (4H, t, J=8.9 Hz, N$\underline{C}H_2CH_2$), 3.20 (4H, d, ^2J_P=8.7 Hz, PC$\underline{H}_2$N), 7.27 (8H, dd, J=8.3 Hz, J=6.8 Hz, Ts$\underline{H}$), 7.47-7.54 (6H, m, *m*-Ph$\underline{H}$), 7.59-7.66 (4H, m, *o*- *p*-Ph$\underline{H}$); **^{13}C NMR** (62.9 MHz, D_2O/NaOD, pD14) δ_C 23.41 (s, NCH$_2\underline{C}H_2$), 25.15 (s, $\underline{C}H_3$), 47.60 (s, N$\underline{C}H_2CH_2$), 49.09 (d, J_P=107 Hz, N$\underline{C}H_2$P), 129.47 (s, Ts), 131.19 (d, ^{3}J=12

Hz, *m*-Ph), 132.78 (s, Ts), 133.98 (s, *p*-Ph), 134.20 (d, ^2J=8 Hz, *o*-Ph), 137.17 (s, Ts), 137.69 (d, ^1J_P=128.6 Hz, PPh), 147.65 (s, Ts); **m/z** (ESMS$^+$, CH_3OH) 757.35 (100%, M -2H$^+$ + 2-OCH_3); **IR** ν_{max} 3450, 3060, 2955, 2920, 2250, 1600, 1490, 1440, 1160, 1090, 960, 815, 740, 690, 650, 550, 520 cm^{-1}; Found: C, 52.6; H, 5.23; N, 3.80; $C_{31}H_{36}N_2O_8P_2S_2.H_2O$ requires C, 52.5; H, 5.40; N, 3.95%.

N,N'-*Bis*-p-*toluenesulfonyl*-N,N'-*bis(methylenephenylthiophosphinic chloride) -1,2-diaminopropane* (58)

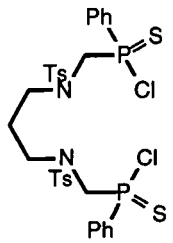

The phosphinic acid, (**55**), (0.95 g, 1.38 mmol) was converted to the thiophosphinic chloride by an analogous procedure to (**46**). Initial treatment of (**55**) with excess oxalyl chloride (1.5 ml, 17 mmol) in dichloromethane (40 ml) gave the intermediate phosphinic chloride as a white solid ($\delta_P[CH_2Cl_2]$ 47.07). This was heated with thiophosphoryl chloride (30 ml) in the presence of a catalytic drop of DMF for 40 h to give a glassy pale brown solid (1.09 g, 96%); **m.p.** 64-68°C; **^{31}P NMR** ($CDCl_3$) δ_P 79.57; **^{1}H NMR** (400 MHz, $CDCl_3$) (two diastereoisomers observed) δ_H 1.84 (2H, t, J=7.6 Hz, $NCH_2C\underline{H}_2$), 2.42 (6H, s, $C\underline{H}_3$), 3.17 (2H, m, $NC\underline{H}_2CH_2$), 3.47 (2H, m, $NC\underline{H}_2CH_2$), 4.17 (1H, dd, $^2J_{HaHb}$=15.2 Hz, J_{HaP}=3.6 Hz, $PC\underline{H}_2N$), 4.18 (1H, dd, $^2J_{HbHa}$=15.2 Hz, J_P=3.6 Hz, $PC\underline{H}_2N$), 4.47 (1H, d, $^2J_{HaHb}$=15.2 Hz, $PC\underline{H}_2N$), 4.48 (1H, d, $^2J_{HaHb}$=15.2 Hz, $PC\underline{H}_2N$), 7.51 (4H, dd, J=8 Hz, J=2.8 Hz, Ts$\underline{H}$), 7.24 (4H, d, J=8 Hz, Ts$\underline{H}$), 7.57 (4H, m, *m*-Ph$\underline{H}$), 7.65 (2H, m, *p*-Ph$\underline{H}$), 8.03 (4H, dd, J=8 Hz, J=15 Hz, *o*-Ph$\underline{H}$); **^{13}C NMR** (62.9 MHz, $CDCl_3$) δ_C 22.29 (s, Ts$\underline{C}H_3$), 25.87 (s, $NCH_2\underline{C}H_2$), 47.08 (s, $N\underline{C}H_2CH_2$), 57.33 (d, J_P=75 Hz, $N\underline{C}H_2P$), 128.15 (s, Ts), 129.47 (d, ^3J=14 Hz, *m*-Ph), 130.58 (s, Ts) 132.63 (d, ^2J=12.3 Hz, *o*-Ph), 132.36 (d, ^1J_P=84.5 Hz, PPh), 134.13 (s, NTs), 136.19 (s, *p*-Ph), 144.75 (s, STs); **m/z** (ESMS$^-$, CH_3CN) 721 (100%, M-Cl_2+OH+H$^+$); **IR** ν_{max} 1596, 1436, 1335, 1155, 1087, 986, 924, 814, 726, 688, 645, 609, 550, 500, 470 cm^{-1}.

N,N'-*Bis*-p-*toluenesulfonyl*-N,N'-*bis[methylene(phenylthiophosphinic) acid)]-1,2-diaminopropane* (61)

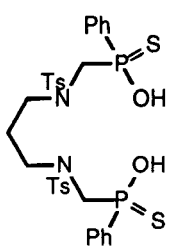

Compound (**58**) (680 mg, 0.90 mmol) was heated under reflux in a solution of potassium hydroxide (5M, 30 ml) for 12 h. The mixture was acidified to pH 2 with hydrochloric acid (4 M) and extracted into dichloromethane (3 x 30 ml), dried (Na_2SO_4) and the solvent evaporated under reduced pressure to give a pale yellow crystalline solid (450 mg, 69%); **m.p.** 85-87°C; **^{31}P NMR** ($CDCl_3$) (two diastereoisomers observed) δ_P 74.88, 74.48; **^{1}H NMR** (250.13 MHz, $CDCl_3$) δ_H 1.73 (2H, br m, $NCH_2C\underline{H}_2$), 2.42 (6H, s, Ts-C$\underline{H}_3$) 3.10 (4H, br m, $NC\underline{H}_2CH_2$), 3.66 (4H, br m, $PC\underline{H}_2N$), 7.28 (4H, d, J=7.6 Hz, Ts$\underline{H}$), 7.45 (6H, m, *m*-, *p*-Ph$\underline{H}$), 7.58 (4H, d, J_P=7.6 Hz, Ts$\underline{H}$), 7.90 (4H, m, *o*-Ph$\underline{H}$); **^{13}C NMR** (62.9 MHz, D_2O) δ_C 23.57 (s, Ts-$\underline{C}H_3$), 25.71 (s, $NCH_2\underline{C}H_2$), 47.64 (s, $N\underline{C}H_2CH_2$), 56.31 (d, J_P=80 Hz, $N\underline{C}H_2P$), 57.19 (d, J_P=80 Hz, $N\underline{C}H_2P$), 129.46 (s, Ts), 130.97 (d, ^{3}J=10.7 Hz, *m*-Ph), 132.51 (s, Ts) 133.64 (s, Ts) 133.87 (d, ^{2}J=18.7 Hz, Ph), 137.47 (s, Ph), 140.80 (d, ^1J_P= 98.75 Hz, Ph), 146.84 (s, Ts); **m/z** (ESIMS $^-$, MeOH) 360 (100%, [M-2H$^+$]/2); **IR** ν_{max} 2950 br, 1600 (Ar-H), 1440, 1330-1300, 1150 s, 1110, 1090, 900, 810, 730-690, 650 cm^{-1}; Found: C, 50.1, H, 5.07, N, 3.89; $C_{31}H_{36}N_2O_6P_2S_4.H_2O$ requires C, 50.3; H, 5.17; N, 3.78%.

Propylenediiminodimethylenebis (phenylthiophosphinic acid) **(64)**

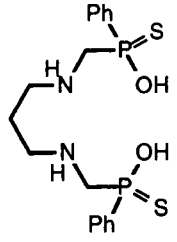

The ditosylamide, (**61**), (320 mg, 0.46 mmol) was added portionwise to a solution of phenol (1 g, 10 mmol) in HBr in glacial acetic acid (45%, 30 ml). The mixture was stirred at 40-50°C for 3 days then slowly dropped into diethyl ether (800 ml) with vigorous stirring to precipitate the solid product. The solid was isolated by centrifugation, redissolved in methanol (1.5 ml) and slowly dropped into fresh ether (800 ml) with vigorous stirring. Again, the precipitate formed was isolated by centrifugation and the resolvation/precipitation process was repeated and the resulting solid dried to give a dark yellow solid (110 mg, 58%); **m.p.** > 250°C; **^{31}P NMR** (CD_3OD) δ_P 67.63; **^{1}H NMR** (250.13 MHz, D_2O) δ_H 1.89 (2H, m, $NCH_2C\underline{H}_2$), 2.98 (4H, t, J=8.1 Hz, $NC\underline{H}_2CH_2$), 3.61 (2H, dd, $^2J_{HaHb}$=14.3 Hz, $^2J_{HaP}$=5.3 Hz, $PC\underline{H}_2N$), 3.84 (2H, dd, $^2J_{HbHa}$=14.3 Hz, $^2J_{HbP}$=11.4 Hz, $PC\underline{H}_2N$), 7.30 (6H, m, *m*-, *p*-Ph$\underline{H}$), 7.72 (4H, m, *o*-Ph$\underline{H}$); **^{13}C NMR** (62.9 MHz, CD_3OD) δ_C 24.27 (s, $NCH_2\underline{C}H_2$) 48.65 (d, ^3J_P=6.2 Hz, $N\underline{C}H_2CH_2$), 52.89 (d, J_P=77.8 Hz, $N\underline{C}H_2P$), 131.04 (d, ^{2}J= 13.1 Hz, *o*-Ph), 133.67 (d, ^{3}J=11.3 Hz, *m*-Ph), 135.09 (s, *p*-Ph), 136.19 (d, ^1J_P=110 Hz, PPh); **m/z** (ESMS $^-$, CH_3OH) 413.21 (100%, M-H$^+$); (ESMS$^+$) 436.4 (M + Na$^+$); **IR** ν_{max} 2920, 2730, 1585, 1540, 1435-1300, 1170, 1113, 910 br, 735-715, 690, 624, 600, 573 cm^{-1}.

Dimethyltetrahydroimidazole-1,3-diyldimethylenebis(methylphosphinate)[3] **(50)**

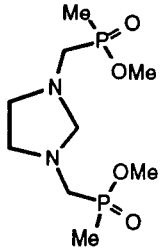

Synthesis of the title compound was carried out according to the procedure for (**39**).[3] Ethane-1,2-diamine (1.47 g, 1.64 ml, 24.5 mmol) was treated with paraformaldehyde (2.8 g, 93 mmol) and diethoxymethylphosphine (10 g, 73 mmol) in dry tetrahydrofuran (150 ml). Purification of the crude product by chromatography on neutral alumina with gradient elution (dichloromethane to 2% methanol-dichloromethane) gave a pale yellow oil (3.8 g, 50%); **^{31}P NMR** ($CDCl_3$) δ_P 51.53; **^{1}H NMR** (250.13 MHz, $CDCl_3$) δ_H 1.31 (6H, t, ^3J=7.1 Hz, $POCH_2C\underline{H}_3$), 1.51 (6H, d, ^2J=14 Hz, $PC\underline{H}_3$), 2.88 (4H, d, ^2J=10 Hz, $PC\underline{H}_2N$), 2.94 (4H, s, $NC\underline{H}_2CH_2$); **^{13}C NMR** (62.9 MHz, $CDCl_3$) δ_C 12.93 (d, J_P=94 Hz, $P\underline{C}H_3$), 16.90 (d, J= 6 Hz, $POCH_2\underline{C}H_3$), 54.36 (d, J=115 Hz, $N\underline{C}H_2P$), 54.56 (d, J=8.3 Hz, $PO\underline{C}H_2CH_3$), 60.55 (d, J= 5 Hz, $N\underline{C}H_2CH_2$), 79.64 (t, J=5 Hz, $N\underline{C}H_2N$); **m/z** (DCI) 313 (100%, MH^+).

Ethylenediiminodimethylenebis(methylphosphinic) Acid[3] **(53)**

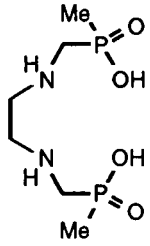

Dimethyltetrahydroimidazole-1,3-diyldimethylenebis(methylphosphinate) (**50**) (2.5 g, 8 mmol) was hydrolysed as described for (**43**) to give a white solid in quantitative yield; **m.p.** 242-244°C (lit.[3] 246-248°C); **^{31}P NMR** (D_2O/NaOD, pD14) δ_P 39.45; **^{1}H NMR** (250.13 MHz, D_2O/NaOD, pD14) δ_H 1.26 (6H, d, ^2J=14 Hz, $PC\underline{H}_3$), 2.69 (4H, d, ^2J=11.5 Hz, $PC\underline{H}_2N$), 2.77 (4H, s, $NC\underline{H}_2CH_2$), 3.58 (2H, s, $NC\underline{H}_2N$), 4.08 (4H, p, ^3J_P=7.3 Hz, $POC\underline{H}_2CH_3$); **^{13}C NMR** (62.9 MHz, D_2O/NaOD, pD14) δ_C 17.35 (d, J_P=91 Hz, $P\underline{C}H_3$), 52.09 (d, J=12.6 Hz, $N\underline{C}H_2CH_2$), 52.36 (d, J=99 Hz, $N\underline{C}H_2P$); **m/z** (ESMS$^-$, CH_3OH) 242.9 (100%, $M\text{-}H^+$).

N,N'-*Bis*-p-*toluenesulfonyl*-N,N'-*bis[methylene(methylphosphinic)acid]-1,2-diaminoethane* **(56)**

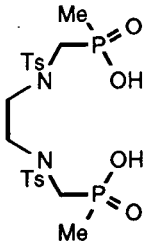

Tosylation was achieved using the same procedure as (**44**). Tosyl chloride (3.4 g, 18 mmol) was added to a solution of ethylenediiminodimethylenebis(methylphosphinic) acid, (**53**), (2 g, 7.13 mmol) in water (40 ml) with the addition of sodium hydroxide to pH 10. The mixture was heated at 50°C for 3 days, maintaining pH 10 by further addition of sodium hydroxide. The solution was cooled and excess tosyl chloride was removed by filtration. The filtrate was acidified with hydrochloric acid (6M) to pH 1 to precipitate a fine white solid which was isolated by centrifugation. The solid was washed with minimal volume of cold water to remove the inorganic salts and *p*-toluenesulfonic acid, and dried to give a white solid (2.4 g, 60%); **m.p.** 108-111°C; **^{31}P NMR** (101.26 MHz, $CDCl_3$) δ_P 47.74; **^{1}H NMR** (250.13 MHz, $CDCl_3$) δ_H 1.51 (6H, d, J_P=9.6 Hz, $PC\underline{H}_3$) 2.46 (6H, s, Ts-$C\underline{H}_3$), 3.43 (4H, d, J_P=9.6 Hz, $PC\underline{H}_2N$), 3.48 (4H, s, $NC\underline{H}_2CH_2$), 7.36 (4H, d, $^{2}J_{HaHb}$=8.2 Hz, Ts$\underline{H}$), 7.72 (4H, d, $^{2}J_{HbHa}$=8.2 Hz, Ts$\underline{H}$); **^{13}C NMR** (62.9 MHz,) δ_C 13.50 (d, J_P=100 Hz, $P\underline{C}H_3$), 22.28 (s, Ts$\underline{C}H_3$), 49.98 (d, J_P=107 Hz, $N\underline{C}H_2P$), 50.84 (s, $N\underline{C}H_2CH_2$), 128.20 (s, *m*-Ts), 130.77 (s, *o*-Ts), 134.93 (NTs), 144.99 (s, STs); **m/z** (ESMS$^-$, CH_3OH) 573.21 (M-2H$^+$ + Na$^+$); **IR** ν_{max} 1350, 1330, 1310, 1270, 1150 s, 1090, 990 960 s cm^{-1}; Found: C, 42.1; H, 5.61; N, 4.74; $C_{20}H_{30}N_2O_8P_2S_2$ requires C, 42.1; H, 5.65; N, 4.91%.

N,N'-*Bis*-p-*toluenesulfonyl*-N,N'-*bis[methylene(methylthiophosphinic)chloride]-1,2-diaminoethane* (59)

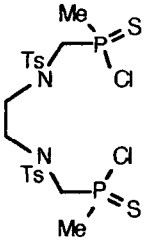

The reaction was carried out as for (**46**) using *N,N'*-bis-*p*-toluenesulfonyl-*N,N'*-bis [methylene(methylphosphinic)]acid-1,2-ethanediamine (**56**) (0.5 g, 0.9 mmol) and oxalyl chloride (0.7 ml, 8 mmol) in dichloromethane (40 ml) to give the phosphinic chloride ($\delta_P[CH_2Cl_2]$ 58.45 and 58.55 corresponding to two diastereoisomers).

Thiophosphorylchloride (35 ml) was added to the phosphinic chloride with a catalytic amount of DMF and the resulting solution stirred at 110°C for 32 h. Upon cooling, a pale yellow solid precipitated and was isolated by filtration and dried *in vacuo* (416 mg, 76%); **m.p.** 114-116°C; **^{31}P NMR** ($CDCl_3$) (two diastereoisomers observed) δ_P 86.83, 87.0; **^{1}H NMR** (400 MHz, $CDCl_3$) δ_H 2.37 (6H, d, $^{1}J_P$=13.2 Hz, $PC\underline{H}_3$), 2.47 (6H, s, Ts-$C\underline{H}_3$), 3.18-3.32 (4H, m, $NC\underline{H}_2C\underline{H}_2N$), 3.78 (1H, dd, J_{HaHb}=15.6 Hz, J_P=3.2 Hz, $PC\underline{H}_2N$) and 4.22 (1H, dd, $^{2}J_{HbHa}$=15.6 Hz, $PC\underline{H}_2N$), 3.85 (1H, dd, $J_{Hb'Ha'}$=15.6 Hz, J_P=3.2 Hz, $PC\underline{H}_2N$) and 4.07 (1H, br d, $^{2}J_{Ha'Hb'}$=15.6 Hz, $^{2}J_P$=3.6 Hz, $PC\underline{H}_2N$), 7.39 (4H, d, ^{3}J=8.0 Hz, Ts$\underline{H}$), 7.80 (4H, t like dd, J=8 Hz, Ph$\underline{H}$); **^{13}C NMR** (62.9 MHz, $CDCl_3$) δ_C 22.36 (s, Ts-$\underline{C}H_3$), 23.03 (d, $^{1}J_P$=85 Hz, $P\underline{C}H_3$), 51.77 (d, $^{3}J_P$=17 Hz, $NC\underline{H}_2C\underline{H}_2N$), 60.55 (d, J_P=73 Hz, $N\underline{C}H_2P$), 60.76 (d, J_P=73 Hz, $N\underline{C}H_2P$),

128.54 (s, *m*-Ts), 130.93 (s, *o*-Ts), 134.41 (s, NTs), 145.63 (s, STs); **IR** ν_{max} 1600, 1350-1260, 1160 s, 1090, 1000-890, 710-700, 650, 540-450 cm^{-1}; **m/z** (ESMS $^-$) 596.67 (100%, M - Cl_2 + OCH_3 + O^-).

N,N'-*Bis*-p-*toluenesulfonyl*-N,N'-*bis[methylene(methylthiophosphinic)acid-1,2-diaminoethane* (62)

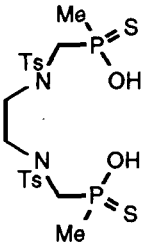

Compound (**59**) (200 mg, 0.20 mmol) was heated under reflux in a solution of potassium hydroxide (6 M, 50 ml) for 12 h. The mixture was acidified to pH 2 with hydrochloric acid (4 M) and extracted with dichloromethane (3 x 40 ml). The combined extracts were dried (Na_2SO_4) and the solvent evaporated to give a pale yellow crystalline solid (160 mg, 85%); **m.p.** 185-188°C; **^{31}P NMR** (D_2O, pD14) δ_P 64.27; **^{1}H NMR** (250.13 MHz, D_2O, pD14) δ_H 1.57 (6H, d, J=13 Hz, $PC\underline{H}_3$), 2.32 (6H, s, Ts-$C\underline{H}_3$), 3.35 (4H, s, $NC\underline{H}_2C\underline{H}_2N$), 3.47 (4H, d, J_P=5.5 Hz, $PC\underline{H}_2N$), 7.32 (4H, d, ^{3}J=8.1 Hz, Ts$\underline{H}$), 7.57 (4H, d, ^{3}J=8.1 Hz, Ts$\underline{H}$); **^{13}C NMR** (62.9 MHz, D_2O, pD14) δ_C 23.71 (s, Ts-$C\underline{H}_3$), 25.82 (d, J=72 Hz, $P\underline{C}H_3$), 49.78 (s, $N\underline{C}H_2\underline{C}H_2$), 57.18 (d, J_P=76 Hz, $N\underline{C}H_2P$), 129.82 (s, *m*-Ts), 132.63 (s, *o*-Ts), 137.25 (NTs), 147.09 (s, Ts); **m/z** (ESMS $^-$, CH_3OH) 582.69 (100%, M-H$^+$); **IR** ν_{max} 3350 b, 1600, 1325-1290, 1150, 1100-1070, 880, 810, 730-690, 660, 540 cm^{-1}; Found: C, 39.9, H, 4.81; N, 4.39; $C_{20}H_{29}N_2O_6P_2S_4$.0.5 HCl requires C, 39.6; H, 4.82; N, 4.62%.

***Ethylenediiminodimethylenebis(methylthiophosphinic) Acid* (65)**

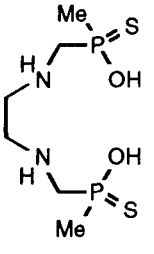

The ditosylamide, (**62**), (150 mg, 0.26 mmol) was added portionwise to a solution of phenol (490 mg, 5.2 mmol) in HBr/glacial acetic acid (45%, 3 ml). The mixture was stirred at 40-50°C for 3 days then slowly dropped into diethyl ether (400 ml) with vigorous stirring to precipitate the solid product. The solid was isolated by centrifugation, redissolved in methanol (0.5 ml) and slowly dropped into fresh ether (300 ml) with vigorous stirring. The precipitate formed was isolated by centrifugation and the resolvation/precipitation process repeated and the resulting solid dried to give a pale yellow solid (37 mg, 51%); **m.p.** 166-173°C; **^{31}P NMR** (101.26 MHz, D_2O) δ_P 67.46; **^{1}H NMR** (400 MHz, D_2O) δ_H 1.49 (6H, d, J=13 Hz, $PC\underline{H}_3$), 2.68 (4H, s,

$NC\underline{H}_2C\underline{H}_2N$), 2.69 (2H, dd, J_{Hab}=14 Hz, J_P=8.8 Hz, $PC\underline{H}_2N$), 2.84 (2H, dd, J_{Hba}=14 Hz, J_P=8.8 Hz, $PC\underline{H}_2N$); **^{13}C NMR** (62.9 MHz, D_2O) δ_C 25.24 (d, J_P=71 Hz, $P\underline{C}H_2N$), 51.38 (d, J=11.5 Hz, $N\underline{C}H_2\underline{C}H_2$), 58.27 (d, J_P=88 Hz, $N\underline{C}H_2P$); **m/z** (ESMS$^-$, CH_3OH) 275.10 (100%, M - H^+); **IR** 3400, 2980, 2770, 2200, 1330, 1150, 930, 880, 820, 710, 660, 550 cm^{-1}.

Dimethyltetrahydroipyrimidine-1,3-diyldimethylenebis(methylphosphinate)[3] **(51)**

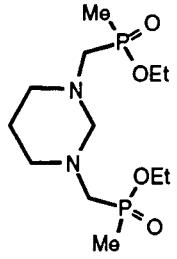

Synthesis was carried out according to the procedure described for (**39**).[3] Propane-1,3-diamine (2.02 g, 2.27 ml, 27 mmol) was treated with paraformaldehyde (2.8 g, 93 mmol) and diethoxymethylphosphine (10g, 73 mmol) in dry tetrahydrofuran (150 ml). Purification of the crude product by chromatography on neutral alumina, with gradient elution (dichloromethane to 2% methanol-dichloromethane) gave a pale yellow oil (3.85 g, 44%); **^{31}P NMR** ($CDCl_3$) δ_P 52.56; **^{1}H NMR** (250.13 MHz, $CDCl_3$) δ_H 1.30 (6H, t, ^{3}J=7.1 Hz, $POCH_2C\underline{H}_3$), 1.49 (6H, d, ^{2}J=14 Hz, $PC\underline{H}_3$), 1.63 (2H, t, J=5 Hz, $NCH_2C\underline{H}_2$), 2.73 (4H, d, ^{2}J=10 Hz, $PC\underline{H}_2N$), 2.75 (4H, m, $NC\underline{H}_2CH_2$) 3.48 (2H, br s, $NC\underline{H}_2N$), 4.04 (4H, qnt, $POC\underline{H}_2CH_3$); **m/z** (DCI) 327 (100%, MH^+); **IR** ν_{max} 2900-2800 (C-H), 1670, 1450-1380 (P-OEt), 1295 (PCH_3), 1200 br s (tertiary amine and P=0), 1040 br s (POEt), 950 s (PCH_3), 800-730 (POEt) cm^{-1}.

Propylenediiminodimethylenebis(methylphosphinic) Acid[3] **(54)**

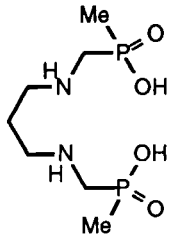

The diester (**51**) (2.85 g, 8.74 mmol) was heated under reflux in hydrochloric acid (6M, 35 ml) for 16 h. The solvent was removed under reduced pressure to leave a white solid in quantitative yield (3.48 g); **m.p.** °C (lit^R. 244-246°C); **^{31}P NMR** (D_2O) δ_P 39.45; **^{1}H NMR** (250.13 MHz, D_2O) δ_H 1.43 (6H, d, ^{2}J=15 Hz, $PC\underline{H}_3$), 1.99 (2H, m, $NCH_2C\underline{H}_2$), 3.06 (4H, s, $NC\underline{H}_2CH_2$), 3.24 (4H, d, ^{2}J=10 Hz, $PC\underline{H}_2N$); **^{13}C NMR** (62.9 MHz, D_2O, NaOD, pD14) δ_C 18.07 (d, ^1J_P=98 Hz, $PC\underline{H}_3$), 24.86 (s, $NCH_2C\underline{H}_2$), 49.06 (d, ^3J_P=6 Hz, $NC\underline{H}_2CH_2$), 49.15 (d, ^1J_P=89 Hz, $PC\underline{H}_2N$); **m/z** (ESMS$^-$, CH_3OH) 256.86 (100%, M-H^+); **IR** ν_{max} 3360, 2600 br, 1610-1590, 1460-1415, 1280, 1210, 1150-1120, 1010, 980-910, 830, 795, 735, 690, 660, 640 cm^{-1}; Found: C, 25.9; H, 6.83; N, 9.18; $C_7H_{20}N_2O_4P_2.2HCl$ requires C, 25.4; H, 6.70; N, 8.46%.

N,N'-*Bis*-p-*toluenesulfonyl*-N,N'-*bis[methylene(methylphosphinic)acid]-1,2-diaminopropane* (57)

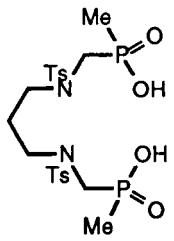

The amino phosphinic acid (**54**) (3.0 g, 9.0 mmol) was treated with tosyl chloride (3.8 g, 20 mmol) with the addition of sodium hydroxide in the same procedure described for (**44**). The mixture was heated at 50°C for 4 days, maintaining pH 10 by addition of sodium hydroxide as required. The excess tosyl chloride was removed by filtration. The filtrate was acidified with hydrochloric acid to pH1 to precipitate a fine white solid which was isolated by centrifugation. The solid was washed with sparing amounts of cold water to remove the salts and *p*-toluenesulfonic acid, and dried to give a white solid (0.6 g, 12%); **m.p.** 188-193 °C; **^{31}P NMR** (D_2O, NaOD, pD14) δ_P 34.74; **^{1}H NMR** (250.13 MHz, D_2O, NaOD, pD14) δ_H 1.19 (6H, d, $^{2}J_P$=13.5 Hz, $PC\underline{H}_3$) 1.41 (2H, m, $NCH_2C\underline{H}_2$), 2.44 (6H, s, Ts-$C\underline{H}_3$), 2.96 (4H, t, ^{3}J=7.5 Hz, $NC\underline{H}_2CH_2$), 3.06 (4H, d, J_P=9 Hz, $PC\underline{H}_2N$), 7.31 (4H, d, ^{3}J=7.7 Hz, Ts$\underline{H}$), 7.54 (4H, d, ^{3}J=8 Hz, Ts$\underline{H}$); **^{13}C NMR** (62.9 MHz, D_2O, NaOD, pD14) δ_C 17.00 (d, $^{1}J_P$=95 Hz, $P\underline{C}H_3$), 23.39 (s, Ts$\underline{C}H_3$), 25.94 (s, $NCH_2\underline{C}H_2$), 48.34 (s, $N\underline{C}H_2CH_2$), 49.49 (d, $^{1}J_P$=103 Hz, $N\underline{C}H_2P$), 129.62 (s, *m*-Ts), 132.87 (d, *o*-Ts), 137.15 (s, NTs) 147.83 (s, STs); **m/z** (ESMS$^-$, CH_3OH) 564.78 (40%, M - H^+), 282.06 (100%, [M- $2H^+$]/2); **IR** ν_{max} 1600 w, 1335, 1150 s, 1090, 970 s, 890-750, 730, 660, 550, 450 cm^{-1}; Found: C, 43.9; H, 5.65; 4.87; $C_{21}H_{32}N_2O_8P_2S_2.0.5H_2O$ requires C, 43.8; H, 5.77; N, 4.87%.

N,N'-*Bis*-p-*toluenesulfonyl*-N,N'-*bis-[methylene(methylthiophosphinic) chloride-1,2-diaminopropane* (60)

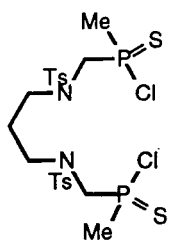

The reaction was carried out as for (**46**) using *N,N'*-bis-*p*-toluenesulfonyl-*N,N'*-bis[methylene(methylphosphinic)acid]-1,3-propanediamine (**57**) (200 mg, 0.35 mmol) and oxalyl chloride (0.7 ml, 8 mmol) in dichloromethane (40 ml) to give the phosphinic chloride (δ_P[CH_2Cl_2] 57.90 and 58.11).

Thiophosphorylchloride (35 ml) was added to the solid phosphinic chloride with a catalytic drop of DMF and the reaction mixture was stirred at 115°C for 18 hours. The solvent was removed under reduced pressure to give a pale yellow solid (165 mg, 70%), **m.p.** 75-78°C, **^{31}P NMR** ($CDCl_3$) δ_P 85.94, 86.01; **^{1}H NMR** (250.13 MHz, $CDCl_3$) δ_H

2.01 (2H, d m, $NCH_2C\underline{H}_2$), 2.38 (6H, d, ^1J_P= 13 Hz, $PC\underline{H}_3$), 2.44 & 2.45 (6H, s, Ts-$C\underline{H}_3$ diastereoisomers), 3.15-3.40 (4H, m, $NC\underline{H}_2CH_2$), 3.76 (2H, m, $PC\underline{H}_2N$), 4.19 (2H, m, $PC\underline{H}_2N$), 7.35 (4H, m, Ts$\underline{H}$), 7.69 (4H, m, Ts$\underline{H}$); **^{13}C NMR** (62.9 MHz, $CDCl_3$) δ_C 22.29 (s, Ts-$\underline{C}H_3$), 26.81 (s, $NCH_2\underline{C}H_2$), 27.94 (d, J_P=58 Hz, $PC\underline{H}_3$), 48.34 (s, $N\underline{C}H_2CH_2$), 58.03 (d, J_P=72 Hz, $N\underline{C}H_2P$), 128.08 (s, Ts), 130.90 (s, Ts) 135.41 (s, NTs), 145.37 (s, STs); **m/z** (ESMS $^-$, MeOH) 597.08 (100%, M- Cl_2 + OH + O^-); **IR** ν_{max} 2850 br, 1597, 1450, 1400, 1330, 1290, 1150, 1190, 920 br, 895, 810, 730-710, 655, 600, 550 cm^{-1}; Found C, 38.2; H, 5.44; N, 4.28; $C_{21}Cl_2H_{32}N_2O_4P_2S_4$ .H_2O requires C, 38.6; H, 4.93; N, 4.29%

N,N'-*Bis*-p-*toluenesulfonyl*-N,N'-*bis[methylene(methylthiophosphinic)acid]-1,2-diaminopropane* (63)

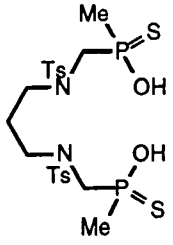

Ligand (**60**) (100 mg, 0.16 mmol) was heated under reflux in a solution of potassium hydroxide (4M, 50ml) for 12 h. The mixture was acidified to pH3 with hydrochloric acid (4M) and extracted with dichloromethane (4 x 40 ml). The combined extracts were dried (Na_2SO_4) and the solvent evaporated to give a pale yellow crystalline solid (75 mg, 79%); **m.p.** 68-71°C ; **^{31}P NMR** (CD_3OD) δ_P 86.00, 86.46; **^{1}H NMR** (250.13 MHz, CDCl3) δ_H 1.91 (6H, d, J_P=13.5 Hz, $PC\underline{H}_3$), 2.52 (6H, s, Ts-$C\underline{H}_3$) 3.2-3.54 (6H, m, $NC\underline{H}_2CH_2$ and $PC\underline{H}_2N$), 3.70-3.91 (2H, m, $PC\underline{H}_2N$), 5.86 (2H, br, PO$\underline{H}$), 7.31 (4H, m, Ts$\underline{H}$), 7.65 (4H, m, Ts$\underline{H}$); **^{13}C NMR** (62.9 MHz,) δ_C 22.30 (s, Ts-$\underline{C}H_3$), 26.82 (s, $NCH_2\underline{C}H_2$), 27.96 (d, J_P=58 Hz, $P\underline{C}H_3$), 48.35 (s, $N\underline{C}H_2CH_2$), 58.04 (d, J_P=72 Hz, $N\underline{C}H_2P$), 128.09 (s, *m*-Ts), 130.92 (s, *o*-Ts) 135.43 (s, NTs), 145.38 (s, STs); **m/z** (ESMS$^-$, CH_3OH) 596.74 (100%, M-H^+), 298.20 (30%, [M-2H^+]/2); **IR** ν_{max} 2930 br, 1597, 1330-1290, 1153, 1090, 1020, 940, 887, 815, 650, 545 cm^{-1}.

***Propylenediiminodimethylenebis(methylthiophosphinic acid)* (66)**

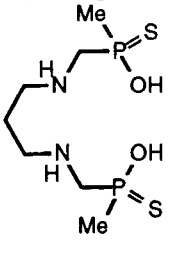

The ditosylamide, (**63**), (70 mg, 0.12 mmol) was added portionwise to a solution of phenol (0.22 g, 2.4 mmol) in HBr in glacial acetic acid (45%, ml). The mixture was stirred at 40-50°C for 3 days then slowly dropped into diethyl ether with vigorous stirring to precipitate the solid product as described previously for (**65**). The solid was

washed with ether and dried to give a pale yellow oil (16 mg, 48%);**^{31}P NMR** (D_2O) δ_P 63.06; **^{1}H NMR** (250.13 MHz, D_2O) δ_H 1.79 (6H, d, J=13.5 Hz, $PC\underline{H}_3$), 2.17 (4H, m, $NCH_2C\underline{H}_2$), 3.15 (2H, m, $PC\underline{H}_2N$), 3.26 (4H, m, $NC\underline{H}_2CH_2$), 3.42 (2H, m, $PC\underline{H}_2N$); **^{13}C NMR** (62.9 MHz,) δ_C 26.14 (s, $NCH_2\underline{C}H_2$), 26.34 (d, J_P=75 Hz, $PC\underline{H}_3$), 49.0 (d, J=6 Hz, $N\underline{C}H_2CH_2$), 53.33 (d, J_P=66 Hz, $N\underline{C}H_2P$), **m/z** (ESMS $^-$, CH_3OH) 288.89 (100%, M - H^+), 730.73 (90%, M + Br^-).

***Ethylenediimino*-N,N'-*dimethyldimethylenebis(phenylphosphinic) acid* (68)**
- *method A*

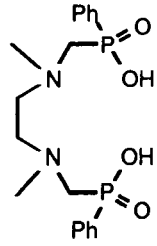

The title compound was prepared following the reductive methylation procedure of Pine and Sanchez.[4] Formic acid (1 ml, 1.1 mmol) was added to ethylenediimino-dimethylenebis(phenylthiophosphinic)acid.2HBr (**48**) (200 mg, 36 mmol) at 0°C. Formaldehyde (0.8 ml) was added and the reaction mixture heated at 80°C for 16h. All volatile material was removed from the mixture under reduced pressure to give a pale yellow solid (120 mg, 85%); **m.p.** 160-162°C; **^{31}P NMR** (101.26 MHz, D_2O) δ_P 19.15; **^{1}H NMR** (250.13 MHz, D_2O) δ_H 2.91 (6H, s, $NC\underline{H}_3$), 3.47 (4H, d, ^2J_P=8.9 Hz, $PC\underline{H}_2N$), 3.64 (4H, s, $NC\underline{H}_2CH_2$), 7.48-7.53 (6H, m, *m*-, *p*- Ar), 6.77 (4H, m, *o*-Ar); **^{13}C NMR** (62.9 MHz, D_2O) δ_C 46.29 (s, $NC\underline{H}_3$) 54.35 (s, $N\underline{C}H_2CH_2$), 58.82 (d, ^{1}J= 91 Hz, $N\underline{C}H_2P$), 131.67 (d, ^{3}J=12 Hz, *m*-Ph), 133.74 (d, ^{2}J=9.3 Hz, *o*-Ph), 135.43 (s, *p*-Ph), 135.47 (d, ^1J_P=137 Hz); **m/z** (ESMS$^-$, CH_3OH) 394.94 (100%, M - H^+); **IR** ν_{max} 2790 br, 1440, 1350, 1220, 1125, 1100, 1070, 990, 915, 840, 780, 745, 690, 860 cm^{-1}.

method B

Following the mild conditions for reductive methylation described by Hemo and Charles[5], a solution of formaldehyde (35% in H_2O, 2.25 mmol) was added to a stirred solution of ethylenediiminodimethylenebis(phenylthiophosphinic)acid.2HBr (**48**) (90 mg, 0.22 mmol) and the reaction mixture heated at 60°C for 0.5 h. Sodium borohydride (200 mg tablet) was added and the mixture stirred for a further 3 h. All volatile material was removed from the mixture under reduced pressure leaving a pale yellow solid containing a single phosphorus-containing species, **^{31}P NMR** (101.26 MHz, D_2O) δ_P 19.15 as above; crude product not purified.

Ethylenediiminodimethylenebis(phenylthiophosphinate) metal oligomeric complexes

Copper(II) (131)

Ligand (**48**) (50 mg, 0.09 mmol) was dissolved in methanol (2 ml) and crushed K_2CO_3 (24 mg) was added. Copper triflate (32 mg, 0.09 mmol) was added as a solution in methanol and a precipitate formed. The solid was isolated by centrifugation, washed with methanol (2 ml) then with water (2 ml) and dried *in vacuo* to give an insoluble green solid (40 mg, 97%); **IR** ν_{max} 1435, 1164, 1140, 1102, 1023 w, 980 w, 734, 715, 692, 585, 575, 552, 515, 460 cm^{-1}; Found C, 37.2; H, 4.06; N, 5.26; $C_{16}H_{19}N_2O_2P_2S_2CuK.H_2O$ requires C, 37.1; H, 4.09; N, 5.41%

Zinc(II) (132)

Ligand (**48**) (50 mg, 0.09 mmol) was dissolved in methanol (2 ml) and crushed K_2CO_3 (24 mg) was added. Zinc triflate (32 mg, 0.09 mmol) was added as a solution in methanol and a precipitate formed. The solid was isolated by centrifugation and washed with methanol (2 ml), water (2 ml) and dried *in vacuo* to give an insoluble white solid (42 mg, 98%); **IR** ν_{max} 1435, 1130, 1091, 1023, 956 w, 870-850 w, 736, 715, 696, 591, 574, 513 cm^{-1}; Found C, 40.9; H, 4.33; N, 5.91; $C_{16}H_{20}N_2O_2P_2S_2Zn.\ 0.5H_2O$ requires C, 40.7; H, 4.48; N, 5.93%

Nickel(II) (133)

A similar procedure to the above was employed using ligand (**48**) (50 mg, 0.09 mmol) dissolved in methanol (2 ml) with the adition of crushed K_2CO_3 (24 mg). Nickel(II) chloride (21 mg, 0.09 mmol) was added as a solution in methanol and a pale green precipitate formed. The solid was isolated by centrifugation and washed with methanol (2 ml), water (2 ml) and dried *in vacuo* to give an insoluble pale green solid (42 mg, 98%); **IR** ν_{max} 1435, 1127, 1095, 1050-1030, 992 w, 737, 715, 695, 588, 513 cm^{-1}; Found C, 40.78; H4.48; N, 5.87; $C_{16}H_{20}N_2O_2P_2S_2Ni.H_2O$ requires C, 40.45; H, 4.67; N, 5.89%

Cadmium(II) (134)

A similar procedure to the above was employed using ligand (**48**) (50 mg, 0.09 mmol) dissolved in methanol (2 ml) with the adition of crushed K_2CO_3 (24 mg). Cadmium(II) triflate (37 mg, 0.09 mmol) was added as a solution in methanol and a pale green precipitate formed. The solid was isolated by centrifugation and washed with methanol (2 ml), water (2 ml) and dried *in vacuo* to give an insoluble colourless solid (43 mg, 93%); **IR** ν_{max} 1435, 1130, 1097, 998 w, 934 w, 860, 736, 714, 696, 599, 513, 465 cm^{-1}; Found C, 36.8; H, 3.95; N, 5.40; $C_{16}H_{20}N_2O_2P_2S_2Cd.0.5H_2O$ requires C, 37.0; H, 4.02; N, 5.39%

Ethylenediiminodimethylenebis(phenylthiophosphinate) copper(II) **Cu(48)**

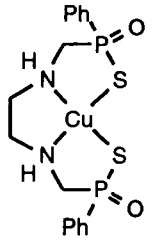

To a solution of $Cu(BF_4)_2$ (8 mg, 0.03 mmol) in methanol (3 ml) was added a solution of the dihydrobromide of (**48**) (16 mg, 0.03 mmol) in methanol (5 ml). The resultant dark green coloured solution was formed instantly and left to stand, however, crystallisation did not occur. $ESMS^-$ (MeOH) 541.77 ($CuLBr^-$) isotope model $C_{16}H_{20}N_2O_2P_2S_2CuBr$ 541.89; λ_{max} (H_2O), 598, ε=300 mol^{-1} dm^3 cm^{-1}, 332, ε=8.3 x 10^3 mol^{-1} dm^3 c m^{-1}; HPLC: C18 reversed phase (1.4 ml min-1), elution A=CH_3CN/TFA; B=H_2O/TFA from 80% B/20% A to 100% A over 25 minutes, observed λ=254 nm, R_t=11 minutes.

Propylenediiminodimethylene bis (Phenylthiophosphinate) copper(II) **Cu(64)**

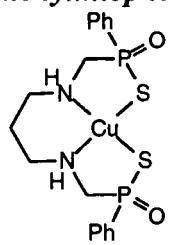

To a solution of $Cu(BF_4)_2$ (8 mg, 0.03 mmol) in methanol (3 ml) was added a solution of the dihydrobromide of (**64**) (17 mg, 0.03 mmol) in methanol (5 ml). The dark green colour of the solution was instantly visible; $ESMS^-$ (MeOH) 555.82 ($CuLBr^-$) isotope model $C_{17}H_{22}N_2O_2P_2S_2CuBr$ 555.91; λ_{max} (H_2O), 628, ε=350 mol^{-1} dm^3 cm^{-1}; HPLC: C18 reversed phase (1.4 ml min-1), elution A=CH_3CN/TFA; B=H_2O/TFA from 80% B/20% A to 100% A over 25 minutes, observed λ=254 nm, R_t=12.5 minutes.

Ethylenediiminodimethylene bis (Methylthiophosphinic Acid) Copper (II) **Cu(65)**

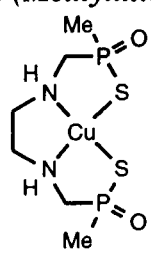

To a solution of $Cu(BF_4)_2$ (5 mg, 0.02 mmol) in water (2 ml) was added a solution of the dihydrobromide of (**65**) (10 mg, 0.02 mmol) in water (4 ml). The pale green colour of the solution was instantly visible; $ESMS^-$ (MeOH) 440.62 (CuLNaBr) isotope model $C_6H_{16}N_2O_2P_2S_2CuBrNa$ 440.85; λ_{max} (H_2O), 598, ε=150 mol^{-1} dm^3 cm^{-1}, 334, ε=10^4 mol^{-1} dm^3 cm^{-1}.

Oxotrichlorobis(triphenylphosphine)rhenium(V)[6] **(135)**

The oxorhenium complex was prepared according to the procedure of Wilkinson *et al.*[6] A boiling solution of triphenylphosphine (5g) in ethanol (5 ml) was added carefully to a boiled but cooling solution of perrhenic acid (1 ml, 8.6 mmol) and concentrated hydrochloric acid (1 ml) in ethanol (10 ml) and heated at reflux for 10 minutes. A yellow-green precipitate formed which was recrystallised from hot toluene (5.73 g, 80%); **IR** ν_{max} 1480, 1433, 1092, 1030, 969 (Re=O), 740, 690, 520, 500 cm^{-1}; Found: C, 51.8; H, 3.66; $C_{36}H_{30}Cl_3OP_2Re$ requires C, 51.9; H, 3.63%.

$[ReOCl_2(OCH_2CH_3)(PPh_3)_2]$ (136)

The above procedure (**135**), carried out in a hot but not boiling solution, gave rise to a dark green solid and was recrystallised in toluene to give brown crystals (5.6 g, 77%); **IR** ν_{max} 1480, 1433, 1094, 1074, 997, 947 (Re=O), 906 (OCH_2), 742, 690, 570, 506; Found: C, 54.2; H, 4.14; $C_{38}H_{35}Cl_2O_2P_2Re$ requires C, 54.2; H, 4.19%.

Conversion to $[ReOCl_3(PPh_3)_2]$ was achieved by the method described by Wilkinson *et al.*[6] The solid $[ReOCl_2(OCH_2CH_3)(PPh_3)_2]$ was stirred in dichloromethane and stirred vigorously with an equal volume of 6M hydrochloric acid for 1 h. A yellow-green powder precipitated from the mixture and was isolated by filtration and dried *in vacuo* (g, %); Found: C, 51.7; H, 3.58% characterisation of $[ReOCl_3(PPh_3)_2]$ as above.

Ethylenediiminodimethylenebis(phenylthiophosphinate) oxorhenium(V) **ReO(48)**

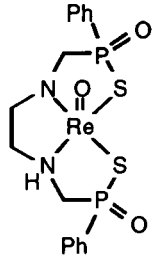

Oxotrichlorobis(triphenylphosphine)rhenium(V) (67 mg, 0.9 mmol) was suspended in hot benzene (20 ml) and stirred under an inert atmosphere and a methanol solution of (**48**) (50 mg, 0.9 mmol) was added to the reaction mixture which was then heated at reflux for 18 h. Upon cooling, the solvent was removed under reduced pressure and the remaining solid was washed with benzene (2 x 10 ml), then dichloromethane (5 ml) and dried in vacuo to give a deep pink coloured solid (43 mg, 80%); **^{31}P NMR** (CH_3OH) δ_P 100.7; **IR** ν_{max} 1110, 1030, 997, 927, 859, 800, 738, 713, 1120, 950, 910, 800, 775, 740 cm^{-1}; λ_{max} 526 (ε=240 $dm^3\ mol^{-1}\ cm^{-1}$); ESMS$^-$ (CH_3OH) 599.11 and 597.13 (55% and 100% respectively corresponding to Re isotopes, ReO(**48**) -H^+), no other species observed.

Chapter 3

Tetramethyldiphosphinedisulfide[7,8,9] **(77)**

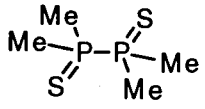

The title compound (**77**) was prepared according to the literature procedure.[7,8,9] A solution of methylmagnesium bromide (2M in diethyl ether, 120 ml, 240 mmol) was cooled to -15°C under an inert atmosphere. To this was slowly added a solution of thiophosphoryl chloride (13.5 g, 80 mmol) in diethyl ether (30 ml) maintaining a temperature of -20° to -10°C. The reaction mixture was stirred for 1 h, after which time the resultant white precipitate was poured *slowly* onto crushed ice (300 g). Sulfuric acid (10%, 90 ml) was added with stirring and the white precipitate was removed by filtration, washed with water and recrystallised from ethanol to give white needle-like crystals (4.16 g, 56%) **m.p.** 225-227°C (lit.[ref] 225-229°C); **^{31}P NMR** ($CDCl_3$) δ_P 35.5; **^{1}H NMR** (250.13 MHz, $CDCl_3$) δ_H 2.07 (dd, J_P=11.55 Hz, J_{P2}=5.8 Hz); **^{13}C NMR** (62.9 MHz, $CDCl_3$) δ_C 16.20 ; **IR** ν_{max} 1400, 1280, 935, 880, 860, 820, 730 b, 560 cm^{-1}; Found: C, 25.9; 6.29; $C_4H_{12}P_2S_2$ requires C, 25.8; H, 6.50.

Dimethylthiophosphinic Bromide[10,11] **(76)**

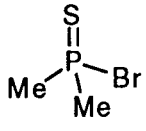

Tetramethyldiphosphine disulphide (**77**) (370 mg, 1.98 mmol) was suspended in dry carbon tetrachloride (7 ml) and a solution of bromine (316 mg, 1.98 mmol) in carbon tetrachloride (4 ml) was added dropwise maintaining the temperature around 0°C. Removal of the solvent at atmospheric pressure gave a residue which was purified by distillation under reduced pressure to yield a colourless liquid which solidified upon standing (0.5 g, 75%); **m.p.** 32-34°C (lit.[10] 34°C); **^{31}P NMR** ($CDCl_3$) δ_P 65.62; **^{1}H NMR** (250.13 MHz, $CDCl_3$) δ_H 2.59 (d, J_P=13.1 Hz); **^{13}C NMR** (62.9 MHz, $CDCl_3$) δ_C 33.12 (d, J_P=57.2 Hz).

Benzildihydrazone[12,13] **(81)**

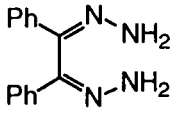

Preparation of the title compound was carried out according to the standard procedure[12,13] of Cope *et al.* To a solution of benzil (5 g, 24 mmol) stirred in *n*-butanol (15 ml) was added hydrazine hydrate (3.09 g, 3 ml, 62 mmol). The resulting solution was heated at reflux for 48 h. Upon cooling to 0°C, a precipitate formed which was isolated by filtration, washed with cold ethanol and dried at the pump to give fine needle-like white crystals (4.5 g, 79%), **m.p.** 138-139°C (lit.[12] 150-151.5°C); **^{1}H NMR** (250.13 MHz, $CDCl_3$) δ_H 5.74 (4H, b s, $N\underline{H}_2$), 7.25-7.32 (6H, m, *m-p*-Ph$\underline{H}$), 7.52-7.55

(4H, m, *o*-PhH); **^{13}C NMR** (62.9 MHz, $CDCl_3$) δ_C 51.9 (Ph-C), 126.18 (*m*-Ph), 129.48 (*o*-Ph), 135.22 (*p*-Ph), 142.86 (Ph); **m/z** (ESMS$^+$ CH_3OH) 499.13 (25%, M_2Na^+), 260.99 (100%, MNa^+), 238.99 (30%, MH^+); **IR** ν_{max} 3290 (Ar-H), 1580, 1560, 1490, 1410, 1380, 1290, 1125, 1070, 1035, 1010, 950, 910, 860, 770, 740, 690, 600 cm^{-1}; Found: C, 70.4; H, 5.94, N, 23.5; $C_{14}H_{14}N_4$ requires C, 70.6; H, 5.92; N, 23.5%

Butane-2,3-dihydrazone **(82)**

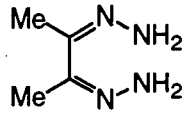

Preparation of the title compound was carried out using an analogous procedure to that for (**81**). Butane-2,3-dione (2.11 ml, 24 mmol) was treated with hydrazine hydrate (3.09 g, 3 ml, 62 mmol) in *n*-butanol (15 ml) to give white needle-like crystals (2.3 g, 84%), **m.p.** 153-154°C (lit.[14] 155-157°C); **^{1}H NMR** (250.13 MHz, $CDCl_3$) δ_H 1.96 (6H, s, CH_3), 5.31 (4H, b s, NH_2); **^{13}C NMR** (62.9 MHz, $CDCl_3$) δ_C 9.22 (s, CH_3), 149.21 (s, C=N); **m/z** (DCI) 115 (100%, MH^+), 87 (100%, $MH^+ - N_2$); **IR** (KBr) ν_{max} 1640, 1575, 1460, 1440, 1360, 1280, 1130, 1080, 940, 740, 450 cm^{-1}; Found: C, 42.1; H, 8.83, N, 49.1; $C_4H_{10}N_4$ requires C, 42.3; H, 8.98; N, 49.3%

Diphenyl-1,2-ethane-1,2-bis[(dimethylthiophosphoryl)hydrazide] **(84)**

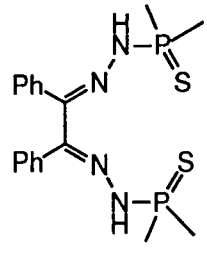

To a solution of dimethylthiophosphinic bromide (2.9 mmol) in carbon tetrachloride (10 ml) was added benzildihydrazone (**81**) (328 mg, 1.4 mmol) and triethylamine (0.42 ml, 3.03 mmol). The reaction mixture was stirred under an inert atmosphere for 15 h resulting in the formation of a white precipitate. The solid was removed by filtration and the solvent was evaporated from the mother liquor under reduced pressure to leave an orange oil. This was dissolved in ether and dark yellow crystals formed. If crystals did not from easily, the ether solution was, instead, washed with water (3 x 30 ml), dried (Na_2SO_4) and the solvent was removed under reduced pressure to give the pale orange solid product (4.0 g, 70%); **m.p.** 164-167°C; **^{31}P NMR** ($CDCl_3$) δ_P 66.71; **^{1}H NMR** (250.13 MHz, $CDCl_3$) δ_H 2.05 (12H, t-like dd, ^2J_P=12.1 Hz, P(S)(CH_3)$_2$), 6.15 (2H, d, ^2J_P=21.4 Hz, PNHN), 7.26-7.37 (6H, m, *m*-, *p*-PhH), 7.51-7.55 (4H, m, *o*-PhH); **^{13}C NMR** (62.9 MHz, $CDCl_3$) δ_C 22.71 (d, J_P=68 Hz, -P(S)(CH_3)$_2$), 23.20 (d, J_P=68 Hz, -P(S)(CH_3)$_2$), 126.52 (*m*-Ph), 129.74 (*o*-Ph), 130.88 (*p*-Ph), 133.53 (PPh), 143.00 (d, J= 14.5 Hz, Ph-C=N-NH-); **m/z** (ESMS$^+$ MeOH) 423.07 (100%, MH^+); **IR** ν_{max} 3290, 1440, 1380, 1290, 1125, 1060, 1035, 1010, 990, 950, 910, 860, 740 s, 670 s, 600

s cm^{-1}; Found: C, 51.3; H, 5.78; N, 13.0; $C_{18}H_{24}N_4P_2S_2$ requires C, 51.2; H, 5.73; N, 13.3;% λ_{max} (acetonitrile) 280, $\varepsilon = 3.1 \times 10^4$ mol^{-1} dm^3.
for crystal data, see Appendix B

Butane-2,3-bis[(dimethylthiophosphoryl)hydrazide] **(85)**

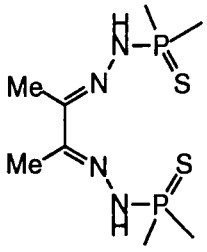

To a solution of dimethylthiophosphinic bromide (27.6 mmol) in carbon tetrachloride (10ml) was added butane-2,3-dihydrazone (**82**) (1.5 g, 13.2 mmol) and triethylamine (3 g, 30 mmol). The reaction mixture was stirred under an inert atmosphere for 15 h. A yellow precipitate formed which was isolated by filtration and washed thoroughly with water to remove the triethylamine salts. The pale yellow solid was dried *in vacuo* (3.5 g, 89%); **m.p.** > 250°C; **^{31}P NMR** ($CDCl_3$) δ_P 65.43; **^{1}H NMR** (250.13 MHz, $CDCl_3$) δ_H 1.92 (12H, d, J=13.5 Hz, $P(C\underline{H}_3)_2$) 1.98 (6H, s, $C\underline{H}_3C$), 5.99 (2H, d, J=21.3 Hz, PN<u>H</u>N); **^{13}C NMR** (62.9 MHz, $CDCl_3$) δ_C 9.93 (C-$\underline{C}H_3$), 22.64 (d, J=68.2 Hz, $P(S)\underline{C}H_3)_2$) 148.30 (s, CH_3-<u>C</u>=NNP); **m/z** (EI^+) 298 (20%, M^+), 205 (100%, M-$P(S)(CH_3)_2$); **IR** ν_{max} 3270 br (NH), 1580, 1410-1400, 1375, 1350, 1290, 1280, 1060 s, 940, 900, 850, 730, 630, 580 cm^{-1}; Found: C, 31.8; H, 6.67; N, 18.3; $C_8H_{18}N_4P_2S_2$ requires C, 32.2; H, 6.76; N,18.8%; λ_{max} 274, ε=3.1 x 10^4 mol^{-1} dm^3.
for crystal data, see Appendix B

2-(Dimethyl thiophosphoramino)-6-picoline **(86)**

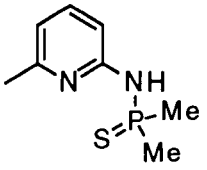

To a solution of dimethylphosphinic bromide (**76**) (5.46 mmol) in carbon tetrachloride (50 ml) was added 2-amino-6-picoline (1.78 g, 16.4 mmol) and the resultant solution stirred for 5 h at room temperature under an inert atmosphere. A white precipitate formed and was isolated by filtration then washed thoroughly with diethyl ether. White crystals formed in the ether layer and were isolated by filtration and dried *in vacuo* (0.9 g, 82%); **m.p.** 138-140°C; **^{31}P NMR** ($CDCl_3$) δ_P 59.96; **^{1}H NMR** (250.13 MHz, $CDCl_3$) δ_H 2.17 (6H, d, ^2J_P=14.17 Hz, $P(C\underline{H}_3)_2$), 2.41 (3H, s, py-$C\underline{H}_3$), 5.14 (1H, br s, N<u>H</u>), 6.41 (1H, d, ^{3}J=8.15 Hz, Py-H(3)), 6.68 (1H, d, ^{3}J=7.39 Hz, Py-H(4)), 7.41 (1H, t, ^{3}J=7.9 Hz); **^{13}C NMR** (62.9 MHz, $CDCl_3$) δ_C 23.53 (d, J_P=68.2 Hz, $P\underline{C}H_3$), 24.74 (s, $\underline{C}H_3$), 130.81, 131.31, 131.82, 162.17, 169.65, 192.72; **IR** ν_{max} 3280 (Ar-H), 1600 (Ar-H), 1570, 1450-1370, 1280 s, 950 s, 910-860, 780, 740 s, 700, 580, 530 cm^{-1}; **m/z**

(DCI) 201 (100%, MH^+), 185 (5%, $M\text{-}CH_3$); Found: C, 47.6; H, 6.50; N, 13.80; $C_8H_{13}N_2PS$ requires C, 48.0; H, 6.54; N, 13.99%; λ_{max} (acetonitrile) 232, ε=1.6 x 10^4 mol^{-1} dm^3; 286, ε= 6.3 x 10^3 mol^{-1} dm^3.

for crystal data, see Appendix B

2,6,-Bis(dimethylthiophosphoramino)pyridine **(89)**

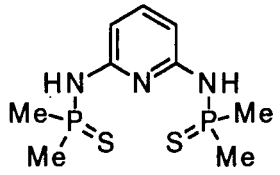

To a stirred solution of dimethylphosphinic bromide (**76**) (4.28 mmol) in carbon tetrachloride (15 ml) was added 2,6 diaminopyridine (110 mg, 1.02 mmol) and triethylamine (0.31 ml, 2.24 mmol) and the reaction mixture stirred for 16 h at room temperature under an inert atmosphere. A white precipitate formed which was isolated by filtration, washed with water and dried *in vacuo* (0.75 g, 60%); **m.p.** 199-203°C (decomp.); **^{31}P NMR** ($CDCl_3$) δ_P 56.99; **^{1}H NMR** (250.13 MHz, $CDCl_3$) δ_H 2.14 (12H, d, J=13.7 Hz, P-($C\underline{H}_3$)$_2$), 5.19 (2H, d, ^2J_P=5.5 Hz, N$\underline{H}$), 6.31 (2H, d, ^{3}J=8 Hz, Py-$\underline{H}$(3), $\underline{H}$(5)), 7.43 (1H, t, ^{3}J=8 Hz, Py-$\underline{H}$(4)); **^{13}C NMR** (62.9 MHz, $CDCl_3$) δ_C 24.06 (d, J_P=68 Hz, P($\underline{C}H_3$)$_2$), 104.42 (d, J =4.3 Hz, Py-$\underline{C}$(3) & $\underline{C}$(5)), 140.92 (Py-$\underline{C}$(4)), 153.9 (Py-$\underline{C}$(2) & $\underline{C}$(4)); **IR** ν_{max} 3150 (Ar-H), 1600 s, 1580 s, 1450 s, 1400, 1290, 1210, 1160, 1040, 950-930, 890, 790 s, 720 s, 650, 850; **m/z** (DCI) 294 (100%, MH^+), 202 (20%, M - P(S)Me_2 + $2H^+$); Found: C, 36.1; H, 5.81; N, 14.17; $C_9H_{17}N_3P_2S_2.0.5H_2O$ requires C, 35.8, H, 6.00; N, 13.90%; λ_{max} (acetonitrile) 244, ε=7.5 x 10^3 mol^{-1} dm^3, 300, ε=6 x 10^3 mol^{-1} dm^3.

Dimethylthiophosphorylhydrazine **(95)**

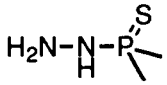

A solution of dimethylthiophosphinic bromide (**76**) (2.7 mmol) in carbon tetrachloride (20 ml) was added dropwise to hydrazine hydrate (200 mg, 4 mmol) under an inert atmosphere. The reaction mixture was stirred for 15 h and the solvents were removed under reduced pressure to give a colourless oil (325 mg, 97%); **^{31}P NMR** (101.26 MHz, $CDCl_3$) δ_P 68.74; **^{1}H NMR** (250.13 MHz, $CDCl_3$) δ_H 1.88 (6H, d, J_P=13.1 Hz, P$\underline{C}H_3$)$_2$), 3.5 (s, br, -N$\underline{H}_2$), 4.1 (1H, d, P-N$\underline{H}$); **^{13}C NMR** (62.9 MHz, $CDCl_3$) δ_C 33.12 (d, J_P=57.2 Hz, P$\underline{C}H_3$)$_2$); **m/z** (ESMS$^+$, MeOH) 124.85 (MH^+) **IR** ν_{max} 3330 b, 3180 b, 1610 b, 1420, 1290, 1050, 930, 860, 710, 550 cm^{-1}.

Tetrakis(acetonitrile)copper(I)tetrafluoroborate **(137)**

This preparation was carried out in a similar manner to Kubas's synthesis of $Cu[(CH_3CN)_4]$ $[PF_6]$.[15] To a stirred suspension of copper(I) oxide (9g, 63 mmol) in acetonitrile (200 ml) was added fluoroboric acid (20 ml of 40% solution) in roughly 2 ml portions over 15-20 min. After stirring for 1 h, some red solid still remained. The reaction mixture was heated gently for 10 mins to give a pale blue solution and was filtered to remove any traces of undissolved solid. The solution was kept at -20°C while large white crystals formed. The crystals were isolated by filtration and recrystallised from acetonitrile (120 ml) to give large colourless crystals (15.6 g, 79%); **m/z** ($ESMS^+$, 144.80 (100%, $Cu(CH_3CN)_2$), 103.82 (45%, $Cu(CH_3CN)$); Found: C, 30.5; H, 3.83; N, 17.5; $C_8H_{12}N_4CuBF_4$ requires C, 30.6, H, 3.85; N, 17.8%.

Butane-2,3-bis[(dimethylthiophosphoryl)hydrazide] Copper(I) Cu(I)(85)

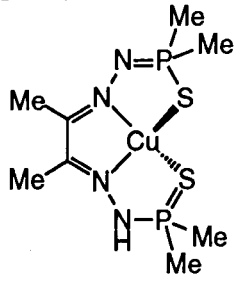

To a solution of [tetrakis(acetonitrile)copper(I)]tetrafluoroborate (295 mg, 0.94 mmol) in acetonitrile (35 ml) was added a solution of butane-2,3-bis[(dimethylthiophosphoryl)hydrazide] (**85**) (280 mg, 0.94 mmol) in dichloromethane (30 ml). After mixing the deep orange coloured solution, a precipitate formed which was isolated by centrifugation, washed with acetonitrile (2 x 10 ml) and dried *in vacuo* to give an orange solid (350 g, 85%); **^{31}P NMR** (101.26 MHz, CH_3CN) δ_P 66.74; **m/z** ($ESMS^+$, CH_3OH) 360.82 (CuL^+); Found: C, 26.5, H, 5.47; N, 15.1; $C_8H_{19}N_4P_2S_2Cu$ requires C, 26.6; H, 5.30; N, 15.5%; λ_{max} (acetonitrile), 274, ε=3.5 x 10^4 M^{-1} cm^{-1}, 430, dm^3, ε=2.0 x 10^3 M^{-1} cm^{-1}.

Butane-2,3-bis[(dimethylthiophosphoryl)hydrazide] Copper(II) Cu(II)(85)

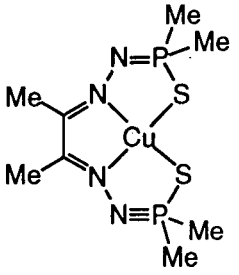

To a stirred solution of Cu(II)triflate (120 mg, 0.34 mmol) in dry acetonitrile (7 ml) was added solid butane-2,3-bis[(dimethylthiophosphoryl)hydrazide] (**85**) (100 mg, 0.34 mmol). The reaction mixture immediately turned deep green and was heated at 80°C for 4 h then left to cool. Diethyl ether (15 ml) was added and the solution left to stand at -5°C, however, crystallisation failed to occur. The solvents were removed under reduced pressure to give a green oil. Crystallisation was attempted using

tetrahydrofuran but no solid was formed although visible spectroscopy and mass spectral analysis confirmed the formation of the complex; **m/z** (ESMS$^+$, CH_3OH) 360.29 (100%, M^+), 363.02 (50%) corresponding to Cu isotopes; λ_{max} (acetonitrile) 206, ε=1.96 x 10^4 mol^{-1} dm^3, 302, ε=1.25 x 10^4 mol^{-1} dm^3, 392, ε=4.7 x 10^3 mol^{-1} dm^3, 636, ε=210 mol^{-1} dm^3.

***Diphenyl-1,2-ethane-1,2-bis[(dimethylthiophosphoryl)hydrazide] copper(I) Cu(I)* (84)**

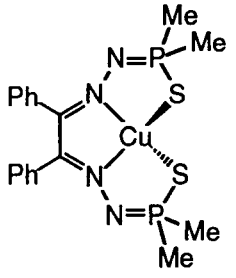

To a solution of [tetrakis(acetonitrile)copper(I)]tetrafluoroborate (37 mg, 0.12 mmol) in acetonitrile (5 ml) was added a solution of (**84**) (50 mg, 0.12 mmol) in acetonitrile (5 ml). After mixing, the yellow coloured solution was cooled to -5°C but crystallisation failed to occur, even following the dropwise addition of diethyl ether. Visible spectroscopy and mass spectral analysis confirmed the formation of the complex; ESMS$^+$ (MeOH) 485.02 $C_{18}H_{23}N_4P_2S_2Cu$ .H^+ (CuL 485.02 with Cu isotope pattern by modelling) λ_{max} (acetonitrile), 280, ε=7.8 x 10^4 M^{-1} cm^{-1}.

Chapter 4

N-*Tosyl-2-bromoaniline* (138)

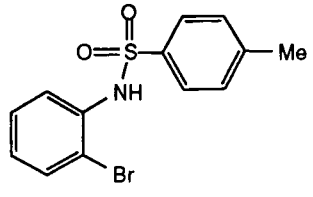

Tosyl chloride (8.0 g, 46.5 mmol) was added to a stirred solution of 2-bromoaniline (8.87 g, 46.5 mmol) in pyridine (100 ml). The yellow solution was stirred for 20 h at room temperature and poured over crushed ice to precipitate the solid product which was isolated by filtration then dried. Recrystallisation from diethyl ether/light petroleum gave pale orange crystals (14.2 g, 93%); **m.p.** 90-93°C; **^{1}H NMR** (250.13 MHz, $CDCl_3$) δ_H 2.29 (3H, s, Ts-CH_3), 6.91 (1H, t, J=7.7 Hz, Ar<u>H</u>), 6.94 (1H, s, NH), 7.13 (2H, d, J=8.3 Hz, TsH), 7.19 (1H, t, J=7 Hz, Ar<u>H</u>), 7.32 (1H, d, J=7.8 Hz, Ar<u>H</u>), 7.57 (2H, d, J=8.3 Hz, TsH), 7.59 (1H, d, J=7.5 Hz, Ar<u>H</u>); **^{13}C NMR** (62.9 MHz, $CDCl_3$) δ_C 22.27 (Ts<u>C</u>H_3), 116.37 (Ar), 123.22 (Ar), 126.94 (Ar), 128.01 (*m*-Ts), 129.25 (Ar), 130.34 (*o*-Ts), 133.25 (Ar), 135.37 (NTs), 136.49 (Ar), 144.93 (STs); **m/z** (DCI) 345 (100%, M + NH_3); (ESMS $^+$, CH_3OH) 327.84 (100%, MH^+); **IR** ν_{max} 3300

br, 2360-2340, 1600 s, 1480, 1400, 1330 s (-$S(O)_2$-N), 1180-1160 s (-$S(O)_2$-N) 1090, 910, 820, 760, 650, 620, 530, 500-440 cm^{-1}; Found: C, 48.4; H, 3.79; N, 4.20 %; $C_{13}H_{12}NOS_2$ requires C, 47.9; H, 3.71; N, 4.29%.

N,N'-*Bis*-p-*toluenesulfonyl*-N,N'-bis(o-*phenylenebromide)-1,2-diaminoethane* (109)

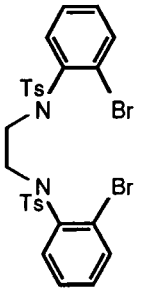

A solution of 1,2-bis(*p*-toluenesulfonato)ethane (0.73 g, 2.0 mmol) in DMF (12 ml) was added dropwise over a period of 1 h to a stirred mixture of *N*-tosyl-2-bromoaniline (1.3 g, 4 mmol) and Cs_2CO_3 (1.37 g, 4.2 mmol) in DMF (12 ml) under an inert atmosphere. The reaction mixture was stirred for 18 h with heating at reflux. The volume of solvent was reduced prior to the addition of water (30 ml) and extraction into CH_2Cl_2 (3 x 30 ml). The combined organic extracts were dried (Na_2SO_4) and the solvent removed under reduced pressure to leave a yellow oil. Crystallisation from ethyl acetate/light petroleum afforded a white solid (0.88 g, 65%); **m.p.** 173-176°C; **^{1}H NMR** (250.13 MHz, CDCl3) δ_H 2.43 (6H, s, $TsC\underline{H}_3$), 3.75 (4H, m, $NC\underline{H}_2C\underline{H}_2N$), 7.07-7.26 (10H, m, Ar), 7.49-7.63 (6H, br m, Ar); **^{13}C NMR** (62.9 MHz, $CDCl_3$) δ_C 22.23 ($TsC\underline{C}H_3$), 50.67 ($NC\underline{C}H_2C\underline{C}H_2N$), 126.08 (Ar$\underline{C}$Br), 128.49 (*m*-Ts), 128.89 (ArBr), 130.22 (*o*-Ts), 130.67 (ArBr), 132.56 (ArBr), 134.67 (ArBr), 136.40 (NTs), 138.90 (ArBr), 144.51 (STs); **m/z** DCI 695 (15%, M + NH_3), 678 (10%, M^+), 524 (25%, M-Ts + H^+); **IR** ν_{max} 1600, 1470, 1340, 1150, 1090, 1040, 930, 810, 770, 760, 710, 660, 570, 550 cm^{-1}: Found C, 49.3; H, 3.80; N, 4.04; $C_{28}H_{26}Br_2N_2O_4S_2$ requires C, 49.6; H, 3.86; N, 4.13%.

***P-Methyl*-o-*nitrophenylphosphinate*[16] (111)**

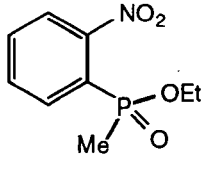

Dinitrobenzene (713 mg, 4.24 mmol) and methyldiethoxyphosphine (7.63 mmol, 20 ml of a 0.38 M solution in ether) were stirred in dry acetonitrile for 24 h. The solvent was removed under reduced pressure and vacuum distillation gave an orange oil (810 mg, 83%); **^{31}P NMR** ($CDCl_3$) δ_P 38.87; **^{1}H NMR** (250.13 MHz, $CDCl_3$) δ_H 1.23 (3H, t, ^{3}J=7 Hz, $POCH_2C\underline{H}_3$), 1.90 (3H, d, ^{2}J=15 Hz, $PC\underline{H}_3$), 3.83 (1H, m, $POC\underline{H}_2CH_3$), 4.05 (1H, m, $POC\underline{H}_2CH_3$), 7.69 (2H, m, ArH), 7.85 (2H, m, ArH); **^{13}C NMR** (62.9 MHz, $CDCl_3$) δ_C 16.76 (s, $POCH_2\underline{C}H_3$), 17.61 (d, J_P=108 Hz, $P\underline{C}H_3$), 62.03 (d, ^3J_P= 5 Hz, $PO\underline{C}H_2CH_3$), 124.82 (d, J=5.5 Hz Ar), 127.36 (d, ^1J_P=119 Hz, Ar), 133.33 (d, J=11 Hz, Ar), 133.76 (s, Ar), 135.83 (d, J=5.5 Hz), 152.48 (s, Ar-NO_2); **m/z** (DCI) 230 (100%,

MH^+); **IR** ν_{max} 1532 s (NO_2), 1360 (NO_2), 1300 (P-O), 1210, 1130, 1023 s, 950, 900-850, 780, 730 s, 490 cm^{-1}.

P-Methyl-o-aminophenylphosphinate[17] **(112)**

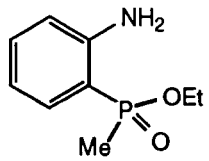

P-Methyl-o-nitrophenylphosphinate (**111**) (700 mg, 3.06 mmol) was added to a stirred mixture of iron powder (570 mg, 10.3 mmol) and ammonium chloride (150 mg, 2.8 mmol) in water (15 ml) and heated under reflux for 16 h. The black powder was removed by filtration and the aqueous solution was made basic by addition of sodium hydroxide solution (10%) to pH 10.5. This was extracted with ethyl acetate (3 x 30 ml), dried (K_2CO_3) and the solvent was removed under reduced pressure to give a yellow oil which solidified upon cooling (500 mg, 82%); **m.p.** 59-62°C (lit. m.p. not reported); **^{31}P NMR** ($CDCl_3$) δ_P 47.63; **^{1}H NMR** (250.13 MHz, $CDCl_3$) δ_H 1.31 (3H, t, ^3J=7 Hz, $POCH_2\underline{C}H_3$), 1.66 (3H, d, ^2J=15 Hz, $PC\underline{H}_3$), 3.91 (1H, m, $POC\underline{H}_2CH_3$), 4.06 (1H, m, $POC\underline{H}_2CH_3$), 5.32 (2H, s, $N\underline{H}_2$), 6.61-6.73 (2H, m, ArH), 7.22-7.35 (2H, m, ArH); **^{13}C NMR** (62.9 MHz, $CDCl_3$) δ_C 16.89 (d, J_P=104 Hz, $P\underline{C}H_3$), 17.06 (s, $POCH_2\underline{C}H_3$), 61.18 (d, ^3J_P= 6 Hz, $PO\underline{C}H_2CH_3$), 117.21 (d, J=10 Hz Ar), 117.66 (d, J=12 Hz, Ar), 132.80, 132.96, 134.27, 152.34; **m/z** (DCI) 200 (100%, MH^+); **IR** ν_{max} 3410 s, 3300 s, 2990-2900, 1620 s, 1600, 1480, 1550, 1330, 1300, 1170-1120, 1020 s, 950 s, 890-880, 780-730 cm^{-1}; $C_9H_{14}NO_2P.H^+$ requires 200.0840; found 200.0840 .

N,N'-bis[phenyl(2-ethoxymethylphosphinyl)] oxamide **(113)**

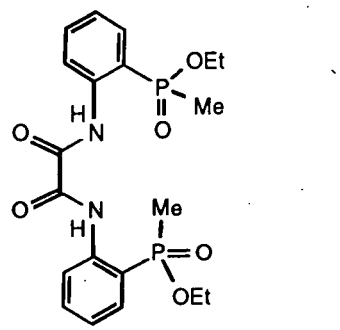

Oxalyl chloride (50 µl, 0.58 mmol) was added to a stirred solution of P-Methyl-*o*-aminophenylethylphosphinate (**112**) (260 mg, 1.2 mmol) and triethylamine (0.2 ml, 1.4 mmol) in dichloromethane (6 ml) under an inert atmosphere. After 2 h the reaction mixture was washed with HCl (0.5 M, 2 x 10 ml) and water (10 ml) and dried over (K_2CO_3). The solvent was evaporated under reduced pressure to give a pale yellow solid which was recrystallised from ethyl acetate/diethyl ether to give a white solid (220 mg, 84%); **m.p.** 167-170°C (decomp.); **^{31}P NMR** ($CDCl_3$) δ_P 46.30; **^{1}H NMR** (250.13

MHz, $CDCl_3$) δ_H 1.32 (6H, t, ^3J=7 Hz, $POCH_2\underline{CH_3}$), 1.74 (6H, d, ^2J=15 Hz, $PC\underline{H_3}$), 4.01 (2H, dm, $POC\underline{H_2}CH_3$), 7.21 (2H, m, ArH), 7.54 (2H, q, ArH), 8.88 (2H, dd, ArH), 10.99 (2H, s, br, N<u>H</u>); **^{13}C NMR** (62.9 MHz, $CDCl_3$) δ_C 15.82 (s, $POCH_2\underline{C}H_3$), 17.13 (d, J_P=79 or 85 Hz, $P\underline{C}H_3$), 61.18 (d, ^3J_P=6 Hz, $PO\underline{C}H_2CH_3$), 118.05 (d, J_P=120 Hz, P-Ar), 121.09 (d, J_P=8.7 Hz, Ar), 124.11 (d, J_P=12 Hz, Ar), 131.84 (d, J_P=8.8 Hz, Ar), 133.74 (d, J=2.3 Hz, Ar), 141.68 (d, J_P=5 Hz, N-Ar), 158.41 (s, C=O); **m/z** (ESMS $^-$, CH_3OH) 450.91 (100%, M-H$^+$); **IR** ν_{max} 3200-2900 br (NH), 1690 s (C=O), 1600, 1580 s, 1510 s, 1460-20, 1300 s, 1190-1130, 1080 w, 1040-1020, 950 s, 880-860, 800, 750, 720, 670 cm^{-1}; Found C, 52.8; H, 5.81; N, 6.13; $C_{20}H_{26}N_2O_6P_2$ requires C, 53.1; H, 5.79; N, 6.19%; $C_{20}H_{26}N_2O_6P_2$ .H$^+$ requires 453.1344; found 453.1344

N,N'-bis[phenyl(2-methylphosphinoxy)] oxamide **(115)**

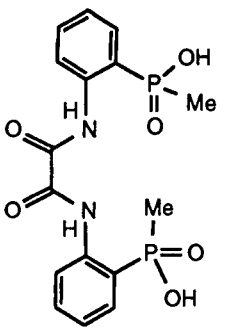

The diester (**113**) (150 mg, 99 mmol) was stirred in a solution of lithium hydroxide (0.5M, 10 ml) for 24 h at room temperature. The solvent was removed under reduced pressure to give a white solid in quantitative yield; **m.p.** >250°C; **^{31}P NMR** (D_2O) δ_P 32.18; **^{1}H NMR** (250.13 MHz, D_2O) δ_H 1.16 (6H, d, ^2J=14 Hz, $PC\underline{H_3}$), 6.62 (4H, m, ArH), 7.09 (2H, t, J=8 Hz, ArH), 7.30 (2H, dd, J=8 Hz, J=13 Hz, ArH); **^{13}C NMR** (50 MHz, D_2O) δ_C 21.27 (d, J_P=97 Hz, $P\underline{C}H_3$), 121.46 (d, J=8.8 Hz, *m*-Ar), 122.85 (d, J_P=11.3 Hz, *m*-Ar), 125.44 (d, J_P=123 Hz, PAr), 136.43 (d, J_P=8.3 Hz, *o*-Ar), 136.62 (d, J=2 Hz, *p*-Ar), 152.53 (d, J=6.5 Hz, NAr), 176.39 (s, C=O); **IR** ν_{max} 3670, 2710, 1660 s (C=O), 1600, 1470-1440, 1320, 1300, 1135, 1090, 1030 br, 890, 750 cm^{-1}.

N,N'-bis[phenyl(2-ethoxymethylphosphinyl)] malonamide **(114)**

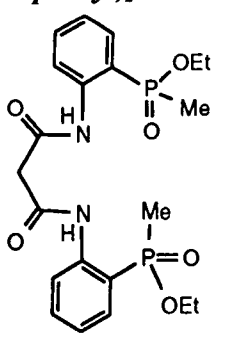

Malonyl dichloride (61 mg, 42 µl, 0.43 mmol) was added to a stirred solution of P-methyl-*o*-aminophenylethylphosphinate (**112**) (180 mg, 0.91 mmol) and triethylamine (0.2 ml) in dichloromethane (5 ml) under an inert atmosphere. After 2 h the reaction

mixture was washed with hydrochloric acid (0.5 M, 2 x 10 ml) and water (10 ml) and dried over (K_2CO_3). The solvent was evaporated under reduced pressure to give a dark yellow oil which was recrystallised from CH_2Cl_2/ light petroleum to give a pale orange oil (150 mg, 75%) with slight impurities observed by NMR analysis; **^{31}P NMR** ($CDCl_3$) δ_P 47.60; **^{1}H NMR** (250.13 MHz, $CDCl_3$) δ_H (6H, t, ^{3}J= Hz, $POCH_2\underline{C}H_3$), (6H, d, ^{2}J=15 Hz, $PC\underline{H}_3$), (2H, dm, $POC\underline{H}_2CH_3$), (2H, m, ArH), (2H, q, ArH), (2H, dd, ArH), (2H, s, br, N$\underline{H}$); **^{13}C NMR** (100 MHz, $CDCl_3$) δ_C 16.19 (d, J_P=13.6 Hz, $POCH_2\underline{C}H_3$), 16.57 (d, ^2J_P=210 Hz, $P\underline{C}H_3$), 47.86 (s, $C(O)\underline{C}H_2$), 61.16 (d, ^3J_P=12.6 Hz, $PO\underline{C}H_2CH_3$), 116.8 (d, J_P=238 Hz, Ar$\underline{C}$(2)P), 121.26 (d, J_P=17.3 Hz, Ar$\underline{C}$3), 123.35 (d, J_P=24.5 Hz, ArAr$\underline{C}$4), 131.41 (d, J_P=18 Hz, Ar$\underline{C}$5), 133.65 (d, J=4 Hz, Ar$\underline{C}$6), 142.71 (d, J_P=11.6 Hz, N-$\underline{C}$Ar), 164.92 (s, C=O); **m/z** (ESMS $^-$) 466 (100%, M-H$^+$), **IR** ν_{max} 3460, 3250, 2980, 1685 (C=O), 1610, 1580, 1520, 1440, 1290, 1180, 1020, 950, 880, 790, 760, 490 cm^{-1}.

N-*Tosyl*-P-*methyl*-o-*aminophenylphosphinate* (116)

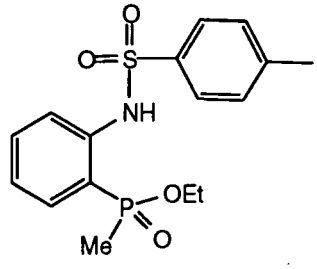

The amine (**112**) (0.91 g, 4.56 mmol) was stirred in pyridine (20 ml) and tosyl chloride (1.83 g, 9.6 mmol) was added. The solution was strried at room temperature for 18 h then poured over crushed ice. The aqueous mixture was extracted with CH_2Cl_2 (3 x 40 ml) and the combined organic extracts were washed with Na_2CO_3 (10%, 40 ml) and water (3 x 30 ml), and dried over Na_2SO_4. The solvent was removed under reduced pressure to give a pale orange oil (1.01 g, 63%); **^{31}P NMR** ($CDCl_3$) δ_P 48.21; **^{1}H NMR** (250.13 MHz, $CDCl_3$) δ_H 1.27 (3H, t, ^{3}J=7.1 Hz, $POCH_2\underline{C}H_3$), 1.51 (3H, d, ^{2}J=15.1 Hz, $PC\underline{H}_3$), 2.43 (3H, s, $TsC\underline{H}_3$), 3.60 (1H, m, $POC\underline{H}_2CH_3$), 3.93 (1H, m, $POC\underline{H}_2CH_3$), (2H, m, ArH), 7.29 (2H, d, J=8.2 Hz, Ts$\underline{H}$), 7.82 (2H, d, J=8.2 Hz, Ts$\underline{H}$), (2H, m, ArH), 10.94 (1H, s, N$\underline{H}$); **^{13}C NMR** (62.9 MHz, $CDCl_3$) δ_C 16.46 (d, J=4.8 Hz, $POCH_2\underline{C}H_3$), 16.69 (d, J_P=106 Hz, $P\underline{C}H_3$), 21.75 (s, $TsCH_3$), 61.38 (d, ^3J_P=5.7 Hz, $PO\underline{C}H_2CH_3$), 117.53 (d, J=119.6 Hz, Ar), 120.92 (d, J=8.6 Hz, Ar), 124.37 (d, J=11.9 Hz, Ar), 127.77 (s, Ts), 129.85 (s, Ts), 132.34 (d, J=9.1 Hz, Ar), 134.24 (s, Ts), 136.77 (s, Ar), 142.82 (d, J=4.3 Hz, Ar), 144.17 (s, Ts); **m/z** (ESMS$^+$, CH_3OH) 353.96 (100%, MH$^+$); **IR** ν_{max} 3000, 1600, 1580, 1500, 1350, 1160, 1100, 1040, 970-900, 820-710, 660, 560, 490 cm^{-1}.

***Diethyl-1,10-phenanthroline-2,9-bis[methylene(methylphosphinate)]*^{3} (117)**

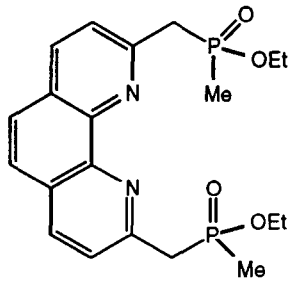

The title compound was prepared using a modified literature procedure.[3] Diethylmethylphosphonite (5.0 g, 36 mmol) and one drop of triethylamine were added to a suspension of 2,9-dibromo-1,10-phenanthroline (4.5 g, 12 mmol) in dry acetonitrile (120 ml). The mixture was stirred for 2 h at room temperature, resulting in a dark brown solution which was heated at 80°C for 18 h to give a golden coloured solution. The solvent was removed under reduced pressure and the residue was purified by chromatography on alumina with gradient elution (dichloromethane to 1.5% methanol) to give a crystalline solid (3.5 g, 70%); **^{31}P NMR** ($CDCl_3$) δ_P 51.24; **^{1}H NMR** (250.13 MHz, $CDCl_3$) δ_H 1.28 (6H, t, ^3J=7 Hz, $POCH_2C\underline{H}_3$), 1.61 (6H, d, ^2J=14 Hz, $PC\underline{H}_3$), 3.76 (4H, d, ^2J=18 Hz, $PC\underline{H}_2N$), 4.10 (4H, qnt, J=7 Hz, $POC\underline{H}_2CH_3$), 7.65 (2H, dd, ^4J_P=1.64, ^3J_H=8.3 Hz, ArH(3), H(8)), 7.76 (2H, s, ArH(5), H(6)), 8.20 (2H, d, J=8.4 Hz, ArH(4), H(7)); **^{13}C NMR** (62.9 MHz, $CDCl_3$) δ_C 14.51 (d, J_P=96 Hz, $P\underline{C}H_3$), 17.27 (s, $POCH_2\underline{C}H_3$), 42.03 (d, ^1J_P=84 Hz, $Ar\underline{C}H_2P$), 61.25 (d, J=6 Hz, $PO\underline{C}H_2CH_3$), 124.88 (Ar-C3), 126.74 (Ar-C5), 128.08 (Ar-C4a), 137.52 (Ar-C4), 146.08 (Ar-C10b), 154.40 (d, ^2J_P= 6, Ar-C2); **m/z** (DCI) 421 (100%, MH^+); **IR** ν_{max} 3758, 3436 br, 2986, 2928, 2864, 2366, 2340 s, 1565, 1504, 1370, 1302, 1206, 1040, 964, 864, 670 cm^{-1}.

1,10-Phenanthroline-2,9-diylmethylenebis(methylphosphinic acid) **(121)**

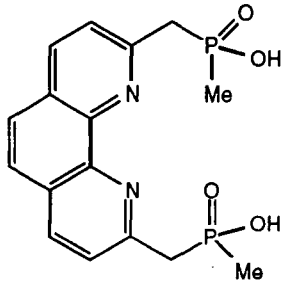

The diester (**117**) (1.0 g, 2.4 mmol) was heated under reflux in HCl (6M) for 20 h as described previously.[3] The solvent was removed under reduced pressure to give a yellow glassy solid in quantitative yield (0.96 g); **^{31}P NMR** (D_2O) δ_P 46.37; **^{1}H NMR** (250.13 MHz, D_2O) δ_H 1.47 (6H, d, ^2J=14 Hz, $PC\underline{H}_3$), 3.71 (4H, d, ^2J=17 Hz, $PC\underline{H}_2N$), 7.43 (2H, s, ArH(3), H(8)), 7.66 (2H, d, J=8 Hz, ArH(5), H(6)), 8.26 (2H, d, J=8.5 Hz, ArH(4), H(7)); **^{13}C NMR** (62.9 MHz, D_2O) δ_C 17.44 (d, J_P=95 Hz, $P\underline{C}H_3$), 41.75 (d, ^1J_P=75.4 Hz, $Ar\underline{C}H_2P$), 125.1 (Ar-C3), 129.34 (Ar-C5), 130.69 (Ar-C4a), 139.33 (Ar-C4), 144.66 (Ar-C10b), 156.20 (d, ^2J_P= 8 Hz, Ar-C2).

6.3 Radiolabelling

Technetium Radiolabelling procedures

General

Pertechnetate-99m was eluted from an Amertec generator using saline solution. activities were measured on a Capintec CRC-15R ion chamber. HPLC analysis was carried out using Gilson Gradient HPLC with a Gilson UV detector and a gamma detector with a C18 reversed phase column with gradient elution of 100% water (0.1% TFA) to 100% acetonitrile (0.1% TFA) at a flow rate of 1ml min^{-1}. Gilson 715 software was used to analyse the HPLC chromatograms. TLC was carried out using three different systems simultaneously: (1) silica gel paper in MEK (methylethylketone) (2) silica gel paper in saline (3) Watman no.1 paper in 50:50 acetonitrile:water, and the results scanned on a Packard InstantImager.

^{99m}Tc Complex preparation

A solution of ligand (**48**) (100 µl of 5 mg ml-1) in methanol was placed in a sealed sample vial together with NaOH solution (20 µl, 1M), saline (1 ml) and ^{99m}pertechnetate (1 ml, 0.4 GBq ml^{-1}). To this was added a solution of stannous chloride in saline (10 µg, 0.1 ml). The preparation was pH6 and 0.345 GBq and was left to stand for 30 min prior to TLC analysis and HPLC injection.

The above procedure was carried out using NaOH (0.1 M) raising the pH of the preparation to 8.

Preparations of ligands (**64**)-(**66**) with technetium-99m were carried out in an analogous manner to that described above, at pH 8.

Copper Radiolabelling procedures

General

HPLC analysis was carried out using a Thermo Separation Products Spectral System P2000 equipt with a 50µl injection loop, a Bioscan gamma-detector and a Spectrasystem UV2000 UV detector.

Production of ^{64}Cu[18]

No carrier added (NCA) ^{64}Cu was produced by the ^{64}Ni(d, 2n)^{64}Cu reaction on 96% enriched ^{64}Ni. Approximately 50 mg enriched ^{64}Ni metal powder was pressed into a 10 mm diameter disc. Once assembled inside an aluminium target holder, the nickel pellet was irradiated with a beam of deuterons (16.5 MeV) from the MC-40 Cyclotron at the

Hammersmith Hospital. After bombardment the target was allowed to cool for several hours prior to chemical processing. The target was dissolved in a small volume of hydrochloric acid (7M) and a few drops of aqueous hydrogen peroxide with heating. The solution was concentrated at 60°C, redissolved in hydrochloric acid (7M) and loaded onto an anion exchange column (AG-1 x 8 resin, 100-200 mesh) of 3 cm x 1.1 cm diameter, preconditioned with HCl solution (7M). Elution of the column with hydrochloric acid (7M) removed the nickel(II) and trace amounts of cobalt(III) isotopes was followed by elution with water to elute the 64-copper(II) which was concentrated under reduced pressure and taken up into fresh water (2.5 ml). The initial concentration of the stock solution of copper-64 was 450 MBq ml^{-1} decaying to 9.6 MBq ml^{-1} due to the decay ($T_{1/2}$=12.7 h) of the radionuclide.

Preparation of ^{64}Cu-ligand complexes

Initial preparations of copper-64 radiolabelled complex were undertaken using ligand (**48**) (0.7 mg) dissolved in pure water (20 µl) and NaOH (1M, 20 µl). This was added to a solution of $^{64}CuCl_2$ (20 µl, from the stock prepared above) and sodium acetate (3M, 20 µl) (pH of the $^{64}CuCl_2$ solution pH 5.5) and mixed thoroughly with a vortex mixer. For HPLC-analysed preparations, typically, a solution of ligand (**48**) in methanol (20 µl of a 5-10 mg ml^{-1}) was mixed thoroughly by vortex mixing with a solution of the stock solution of activity (20-60 µl) (depending upon the radioactive concentration of the sample as it decayed). The pure radiolabelled species was collected as it eluted from the HPLC system. Slight variations in the amount of activity (MBq) and the quantity of ligand used for each radiotracer preparation were found to have no effect upon complex formation. The control for HPLC analysis was the analysis of the $^{64}CuCl_2$ stock solution (20 µl in 40 µl water).

Radiolabelling of ligands (**64**)-(**66**) was carried out in a similar manner described above, using water to dissolve ligands (**65**) and (**66**), and methanol for ligand (**64**).
The dimethylthiophosphoryldihydrazide ligand (**84**) (15 mg ml^{-1} in acetonitrile) showed no evidence of radiolabelling with 60 µl of the stock solution of aqueous $^{64}CuCl_2$. Successful radiolabelling was achieved when the ligand solution (60 µl, 15 mg ml^{-1} in acetonitrile) was treated with 20 µl triethylamine and mixed for 0.5 minutes with a vortex mixer prior to the addition of 60 µl of the aqueous $^{64}CuCl_2$ solution. This was mixed with a vortex mixer and analysed immediately by HPLC.

A solution of ligand (**85**) (5 mg ml^{-1} in acetonitrile) was attempted under the conditions described for (**84**), but showed no radiolabellling.

Lipophilicity measurements

Typically, a 10 μl solution of each radiolabelled complex was added to a microcentrifuge tube containing 0.5 ml water and 0.5 ml octanol. A vortex mixer was used to mix the contents of the tube thoroughly for 2 minutes and centrifugation for 5 minutes (1000 rpm) ensured complete separation of the two layers. A portion of 200 μl from each layer was carefully removed and its radioactivity was counted using an LKB Wallac automatic gamma-counter. Each radiotracer was partitioned in duplicate. Samples were taken from the reaction mixture directly or from the HPLC-purified complex which had been evaporated to near dryness and taken up into fresh solvent (usually water).

Plasma-Protein Binding Studies

Whole human blood was centrifuged for 5 minutes (4000 rpm) to separate the plasma and the blood elements. A sample of the radiolabelled complex (typically 50 μl and 0.5-2 MBq) was added to a sample of 0.5 ml serum, 'vortexed' for 2 minutes and incubated at 37°C for 1 h. The sample was loaded onto a PD10 column (Sephadex G25, Pharmacia UK) pre-equilibrated with 5 ml phosphate buffered saline (PBS) (pH 7.4, physiological saline) and preconditioned with 0.5 ml human serum albumin (2 mg ml^{-1}) followed by more PBS. The column was eluted with the same PBS solution and around fifteen fractions of 0.5 ml were collected and γ-counted.

Partitioning of ^{64}Cu-Complexes Between Plasma and Red Blood Cells

Typically, ^{64}Cu(**48**) (ca. 0.5 MBq) (200 μl) was added to human blood (2 ml) in a microcentrifuge tube. The contents of the tube were mixed thoroughly by a vortex mixer and aliquots of 250 μl were incubated at 37°C. Samples were removed after 10, 15, 30 and 60 minutes in duplicate and were centrifuged for 5 minutes (1000 rpm) to separate the blood samples into two layers of plasma and red blood cells. The plasma was withdrawn and placed in a counting tube and PBS (pH 7.4) was used to transfer the thick blood elements into a separate counting tube.

6.4 References

1. L. Collie, J.E. Denness, D. Parker, F. O'Carroll and C. Tachon, *J. Chem. Soc., Perkin Trans. 2*, 1993, 1747; using a routine in 'Kaleidagraph'
2. D.E.C. Corbridge, '*Phosphorus: An Outline of its Chemistry, Biochemistry and Technology*', 4th Ed., Elsevier,1990, p329
3. G.B. Bates, E. Cole, D. Parker and R. Kataky, *J. Chem. Soc., Dalton Trans*, 1996, 2693
4. S.H. Pine and B.L. Sanchez, *J. Org. Chem.*, 1971, **36**, 829

5. B.L. Sondengam; J.H. Hemo and G. Charles, *Tetrahedron Lett.*; 1973; **3**, 261
6. N.P. Johnson, C.J.L. Lock and G. Wilkinson, *J. Chem. Soc.*, 1964, 1054
7. G.W. Parshall,*Org. Synth.*, 1965, **45**, 102
8. K.A. Pollart, H.J. Harwood, *J.Org.Chem.*, 1962, **27**, 4444
9. H. Reinhardt, D. Bianchi, D. Molle, *Chem. Ber.*, 1957, 1656
10. R. Schmultzler, *Inorg. Synth.*, 1970, **12**, 287
11. W. Kuchen and H. Buchwald, *Agnew. Chem*, 1959, **4**, 162
12. A.C Cope, D.S. Smith, R.J. Cotter, *Org.Synthesis Coll. Vol. 4*, 1963, p377 *et seq.*
13. J. Tsuji, H. Kezuka, Y. Toshida, H. Takayangi and K. Yakamoto, *Tetrahedron*, 1983, **39**, 3279
14 · S. Wolfe *et al*, *Can. J. Chem.*, 1971, **49**, 1099
15. G.J. Kubas, *Inorg. Synth.*, 1979, **19**, 90; *ibid*, 1990, **28**, 68
16. J.I.G. Cadogan, D.J. Sears and D.M. Smith, *J. Chem. Soc. (C)*; 1969, 1314
17. E.P. Kyba and C.N. Clubb, *Inorg. Chem.*, 1984, **23**, 4766
18. J. Zweit, A.M. Smith, S. Downey and H.L. and H.L. Sharma, *Appl. Radiat. Isot.*, 1991, **42**, 193

Appendices

Appendix A Experimental for X-ray crystal structures (43), (84), (85) and (86)

Experimental

X-Ray diffraction experiments were carried out on a Siemens SMART 3-circle diffractometer with a CCD area detector, using graphite-monochromated Mo-K_α radiation (λ=0.71073 Å) and a Cryostream open-flow cryostat. Data were collected by scanning over a full hemisphere of reciprocal space in frames of 0.3° ω and corrected for absorption by a semi-empirical method based on Laue equivalents of strong reflections. The data for (**43**) was corrected for absorption errors using SADABS.[1] Structures (**84**), (**85**) and (**86**) were solved by direct methods and refined by full martix least squares against F^2 of all data, using SHELXTL software.[2] All non-H atoms were refined with anisotropic displacement parameters, all H atoms were located from difference Fourier map and refined in isotropic approximation. Atomic coordinates and displacement parameters, bond distances and angles have been deposited at the Cambridge Crystallographic Data Centre.

1. G.M. Sheldrick, SADABS 1996, Program for the correction of Area Detector data, University of Göttingen, Germany.
2. G.M. Sheldrick, SHELXTL Version 5/VMS, 1995, Analytical X-Ray Systems GmbH, Madison, WI, USA.

Appendix B X-ray crystal structure (43)

Table 1. Crystal data and structure refinement for (**43**).

Empirical formula	C16 H22 N2 O6.50 P2		
Formula weight	408.30		
Temperature	150(2) K		
Wavelength	.71073 Å		
Crystal system	Monoclinic		
Space group	$P2_1/c$		
Unit cell dimensions	a = 7.590(2) Å b = 23.469(5) Å c = 11.312(3) Å		alpha = 90 deg. beta = 92.91(2) deg. gamma = 90 deg.
Volume	2012.4(1) $Å^3$		
Z	4		
Number of reflexions used	Total Unique Observed	16056 4599 2847	 [Fo > 4.sigma(Fo)]
Crystal description	Plate		
Crystal colour	Pale Yellow		
Density (calculated)	1.348 g/cm^3		
Absorption coefficient	0.252 mm^{-1}		
F(000)	856		
Crystal size	0.40 x 0.20 x 0.20 mm		
Theta range for data collection	1.74 to 27.48 deg.		
Index ranges	-9<=h<=8, -27<=k<=30, -14<=l<=14		
Experiment device	Siemens SMART-CCD		
Experiment methods	Omega scans		
Reflections collected	15808		
Independent reflections	4599 [R(int) = 0.0867]		
Refinement method	Full-matrix least-squares on F^2		
Data / restraints / parameters	4593 / 0 / 317		
Goodness-of-fit on F^2	1.062		

Final R indices [I>2sigma(I)]	$R_1 = 0.0621$, $wR_2 = 0.1418$
R indices (all data)	$R_1 = 0.1180$, $wR_2 = 0.1794$
Largest diff. peak and hole	0.756 and -0.617 e.Å^{-3}

Table 2. Atomic coordinates (x 10^4) and equivalent isotropic displacement parameters (Å^2 x 10^3) for (**43**). U_{eq} is defined as one third of the trace of the orthogonalized U_{ij} tensor.

	x	y	z	U_{eq}
P(1)	2596(1)	5910(1)	1218(1)	18(1)
P(2)	-7372(1)	4108(1)	1264(1)	18(1)
O(1)	3907(3)	5631(1)	2089(2)	24(1)
O(2)	2290(3)	5659(1)	10(2)	25(1)
O(3)	-8488(3)	4436(1)	2103(2)	24(1)
O(4)	-7262(3)	4309(1)	13(2)	25(1)
N(1)	-525(4)	5373(1)	1741(3)	17(1)
N(2)	-4180(4)	4656(1)	1768(3)	18(1)
C(1)	455(5)	5925(2)	1896(4)	20(1)
C(2)	-1842(5)	5306(2)	2674(3)	22(1)
C(3)	-2698(5)	4725(2)	2682(3)	21(1)
C(4)	-5121(5)	4101(2)	1929(3)	20(1)
C(11)	3101(5)	6661(2)	1125(3)	19(1)
C(12)	2463(5)	6981(2)	148(4)	24(1)
C(13)	2790(6)	7559(2)	92(4)	31(1)
C(14)	3726(6)	7832(2)	1017(4)	32(1)
C(15)	4355(6)	7521(2)	1997(4)	31(1)
C(16)	4057(5)	6940(2)	2053(3)	24(1)
C(21)	-7954(5)	3362(2)	1319(3)	20(1)
C(22)	-7425(5)	2995(2)	431(3)	24(1)
C(23)	-7785(6)	2414(2)	494(4)	30(1)
C(24)	-8682(6)	2203(2)	1445(4)	35(1)
C(25)	-9235(6)	2566(2)	2318(4)	31(1)
C(26)	-8869(5)	3145(2)	2258(4)	26(1)
O(1S)	4253(5)	5755(2)	4498(3)	55(1)
O(2S)	-7477(5)	4636(2)	4428(3)	64(1)
O(3S)	591(16)	6057(5)	5003(10)	104(3)

Table 3. Selected Intermolecular bond lengths [Å] and angles [deg] for (**43**).

Distance O..H

1.827 (0.046) O3 - H2N_$1
1.800 (0.055) O4 - H1N_$2
1.842 (0.054) O1 - H3N_$3
2.518 (0.041) O1 - H2B_$3

Distance O..N

2.708 (0.004) O3 - N1_$1
2.641 (0.004) O4 - N1_$2
2.742 (0.004) O1 - N2_$3

Distance O..C

3.349 (0.005) O1 - C2_$3

Angle XHY

165.50 (3.92) O3 - H2N_$1 - N1_$1
142.90 (4.58) O4 - H1N_$2 - N1_$2
166.25 (4.66) O1 - H3N_$3 - N2_$3
137.21 (2.86) O1 - H2B_$3 - C2_$3

Symmetry transformations used to generate equivalent atoms:

$1: X-1, Y, Z
$2: -X-1, -Y+1, -Z
$3: X+1, Y, Z

Table 4. Bond lengths [Å] and angles [deg] for (**43**).

P(1)-O(2)	1.495(3)
P(1)-O(1)	1.514(3)
P(1)-C(11)	1.807(4)
P(1)-C(1)	1.832(4)
P(2)-O(4)	1.499(3)
P(2)-O(3)	1.514(3)
P(2)-C(21)	1.807(4)
P(2)-C(4)	1.831(4)
N(1)-C(2)	1.498(5)
N(1)-C(1)	1.499(5)
N(1)-H(2N)	0.90(5)
N(1)-H(1N)	0.97(5)
N(2)-C(3)	1.497(5)
N(2)-C(4)	1.502(5)
N(2)-H(3N)	0.92(5)
N(2)-H(4N)	0.95(4)
C(1)-H(1A)	1.00(4)
C(1)-H(1B)	0.99(4)
C(2)-C(3)	1.511(5)
C(2)-H(2B)	1.03(4)
C(2)-H(2A)	1.02(5)
C(3)-H(3A)	1.02(4)
C(3)-H(3B)	0.99(5)
C(4)-H(4B)	1.00(4)
C(4)-H(4A)	0.96(4)
C(11)-C(12)	1.403(5)
C(11)-C(16)	1.407(5)
C(12)-C(13)	1.381(6)
C(12)-H(12)	0.99(4)
C(13)-C(14)	1.391(6)
C(13)-H(13)	0.89(4)
C(14)-C(15)	1.392(6)
C(14)-H(14)	0.93(5)
C(15)-C(16)	1.384(6)
C(15)-H(15)	0.95(4)
C(16)-H(16)	1.01(4)
C(21)-C(26)	1.395(5)
C(21)-C(22)	1.398(5)
C(22)-C(23)	1.392(6)
C(22)-H(22)	1.00(4)
C(23)-C(24)	1.394(6)
C(23)-H(23)	0.99(4)
C(24)-C(25)	1.385(6)
C(24)-H(24)	0.99(5)
C(25)-C(26)	1.389(6)
C(25)-H(25)	0.94(4)
C(26)-H(26)	1.00(4)
O(2)-P(1)-O(1)	119.4(2)
O(2)-P(1)-C(11)	110.8(2)
O(1)-P(1)-C(11)	109.0(2)
O(2)-P(1)-C(1)	106.9(2)
O(1)-P(1)-C(1)	107.6(2)
C(11)-P(1)-C(1)	101.6(2)
O(4)-P(2)-O(3)	119.4(2)
O(4)-P(2)-C(21)	111.3(2)
O(3)-P(2)-C(21)	109.0(2)

O(4)-P(2)-C(4)	107.2(2)
O(3)-P(2)-C(4)	106.7(2)
C(21)-P(2)-C(4)	101.7(2)
C(2)-N(1)-C(1)	110.7(3)
C(2)-N(1)-H(2N)	109(3)
C(1)-N(1)-H(2N)	115(3)
C(2)-N(1)-H(1N)	112(3)
C(1)-N(1)-H(1N)	109(3)
H(2N)-N(1)-H(1N)	100(4)
C(3)-N(2)-C(4)	110.8(3)
C(3)-N(2)-H(3N)	108(3)
C(4)-N(2)-H(3N)	118(3)
C(3)-N(2)-H(4N)	108(3)
C(4)-N(2)-H(4N)	109(3)
H(3N)-N(2)-H(4N)	102(4)
N(1)-C(1)-P(1)	112.3(2)
N(1)-C(1)-H(1A)	109(2)
P(1)-C(1)-H(1A)	110(2)
N(1)-C(1)-H(1B)	110(3)
P(1)-C(1)-H(1B)	111(3)
H(1A)-C(1)-H(1B)	106(3)
N(1)-C(2)-C(3)	113.7(3)
N(1)-C(2)-H(2B)	109(2)
C(3)-C(2)-H(2B)	109(2)
N(1)-C(2)-H(2A)	109(3)
C(3)-C(2)-H(2A)	106(3)
H(2B)-C(2)-H(2A)	110(3)
N(2)-C(3)-C(2)	113.7(3)
N(2)-C(3)-H(3A)	109(2)
C(2)-C(3)-H(3A)	102(2)
N(2)-C(3)-H(3B)	109(3)
C(2)-C(3)-H(3B)	112(3)
H(3A)-C(3)-H(3B)	112(4)
N(2)-C(4)-P(2)	112.5(2)
N(2)-C(4)-H(4B)	109(2)
P(2)-C(4)-H(4B)	109(2)
N(2)-C(4)-H(4A)	106(3)
P(2)-C(4)-H(4A)	112(3)
H(4B)-C(4)-H(4A)	109(3)
C(12)-C(11)-C(16)	118.9(3)
C(12)-C(11)-P(1)	120.1(3)
C(16)-C(11)-P(1)	120.9(3)
C(13)-C(12)-C(11)	120.4(4)
C(13)-C(12)-H(12)	121(2)
C(11)-C(12)-H(12)	118(2)
C(12)-C(13)-C(14)	120.3(4)
C(12)-C(13)-H(13)	121(3)
C(14)-C(13)-H(13)	118(3)
C(13)-C(14)-C(15)	120.0(4)
C(13)-C(14)-H(14)	120(3)
C(15)-C(14)-H(14)	120(3)
C(16)-C(15)-C(14)	120.2(4)
C(16)-C(15)-H(15)	121(3)
C(14)-C(15)-H(15)	119(3)
C(15)-C(16)-C(11)	120.3(4)
C(15)-C(16)-H(16)	121(2)
C(11)-C(16)-H(16)	118(2)
C(26)-C(21)-C(22)	119.6(4)
C(26)-C(21)-P(2)	120.8(3)
C(22)-C(21)-P(2)	119.5(3)

C(23)-C(22)-C(21)	120.2(4)
C(23)-C(22)-H(22)	120(2)
C(21)-C(22)-H(22)	120(2)
C(22)-C(23)-C(24)	119.5(4)
C(22)-C(23)-H(23)	121(3)
C(24)-C(23)-H(23)	120(3)
C(25)-C(24)-C(23)	120.6(4)
C(25)-C(24)-H(24)	125(3)
C(23)-C(24)-H(24)	115(3)
C(24)-C(25)-C(26)	119.9(4)
C(24)-C(25)-H(25)	121(3)
C(26)-C(25)-H(25)	119(3)
C(25)-C(26)-C(21)	120.2(4)
C(25)-C(26)-H(26)	120(3)
C(21)-C(26)-H(26)	120(3)

Table 5. Anisotropic displacement parameters ($Å^2$ x 10^3) for (**43**). The anisotropic displacement factor exponent takes the form: $-2\pi^2 [h^2 a^{*2} U_{11} + ... + 2 h k a^* b^* U_{12}]$

	U11	U22	U33	U23	U13	U12
P(1)	13(1)	18(1)	23(1)	-2(1)	3(1)	-1(1)
P(2)	13(1)	18(1)	23(1)	2(1)	-1(1)	0(1)
O(1)	19(1)	22(1)	30(1)	1(1)	0(1)	3(1)
O(2)	21(1)	29(2)	25(1)	-4(1)	5(1)	-3(1)
O(3)	18(1)	25(2)	29(2)	-1(1)	0(1)	4(1)
O(4)	21(1)	27(2)	26(1)	6(1)	-2(1)	-2(1)
N(1)	16(2)	16(2)	20(2)	-1(1)	3(1)	0(1)
N(2)	14(2)	18(2)	20(2)	2(1)	1(1)	-1(1)
C(1)	15(2)	16(2)	30(2)	-3(2)	4(2)	0(1)
C(2)	17(2)	28(2)	21(2)	-6(2)	6(2)	-4(2)
C(3)	16(2)	28(2)	20(2)	0(2)	-1(2)	-4(2)
C(4)	17(2)	15(2)	27(2)	1(2)	1(2)	-1(2)
C(11)	15(2)	17(2)	25(2)	-3(2)	3(1)	-3(1)
C(12)	19(2)	25(2)	29(2)	1(2)	-2(2)	-3(2)
C(13)	29(2)	27(2)	35(2)	9(2)	-1(2)	-1(2)
C(14)	30(2)	18(2)	46(3)	2(2)	1(2)	-7(2)
C(15)	34(2)	27(2)	31(2)	-7(2)	-4(2)	-7(2)
C(16)	25(2)	24(2)	25(2)	0(2)	-3(2)	-3(2)
C(21)	13(2)	21(2)	25(2)	1(2)	-4(1)	-2(1)
C(22)	21(2)	25(2)	25(2)	-1(2)	-1(2)	-4(2)
C(23)	32(2)	25(2)	33(2)	-3(2)	-4(2)	-4(2)
C(24)	36(3)	25(2)	42(3)	3(2)	-7(2)	-11(2)
C(25)	32(2)	31(2)	30(2)	9(2)	0(2)	-9(2)
C(26)	22(2)	29(2)	28(2)	1(2)	1(2)	-4(2)

Table 6. Hydrogen coordinates (x 10^4) and isotropic displacement parameters ($Å^3$ x 10^3) for (**43**).

	x	y	z	U(eq)
H(3N)	-4835(74)	4985(21)	1746(44)	50(15)
H(16)	4515(53)	6707(17)	2749(34)	22(10)
H(1A)	-287(55)	6236(17)	1530(34)	23(11)
H(2N)	155(61)	5059(18)	1727(36)	28(11)
H(12)	1769(58)	6781(18)	-495(36)	30(11)
H(3A)	-3202(56)	4714(18)	3502(37)	28(11)
H(14)	3911(60)	8225(21)	988(38)	36(12)
H(22)	-6772(51)	3146(16)	-247(32)	17(10)
H(2B)	-2814(53)	5610(17)	2553(33)	19(10)
H(25)	-9827(56)	2424(17)	2968(37)	27(11)
H(2A)	-1220(60)	5351(19)	3491(40)	37(12)
H(23)	-7390(58)	2149(19)	-116(38)	33(12)
H(1B)	604(59)	6022(18)	2749(39)	34(12)
H(15)	5016(59)	7709(19)	2611(37)	31(12)
H(3B)	-1839(61)	4417(20)	2578(38)	35(12)
H(13)	2350(59)	7770(19)	-506(38)	32(12)
H(4B)	-5178(47)	4018(15)	2790(33)	13(9)
H(26)	-9294(61)	3405(19)	2879(39)	34(12)
H(4A)	-4401(58)	3818(18)	1584(36)	29(11)
H(4N)	-3689(57)	4656(18)	1010(38)	29(11)
H(24)	-8860(61)	1786(21)	1438(39)	41(13)
H(1N)	-1071(71)	5360(22)	945(47)	55(15)

Appendix C X-ray crystal structure (84)

Table 1. Crystal data and structure refinement for (**84**).

Empirical formula	C18 H24 N4 P2 S2
Formula weight	422.47
Temperature	150(2) K
Wavelength	0.71073 A
Crystal system	Triclinic
Space group	P-1
Unit cell dimensions	a = 9.588(1) Å alpha = 69.43(1) deg. b = 11.402(1) Å beta = 87.11(1) deg. c = 11.620(1) Å gamma = 69.74(1) deg.
Volume	1112.1(2) $Å^3$
Z	2
Density (calculated)	1.262 g/cm^3
Absorption coefficient	0.393 mm^{-1}
F(000)	444
Crystal size	0.5 x 0.5 x 0.3 mm
Crystal colour	pale yellow
Theta range for data collection	1.88 to 25.52 deg.
Index ranges	-11<h<11, -7<k<13, -11<l<13
Reflections collected	4911
Independent reflections	3567 [R(int) = 0.0270]
Observed reflections	I>2sigma(I) 3319
Absorption correction	Semi-empirical (equivalents)
Max. and min. transmission	0.906 and 0.828
Refinement method	Full-matrix least-squares on F^2
Data / restraints / parameters	3545 / 0 / 332
Goodness-of-fit on F^2	1.054
Final R indices [I>2sigma(I)]	R_1 = 0.0324, wR_2 = 0.0846
R indices (all data)	R_1 = 0.0354, wR_2 = 0.0944
Extinction coefficient	0.010(2)

Largest shift/e.s.d. ratio	-0.006
Largest diff. peak and hole	0.264 and -0.300 e.Å^{-3}

Table 2. Atomic coordinates (x 10^4) and equivalent isotropic displacement parameters (Å^2 x 10^3) for (**84**). U(eq) is defined as one third of the trace of the orthogonalized U_{ij} tensor.

	x	y	z	U(eq)
P(1)	6937(1)	7056(1)	3556(1)	27(1)
P(2)	2389(1)	8494(1)	5837(1)	28(1)
S(1)	6134(1)	8943(1)	2571(1)	42(1)
S(2)	1323(1)	7654(1)	5189(1)	40(1)
N(1)	7176(2)	5633(2)	5935(1)	29(1)
N(2)	6933(2)	6879(2)	5054(2)	37(1)
N(3)	4993(2)	7602(2)	7132(1)	28(1)
N(4)	4029(2)	7301(2)	6535(2)	32(1)
C(1)	6925(2)	5554(2)	7057(2)	25(1)
C(2)	6348(2)	6770(2)	7423(2)	25(1)
C(3)	5894(4)	6085(3)	3401(3)	56(1)
C(4)	8820(3)	6182(3)	3352(3)	61(1)
C(5)	1500(2)	9142(2)	6980(2)	35(1)
C(6)	2823(3)	9844(2)	4719(2)	41(1)
C(11)	7129(2)	4223(2)	7996(2)	24(1)
C(12)	7776(2)	3057(2)	7727(2)	29(1)
C(13)	7859(2)	1828(2)	8584(2)	36(1)
C(14)	7303(3)	1739(2)	9725(2)	39(1)
C(15)	6673(2)	2882(2)	10007(2)	35(1)
C(16)	6587(2)	4119(2)	9153(2)	29(1)
C(21)	7366(2)	7009(2)	8163(2)	26(1)
C(22)	8900(2)	6386(2)	8197(2)	37(1)
C(23)	9859(3)	6573(2)	8916(2)	43(1)
C(24)	9301(3)	7379(2)	9601(2)	41(1)
C(25)	7785(3)	8007(2)	9568(2)	41(1)
C(26)	6809(2)	7830(2)	8854(2)	34(1)

Table 3. Bond lengths [Å] and angles [deg] for (**84**).

P(1)-N(2)	1.680(2)
P(1)-C(3)	1.784(2)
P(1)-C(4)	1.785(3)
P(1)-S(1)	1.9346(8)
P(2)-N(4)	1.689(2)
P(2)-C(5)	1.782(2)
P(2)-C(6)	1.794(2)
P(2)-S(2)	1.9469(7)
N(1)-C(1)	1.292(2)
N(1)-N(2)	1.376(2)
N(3)-C(2)	1.291(2)

N(3)-N(4)	1.380(2)
C(1)-C(11)	1.478(3)
C(1)-C(2)	1.506(2)
C(2)-C(21)	1.483(3)
C(11)-C(16)	1.397(3)
C(11)-C(12)	1.397(3)
C(12)-C(13)	1.383(3)
C(13)-C(14)	1.387(3)
C(14)-C(15)	1.381(3)
C(15)-C(16)	1.387(3)
C(21)-C(22)	1.390(3)
C(21)-C(26)	1.394(3)
C(22)-C(23)	1.388(3)
C(23)-C(24)	1.377(3)
C(24)-C(25)	1.376(3)
C(25)-C(26)	1.390(3)

N(2)-P(1)-C(3)	104.85(13)
N(2)-P(1)-C(4)	105.03(12)
C(3)-P(1)-C(4)	105.6(2)
N(2)-P(1)-S(1)	108.72(7)
C(3)-P(1)-S(1)	115.42(9)
C(4)-P(1)-S(1)	116.21(11)
N(4)-P(2)-C(5)	105.77(10)
N(4)-P(2)-C(6)	106.82(10)
C(5)-P(2)-C(6)	104.97(11)
N(4)-P(2)-S(2)	107.18(6)
C(5)-P(2)-S(2)	115.52(8)
C(6)-P(2)-S(2)	115.86(9)
C(1)-N(1)-N(2)	118.1(2)
N(1)-N(2)-P(1)	119.30(13)
C(2)-N(3)-N(4)	117.9(2)
N(3)-N(4)-P(2)	119.89(13)
N(1)-C(1)-C(11)	118.2(2)
N(1)-C(1)-C(2)	122.5(2)
C(11)-C(1)-C(2)	119.2(2)
N(3)-C(2)-C(21)	118.8(2)
N(3)-C(2)-C(1)	122.4(2)
C(21)-C(2)-C(1)	118.8(2)
C(16)-C(11)-C(12)	118.7(2)
C(16)-C(11)-C(1)	120.0(2)
C(12)-C(11)-C(1)	121.2(2)
C(13)-C(12)-C(11)	120.5(2)
C(12)-C(13)-C(14)	120.2(2)
C(15)-C(14)-C(13)	119.8(2)
C(14)-C(15)-C(16)	120.3(2)
C(15)-C(16)-C(11)	120.4(2)
C(22)-C(21)-C(26)	119.0(2)
C(22)-C(21)-C(2)	119.9(2)
C(26)-C(21)-C(2)	121.0(2)
C(23)-C(22)-C(21)	120.3(2)
C(24)-C(23)-C(22)	120.4(2)
C(25)-C(24)-C(23)	119.8(2)
C(24)-C(25)-C(26)	120.6(2)
C(25)-C(26)-C(21)	120.0(2)

Table 4. Anisotropic displacement parameters ($Å^2$ x 10^3) for (**84**). The anisotropic displacement factor exponent takes the form: $-2\pi^2 [h^2 a^{*2} U_{11} + ... + 2 h k a^* b^* U_{12}]$

	U11	U22	U33	U23	U13	U12
P(1)	30(1)	26(1)	24(1)	-8(1)	2(1)	-10(1)
P(2)	30(1)	24(1)	26(1)	-9(1)	-1(1)	-6(1)
S(1)	62(1)	27(1)	31(1)	-4(1)	5(1)	-14(1)
S(2)	42(1)	35(1)	43(1)	-18(1)	-10(1)	-9(1)
N(1)	35(1)	24(1)	25(1)	-5(1)	4(1)	-11(1)
N(2)	60(1)	23(1)	25(1)	-8(1)	10(1)	-14(1)
N(3)	31(1)	27(1)	27(1)	-9(1)	1(1)	-10(1)
N(4)	32(1)	26(1)	39(1)	-17(1)	-7(1)	-4(1)
C(1)	24(1)	25(1)	24(1)	-8(1)	2(1)	-9(1)
C(2)	29(1)	24(1)	22(1)	-6(1)	5(1)	-10(1)
C(3)	74(2)	40(1)	55(2)	-5(1)	-26(1)	-28(1)
C(4)	44(2)	66(2)	44(2)	-8(1)	15(1)	2(1)
C(5)	35(1)	33(1)	31(1)	-13(1)	1(1)	-6(1)
C(6)	45(1)	31(1)	37(1)	-4(1)	6(1)	-10(1)
C(11)	21(1)	26(1)	26(1)	-8(1)	0(1)	-9(1)
C(12)	32(1)	29(1)	28(1)	-11(1)	5(1)	-11(1)
C(13)	46(1)	24(1)	37(1)	-11(1)	2(1)	-12(1)
C(14)	50(1)	30(1)	33(1)	-1(1)	1(1)	-20(1)
C(15)	38(1)	37(1)	27(1)	-7(1)	7(1)	-15(1)
C(16)	28(1)	30(1)	28(1)	-10(1)	2(1)	-9(1)
C(21)	33(1)	24(1)	22(1)	-5(1)	3(1)	-13(1)
C(22)	32(1)	40(1)	43(1)	-21(1)	6(1)	-14(1)
C(23)	31(1)	49(1)	56(1)	-21(1)	1(1)	-16(1)
C(24)	48(1)	46(1)	37(1)	-11(1)	-3(1)	-27(1)
C(25)	51(1)	43(1)	39(1)	-22(1)	6(1)	-23(1)
C(26)	35(1)	33(1)	36(1)	-15(1)	4(1)	-12(1)

Table 5. Hydrogen coordinates (x 10^4) and isotropic displacement parameters ($Å^2$ x 10^3) for (**84**).

	x	y	z	U(eq)
H(2N)	6627(25)	7567(25)	5242(21)	38(6)
H(4N)	4361(25)	6630(24)	6323(21)	36(6)
H(3A)	5928(33)	6144(30)	2601(30)	68(9)
H(3B)	4876(42)	6536(36)	3596(32)	91(11)
H(3C)	6348(32)	5170(32)	3920(28)	65(8)
H(4A)	8865(35)	6259(32)	2517(33)	80(10)
H(4B)	9209(35)	5232(35)	3883(31)	77(9)
H(4C)	9391(48)	6617(42)	3517(39)	116(16)
H(5A)	591(29)	9876(26)	6646(23)	50(7)
H(5B)	2132(28)	9449(24)	7294(23)	47(7)
H(5C)	1243(27)	8475(27)	7615(25)	50(7)
H(6A)	1896(29)	10566(26)	4407(23)	47(7)
H(6B)	3299(27)	9552(24)	4111(23)	45(7)
H(6C)	3465(30)	10111(26)	5146(24)	54(7)
H(12)	8095(23)	3092(20)	6981(21)	29(5)

H(13)	8294(26)	1089(25)	8393(21)	42(6)
H(14)	7339(26)	956(26)	10266(23)	45(6)
H(15)	6284(26)	2845(23)	10799(23)	42(6)
H(16)	6167(24)	4900(23)	9345(20)	35(6)
H(22)	9279(26)	5834(24)	7719(22)	45(6)
H(23)	10884(32)	6136(26)	8904(24)	56(7)
H(24)	9995(27)	7506(23)	10087(22)	43(6)
H(25)	7389(27)	8568(24)	10035(23)	47(7)
H(26)	5794(27)	8275(23)	8824(20)	39(6)

Table 6. Torsion angles (degrees) for (**84**).

S(1)-P(1)-N(2)-N(1)	167.36(13)
P(1)-N(2)-N(1)-C(1)	-168.68(14)
N(2)-N(1)-C(1)-C(2)	1.4(3)
N(1)-C(1)-C(2)-N(3)	71.9(2)
C(1)-C(2)-N(3)-N(4)	4.4(3)
C(2)-N(3)-N(4)-P(2)	-165.62(14)
N(3)-N(4)-P(2)-S(2)	-177.05(13)

Appendix D X-ray crystal structure (85)

Table 1. Crystal data and structure refinement for (**85**).

Identification code	ps	
Empirical formula	C8 H20 N4 P2 S2	
Formula weight	298.34	
Temperature	120(2) K	
Wavelength	0.71073 Å	
Crystal system	Monoclinic	
Space group	P 1 21/n 1	
Unit cell dimensions	a = 6.2200(1) Å b = 12.1463(2) Å c = 10.1414(1) Å	alpha = 90 deg. beta = 97.937(1) deg. gamma = 90 deg.
Volume	758.84(2) $Å^3$	
Z	2	
Density (calculated)	1.306 g/cm^3	
Absorption coefficient	0.545 mm^{-1}	
F(000)	316	
Crystal size	0.40 x 0.20 x 0.15 mm	
Theta range for data collection	2.63 to 27.45 deg.	
Index ranges	-7<h<8, -15<k<14, -12<l<13	
Reflections collected	5381	
Independent reflections	1735 [R(int) = 0.0238]	
Observed reflections, I>2sigma(I)	1595	
Absorption correction	Multi-scan	
Max. and min. transmission	0.843 and 0.726	
Refinement method	Full-matrix least-squares on F^2	
Data / restraints / parameters	1718 / 0 / 114	
Goodness-of-fit on F^2	1.056	
Final R indices [I>2sigma(I)]	R_1 = 0.0253, wR_2 = 0.0661	
R indices (all data)	R_1 = 0.0284, wR_2 = 0.0726	

Extinction coefficient	0.006(2)
Largest diff. peak and hole	0.382 and -0.266 e.Å^{-3}
Largest shift/e.s.d.	0.001

Table 2. Atomic coordinates (x 10^4) and equivalent isotropic displacement parameters (Å^2 x 10^3) for (**85**). U(eq) is defined as one third of the trace of the orthogonalized U_{ij} tensor.

	x	y	z	U(eq)
P	1969(1)	1740(1)	8712(1)	17(1)
S	981(1)	1785(1)	10459(1)	25(1)
N(1)	508(2)	802(1)	7764(1)	24(1)
N(2)	957(2)	692(1)	6474(1)	19(1)
C(1)	-291(2)	54(1)	5679(1)	16(1)
C(2)	-2217(2)	-548(1)	6066(1)	22(1)
C(3)	4789(2)	1389(1)	8730(2)	30(1)
C(4)	1602(2)	2993(1)	7762(1)	22(1)

Table 4. Bond lengths [Å] and angles [deg] for (**85**).

P-N(1)	1.6757(11)
P-C(4)	1.7984(14)
P-C(3)	1.8026(14)
P-S	1.9550(4)
N(1)-N(2)	1.3817(14)
N(1)-H(1)	0.83(2)
N(2)-C(1)	1.296(2)
C(1)-C(1)#1	1.478(2)
C(1)-C(2)	1.500(2)
C(2)-H(2A)	0.97(2)
C(2)-H(2B)	0.92(2)
C(2)-H(2C)	0.94(2)
C(3)-H(3A)	0.99(2)
C(3)-H(3B)	0.97(2)
C(3)-H(3C)	0.93(2)
C(4)-H(4A)	0.99(2)
C(4)-H(4B)	0.93(2)
C(4)-H(4C)	0.94(2)
N(1)-P-C(4)	104.47(6)
N(1)-P-C(3)	107.15(7)
C(4)-P-C(3)	104.90(7)
N(1)-P-S	109.01(4)
C(4)-P-S	115.40(5)
C(3)-P-S	115.11(5)

N(2)-N(1)-P	116.36(9)
N(2)-N(1)-H(1)	121.1(13)
P-N(1)-H(1)	122.1(13)
C(1)-N(2)-N(1)	117.63(10)
N(2)-C(1)-C(1)#1	115.41(13)
N(2)-C(1)-C(2)	124.07(10)
C(1)#1-C(1)-C(2)	120.52(13)
C(1)-C(2)-H(2A)	109.5(12)
C(1)-C(2)-H(2B)	111.2(12)
H(2A)-C(2)-H(2B)	108(2)
C(1)-C(2)-H(2C)	112.4(11)
H(2A)-C(2)-H(2C)	109(2)
H(2B)-C(2)-H(2C)	107(2)
P-C(3)-H(3A)	108.2(11)
P-C(3)-H(3B)	108.0(12)
H(3A)-C(3)-H(3B)	108(2)
P-C(3)-H(3C)	109.9(11)
H(3A)-C(3)-H(3C)	110(2)
H(3B)-C(3)-H(3C)	113(2)
P-C(4)-H(4A)	109.9(10)
P-C(4)-H(4B)	106.4(12)
H(4A)-C(4)-H(4B)	110(2)
P-C(4)-H(4C)	109.5(11)
H(4A)-C(4)-H(4C)	109(2)
H(4B)-C(4)-H(4C)	112(2)

Symmetry transformations used to generate equivalent atoms:
#1 -x,-y,-z+1

Table 5. Anisotropic displacement parameters ($Å^2$ x 10^3) for (**85**). The anisotropic displacement factor exponent takes the form: $-2\pi^2 [h^2 a^{*2} U_{11} + ... + 2 h k a^* b^* U_{12}]$

	U11	U22	U33	U23	U13	U12
P	17(1)	22(1)	12(1)	-3(1)	2(1)	-1(1)
S	27(1)	38(1)	12(1)	-5(1)	5(1)	-5(1)
N(1)	36(1)	26(1)	12(1)	-5(1)	9(1)	-12(1)
N(2)	28(1)	18(1)	12(1)	-1(1)	6(1)	-2(1)
C(1)	22(1)	15(1)	12(1)	1(1)	4(1)	2(1)
C(2)	25(1)	26(1)	15(1)	-2(1)	5(1)	-6(1)
C(3)	22(1)	43(1)	26(1)	6(1)	5(1)	8(1)
C(4)	23(1)	21(1)	21(1)	-2(1)	5(1)	-2(1)

Table 6. Hydrogen coordinates (x 10^4) and isotropic displacement parameters (Å^2 x 10^3) for (**85**).

	x	y	z	U(eq)
H(1)	-339(31)	373(16)	8072(18)	40(5)
H(2A)	-3258(32)	-21(17)	6316(18)	44(5)
H(2B)	-1817(30)	-1004(16)	6782(19)	40(5)
H(2C)	-2903(29)	-988(15)	5375(18)	36(5)
H(3A)	5033(31)	647(17)	9133(19)	47(5)
H(3B)	5653(33)	1910(16)	9304(20)	42(5)
H(3C)	5133(30)	1388(16)	7866(19)	37(5)
H(4A)	37(32)	3146(14)	7519(18)	33(5)
H(4B)	2251(32)	3547(17)	8310(20)	44(5)
H(4C)	2245(29)	2920(15)	6986(18)	34(4)

Appendix E X-ray crystal structure (86)

Table 1. Crystal data and structure refinement for (**86**).

Empirical formula	C8 H13 N2 P S	
Formula weight	200.23	
Temperature	150(2) K	
Wavelength	0.71073 A	
Crystal system	Monoclinic	
Space group	$P2_{(1)/c}$	
Unit cell dimensions	a = 11.415(1) Å b = 8.348(1) Å c = 11.983(1) Å	alpha = 90 deg. beta = 114.54(1) deg. gamma = 90 deg.
Volume	1038.7(2) $Å^3$	
Z	4	
Density (calculated)	1.280 g/cm^3	
Absorption coefficient	0.416 mm^{-1}	
F(000)	424	
Crystal size	0.4 x 0.3 x 0.2 mm	
Crystal colour	colourless	
Theta range for data collection	1.96 to 30.43 deg.	
Index ranges	-15<h<15, -11<k<11, -17<l<16	
Reflections collected	8012	
Independent reflections	2815 [R(int) = 0.0279]	
Observed reflections, I>2sigma(I)	2425	
Absorption correction	Semiempirical	
Max. and min. transmission	0.9518 and 0.8574	
Refinement method	Full-matrix least-squares on F^2	
Data / restraints / parameters	2806 / 0 / 161	
Goodness-of-fit on F^2	1.163	
Final R indices [I>2sigma(I)]	R_1 = 0.0329, wR_2 = 0.0727	
R indices (all data)	R_1 = 0.0432, wR_2 = 0.0824	

Largest shift/e.s.d. ratio	-0.001
Largest diff. peak and hole	0.353 and -0.255 e.Å^{-3}

Table 2. Atomic coordinates (x 10^4) and equivalent isotropic displacement parameters (Å^2 x 10^3) for (**86**). U(eq) is defined as one third of the trace of the orthogonalized U_{ij} tensor.

	x	y	z	U(eq)
S	5793(1)	6961(1)	1449(1)	27(1)
P	3961(1)	7376(1)	1018(1)	19(1)
N(1)	1063(1)	6969(2)	-278(1)	19(1)
N(2)	3079(1)	6056(2)	-60(1)	22(1)
C(2)	1735(1)	5985(2)	-671(1)	18(1)
C(3)	1161(2)	4909(2)	-1643(2)	26(1)
C(4)	-169(2)	4867(2)	-2214(2)	29(1)
C(5)	-884(1)	5879(2)	-1815(2)	24(1)
C(6)	-239(1)	6910(2)	-846(1)	20(1)
C(7)	-960(2)	8052(2)	-387(2)	28(1)
C(8)	3546(2)	7175(3)	2304(2)	31(1)
C(9)	3467(2)	9355(2)	415(2)	27(1)

Table 3. Bond lengths [Å] and angles [deg] for (**86**)

S-P	1.9655(5)
P-N(2)	1.6771(13)
P-C(9)	1.797(2)
P-C(8)	1.799(2)
N(1)-C(2)	1.336(2)
N(1)-C(6)	1.354(2)
N(2)-C(2)	1.400(2)
N(2)-H(2)	0.80(2)
C(2)-C(3)	1.399(2)
C(3)-C(4)	1.382(2)
C(3)-H(3)	0.92(2)
C(4)-C(5)	1.391(2)
C(4)-H(4)	0.95(2)
C(5)-C(6)	1.386(2)
C(5)-H(5)	0.94(2)
C(6)-C(7)	1.505(2)
C(7)-H(71)	0.95(2)
C(7)-H(72)	0.96(2)
C(7)-H(73)	0.96(2)

C(8)-H(81)	0.96(2)
C(8)-H(82)	0.93(2)
C(8)-H(83)	0.99(2)
C(9)-H(91)	0.95(2)
C(9)-H(92)	0.95(2)
C(9)-H(93)	0.96(2)

N(2)-P-C(9)	107.84(8)
N(2)-P-C(8)	108.14(8)
C(9)-P-C(8)	106.24(9)
N(2)-P-S	108.66(5)
C(9)-P-S	112.91(6)
C(8)-P-S	112.83(6)
C(2)-N(1)-C(6)	118.11(13)
C(2)-N(2)-P	127.43(11)
C(2)-N(2)-H(2)	115(2)
P-N(2)-H(2)	118(2)
N(1)-C(2)-C(3)	123.30(13)
N(1)-C(2)-N(2)	116.98(13)
C(3)-C(2)-N(2)	119.72(13)
C(4)-C(3)-C(2)	117.8(2)
C(4)-C(3)-H(3)	121.2(11)
C(2)-C(3)-H(3)	121.0(12)
C(3)-C(4)-C(5)	119.7(2)
C(3)-C(4)-H(4)	119.3(12)
C(5)-C(4)-H(4)	121.0(12)
C(6)-C(5)-C(4)	118.77(14)
C(6)-C(5)-H(5)	120.3(12)
C(4)-C(5)-H(5)	120.9(12)
N(1)-C(6)-C(5)	122.28(14)
N(1)-C(6)-C(7)	116.51(13)
C(5)-C(6)-C(7)	121.20(13)
C(6)-C(7)-H(71)	110.8(13)
C(6)-C(7)-H(72)	110.9(13)
H(71)-C(7)-H(72)	104(2)
C(6)-C(7)-H(73)	110.8(14)
H(71)-C(7)-H(73)	111(2)
H(72)-C(7)-H(73)	109(2)
P-C(8)-H(81)	110.8(13)
P-C(8)-H(82)	110.2(14)
H(81)-C(8)-H(82)	108(2)
P-C(8)-H(83)	107.6(14)
H(81)-C(8)-H(83)	111(2)
H(82)-C(8)-H(83)	110(2)
P-C(9)-H(91)	108.6(13)
P-C(9)-H(92)	105.2(14)
H(91)-C(9)-H(92)	109(2)
P-C(9)-H(93)	109.1(14)
H(91)-C(9)-H(93)	112(2)
H(92)-C(9)-H(93)	113(2)

Table 4. Anisotropic displacement parameters ($Å^2 \times 10^3$) for (**86**)
The anisotropic displacement factor exponent takes the form:
$-2\ Å^2\ [\ h^2\ a^{*2}\ U_{11} + ... + 2\ h\ k\ a^*\ b^*\ U_{12}\ ]$

	U11	U22	U33	U23	U13	U12
S	13(1)	31(1)	33(1)	-6(1)	5(1)	2(1)
P	13(1)	22(1)	19(1)	-3(1)	5(1)	0(1)
N(1)	16(1)	20(1)	20(1)	0(1)	7(1)	0(1)
N(2)	13(1)	24(1)	26(1)	-7(1)	5(1)	2(1)
C(2)	15(1)	20(1)	18(1)	1(1)	5(1)	1(1)
C(3)	20(1)	28(1)	27(1)	-9(1)	7(1)	3(1)
C(4)	20(1)	30(1)	29(1)	-10(1)	3(1)	-1(1)
C(5)	14(1)	25(1)	29(1)	0(1)	4(1)	0(1)
C(6)	16(1)	19(1)	23(1)	4(1)	8(1)	1(1)
C(7)	20(1)	28(1)	36(1)	-3(1)	13(1)	3(1)
C(8)	25(1)	47(1)	22(1)	-4(1)	10(1)	-4(1)
C(9)	21(1)	23(1)	35(1)	-2(1)	10(1)	1(1)

Table 5. Hydrogen coordinates ($\times 10^4$) and isotropic displacement parameters ($Å^2 \times 10^3$) for (**86**)

	x	y	z	U(eq)
H(2)	3457(20)	5423(26)	-290(18)	33(5)
H(3)	1653(18)	4242(23)	-1886(16)	26(5)
H(4)	-579(19)	4140(26)	-2869(18)	36(5)
H(5)	-1793(18)	5846(23)	-2178(17)	29(5)
H(71)	-928(20)	9117(28)	-664(19)	39(6)
H(72)	-554(21)	8133(26)	495(22)	43(6)
H(73)	-1830(23)	7704(27)	-626(21)	44(6)
H(81)	2648(21)	7392(25)	2066(19)	37(6)
H(82)	4013(21)	7899(26)	2914(21)	39(6)
H(83)	3759(22)	6068(30)	2618(21)	49(7)
H(91)	2556(20)	9422(25)	110(18)	35(5)
H(92)	3837(21)	10047(28)	1097(20)	44(6)
H(93)	3759(22)	9559(29)	-218(21)	51(7)

Table 6. Torsion angles (degrees) for (**86**)

S-P-N(2)-C(2)	-176.19(12)
P-N(2)-C(2)-N(1)	-7.2(2)

Appendix F Publications

M.A.M. Easson and D. Parker, Synthesis of New Aza-thiophosphinate Ligands, *Tetrahedron Letters*, 1997, **38**, 6091

M.A.M. Easson and D. Parker, Aza-thiophosphinate Acids and Metal Complexes Thereof, British Patent Application no. 9616995.8; 1996; priority 130896

M.A.M. Easson, Drug Suspects and Electronic Tagging, *Chemistry and Industry*, 1996, 461

Appendix G Conferences, Lectures, Research Colloquia and Seminars

The author attended the following meetings:

Stereochemistry at Sheffield, University of Sheffield, 20th December 1994

RSC UK Macrocycles Group Meeting, University of Newcastle, 4-5th January 1995

Stereochemistry at Sheffield, University of Sheffield, 19th December 1995

RSC UK Macrocycles Group Meeting, University of Sheffield, 4-5th January 1996

31st International Conference of Coordination Chemistry,* Vancouver, BC, Canada, 18-23rd August 1996

ICI Poster Presentation, University of Durham,* 18th December, 1996 (prize winner)

Graduate Symposium,† University of Newcastle, 7th April 1997

21st Century Heterocyclic Chemistry, University of Sunderland, 7th May 1997

* indicates a poster presentation by the author

† indicates an oral presentation by the author

The author attended the following lecture courses:

NMR Spectroscopy, by Dr A.M. Kenwright
Organometallic Chemistry, by Prof. V. Gibson and Prof. Parker
Polymers, by Prof. W. Feast

The author attended the following colloquia between October 1994 and September 1997

1994

October 5 Prof. N. L. Owen, Brigham Young University, Utah, USA
Determining Molecular Structure - the INADEQUATE NMR way

October 19 Prof. N. Bartlett, University of California
Some Aspects of Ag(II) and Ag(III) Chemistry

November 2 Dr P. G. Edwards, University of Wales, Cardiff
The Manipulation of Electronic and Structural Diversity in Metal Complexes - New Ligands

November 3 Prof. B. F. G. Johnson, Edinburgh University
Arene-metal Clusters

November 9 Dr G. Hogarth, University College, London
New Vistas in Metal-imido Chemistry

November 10 Dr M. Block, Zeneca Pharmaceuticals, Macclesfield
Large-scale Manufacture of ZD 1542, a Thromboxane Antagonist Synthase Inhibitor

November 16 Prof. M. Page, University of Huddersfield
Four-membered Rings and β-Lactamase

November 23 Dr J. M. J. Williams, University of Loughborough
New Approaches to Asymmetric Catalysis

December 7 Prof. D. Briggs, ICI and University of Durham
Surface Mass Spectrometry

1995

January 11 Prof. P. Parsons, University of Reading
Applications of Tandem Reactions in Organic Synthesis

January 25 Dr D. A. Roberts, Zeneca Pharmaceuticals
The Design and Synthesis of Inhibitors of the Renin-angiotensin System

February 22 Prof. E. Schaumann, University of Clausthal
Silicon- and Sulphur-mediated Ring-opening Reactions of Epoxide

April 26 Dr M. Schroder, University of Edinburgh
Redox-active Macrocyclic Complexes : Rings, Stacks and Liquid Crystals

May 4 Prof. A. J. Kresge, University of Toronto
The Ingold Lecture Reactive Intermediates : Carboxylic-acid Enols and Other Unstable Species

1995

October 13 Prof. R. Schmutzler, Univ Braunschweig, FRG.
Calixarene-Phosphorus Chemistry: A New Dimension in Phosphorus Chemistry

October 18 Prof. A. Alexakis, Univ. Pierre et Marie Curie, Paris,
Synthetic and Analytical Uses of Chiral Diamines

October 25 Dr.D.Martin Davies, University of Northumbria
Chemical reactions in organised systems.

November 1 Prof. W. Motherwell, UCL London
New Reactions for Organic Synthesis

December 8 Professor M.T. Reetz, Max Planck Institut, Mulheim
Perkin Regional Meeting

1996

January 10 Dr Bill Henderson, Waikato University, NZ
Electrospray Mass Spectrometry - a new sporting technique

January 11 Dr Terry O' Brien, Rayne Institute, St. Thomas' Hospital
Medical Sensors: The Changing Face of Critical Care

January 24 Dr Alan Armstrong, Nottingham Univesity
Alkene Oxidation and Natural Product Synthesis

February 12 Dr Paul Pringle, University of Bristol
Catalytic Self-Replication of Phosphines on Platinum(O)

March 7 Dr D.S. Wright, University of Cambridge
Synthetic Applications of Me_2N-p-Block Metal Reagents

March 12 RSC Endowed Lecture - Prof. V. Balzani, Univ of Bologna
Supramolecular Photochemistry

April 30 Dr L.D.Pettit, Chairman, IUPAC Commission of Equilibrium Data
pH-metric studies using very small quantities of uncertain purity

1996

October 22 Professor Lutz Gade, Univ. Wurzburg, Germany
Organic transformations with Early-Late Heterobimetallics: Synergism and Selectivity

October 22 Professor B. J. Tighe, Department of Molecular Sciences and Chemistry, University of Aston
Making Polymers for Biomedical Application - can we meet Nature's Challenge?

October 23 Professor H. Ringsdorf (Perkin Centenary Lecture), Johannes Gutenberg- Universitat, Mainz, Germany
Function Based on Organisation

November 18 Professor G. A. Olah, University of Southern California, USA
Crossing Conventional Lines in my Chemistry of the Elements

November 19 Professor R. E. Grigg, University of Leeds
Assembly of Complex Molecules by Palladium-Catalysed Queueing Processes

December 11 Dr Chris Richards, Cardiff University
Stereochemical Games with Metallocenes

1997

January 15 Dr V. K. Aggarwal, University of Sheffield
Sulfur Mediated Asymmetric Synthesis

January 16 Dr Sally Brooker, University of Otago, NZ
Macrocycles: Exciting yet Controlled Thiolate Coordination Chemistry

March 3 Prof. Jim Riehl, Michigan,
The Enantioselective Quenching of Lanthanide complexes

March 5 Dr J. Staunton FRS, Cambridge University
Tinkering with biosynthesis: towards a new generation of antibiotics

March 11 Dr A. D. Taylor, ISIS Facility, Rutherford Appleton Laboratory
Expanding the Frontiers of Neutron Scattering

March 19 Dr Katharine Reid, University of Nottingham
Probing Dynamical Processes with Photoelectrons

May 29 Prof. R. Grubbs, California Institute of Technology,
Olefin Metathesis Catalysts